Experimental Studies on Bio-mitigation of CO_2 and its Utilization for Product Recovery and Process Development

THESIS

Submitted in partial fulfillment
of the requirements for the degree of

DOCTOR OF PHILOSOPHY
by

SOMESH MISHRA

Under the
Supervision of

Dr. SMITA RAGHUVANSHI

and

Co-supervision of

Prof. SURESH GUPTA

BIRLA INSTITUTE OF TECHNOLOGY AND SCIENCE, PILANI
2017

BIRLA INSTITUTE OF TECHNOLOGY & SCIENCE
PILANI-333031 (RAJASTHAN) INDIA

CERTIFICATE

This is to certify that the thesis entitled "**Experimental Studies on Bio-mitigation of CO_2 and its Utilization for Product recovery and Process Development**" and submitted by **SOMESH MISHRA**, ID. No. **2011PHXF007P** for the award of **PhD** Degree of the Institute embodies the original work done by him under our supervision.

Signature of the Supervisor
Name in capital letters **Dr. SMITA RAGHUVANSHI**
Designation Assistant Professor
Department of Chemical Engineering
BITS-PILANI, Pilani Campus, India

Date:

Signature of the Co-Supervisor
Name in capital letters **Prof. SURESH GUPTA**
Designation Associate Professor
Department of Chemical Engineering
BITS-PILANI, Pilani Campus, India

Date:

ॐ

दृषद्विचित्रतल्पयोर्भुजङ्गमौक्तिकस्रजोर्
गरिष्ठरत्नलोष्ठयोः सुहृद्विपक्षपक्षयोः ।
तृणारविन्दचक्षुषोः प्रजामहीमहेन्द्रयोः
समप्रवृत्तिकः कदा सदाशिवं भजाम्यहम्

"When will I see the sameness in the Touch between a Variegated Comfortable Bed (and Hard Ground)? When will I see the sameness in Value between the Garland made of Pearls of Serpents which is a Highly Valued Gem (i.e. ornament) and a Lump of Clay? When will I feel the sameness in Relationship between a Friend and an Enemy? When will I feel the sameness in Vision between a Grass-like Eye (representing ordinary look) and a Lotus-like Eye (representing beautiful look)? When will I feel the sameness in the soul of an ordinary Subject and the King of the World? When will I Worship Mahadeva with the Equality of Vision and Conduct?"

-: Shiv tandav strotam;12th Shloka; Ravana

To My Grandparents, Parents and Nishi
Who
always picked me up on time
and
encourage me to go on every adventure,
especially this one

ACKNOWLEDGEMENTS

I would like to thank all the people who contributed in some way to the work described in this thesis. First and foremost, I thank my Supervisor **Dr. Smita Raghuvanshi**, Assistant Professor, Department of Chemical Engineering, BITS-Pilani, Pilani Campus for accepting me into her research group. Madam has supported me academically and emotionally through the rough road to finish this thesis. During my tenure, she contributed to a rewarding doctorate experience by giving me intellectual freedom in my work, supporting my attendance at various conferences, engaging me in new ideas, and demanding a high quality of work in all my endeavors. I could not have imagined having a better advisor and mentor for my Ph.D. programme.

My sincere gratitude is reserved for my Co-Supervisior **Prof. Suresh Gupta,** Associate Professor & Former Head, Department of Chemical Engineering, BITS-Pilani, Pilani Campus for his invaluable insights and suggestions. I am very grateful for his patience, motivation, enthusiasm, and immense knowledge in analytical techniques, bio-based process development and process calculations that, taken together, make him a great mentor. I really appreciate his willingness to meet me at short notice every time and going through several drafts of my thesis. I remain amazed that despite his busy schedule, he was able to go through the final draft of my thesis and meet me in less than a week with comments and suggestions on almost every page. He is an inspiration.

I would like to thank the members of Doctoral Advisory Committee, Prof. Arvind Kumar Sharma, Associate Professor & Former Head, Department of Chemical Engineering, BITS-Pilani, Pilani campus and Prof. H. K. Mohanta, Associate Professor & Head, Department of Chemical Engineering, BITS-Pilani, Pilani Campus not only for their insightful comments and encouragements but also for the hard questions which incented me to widen my research from various perspectives.

I extended my sincere thanks to Prof. Souvik Bhattacharyya, Vice-Chancellor, BITS-Pilani for giving me the opportunity to carry out the Ph.D. work in BITS-Pilani, Pilani Campus. My sincere thanks go to Prof. A. K. Sarkar, Director, BITS-Pilani, Pilani Campus for providing the necessary infrastructure to carry out this research work. I am indebt to Dr. S. K Verma, Dean, Academic Research Division (Ph.D programme), BITS-Pilani and Prof. H. R. Jadhav, Associate Dean, Academic Research Division (Ph.D. programme), BITS-Pilani, Pilani Campus for providing the necessary research facilities required for my work.

I would like to thank Dr. Pratik N. Sheth, Assistant Professor, Department of Chemical Engineering, BITS-Pilani, Pilani campus for giving me valuable inputs for GC equipment utilization and suggestions which were helpful in improving the quality of my research work. I also thank Ms. Ambika Arkatker for helping me to understand protocols used in isolation and identification of microbial strains. I also thank Mr. Sandeep Ponia and Ms. Shraddha Mishra, Research Scholars, Biological Sciences for their help in protein estimation.

I extend my special thanks to Mrs. Ambika Arketkar for making me familiar with the basics of the biological experiments. I would like to thank Dr. Dipaloy Datta, Dr. Ajay Kumar Pani and Dr. Utkarsh Maheshwari for their constant support and brain storming sessions. I am thankful to Dr. Banasri Roy, Dr. Pradipta Chattopadhyay, Dr. Sushil Kumar, Dr. Amit Jain, Dr. Nikhil Prakash Saxena, Dr. Raman Sharma, Dr. Srinivas Appari, Dr. (Ms.) Priya C. Sande and Dr. Sonal Mazumdar for their support throughout the work.

The greatest gift of life is friendship and I have received it in the form of Mr. Nishkam Batta, Mr. Sudershan Singh, Ms. Shweta Sharma, Ms. Prachi Venkat, Ms. Prachi Varseney, Mr. Rajeev Sharma. My special thanks to Ms. Indu Sharma to keep me intact in my childhood regime. I would like to thank Mr. Saswat Kumar Pradhan for the discussions revolving around various religious and political issues.

I thank my fellow labmates Ms. Pratibha Pal, Mr. Ajinkya Rahane, Mr. Isha Nagarpukar, Mr. Anand Sarit, Mr. Kaushik Raj, Mr. Piyush Chauhan, Mr. Aditya Bhatt, Ms. Gayathri Gangadhar, Ms. Amrita Singh, Mr. Silbrata Pahari and Mr. Debashish Mohanty for the stimulating discussions, for the sleepless nights we were working together before timelines, and for all the fun we have had in the last five years.

I thank Center for Scientific and Industrial Research (CSIR) and University Grants Commission (UGC) for providing fellowships and necessary supports to carry out research at department laboratories.

I would like to express my special thanks to Mr. Ashok Saini for his help and support in fabricating the packed bed bioreactor column and time to time technical assistance. I would like to thank Mr. Subodh Kumar Azad, demonstrator for his help in handling various analytical equipments. I specially thank Mr. Babulal Saini for his continuous support, time to time guidance and maintaining disclipline throughout course of work. Thanks are also due to Mr. Jeevan Lal Verma and Mr. Jangvir Sheron for their help and co-operation during this work.

I would like to acknowledge my teachers Dr. A. K. Jha, Dr. Ramayan Tripathi, Dr. S. L. Maurya and Dr. N. K. Upadhaya, Central Hindu Boys School, B.H.U, Varanasi, I learnt from them since my childhood, I would not have been here without their guidance, blessings and support. My special thanks to Dr. O. P. Singh, Central Hindu Boys School, B.H.U, Varanasi for being another role model for me. I feel privileged to be his student once, a feeling that every student of his will second.

A special thanks to my parents, younger sister Nishi, family members and Uncle Ranjan Sinha for their love, understanding and affection and for supporting me throughout this research work and my life in general.

I thank the Almighty for giving me the strength and patience to work through all these years so that today I can stand proud with my head held high.

SOMESH MISHRA

ABSTRACT

Continuous increase in the environmental concentration green house gases (GHG's) chiefly CO_2(g) from anthropogenic sources results in global warming and climate change. Currently, CO_2 concentration in Earth's atmosphere has reached to 405 ppm. The world community has taken different steps such as carbon capture and sequestration (CCS), carbon capture and utilization (CCU), development of processes having zero carbon discharge, etc. to reduce the emissions of CO_2 into the Earth atmosphere. Out of these, CCU via biological route employing photoautotrophs is found to be the attractive solution and has got immense attention in the past decade. Most of the studies are dedicated for the development of CO_2 bio-mitigation system and production of valuable metabolites using photoautotrophs. However, the limitations such as low tolerance to CO_2, low biomass productivity, costly downstream processing, lower rate of CO_2 etc. are associated with photoautotrophs and has lead researchers to search for other biological alternatives. Thus, the focus was shifted towards chemoautotrophic microorganisms. These microorganism by virtue of their faster growth rate, use inorganic salt as energy source, adaptability under harsh conditions, capability to produce valuable metabolites, are able to utilize CO_2 and has high CO_2 tolerance capability to replace photoautotrophs for the development of sustainable and efficient CO_2 bio-mitigation system. The necessity of future prespective of CCU via biological route explored in the present work.

Bacterium *B. cereus*, mixed microbial population, *E. cloacae*, *P. putida* obtained from sewage treatment plant (STP) and *P. aeruginosa* and *H. stevensii* obtained from Sambhar salt lake (SSL) were subjected to carry out extensive batch CO_2(g) bio-mitigation studies at different concentrations of Fe[II] or $S_2O_3^{2-}$ as an energy substrate. Among all microbial cultures used in the present study, *H. stevensii* has shown maximum CO_2(g) removal efficiency [η_{CO2}(g)], biomass productivity per day (P, g L^{-1} d^{-1}), biomass produced (X_{Max}, g L^{-1}), CO_2(g) utilization per day (R_{CO2}, g_{CO2} L^{-1} d^{-1}) as 98.4%, 0.174 (±0.016), 1.05 (±0.07) and 0.215 (±0.02), respectively at 100 mM $S_2O_3^{2-}$ concentration.

Leachate (biomass & supernatant) obtained from CO_2 bio-mitigation batch studies were analyzed using Fourier-Transform Infrared Spectroscopy (FT-IR) and Gas Chromatography - Mass Spectroscopy (GC-MS). The obtained results revealed the presence of fatty acids, hydrocarbons for STP cultures and fatty alcohols for SSL cultures in extractable amount. The elemental carbon balance and thermodynamic analysis of the CO_2 bio-mitigation batch studies

w.r.t electron acceptor/donor component were carried out to estimate the actual CO_2 removal efficiency ($R.R_{CO2}$) and thermodynamic feasibility of the process.

Based on the CO_2(g) utilization capability of *H. stevensii* additional experiments were performed using *H. stevensii* for understanding the possible assimilation of CO_2(g) into cellular biomass and its allocation among different cellular organic pool. The optimum salt concentration, pH and temperature for CO_2 utilization of *H. stevensii* were found as 0.5 M, 8 and 37 ^{o}C, respectively. The studies have indicated that the fatty alcohols were produced at the expense of cellular carbohydrates and protein content and their concentrations increase with increase in the concentration of CO_2.

Scale up studies were also carried out in a lab scale bioreactor by continuous supply of 15% (v/v) CO_2(g) concentration for 72 h using *H. stevensii*. The calculated values of P (g $L^{-1}d^{-1}$), μ (d^{-1}) and R_{CO2} were found as 1.55 (± 0.035), 0.19 (± 0.034) and 1.94 (± 0.044), respectively for semi-continuous studies which were found to be better than the values obtained during batch studies. The downstream bio-processing strategy was tested and biomass obtained from filtration and direct recovery of metabolites using solvent extraction from wet biomass was found as an efficient and cost effective downstream processing strategy. Economic feasibility analysis of the developed downstream bio-processing method suggested that it can be utilized for the production of dodecanol as compared to the tetradecanol.

Packed bed column was developed using mixture of coal and matured compost and biofilm was developed by inoculating the column with mixed population of *B. cereus*, *E. cloacae*, *P. putida*, *P. aeruginosa* and *H. stevensii* for the total duration of 7 days. The column was operated for 77 days at three different inlet CO_2 concentrations of 5, 10 and 15 % (v/v). The maximum steady CO_2(g) removal efficiency was observed as 100% (v/v) at inlet CO_2(g) concentration of 5, 10 and 15% (v/v). The obtained results of sudden change in inlet CO_2(g) concentration indicated that biofilm developed in the bioreactor was quite stable.

Keywords**:** *Approximate material balance; Biodiesel; CO_2 bio-mitigation; Downstream bio-processing strategy; Energy substrate; Fatty acids; Fatty alcohol; FT-IR; GC-MS; Halomonas stevensii; Mixed microbial population; Process economics; packed bed bioreactor; Scale-up studies SSL; STP; Thermodynamic assessment.*

TABLE OF CONTENTS

LIST OF FIGURES

LIST OF PLATES

LIST OF TABLES

NOMENCLATURE

C	Cost of biomass	Rs.
C_C	Carbon content in biomass	
CFU	Colony forming unit	CFU g^{-1}
F	Total cost of production	Rs.
ΔG	Gibb's free energy change,	kJ mol^{-1}
M	Molarity	
M_A	Amount of biomass	g
M_C	Molecular weight of carbon	g $mole^{-1}$
$M_{C, in}$	Mass of C supplied as CO_2(g)	g
$M_{C, go}$	C left in gaseous phase as CO_2 at the end of batch study	g
$M_{C,bo}$	C assimilated as biomass	g
$M_{C,CO2(l)}$	Dissolved CO_2 in aqueous phase	g
$M_{Cin,CO2(g)}$	Mass of CO_2(g) present in the head space of flask	g
$M_{Cin,CO2(l)}$	CO_2 present in dissolved form in the liquid media	g
M_{CO2}	Molecular weight of CO_2	g $mole^{-1}$
P_T	Total production cost	Rs.
P_R	Cost of raw material as coconut oil	Rs.
P_{Max}	Biomass productivity	g L^{-1} d^{-1}
R	Experimentally obtained product recovery	%
$R.R_{CO2}$	Actual CO_2 removal efficiency	% w/w
R^2	Co-relation factor	
R_{CO2}	CO_2(g) fixation rate	g_{CO2} L^{-1} d^{-1}
$W_{(Fatty\ alcohol\ obtained)}$	Weight of Fatty alcohol obtained	mg
$W_{Biomass}$	Weight of Biomass taken	mg
W_{FAME}	Weight of FAME obtained	mg
X_{Max}	Maximum biomass obtained in terms of dry weight	g L^{-1}
Y	Factor correcting for the differences in the solvent recovery costs	
y_{in}	Initial concentration of CO_2(g)	atm
$y_{CO2, final}$	Initial (t = 0) head space CO_2 concentration,	% v/v
$y_{CO2, in}$	Final ($t = t_x$) head space CO_2 concentration,	% v/v
y_{CO2out}	Final concentration of CO_2,	% v/v
z	Mass fraction of fatty alcohol in the biomass	
S	Salt concentration	% w/v
T	Temperature	^oC
t	Time	

Greek Symbols

μ_{Max}	Specific growth rate	d^{-1}
η_{CO2}	CO_2(g) removal efficiency	% v/v

Abbreviations

16S rRNA	16S ribosomal RNA
ATR	Attenuated total reflectance
CA	Carbonic anhydrase
CCM	Carbon concentration mechanism
CCS	Carbon capture and sequestration
CCU	Carbon capture and utilization
COP22	22^{nd} Conference of the parties
DIC	Dissolved inorganic carbon
DO	Dissolved oxygen
EGR	Enhanced gas recovery
EOR	Enhanced oil recovery
FAME	Fatty acid methyl ester
FT-IR	Fourier transform infra red
GC-MS	Gas chromatography and mass spectroscopy
GHGs	Green house gases
GPC	Generalized predictive controller
LPM	Liter per minute
FAME	Fatty acid methyl ester
MSM	Minimal salt media
NAD(P)H	Nicotinamide adenine dinucleotide phosphate
NCBI	National center for biotechnology information
MSM	Minimal salt media
NAD(P)H	Nicotinamide adenine dinucleotide phosphate
NPK	Nitrogen phosphorus potassium
PBRs	Photobioreactors
PMMA	Polymethyl methacrylate
RE	Reactive extraction
SSE	Solvent solvent extraction
SSL	Sambhar salt lake
STP	Sewage treatment plant
UNFCCC	United Nation Framework on Climate Change Convention

Chapter 1

Introduction

A brief background of the origin of problem statement, carbon capture utilization, algal and cyanobacteria system limitations, motivation, hypothesis as well as research objectives of the present work are presented in this chapter.

1.1 Green House gases (GHGs) and their environmental impact

Energy is indispensable for human well-being and for sustainable economic growth. The exploitation of easy-to-transform fossil fuel for human comfort and to meet sustainable energy demand result's to the addition of green house gases (GHGs) into the atmosphere (Kais and Sami, 2016). The gases which are categorized as GHGs, include carbon dioxide (CO_2), nitrous oxide (N_2O), methane (CH_4), water vapor (H_2O), fluorocarbons (CFs) and chlorofluorocarbons (CFCs). GHGs have ability to trap the outgoing solar radiation, which results in global rise in environmental temperature, a phenomenon known as global warming (IPCC, 2014). The impact of increasing GHGs concentration in the Earth's atmosphere may lead to adverse phenomena such as climate change, rising of sea level, melting of glacier, droughts, floods, etc (IPCC, 2014). Considering the importance of the issue of global warming and climate change, the international community adopted United Nation Framework on Climate Change Convention (UNFCCC) in Rio (Brazil) Earth summit in 1992. The frame work was focused on stabilizing the concentration of GHGs in the Earth's atmosphere, which was outpaced due to anthropogenic intervention. Presently, UNFCCC has 195 countries as members. At 22nd Conference of the Parties (COP22) (UNFCCC Marrakech, Morocco, 2016), members were reasserting to limit the increase in global temperature below 2 ^{o}C and were insisting for attempts to limit the rise below 1.5 ^{o}C (Johannsdottir, 2016). Carbon dioxide (CO_2) is one of the chief GHGs having lowest global warming potential. However, its concentration in the atmosphere is increasing at more alarming rate as compared to other GHGs. CO_2(g) was comprising 78% of the total GHGs emitted globally during the period 1970 to 2015 (IPCC, 2014).

The accumulation of CO_2(g) into the Earth's atmosphere is understood by the existing balance between CO_2(g) source and sink. The extensive uses of fossil fuels and change of land

uses (deforestation, logging and intensive cultivation of crop land soils) are the major anthropogenic CO_2 sources (Le Quéré et al., 2009). The combined CO_2(g) emission due to extensive fossil fuels and change of land uses was approximately 9.9±0.9 Pg C/ yr (1 Pg C = 1 petagram or 10^9 metric tons of carbon) in the year 2008. The CO_2(g) emission due to the uses of fossil fuels increased at the rate of 3.4 % yr^{-1} during the period of 2000 to 2008 as compared to 1 % yr^{-1} from 1990 to 2000 (Le Quéré et al., 2009). Cement industry is one of the important contributors of CO_2 emission in the atmosphere (Peters et al., 2012). The terrestrial plantation, inland water systems and oceans are the largest CO_2(g) sink. The green plants assimilate CO_2(g) as a product of photosynthesis into the plant biomass. The planktons and phytoplankton present in different water bodies (including oceans) are capable of assimilating CO_2(g) as biomass. Various phenomena such as the dissolution of CO_2(g) into the oceans, acid base reactions and carbonate forming capability of many micro-organisms also act as sink for CO_2(g) (Battin et al., 2009). Out of 9.1 PgC yr^{-1} of CO_2(g) emitted from anthropogenic sources during period of 2000 to 2006, 4.1 PgC yr^{-1} was accumulated to atmosphere, 2.2 PgC yr^{-1} was sequestered into marine ecosystem and 2.8 PgC yr^{-1} mitigated within terrestrial biosphere (Battin et al., 2009). Therefore, the emission of CO_2(g) from anthropogenic sources has outpaced the existing balance between CO_2 source and sink. This resulted in the accumulation of CO_2(g) and thus increase in CO_2(g) concentration in the Earth's atmosphere.

The higher CO_2(g) concentration in the Earth's atmosphere has physical, ecological and biological impact (Rosenzweig et al., 2008). Increase of CO_2(g) concentration up to the level of 450 ppmv - 600 ppmv (parts per million volumes) would result in an irreversible dry climate.
In 21^{st} century, if the CO_2(g) concentration reaches upto the value of 600 ppm that would result in the rise in the sea level from 0.4 to 1 m (Solomon et al., 2009). The accumulation of CO_2(g)

into oceans resulted in ocean acidification, which is another mankind induced problem due to increased CO_2(g) concentration in Earth's atmosphere. The changing pH of ocean has not only adversely affected the climate but has also affected the marine biota to a larger extent (Baumann et al., 2012). Currently, CO_2(g) in the Earth's atmosphere is at a concentration of 406.42 ppm which is 40% higher as compared to pre-industrial level of 285 ppm (www.co2.earth). The increasing dependency on fossil fuels to meet energy requirement has forecasted further increase in CO_2(g) concentration in the Earth's atmosphere.

Hence, the anthropogenic induction of CO_2(g) into the atmosphere resulted in global warming, which has further lead to climate change. Therefore, CO_2(g) mitigation from anthropogenic sources is the prime focus of the present work.

1.2 Existing solution (Carbon Capture and Sequestration) and their limitations

The escalating level of CO_2(g) in the Earth's atmosphere and its related adverse effects have propelled the researchers to look into the options for curbing down the CO_2(g) emissions. The options include: (1) switching to renewable sources of energy, (2) development of manufacturing processes having zero CO_2(g) emission and (3) restricting the emission of CO_2(g) from anthropogenic sources into the atmosphere (Lal, 2008; Shukla et al, 2010). Switching to renewable energy sources and development of zero CO_2 emission processes are the acute CO_2(g) controlling options and are still in their developing stage (Lal, 2008). Thus, in the past decades, option of reducing the anthropogenic CO_2(g) emission into the environment was practiced by industries in the name of Carbon Capture and Storage (CCS).

CCS is an "end of the pipe" technique, allowing the utilization of fossil fuels while simultaneously restricting the emissions of CO_2(g) into the Earth's atmosphere. CCS includes the

separation of CO_2(g) from point sources (power plant, natural gas production, synthetic fuel plants etc.), transportation to the storage site and storage in isolation from the Earth's atmosphere (e.g., geological formation, ocean storage) [IPCC, 2014; Mikkelsen et al., 2009; Anderson, 2003]. Therefore, CCS is a direct sequestration option, avoiding the atmospheric emission of CO_2(g) altogether. CCS has three distinct strategies, which include: (1) post combustion capture system, (2) pre combustion capture system and (3) oxygen fired combustion system (MacDowell, 2010).

The disadvantages associated with these three CCS strategies include: high capital cost, energy penalty associated with separation unit, energy penalty of (15%) associated with the regeneration of sorbent, high operating cost for connected sorption system, handling of low CO_2(g) concentration flue gas processing, energy associated with compression of CO_2(g) and its transportation, extensive equipment requirements, control of generated waste, extra energy penalty associated with cryogenic air separation unit and air leakage problems (MacDowell et al., 2010; de Visser et al., 2008; Ramdin et al., 2012; Leung et al., 2014; Kumar et al., 2015).

Looking into the disadvantages, CCS still has to overcome associated technical and economic barriers to become a feasible CO_2 mitigation solution. Hence, the CCS strategy for CO_2 sequestration is still in the development phase and alone it would not be able to control the addition of CO_2(g) into the Earth’s atmosphere.

1.3 Carbon capture and utilization (CCU)

In the past decades, despite of considerable research, drawbacks associated with CCS technology and its inefficacy in delivering a sustainable economic solution for CO_2 mitigation problem led researchers to look for the alternative CO_2 mitigation technologies. Carbon capture and

utilization (CCU) is one such technology, which involves the conversion of waste CO_2(g) into valuable molecules such as chemicals, fuels etc., and in process contributing significantly towards CO_2 mitigation. Thus, CCU provides value addition to the waste CO_2(g), rather being treated as garbage in CCS. Furthermore, CO_2(g) can be considered as low-cost available feedstock for the production of different chemicals as long as it is emitted from different anthropogenic sources (Cue´ llar-Franca et al., 2015; Mikkelsen et al., 2009). Different means for CO_2(g) utilization are further categorized into chemical, physical and biological means.

Chemically, CO_2(g) is utilized as a feedstock for the commercial production of compounds such as urea, methanol and salicylic acid (Aresta et al., 2004). Different high commercial value chemicals that can be produced using CO_2(g) as a feedstock are shown in Fig. 1.1 (Sakakura et al., 2007).

The physical means of CO_2(g) utilization include application as a coolant and refrigerant, use in fire extinguishers, extraction of residual oil and gas for Enhanced Oil Recovery (EOR) and Enhanced Gas Recovery (EGR), extraction of natural materials, processing and recycling of polymer and rubber products, and the impregnation of wood (Aresta and Dibenedetto, 2007; Markewitz, 2012; Leung et al., 2014).

The conversion of CO_2(g) into other compounds via chemical and physical schemes as described above required three basic steps: (1) separation, (2) transportation, and (3) utilization. The cost associated with CO_2(g) separation and its compression up to 110 bar is estimated to be \$30 - 50 per ton of CO_2. The estimated transportation cost was \$1 - 3 per ton of CO_2(g) per 100 km and utilization or conversion cost is \$1 - 3 per ton of CO_2(g), respectively (Gupta and Fan 2002; Shi and Shen 2003). CO_2 is an inert molecule, due to which its chemical conversion into

other compounds requires high input of energy and cost, which makes the mitigation benefits marginal (Mikkelsen, 2009).

Thus, the limitations such as energy penalty, associated separation cost, transportation and utilization costs associated with the chemical and physical means of CO_2(g) utilization have compelled researchers to look out for more sustainable and economical solution for CO_2 mitigation problem.

On the lines of CCU, biological route for CO_2 mitigation has gained much attention in the present decade. Biological route ensures the natural assimilation of CO_2(g) into biomass at the expense of very less energy penalty. Biological utilization of CO_2(g) has occurred via natural processes known as photoautotrophy and chemolithotrophy (Mikkelsen, 2009). Bio-mitigation of CO_2 via photoautotrophy route (terrestrial plants, micro-alga and cyanobacteria) has found its way back to year 1991 and research continues till today. On the virtue of their faster growth rate and higher solar energy utilization efficiency (10 - 50 times of terrestrial plants), microalgae and cyanobacteria become the first choice for the development of CO_2 bio-mitigation system (Wang et al., 2008; Li et al., 2008). Microalgae and cyanobacteria were able to utilize CO_2(g) released from anthropogenic sources and assimilate it further into biomass and valuable bio-molecules having high commercial values such as lipids, pigments, cosmetics, pharmaceuticals, bio-polymers, coenzymes, etc. Thus bio-mitigation of CO_2 has satisfactorily fulfilled the CCU requirements (Yen et al., 2013; Skjånes et al., 2013).

Therefore, in the past decades, CO_2 bio-mitigation employing photoautotrophic micro-organisms has gained an immense attraction as a feasible solution. Immense work has been carried out using different microalgal and cyanobacterial strains to check their ability to bio-mitigate CO_2(g) from various sources (Table 1.1). Various micro-algal and cyanobacterial strains

were isolated, identified and characterized from habitat ranging from natural to man-made. Extensive batch studies have been carried out using isolated microalgal and cyanobacterial strains to optimize their cultivation conditions such as CO_2(g) tolerance, nutritional requirements, light intensity/photo-inhibition, temperature, pH, light to dark cycle, photo-quantum efficiency, tolerance to SO_x and NO_x etc (Wang et al., 2008; Li et al., 2008). Biological parameters such as maximum biomass productivity (X_{Max}), specific growth rate (μ_{Max}), CO_2 fixation rate (R_{CO2}) were estimated using either different growth kinetic models or developed mathematical correlation by fitting the biomass growth data (Kumar et al., 2011; Ho et al., 2011). The biomass obtained from CO_2(g) fixation batch studies was further utilized for the characterization of metabolites using different analytical techniques (FT-IR, GC-MS, etc). Quantification of metabolites was carried out in terms of yield, which is defined as amount of product recovered per gram of biomass (Li et al., 2008; Ho et al., 2011; Kumar et al., 2011).

The results obtained from batch studies were utilized for the development of different types of laboratory scale cultivation systems. The cultivation systems were broadly classified into two categories (1) open pond system and (2) closed system. On the basis of their specific design and gas sparging strategy, closed systems were further classified as (1) Tubular, (2) Flat-plate, (3) Air-lift and (4) Bubble column (Chisti, 2007). The lab scale cultivation system would be further scaled-up to pilot plant scale (Ho et al., 2011).

Some of the studies have highlighted not only the CO_2 mitigation problem but also the eutrophication problem. Recently, bio-refinery approach works on the integration and utilization of flue gas as carbon source, waste water from industrial effluent plant as growth medium and extraction of bio-molecules (Cuellar-Bermudeza et al., 2015). The recent literature related to

CO_2 bio-mitigation experimental studies employing photoautotrophs (microalgae/cyanobacteria) are summerized in Table 1.1.

Thus, the development of CO_2 bio-mitigation system utilizing photoautotrophic microorganisms was studied extensively by scientific community. The major hurdles faced in the implementation of CO_2 bio-mitigation system using photoautotrophs at real time industrial scenario include: (1) growth inhibition at high CO_2(g) concentration [> 8% CO_2 (% v/v)], (2) low CO_2(g) utilization, (3) tolerance to NO_x & SO_x presence in flue gas, (4) photoinhibition, (5) decrease in valuable metabolite content at high CO_2(g) concentration, (6) high capital and operating costs of cultivation system, (7) contamination risk in open cultivation system, (8) heavy metal ion tolerance, (9) difficulties in scale up of bioreactor system and (10) higher downstream processing cost. Hence, the work is still in its development phase to become reality in the near future. Most of the studies were limited to the use of photoautotrophs for CO_2 mitigation. These studies were mainly focused on answering the question: "how to make CO_2 bio-mitigation system more realistic, sustainable and economic?". However, along with the bio-mitigation convention, the limitations associated with photoautotrophs can be overcome by the use of chemolihtotrophic organisms.

1.4 Motivation

Energy required for the conversion of CO_2(g) into the cellular organic carbon can be obtained either from light or inorganic compounds depending on the type of organisms (Berg, 2011). Chemoautotrophic fixation of CO_2(g) is represented by catalyzing thermodynamically favored but kinetically inhibited oxidation-reduction or electron donor-acceptor scheme of dissolved inorganic compounds. The compounds such as H_2, Fe [II], H_2S, $S_2O_3^{2-}$, $S_4O_6^{2-}$, sulfide mineral,

CH_4, various mono, di, tri and hydroxy carboxylic acid, alcohols, amino acids, and complex organic substrate are major electron donors whereas, O_2, Fe[III], CO_2, CO, NO_3^-, NO_2^-, NO, N_2O, SO_4^{2-}, SO_3^{2-}, $S_2O_3^{2-}$ and sulfur are major electron acceptors (Fdz-Polanco et al., 2001).

Chemolithotrophs harness the required energy from redox reactions for metabolizing the inorganic form of carbon [CO_2(g)] to accomplish their cellular demand. Hence, in contrast to photoautotrophs, if a chemolithotrophic bacterium is able to assimilate CO_2(g) at high CO_2(g) concentration and at room temperatures (less energy penalty), then it would be economically viable and an efficient route for bio-mitigation of CO_2.

Few recent studies have investigated the prokaryotes for their ability to capture CO_2(g) in the absence of light and its simultaneous conversion into valuable products (Alonso-Sáez et al., 2010; Saini et al. 2011; García et al., 2016). One study has shown the fixation of CO_2 by *Sulfurovum lithotrophicum* 42BKT^T under high pressure of CO_2 + N_2 [$p^o_{CO_2} : p^o_{N_2} = 2:8\,(\text{atm})$] at 29 ^oC. The study confirmed the utilization of 37% of total CO_2(g) and its fixation into metabolites such as glutamate and pyroglutamate (Kwon et al., 2015). The other study has reported the fixation of dissolved CO_2 into lipids by chemolithotrophic bacterium, *Serratia sp.* ISTD04 and 94% conversion of obtained lipids to fatty acid methyl esters (Bharti et al., 2014).

Significant advantages such as faster life cycle, rapid growth rate, ability to sustain in highly-dense culture and ability to utilize CO_2(g) in the absence of light and rapid adaptability to the changing environment associated with bacterium make them an attractive choice over photoautotrophs (Bharti et al., 2014). Different bacterium strains are known for the production of enzymes, metabolites, solutes, exopolysachharides, surfactants, fatty alcohols, hydrocarbons, lipids and pigments, which are valuable products (Khan et al., 2014; Ladingya et al., 2006; Bharti et al., 2014). Thus, the above mentioned major challenges associated with

photoautotrophs may be overcome by chemolithotrophic bacteria. Presently, development of CO_2 mitigation system using bacteria, in dark, for direct conversion of CO_2(g) from point source into cellular biomass and recovery of commercial valued molecules is the most untouched area. This can be utilized for the development of cost effective and sustainable CO_2 bio-mitigation system. Therefore, for the development of sustainable CO_2 mitigation process, the understanding of CO_2 bio-mitigation potential of bacteria belonging to different habitat was necessary. Hence, there is need to study the CO_2(g) utilizing capability of bacteria, isolated from different habitats, utilizing reduced inorganic compound as an energy source.

The mixed microbial population utilization was found to be suitable for long term industrial use. However, the utilization of mixed microbial population for CO_2 bio-mitigation in dark is yet to be investigated. On the line of CCU, to give economic value to the mitigation process, the analysis of by-products obtained from CO_2 mitigation studies is an exciting area to think of and required serious attention. In recent years, no work has been discussed on the development of downstream processing strategy for the economic recovery of primary metabolites from CO_2(g) utilizing bacteria. Further, the development of continuous system for bio-mitigation of CO_2(g) in the absence of light is not reported.

1.5 Research Objectives

Thus, the objectives of the present study are:

1. To isolate and characterize the microbial species obtained from different habitats which are capable of utilizing CO_2(g).
2. To carry out CO_2 bio-mitigation studies utilizing isolated bacterium and mixed microbial population using inorganic energy substrates.

3. To identify and characterize the valuable metabolites produced through microbial utilization of CO_2(g).
4. To carry out the semi-continuous studies in bioreactor for the product recovery from leachate obtained and process economic feasibility analysis.
5. To develop packed bed bio-reactor studies at laboratory scale and determine its performance for the mitigation of CO_2(g) by conducting experiments.

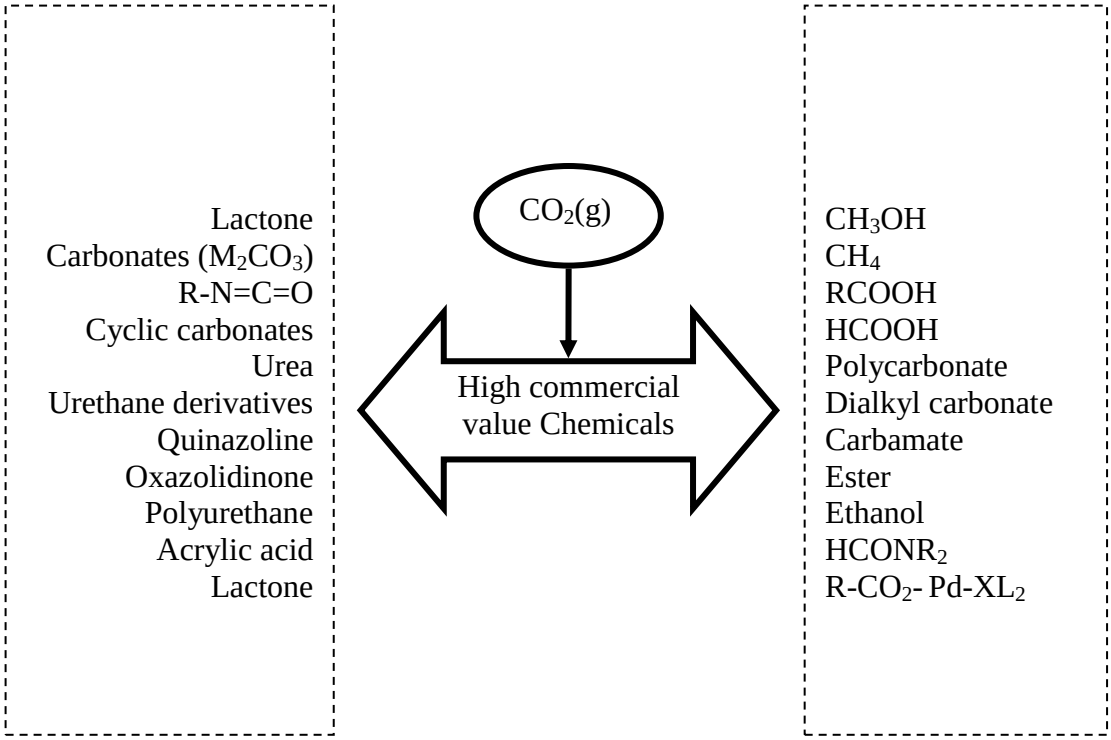

Fig. 1.1 Chemical conversion of CO_2(g) into commodity chemicals

Table 1.1: CO_2 bio-mitigation studies incorporating different species of microalgae and cyanobacteria from 2007 to 2016

S. No.	Microalgae/Cyanobacteria	Inlet CO_2(g) concentration (% v/v)	References
1.	*Scenedesmus obliquus*, *Chlorella Kessleri*	6 & 12	deMorais and Costa, (2007)
2.	*Chlorogleopsis* sp. (SC2)	5	Ono and Cuello (2007)
3.	*Chlorocuccum littorale*	5	Ota et al., (2009)
4.	*Scenedesmus obliquus* CNW-N and AS-6-1	20	Ho et al., (2010)
5.	*Dunaliella tertiolecta* SAD-13.86, *Chlorella vulgaris* LEB-104, *Spirulina platensis* LEB-52 and *Botryococcus braunii* SAG-30.81.	5	Sydney et al., (2010)
6.	*Scenedesmus obliquus* SJTU-3 & *Chlorella pyrenoidosa*	0.03, 5, 10, 20 , 30 and 50	Tang et al., (2011)
7.	*Anabarna* sp. CH1	15	Chiang et al., (2011)
8.	*Cyanothece* sp. ATCC 51142	0.5	Sinetova et al., (2012)
9.	*Synechocystis aquatilis* TISTR8612	5 & 10	Kaiwan-arporn et al., (2012)
10.	*Mutate Chlorella* sp.	15	Cheng et al., (2013)
11.	*Scenedesmus obliquus* SA1	13(±1)	Basu et al., (2013)
12.	*Chlorella vulgaris*	2 , 6 & 10	Anjos et al., (2013)
13.	*Scenedesmus obtusiusculus*	10	Toledo-Cervantes et al., (2013)
14.	*Ettlia* sp. YC001	5	Yoo et al., (2013)
15.	*Thermosynechococcus elongates* TA-1	10 and 20	Leu et al., (2013)
16.	*Chaetoceros muelleri*	0.03, 10, 20, and 30	Wang et al., (2014)
17.	*Chlamydomonas* sp. JSC4	0.04, 2, 4 and 8	Nakanishi et al., (2014)
18.	*Chlorella* sp. MTF-15	22 - 28	Kao et al., (2014)
19.	*Desmodesmus* sp. 3Dp86E-1	20	Solovchenko et al., (2015)
20.	*Chlorella* sp.	5	Yadav et al., (2015)
21.	*Rhizoclonium hieroglyphicum* JUCHE2	5 - 25	Pradhan et al., (2015)
22.	*Chlorella vulgaris*, *Pseudokirchneriella subcapitata*, *Synechocystis salina*, *Microcystis aeruginosa*	10	Gonçalves et al., (2016)
23.	*Chlorella vulgaris* & *Guzmania membranacea*	5 - 15	Mohsenpour and Willoughby, (2016)
24.	Mutant *Chlorella* PY-ZU1	15	Cheng et al., (2017 (a))
25.	Mutant *Haematococcus pluvialis*	15	Cheng et al., (2017 (b))

1.6 Thesis organization

The objectives are achieved by initially carrying out the detailed literature review on available batch studies for CO_2 bio-mitigation, by-products analyzing technique, carbon concentrating mechanism in bacteria, different CO_2 fixing pathways and thermodynamic feasibility analysis of chemoautotrophic growth, which is given in chapter 2. The details on growth media formulation, batch studies, by-product analysis techniques, product yield quantification, downstream processing strategy and design of bio-filter column are described in chapter 3. The methodology followed for estimating the economic analysis of product recovery is reported in chapter 4. The results pertaining to CO_2 bio-mitigation batch studies using bacteria and mixed microbial population, downstream processing strategy and bio-filter column are discussed in chapter 5. Chapter 6 deals with the summary of the work and important conclusions drawn from the present study.

Chapter 2

Literature Review

CO_2 bio-mitigation studies employing microalgae and cyanobacteria, micro-algal and cyanobacteria CO_2 mitigation systems, bacteria CO_2 utilization, energetic requirement, gaps and scope of present work are described in this chapter.

In the past decades, exhaustive studies have been carried out for the development of sustainable phototrophic and chemotrophic CO_2 bio-mitigation systems. The previous studies reporting the use of photoautotrophs and chemoautotrophs for CO_2 bio-mitigation are discussed in following sections.

2.1 Phototrophic CO_2 bio-mitigation

Photoautotrophs utilize solar energy to assimilate CO_2(g) into cellular biomass at expense of very less thermodynamic energy penalty. The kinetics of photosynthetic CO_2(g) reduction reaction by plants (mainly larger trees) is slow and inefficient. However, the efficiency of photosynthesis reaction increases as the plant size decreases. It is found that microalgae are an unicellular plant like organism which are 10 times more efficient than terrestrial plants in CO_2(g) fixation using solar energy (Mikkelsen et al., 2009; Wang et al., 2008; Li et al., 2008). Therefore, in the past decades many studies have been reported for the development of photoautotrophic based CO_2 mitigation system. Several studies have also discussed the production of value-added chemicals such as bio-diesel, pigments, food supplements, cosmetics, fine chemicals, etc from photoautotrophs. Hence, the uses of photoautotrophic microorganisms for CO_2 bio-mitigation were based on two major perspectives: (1) CO_2 mitigation and (2) conversion into other products. Recent studies have highlighted not only the CO_2 mitigation problem but also the eutrophication problem. The studies related to the above mentioned perspectives are discussed in following sub-sections.

2.1.1 CO_2 mitigation batch studies

De Morais and Costa (2007) isolated *Scenedesmus obliquus* and *Chlorella kessleri* from effluent treatment plant of coal fired thermoelectric power plant and their growth characteristics were studied under 6%, 12 % and 18% (v/v) of CO_2(g) stress. The maximum biomass productivities of *C. kessleri* and *S. obliquus* were observed as 0.090 (±0.002) g L^{-1} d^{-1} and 0.085 (±0.002) g L^{-1} d^{-1} at 0.038% and 6% (v/v) CO_2 stresses, respectively. *C. kessleri* and *S. obliquus* were also found to grow well under 18% (v/v) CO_2 stress. However, *C. kessleri* and *S. obliquus* have shown the decrease in biomass productivity with increase in CO_2 concentration from 6% (v/v) to 18% (v/v).

Ono and Cuello (2007) studied the CO_2 bio-fixation capabilities of *Chlorogleopsis* sp. (thermophilic microalgae), isolated from Yellowstone National park. *Chlorogleopsis* sp. was found to grow at 5% (v/v) CO_2(g) for the luminance value of 200 µmol m^{-2} s^{-1} with maximum carbon fixation rate of 20.45 mg(C) L^{-1} d^{-1}.

Seven *Scenedesmus obliquus* strains from fresh water lake (Taiwan) were isolated by Ho et al., (2010) and there CO_2 bio-mitigation capabilities were evaluated. The strains have shown promising growth under 20% (v/v) CO_2(g) concentration in the 12 days of batch study. The maximum biomass concentration (X_{Max}) values were obtained in the range of 1.13 - 2.63 g L^{-1}. Maximum X_{Max} values for *S. obliquus* strains CNW-N and AS-6-1 were obtained as 2.63 g L^{-1} and 1.90 g L^{-1}, respectively. Thus, *S. obliquus* strains CNW-N and AS-6-1 were found to be suitable candidates for CO_2 bio-mitigation process.

Growth characteristics of four microalgal species namely *Dunaliella tertiolecta* SAD-13.86, *Chlorella vulgaris* LEB-104, *Spirulina platensis* LEB-52 and *Botryococcus braunii* SAG-30.81 were studied at 5% (v/v) CO_2(g) concentration for total 15 days of cultivation period by Sydney et al., (2010). CO_2 fixation rate (R_{CO2}) was obtained as 496.98 mg L^{-1} d^{-1}, 318.61 mg L^{-1}

d^{-1}, 272.4 mg L^{-1} d^{-1} and 251.64 mg L^{-1} d^{-1} for *B. braunii* SAG-30.81, *S. platensis* LEB-52, *D. tertiolecta* SAD-13.86 and *C. vulgaris* LEB-104, respectively.

Tang et al., (2011) studied the effect of CO_2(g) concentration on the biomass growth of *Scenedesmus obliquus* SJTU-3 and *Chlorella pyrenoidosa* SJTU-2 at different CO_2 concentrations [0.03, 5, 10, 20 and 50% (v/v)]. This study suggested that the increasing CO_2(g) concentration has an inhibitory effect on the microalgal growth. The highest value of biomass was obtained at 5 and 10% (v/v) CO_2(g) concentrations, which implies that 10% CO_2 concentration was suitable for the microalgal growth.

The shake flask and photobioreactor experiments using *Spirulina platensis* microalgal species was carried out by Zeng et al., (2012) to investigate the effect of various physicochemical parameters such as pH, flow rate and CO_2(g) concentration on growth of microalgal species. Shake flask studies revealed that the maximum biomass concentration was observed at pH value of 9. Utilization of CO_2(g) as HCO_3^- and uptake of nitrate by microalgae to produce ammonia (NH_3) may be the main reasons to increase in pH values. Low biomass productivity was observed at pH values of 10 and 11 were mainly due to the agglomeration of microalgal cells as a result of pH or electromotive burst.

The change in the cellular metabolite composition of *Chlorella vulgaris* (UTEX 259), *Chlorella sorokiniana* (UTEX 2805), *Chlorella minutissima* (UTEX 2341) and *Chlorella variabilis* (NC64A) due to CO_2(g) induction was studied by Cheng et al., (2014). The obtained results have shown that with increase in CO_2(g) concentration from ambient supply (330 ppm) to 2% (v/v), there was a increase in cellular starch composition of *C. vulgaris* and *C. variabilis*. This accumulation of cellular lipid was found to be more at 2% (v/v) CO_2(g) concentration as compared to the ambient supply (330 ppm) for *C. minutissima* and *C. vulgaris*. The

polysaccharide composition of cell wall for all four *Chlorella* strains revealed the presence of higher concentration of uronic acids and lower concentration of neutral sugars at 2% (v/v) CO_2(g) concentration.

The investigation of the CO_2 mitigation capability of *Chlorella pyrenoidosa* (FACHB 9) was carried out by cultivating it at different CO_2(g) concentrations [air, 1, 5, 10, 20 and 100% (v/v)] (Fan et al., 2015). The obtained result indicates that increase in CO_2(g) concentration has an inhibitory effect on the growth of *Chlorella pyrenoidosa* (FACHB 9). The maximum biomass concentration and maximum lipid productivity of *Chlorella pyrenoidosa* (FACHB 9) were observed as 4.3 g L^{-1} and 107 mg L^{-1} d^{-1} at 5% (v/v) CO_2(g) concentration, respectively.

Gonçalves et al., (2016) performed laboratory scale batch cultivation studies utilizing *C. vulgaris*, *Pseudokirchneriella subcapitata*, *Synechocystis salina* and *Microcystis aeruginosa* microagal species to check their CO_2(g) fixation ability, nutrient utilization capability and biomass productivity. The obtained results indicated that the increasing CO_2(g) concentration beyond 5% (v/v) has an inhibitory effect on the biomass production. This study also estimated that mathematically CO_2 concentration of 5.35 (±0.34)% (v/v) was optimum for microalgal growth.

Shene et al., (2016) discussed the biomass productivity of *Nannochloropsis oculata* with/without pH control strategy under varying CO_2 concentration. The highest specific growth was observed without controlling the pH of growth media. The microbial growth might be hindered due to high pH (6.5 - 8), which has limited the nitrate utilization rate under pH control strategy. However, during nitrate limiting phase, with pH control strategy (pH = 8.0), specific growth rate was found to be the highest. This study concluded that pH not only decides the bio-

usable CO_2 availability (HCO_3^-) but also governs the nitrogen source (NO_3^-) uptake [Shene et al., 2016].

2.1.2 Value added products from microalgae

Microalgae, which is a source of various chemicals having economic values is also a promising CO_2 bio-mitigation candidate. Downstream processing of the microalgal biomass produces pigments, vitamins, proteins, cosmetics, fine chemicals, etc. Biodiesel derived from Microalgae has found capability to replace fossil based transportation fuels (Chisti, 2007). The production of chemicals from the microalgae biomass depends on the distribution of elemental carbon (C) and nitrogen (N) among different cellular metabolites (Geider et al., 2002; Fernandes et al., 2016). In nutrient deficient environment, to achieve homeostasis, cell starts producing molecules, which required no or very less amount of undersupplied nutrients (Lynn et al., 2000; Hu et al., 2008). Hence, if there is an inadequate nitrogen supply, microalgae would try to accumulate polysaccharides and fatty acids. On the contrary, the reduction in nitrogen utilization was observed in limited carbon supply due to less availability of carbon chain for the synthesis of amino acids (Geider et al., 2002; Hu et al., 2008).

Ota et al. (2009) reported a sharp increase in cellular fatty acid content of *Chlorocuccum littorale* with decrease in CO_2(g) concentration after nitrate (NO_3^-) depletion. Maximum fatty acid accumulation was obtained as 34% (w/w) in the biomass of *C. littorale* at 5% (v/v) CO_2(g) concentration. The study also reported the higher tolerance of CO_2 for *C. littorale*.

The effect of different nitrogen sources such as ammonium carbonate [$(NH_4)_2CO_3$], urea (CH_4N_2O), sodium nitrate ($NaNO_3$) and mixture of urea and $NaNO_3$ on biomass generation and fatty acid accumulation of *S. rubescens* was studied by Lin and Lin (2011). Their study utilized

different cultivation systems such as photo-bioreactors and outdoor raceway ponds. The microalgal fatty acid content was found to be increase during nitrogen limiting phase.

Ota et al. (2011) found that the lipid accumulation in *C. littorale* at 5% (v/v) CO_2(g) was strongly dependent on gas phase oxygen (O_2) concentration. The results obtained in this study revealed that O_2(g) plays an important role in the accumulation of cellular lipids when nitrogen concentration was limiting.

Scenedesmus sp. AMDD was isolated from municipal waste water and its nutrient utilization capability was investigated in 2 L chemostat. The complete utilization of nitrogen and phosphorus sources from the waste water was observed along with approximate generation of 5.3 - 6.1 MJ m^{-3} d^{-1} of bio-energy. The study reported the near complete biosorption of iron (Fe), zinc (Zn) and cadmium (Cd) from the municipal wastewater using *Scenedesmus sp.* AMDD strain (McGinn et al., 2012).

Wu et al. (2013) isolated the microalgae *Monoraphidium sp.* SB2 from Taiwan ponds and studied the effect of changing temperature on there cellular lipid accumulation. The experiments were carried out by cultivating microalgae *Monoraphidium sp.* SB2 at different temperature values. The obtained results suggested that there was different cellular lipid composition at different values of temperature. The optimum temperature for the growth of microalgae was found to be in the range of 25 - 35 ^{o}C.

The nutrient requirement, light intensity and PBR strategy for the growth of *Chlorella PY-ZU1*, cultivated in flue gas obtained from coal-fired power plants was optimized by Cheng at al. (2013a). The obtained results revealed that there was 125% increase in *Chlorella PY-ZU1* biomass production in sequential bioreactor at optimum nutrient molar ratio of N:C (0.69), P:C (0.096) and Mg:C (0.03). The biomass growth of *Chlorella PY-ZU1* was found to increase with

increase in light intensity and maximum biomass growth of strain was observed as 0.95 g L^{-1} d^{-1} at light intensity of 6000 lux. CO_2 fixation efficiency of *Chlorella PY-ZU1* was observed as 85.6% using multi-stage sequential bioreactor.

Yvon-Durocher et al. (2015) illustrated the temperature dependency of the cellular biochemical composition of the microalgae. The increase in temperature resulted in increase in N:P and C:P ratio. This has indicated the rise in the formation of N- rich proteins in place of P-rich ribosomes.

The effect of temperature on the growth, lipid accumulation and nutrient removal ability of *Chlorella sp.* HQ was studied by Zhang et al. (2016). The obtained results revealed that the *Chlorella sp.* HQ was able to grow up to temperature value of 38 ^oC. The values of maximum biomass growth and lipid content of *Chlorella sp.* HQ were observed as 68.8 (±15.9) mg L^{-1} and 23.8 mg L^{-1} at temperature value of 18 ^oC, respectively. The optimum temperature range for the treatment of wastewater using *Chlorella sp.* HQ was found to be in the range of 18 - 25 ^oC.

Yang et al. (2016) found that the *Chlorella* strains isolated from three distinct natural habitats (arctic glacier, desert soil and native soil) have optimum growth at different temperature ranges. This study concluded that the cellular biochemical compositions (proteins, carbohydrates and lipids) of all *Chlorella* strains were affected by fluctuating temperature range.

2.1.3 Continuous studies

The capabilities of microalgae to utilize CO_2 as sole carbon source and its conversion into valuable chemicals have attracted researchers to investigate the development of suitable microalgal cultivation system. (Chisti, 2007; Mata et al., 2010).

The systems which are utilized for the cultivation of microalgae include: open system and closed system. The open system is the one in which the growth of microalgae was carried out in predetermined growth media (Ugwu et al., 2008).

The growth of microalgae in an open pond for the purpose of CO_2 mitigation was extensively investigated. Open pond systems are inexpensive, require low energy penalty and associated with less capital expenditure. The performance of open pond system depends on the factors such as availability of sunlight, light transmission across the depth, temperature, mixing and CO_2(g) diffusion rate. Many studies have been conducted in an open pond system for CO_2 mitigation in order to investigate the system performance.

Ketheesan and Nirmalakhandan (2012) adopted an air-lift system to supply CO_2(g) in raceway pond for the cultivation of microalgae. This study illustrated the advantages of the present design over traditional designs of raceway ponds and PBRs in terms of energy penalty and CO_2 utilization efficiency. *Nannochloropsis salina* and *Scenedesmus* sp. were utilized as test species from microalgae. The mathmatical model for predicting the biomass growth in airlift raceway pond was developed and validated with experimental results. The coefficient of correlation (r^2) value was found in the range of 0.96-0.98 with $p<0.001$.

Chiaramonti et al. (2013) reported the energy penalty associated with a raceway pond and suggested the ways by which the energy penalties of system can be reduced. This study demonstrated the development of new design for 5 m^2 raceway pond by incorporating the changes which include propeller in place of paddle wheel, reduction of the water depth and installation of baffle boards at the curve. The application of new design avoided the photo-inhibition and photo-limitation which resulted in the improved biomass productivity.

Li et al. (2014) studied the power requirements of four different paddle wheel arrangements in 2.2 m^2 raceway pond. The obtained results indicate that flat blades were the superior arrangement for paddle wheel in terms of energy utilization. The power consumption, fluid velocity and paddle wheel efficiency were found to increase with increase in culture depth. At similar conditions of water head and rotational speed, the value of power consumption was found in the order of blade arrangement as zigzag > flat > forward-curved > backward-curved.

Pawlowski et al. (2014) investigated the CO_2(g) utilization efficiency in raceway ponds at controlled pH. The Generalized Predictive Controller (GPC) with actuator deadband was utilized in their study for controlling the changing pH value of the growth media in the raceway pond. The obtained results revealed that the improved CO_2(g) utilization efficiency was achieved by controlling the pH through GPC controller.

Few studies have also reported the installation of devices such as sumps and mixing columns in raceway pond for increasing the gas/liquid contact time and the CO_2 absorption efficiency (de Godos et al., 2014, Mendoza et al., 2013 and Putt et al., 2011).

Zhang et al. (2015) developed a new design of raceway ponds using flow deflectors and wing baffles for reducing the dead zone and improving the flashing light effect. In this study, the decrease in pressure loss by 14.58%, increase in average fluid velocity by 26.89% and reduction in dead zone by 60.42% were observed for raceway pond installed with flow deflectors and wing baffles. In newly developed raceway pond, the *Chlorella* sp. was utilized as a test species and the biomass growth of strain was observed to increase by 30.11%.

The drawbacks related to open pond system such as low productivity, high risk of contamination, low CO_2(g) utilization, low cell density, large area requirement and loss of water

due to evaporation have led researchers to look for the development of low cost closed cultivation systems (Ugwu et al., 2008; Ho et al., 2011).

Closed systems provide better monitoring and controlling over different physicochemical parameters which have considerable effect on the growth of microalgae. The advantages of closed system include: higher rate of CO_2(g) fixation, lower risk of contamination, controlled hydrodynamics, better control over the operating temperature and reduction in water loss. The reproducibility of the desired cultivation conditions was easy to achieve in closed systems (Fernandes et al., 2015). Closed systems are generally referred as PBRs and various designs of PBRs have been reported in previous studies. PBRs can be categorized as (1) tubular, (2) flat plate and (3) column. The production of valuable products from microalgae has applications in pharmaceutical, cosmetics and food industry which are required to be grown in a contamination free environment. Hence, there is a scope to carry out the research for the development of PBRs. The criteria for good PBRs employed for CO_2 mitigation and biomass production are proficient mixing, high CO_2/O_2(g) mass transfer rate and even distribution of light. The comprehensive works reported by earlier studies for enhancing the efficiency of PBRs are discussed in the following paragraphs.

Kumar and Das (2012) have studied the CO_2 bio-mitigation potential of *Chlorella sorokiniana* in terms of biomass productivity using airlift and bubble column PBR. The growth of *C. sorokiniana* was found to be better in airlift PBR at inlet CO_2(g) load of 5% (v/v). The mixing time pattern in airlift PBR was observed constant as compared to random pattern for bubble column PBR.

Xue et al. (2013) developed novel PBR to address the issue of flashing light effect by placing optical fibers as internal source of light. The higher biomass productivity was reported for developed airlift PBR as compared to the PBR without optical fibre as internal light source.

The design and development of a novel vertical external loop air-lift PBR to overcome the problems of longer mixing time and higher power consumption was reported by Pirouzi et al. (2014). The suggested design used two spargers, one which was placed at the bottom of downcomer and the other one was at the bottom of riser for gas feeding. This design resulted in the shorter mixing time and has lowered the overall power consumption.

Raeesossadati et al., (2014) reviewed the growth response and CO_2(g) utilization efficiency of photoautotrophic microorganisms cultivated under different CO_2(g) concentration. The effect of different physicochemical parameters such as temperature, light intensity and PBR design on CO_2(g) removal efficiency of photoautotrophic microorganisms was discussed. It was reported that the membrane PBRs has the higher CO_2(g) fixation rate as compared to other PBRs. The study concluded that CO_2 removal efficiency of photoautotrophic microorganisms was strongly affected by the geometry of PBR, input CO_2(g) load, light intensity and temperature.

The utilization of thin polyethylene film as a manufacturing material for vertical flat-panel PBRs was discussed by Cue´ llar-Franca and Azapagic (2015). This modification resulted in the lower capital cost and energy requirements. They have presumed that the future of PBRs may be dependent on the use of thin polyethylene film as material for the construction of PBRs.

Yadav et al. (2015) have investigated the capability of *Chlorella* sp. for mitigating CO_2(g) from flue gas using bubble column PBRs. The obtained results indicated that *Chlorella* sp. was able to tolerate 5% (v/v) CO_2(g) concentration. The use of pure flue gas as CO_2(g) inlet

feed has shown inhibitory effect on the growth of microalgae. The obtained biomass from CO_2(g) mitigation study was utilized for identification and characterization of value added by-products in terms of lipids, proteins, polysaccharides and pigment contents. It was found that increase in CO_2(g) concentration has decreased the cellular lipid accumulation. However, carbohydrate and protein contents were found to increase with increase in CO_2(g) concentration.

Sun et al. (2016a) investigated the use of hollow polymethyl methacrylate (PMMA) tubes as secondary light source in flat plate PBR to cultivate *Chlorella vulgaris*. The proposed design of flat plate PBR has shown the even distribution of light for cell growth, which has resulted in the significant increase in biomass growth of *C. vulgaris* by 23.42%. Sun et al. (2016b) improved the flat plate PBR design with the use of planar waveguides doped with light scattering nano-particles. This resulted in homogeneous light distribution and higher biomass production.

The CO_2 bio-fixation efficiency of microalgae *Chlorella fusca* LEB 111 cultivated using flue gas was studied by Duarte et al. (2016). The specific growth rate of *Chlorella fusca* LEB 111 was observed as 0.18 (±0.01) d^{-1} at 10% (v/v) CO_2(g), 200 ppm SO_2 and 200 ppm NO and 40 ppm ash concentration. The biomass productivity was found to decrease with increase in NO (g), SO_2 (g) and ash concentration.

2.2 Bacterium CO_2 fixation

The employment of microalgal CO_2 bio-mitigation system in the real time industrial application is yet to be explored (Cheah et al., 2015). The major hurdles faced in the implementation of CO_2 bio-mitigation system using photoautotroph include: lower tolerance to NO_x & SO_x, growth inhibition at higher CO_2 concentration (> 8% CO_2(g) (v/v)), lower CO_2(g) utilization efficiency, photoinhibition, higher capital and operating costs, risk of contamination, and higher

downstream processing cost (Cheah et al., 2015; Moreira and Pires, 2016). The above issues may be addressed by utilizing bacteria in the absence of light for CO_2 fixation (Chemoautotrophy). Recently, the prokaryotic CO_2 fixation in the absence of light (chemosynthesis) has started gaining attention (Bharti et al., 2014). The chemosynthetic microorganisms due to their faster growth rate and ability to resist higher CO_2(g) concentration may prove to be a prominent alternative to microalgae (Bharti et al., 2014; VenkataMohan et al., 2016).

Three major steps involved in the CO_2(g) utilization mechanism of bacterium in the absence of light are: (1) the anabolism of CO_2(g) by utilizing the generated energy (carbon fixing pathways), (2) accumulation of CO_2(g) into the bacterium cellular micro-compartments (carboxysome) known as carbon concentrating mechanism (CCM) and (3) catabolism of inorganic compounds to generate energy. The studies reporting the uses of above three mechanisms for CO_2(g) fixation are discussed in following sub-sections.

2.2.1 Carbon concentrating mechanism (CCM)

CCM deals with the direct transport of CO_2(g) across the cell of the microorganisms (Alonso-Sa´ez et al., 2010). CO_2(g) was dissolved in aqueous phase and part of it existed as CO_2(aq) or free CO_2. The other part gets reacted with water to form carbonic acid (H_2CO_3). H_2CO_3 is a weak acid and its dissociation scheme is represented by pH dependent equilibrium and is given by Eq. 2.1 with apparent pKa [HCO_3^-/ CO_2] = 6.3 (Prabhu et al., 2011).

$$CO_2 + H_2O \leftrightarrow H_2CO_3 \leftrightarrow H^+ + HCO_3^- \leftrightarrow 2H^+ + CO_3^{2-} \quad (2.1)$$

This bicarbonate ion (HCO_3^-) was utilized by micro-organisms as carbon source (Alonso-Sa´ez et al., 2010). The concentration of HCO_3^- in aqueous phase depends on the solubility of CO_2(g) in the aqueous phase, which in turn relied on the factors such as temperature, pH and

pressure (Lower, 1999). The bacterial cell accumulates the HCO_3^- in the cellular cytosolic pool. HCO_3^- is a charged molecule and hence, was unable to diffuse out through the phospholipid layer of plasma membrane. This accumulation of HCO_3^- ion into the cell was facilitated by the carboxylating enzyme carbonic anhydrase (CA), present in polyhedral protein micro-compartments (Cannon et al., 2010). The micro-compartment carboxysome was found to be present in all cyanobacteria and non-photosynthetic bacteria (Smith and Ferry, 2000; Cannon et al., 2010). CA catalyzes the reversible conversion of cytosolic HCO_3^- into CO_2(g) within the carboxysome and hence has locally increased the concentration of CO_2(g) much above that was required for the efficient working of CO_2 fixing enzyme (Prabhu et al., 2011). However, the very rapid conversion of HCO_3^- into CO_2(g) and vice-versa (Eq. 2.2) is required as high CO_2(g) concentration within the cell may damage the cell and higher intracellular HCO_3^- concentration may disturb the intracellular pH stability (Supuran, 2016).

$$CO_2 + H_2O \xleftrightarrow{CA} HCO_3^- + H^+ \qquad (2.2)$$

Therefore, the carbon concentrating mechanism (CCM) or carbon assimilation into the cell was facilitated by the enzyme CA. Presently, six different classes of CA enzyme are reported and are classified as α, β, γ, δ, ζ and η (Supuran, 2016). The α, β, γ classes of CA were found to be present in all prokaryotes while δ, ζ were present in marine diatoms and η was found only in protozoa. Thus, CA was ubiquitous in nature and found in diverse groups of eukaryotes as well as prokaryotes (Supuran, 2016). Apart from catalyzing the conversion of CO_2(g) and HCO_3^-, the other functions of CA include pH homeostasis, diffusion of CO_2(g) within the cell and ion transport across the cell (Supuran, 2016).

Thus, in order to fulfill the cellular demand of carbon via CCM, prokaryotes are able to accumulate inorganic carbon [CO_2(g)] in the form of bicarbonate (HCO_3^-) into the cell and thus

fixing atmospheric CO_2(g) in the process. Prior to 1963, it was believed that the green plants and some bacterial and cyanobacterial species are capable of fixing CO_2(g) via autotrophy. However, few studies have demonstrated CO_2(g) utilization capability of heterotrophic micro-organisms via CCMs.

Sharma et al. (2008) screened the various groups of bacteria on the basis of their intracellular CA activity. The obtained results revealed that the different isolated strains related to the group *Enterobacter* have significant intracellular CA activity. This study suggested that the *E. taylorae* can be utilized for the development of an effective CO_2 mitigation bioreactor system.

Eminoglu et al. (2015) isolated *Enterobacter sp. B13* from a riverside near to Trabzon, Sürmene, Turkey and purified a new enzyme B13-CA. The purified enzyme was found to belong to β-class CA and significant catalytic activity of the enzyme was observed for hydration of CO_2(g) to HCO_3^- and H^+. The obtained results demonstrated the capability of strain for assimilating CO_2(g) as HCO_3^- ion within the cell.

The chemoautotrophic growth ability of bacterium belongs to group *Pseudomonas* was also known to the researchers for long time. Ilialetdinov and Abdrashitova (1981) isolated the *P. arsenitoxidans* from the water of a gold-arsenic deposit and the ability of strain to grow chemoautotrophically was studied. In this study, the strain was found to utilize arsenite as electron donor and O_2 as electron acceptor and assimilate 41.2 - 41.7% carbonate as carbon source. Thus, this study confirmed the autotrophic growth of *P. arsenitoxidans*.

Lotlikar et al. (2013) reported the presence of three functionally active *β*-classes CAs in *P. aeruginosa* PAO1, which helped in the survival of the bacterium under environments of fluctuating CO_2(g) concentration.

Aggarwal et al. (2015) investigated the adaptability of *P. aeruginosa* PAO1 in the changing environment of CO_2(g) [0.03 - 5% (v/v)]. The proteins PAO102, PA2053 and PA4676 were purified and were found to belong to the *β*-class CA. The catalytic activity of the enzymes was observed at pH value of 7.5 and 8.3 and was found to be significant. The adaptation of the strain to the CO_2(g) was studied by growing the strain in the ambient environment and in the environment of 5% (v/v) concentration. The obtained results revealed that in the environment of different CO_2(g) concentration, enzyme POA1 (β-class CA) was responsible for the growth of the *P. aeruginosa* PAO1.

The cultures from arctic sea water were obtained by Alonso-Sa´ez et al. (2010) and were investigated for the possibility of chemotrophic and heterotrophic assimilation of HCO_3^- in absence of light. The obtained results indicated that mostly heterotroph belongs to the genera *β* and *γ-proteobacteria* which are responsible for the cellular assimilation of HCO_3^-.

Prabhu et al. (2011) partially purified the enzyme CA from microorganisms (heterotrophs) such as *Bacillus pumilus*, *Pseudomonas fragi*, and *Micrococcus lylae*. The microorganisms were isolated from river Ganges and soil present around $CaCO_3$ kiln. The obtained results indicate that the significant CA enzyme activity was present in all three isolates. The CA enzyme activity was found to be highest for *B. pumilus* and lowest for *M. lylae*. The ability of CA enzyme to convert CO_2(g) into carbonate was investigated and better CO_2 sequestration capacity was found as compared to the CO_2 sequestration capacity of pure CA purchased (Sigma-Aldrich Co., St. Louis, USA). This study has further strengthened the CO_2(g) utilization capability of *Bacillus pumilus*, *Pseudomonas fragi*, and *Micrococcus lylae*.

Serratia sp. ISTD04 was isolated from the marble rock and its CO_2 bio-mitigation capability and biodiesel production was investigated. The obtained results indicate that the

Serratia sp. ISTD04 was able to assimilate HCO_3^- ion into cellular biomass using enzyme CA. Furhther, assimilated HCO_3^- was metabolized into different cellular component using enzyme ribulose-1,5-bisphosphate carboxylase/oxygenase (RuBisCO). The production of 0.487 and 0.647 mg of hydrocarbons (C_{13} - C_{24}) and lipids (C_{15} - C_{20}) per mg of biomass was also reported in the study. The obtained lipids were converted into the fatty acid methyl ester via transestrification. The obtained biodiesel has relevant components and their composition can be directly utilized as fuel (Bharti et al., 2014).

Sundaram and Thakur (2015) isolated the chemolithotrophic bacterium, *Bacillus* sp. ISTS2 from marble mining rocks and evaluated its potential to produce biosurfactant using different carbon sources such as 5% (v/v) CO_2(g), 100 mM $NaHCO_3$ and 2% (v/v) hexadecane. The obtained results revealed that the strain was able to assimilate and metabolize CO_2 using enzymes CA and ribulose-1,5-bisphosphate carboxylase/oxygenase (RuBisCO) and can be utilized for the development of CO_2 bio-mitigation system.

The CO_2 bio-mitigation potential of deep sea sulfur oxidizing bacterium *Sulfurovum lithotrophicum* 42BKT^T, at higher partial pressure of CO_2(g) was studied by Kwon et al. (2015). The strain was able to assimilate approximately 0.42 g CO_2 g^{-1} h^{-1} at 2 atm CO_2 partial pressure. The assimilated cellular CO_2(g) was majorly fixed (~37 %) into the biomass as glutamate and pyroglutamate. The study concluded that an efficient and sustainable CO_2 bio-mitigation system can be developed using *Sulfurovum lithotrophicum* 42BKT^T.

The above studies revealed the fact that prokaryotes were able to assimilate CO_2(g) via CCM and CA is the key enzyme responsible for CCM. The presence of CCM was not only limited to autotrophs but also found to be present in heterotrophs. However, the heterotrophic metabolism of assimilated CO_2 is under investigation and yet to be fully understood.

2.2.2 Energy requirements in the absence of light (chemotrophic way of life)

Chemoautotrophy is the metabolic process in which microorganism reduces CO_2(g) into the cellular biomass by utilizing the energy gained from reduced inorganic compounds such as Fe[II], $S_2O_3^{2-}$, H_2, H_2S, CH_4, etc. (Amend and Shock, 2001). The redox scheme of chemoautotrophic CO_2(g) assimilation was accompanied by the loss of electrons from reduced molecules such as Ferrous ion (Fe [II]), thiosulfate ($S_2O_3^{2-}$), ammonium ion (NH_4^+), etc. with simultaneous electron gain by molecules like oxygen (O_2), nitrate (NO_3^-), hydrogen sulfide (H_2S), etc. The energy evolved during the process is utilized for the CO_2 fixation (Amend et al., 2003).

The bio-mass yield of chemoautotrophic microorganism is governed by the supply of adequate amount of reduced inorganic compound in bio-usable form (Mccollom and Amend, 2005). The cellular growth and multiplication of chemoautotrophic microorganism are dependent on the effective utilization of the available energy to reduce CO_2(g) into the cellular biomass. The microorganisms will follow thermodynamically efficient metabolic pathway for CO_2(g) fixation to minimize the energy loss. Therefore, the presence of electron donors and electrons acceptors in bio-usable state and in adequate amount is necessary to meet the energetic requirement of CO_2 metabolization (Mccollom and Amend, 2005).

The bio-usable form of inorganic chemical species is goverened by different physicochemical parameters such as aerobic/anaerobic environment, pH, temperature and pressure. Fe[II] and Fe[III] are the inorganic species, which are utilized by different bacterial species for their autotrophic growth (Mignone and Donati, 2004). However, the stability of Fe[II] and Fe[III] depends on the pH and the redox potential of that environment. In presence of O_2 and at pH value > 6, Fe[II] readily oxidizes to give Fe[III]. In presence of water, Fe[III] hydrolyzes to

form precipitate. Therefore, there is a limited availability of bio-usable form of iron in oxic environment having value of pH ~ 7 (Tekerlekopoulou et al., 2006).

The rate of reaction was found to increase with increase in temperature. Abiotic reaction rates are so fast at elevated temperature that there is no benefit to an organism, if it catalyzes the reaction. Hence, chemical reaction should be thermodynamically favored but kinetically inhibited to serve as an energy source (Amend et al., 2003). The fate of CO_2(g) as carbon source to the micro-organisms is decided by prevailing pH, temperature and pressure. The bio-usable form of CO_2(g) is HCO_3^- and is found to be stable in the pH range of 6 - 10. The solubility of CO_2(g) in aqueous phase decreases with increase in temperature. The solubility of CO_2(g) increases with increase in CO_2(g) partial pressure at any constant temperature (Carrol et al., 1991; Amend et al., 2003). Thus, the chemoautotrophy requires the presence of adequate amount of inorganic compound as an energy source in bio-usable form in the absence of light. The availability of energy source determines the extent of CO_2(g) fixation and biomass yield. It was found that the various physicochemical parameters govern the availability of energy source and the amount of CO_2(g) in soluble form, which are necessary for the survival of microorganisms.

2.2.3 Carbon fixation general view and pathways

The basic features of the fixation of CO_2(g) into the cellular biomass include: (1) requirement of 4 reducing equivalent [the oxidation state of carbon was changed from +4 [CO_2(g)] to 0 (carbohydrate)], (2) energy requirement provided by the hydrolysis of ATP, (3) presence of carboxylating enzyme such as CA, which associates CO_2(g) or HCO_3^- directly to the organic acceptor molecule and (4) presence of low potential electron donor or reductant such as reduced ferredoxin (E_o = - 400 mV) in anaerobes and NAD(P)H (E_o = - 320 mV) in aerobes (Buckel and

Thauer, 2013). The products obtained from the metabolism of CO_2(g) are the primary metabolites through which other cellular components like nucleic acid, carbohydrate, proteins and lipids are derived. However, the distribution of cellular organic pool (nucleic acid, carbohydrate, proteins and lipids) was dependent on the environmental conditions (T, pH, Salt concentration), nutrient supplies (NPK availability, energy source availability) & habitat (natural or extreme) and also varies from organism to organism as per there metabolic requirement. At present, following six autotrophic CO_2(g) fixation pathways are known (Berg, 2011):

- Reductive pentose phosphate pathway or Calvin-Benson-Bassham pathway (CBB pathway)
- Reductive citric acid cycle or Arnon-Buchanan cycle (rTCA cycle)
- Reductive acetyl-coenzyme A (CoA) pathway (Wood-Ljungdahl pathway)
- 3-Hydroxypropionate cycle (Fuchs-Holo (bi-)cycle)
- 3-Hydroxypropionate/4-hydroxybutyrate (Hydroxypropionate/Hydroxybutyrate) (HP/HB) cycle
- Dicarboxylate/4-hydroxybutyrate (dicarboxylate/hydroxybutyrate) (DC/HB) cycle

2.3 Gaps

Most of the studies carried out in the field of CO_2 bio-mitigation were limited to the use of photoautotrophs. The major focuses of the reported studies were to make CO_2 bio-mitigation system more realistic, sustainable and economic. The major drawbacks associated with photoautotrophs as mentioned in section 2.2 limit their use for the development of efficient CO_2 bio-mitigation system.

Industrial scale CO_2 bio-mitigation system using photoautotrophs are facing the limitations such as low utilization of light, circulation of biomass, accumulation of O_2(g) within

the system, lower mass transfer rates and difficulty in controlling the growth parameters. Direct utilization of flue gas as CO_2(g) source has shown the adverse effect on the growth for microalgae, which has also changed the characteristics of chemicals extracted from biomass.

The limitations associated with photoautotrophs led the researchers to check the possibility of chemoautotroph for CO_2 bio-mitigation. The importance of chemoautotrophs cannot be ignored in carbon cycle as it is demonstrated that their role of CO_2(g) utilization is more than the terrestrial plants (Cardoso et al., 2014). Faster life cycle, rapid growth rates, ability to sustain in highly-dense culture and ability to utilize CO_2(g) in the absence of light are the advantages associated with bacteria that make them attractive choice over photoautotrophs (Bharti et al., 2014; Kwon et al., 2015).

Few recent studies reported the use of chemoautotrophs for their ability to capture CO_2 in the absence of light and its simultaneous conversion into valuable products (Alonso-Sáez, L. et al., 2010, Saini R., 2011, Bharti, 2014; Garcĭa et al., 2015; Kwon et al., 2015; Sundaram et al., 2015). These reported studies were focused on the characterization of bacterium strains which have shown an ability to sequester CO_2(g) and use sodium bicarbonate ($NaHCO_3$) as an inorganic carbon source. Even though the bacterium CO_2(g) utilization capability was known for long time, the employment of bacterium for the development of CO_2 bio-mitigation system and value addition is the most untouched area.

One limitation with the above studies is the use of pure strain, which might not be able to sustain the industrial environment. It has been observed in several studies, that in most of the industrial based applications (engineering based applications) mixed cultures are preferred over pure strains during long term operations (Raghuvanshi and Babu, 2009; Jabeen et al., 2016; Majumder et al., 2016). The reason is the adaptability of mixed culture in any environment

unlike pure strain where certain specified conditions are to be maintained throughout (Subashchandrabose et al., 2011).

The reported studies have not considered the quantification of CO_2(g) fixation in terms of cellular biomass and CO_2(g) fixation efficiency. These studies are necessary for the design and development of sustainable large scale CO_2 bio-mitigation systems. The presence of adequate amount of energy substrate is necessary to get a desired amount of CO_2(g) fixation. The studies have ignored to investigate the effect of energy source on CO_2 bio-mitigation ability of microorganism.

Thermodynamic analysis of the possible CO_2(g) metabolic reactions helps in understanding the suitable mechanism for CO_2(g) utilization using bacterial strains and assists in designing the growth medium to meet the energy requirements for batch and continuous experiments. The reported studies have not carried out the thermodynamic analysis of the overall CO_2(g) metabolic processes, which is an important aspect to check the feasibility of CO_2(g) fixation.

Few studies have reported the production of valuable chemicals from chemoautotrophic microorganisms utilizing CO_2(g) as substrate (Bharti, 2014; Kwon et al., 2015; Sundaram et al., 2015). However, there is very limited literature available, which has reported the utilization of CO_2(g) as substrate for the production of valuable chemicals.

Therefore, the capability of chemoautotroph for utilizing CO_2(g) in dark and the production of valuable chemicals within the framework of CCU was an exciting area to think and requires serious attention. If the CO_2 utilization capability of chemoautotrophic bacteria was exploited well, then it was possible to develop a cost effective and sustainable CO_2 bio-mitigation system.

2.4 Scope of present study

CO_2 bio-mitigation potential of bacteria in the absence of light is the most ignored area of research. Thus, there is a need to investigate the CO_2 mitigation potential of bacteria in the absence of light. The industrial application requires the robustness of bacterium towards harsh environment, which may be fulfilled by the bacteria obtained from the extreme habitat. Therefore, there is need to investigate the different habitats such as man-made and extreme to obtain the strains capable of utilizing CO_2(g). Hence, selecting site for obtaining the microbial culture was necessary to obtained microorganisms capable of utilizing CO_2(g). The batch studies were required for the enrichment of culture to obtain microorganisms, which are capable of utilizing CO_2(g). The screening of strains comprising the enriched culture was necessary for comparative CO_2(g) bio-mitigation studies and further, the discovery of new strains gives a perspective for the production of new bio-molecules. Hence, the identification of the screened bacterial strains is to be carried out by following 16S rRNA analysis. The experiments were required to understand the effect of energy substrate concentration on the CO_2 bio-mitigation ability of mixed microbial population and isolated strains. This study is further necessary for the comparative evaluation of CO_2(g) utilization potential of mixed microbial population and isolated strains.

The biomass and the leachate obtained from CO_2 bio-mitigation studies are needed to be analyzed for value addition. Thus, there is a necessity to carry out identification and characterization of valuable metabolic products present in the biomass and leachate obtained from CO_2 bio-mitigation studies using FT-IR and GC-MS. The thermodynamic assessment of the overall CO_2 bio-mitigation process gives theoretical aspects on which the performance of the real process can be evaluated. Hence, there is scope to assess the overall CO_2 bio-mitigation

process thermodynamically by calculating the values of overall Gibb's free energy ($\Delta G_{reaction}$) of possible overall CO_2 bio-fixation reaction.

There is very limited or almost no literature available, which considered the development of continuous system for the bio-mitigation of CO_2 using bacteria in the absence of light. Packed bed columns have already established there importance for the long term industrial applications. However, till date no study has reported the development of packed bed column for CO_2 mitigation using microorganisms. Thus, there is scope for the development of packed bed column using the microbial culture trained for the mitigation of CO_2(g) obtained from batch studies. The bio-filtration experiments need to be carried out for evaluating the column performance.

60% of the production cost of products obtained from bio-based processes depends on downstream processing strategy. Further, the production of valuable chemicals using bacterial strain utilizing CO_2(g) as substrate will solve simultaneously two problems: (1) depleting petroleum feed stock and (2) control of GHGs emissions. Therefore, there is scope in the development of economic downstream bio-processing strategy for the production of valuable compound.

Chapter 3

Materials and Methods

Sample collection sites, bacterial species isolation and identification, growth medium formulation, cultivation systems, analytical and measurement techniques, calculation equations, statistical analysis and experimental steps are described in this chapter.

The present chapter provides the details of experimental methodology adopted for the enrichment, isolation and identification of CO_2 utilizing bacteria from different habitats. It also describes the details of batch, semi-continuous and continuous studies. The different analytical techniques used for the analysis of results are also discussed.

3.1 Glasswares and chemicals utilized

Glasswares (conical flask, beaker, petriplate, test tube, measuring cylinder etc.) used in the present work are reported in Table 3.1. The chemicals used in the present work were of analytical grade and are listed in Table 3.2.

3.2 Microbial culture

3.2.1 Site selection

In the present work two different habitats which resembled to neutral environment (sewage treatment plant) and extreme environment (Sambhar salt lake) were considered. The details of the sampling sites are described in the following sub-sections.

3.2.1.1 Sewage treatment plant (STP)

Activated sludge samples were obtained from the secondary clarifier unit of the sewage treatment plant (STP) located at Birla Institute of Technology and Science (BITS), Pilani (28° 22' 0" N, 75° 36' 0" E), Rajasthan, India. STP comprises the application of physical, chemical and biological processes for the removal of various contaminants such as organic compounds, heavy metal ions, etc. from the waste water and hence represents extreme environment. Therefore, it is a natural habitat for microorganisms ranging from microalgae to bacteria which

are capable to survive under harsh environmental condition. These microorganisms may utilizes the contaminants such as organic compounds, heavy metal ions (Fe[II], Cr[III], Pb[II], etc.) and different inorganic salts present in waste water for their survival. Therefore, the chance of obtaining a microorganism which was capable of utilizing CO_2 is very high. Further, the successful investigation of STP for the presence of CO_2 utilizing strains may demonstrate its capability to be converted into a possible carbon sink. Hence, it was chosen as a sampling site.

The sample (sludge) was collected at the start of the dry season and kept in sterile polypropylene sampling bottle and was immediately transported in ice cooled environment to the laboratory for further enrichment.

3.2.1.2 Extreme environment of Sambhar salt lake (SSL)

The present industrial need is the improvement of the bio-based-method, that can withstand the extreme industrial environment and extremophilic bacterium isolated from soda salt lake can satisfied the need. The extremophiles does not just skilled to adjust the great ecological condition but also require compelling condition for their survival. The Soda salt lakes are depicted as great common natural surroundings for extremophiles on account of their high saltiness and high alkalinity. Sambhal Salt Lake (SSL) is one such haloalkaophilic habitat and was chosen as a sample collecting site. The extreme environment of high alkalinity, salt concentration and presence of high bicarbonate concentration signifies the possibility of obtaining CO2 utilizing extremophilic strain that can withstand in industrial scenario.

In April 2013, sediment and water samples were collected from the hypersaline environment located at Sambhar salt lake, Rajasthan, India (26.9667° N, 75.0833° E). Total salt concentration of the lake was found in the range of 7% (w/v) to 30% (w/v). Major contributors to

salt concentration are sulfates, carbonates, bicarbonates, chlorides, sodium salts and lesser amounts of potassium salts. pH of Sambhar lake is in the range of 9.5-10. Presence of total suspended solids is in the range of 0.7-2.8% (w/v) (Gupta et al., 2014). The obtained samples were kept in the dark at ambient temperature and were transported to the laboratory in autoclaved sample vials. Later, these samples were stored at 4 ^{o}C.

3.2.2 Media preparation

In the present work, de-ionized water (Milli-Q Millipore 15.2 MΩ cm^{-1}) was used to conduct experiments and analysis. All solutions were sterilized in a vertical autoclave (MSW-101, Macro Scientific Works, India) at 15 kPa and 120 ^{o}C for 30 min prior to their use. The operating conditions for sterilization were maintained throughout the experimental studies unless otherwise specified. Based upon the characteristics of microbial samples, four different types of minimal salt media were used in the present study. The details of MSM compositions are given in Table 3.3.

1000 ppm stock solution of Fe[II] was prepared using filter sterilization technique by dissolving 4.96 g of $FeSO_4.7H_2O$ in distilled water and volume of the solution was made up to 1 L. The pH of stock Fe[II] solution was maintained as 3.5 using 0.1 M HCl solution. The medium for plating was prepared by adding 2% agar to the nutrient broth for culture obtained from STP. However, MSM supplemented with 2% agar was used as plate medium for culture obtained from SSL. $NaHCO_3$ stock solution (500 mL) of 1 M concentration was prepared by dissolving appropriate amount of $NaHCO_3$ in deionized water and was sterilized using filter sterilization technique.

Table 3.1: Details of glasswares used in present study

S. No.	Glasswares	Make
1.	Beakers (100 mL, 500 mL, 1L)	Borosil®
2.	Burette	Borosil®
3.	Conical flask (50 mL, 100 mL, 250 mL, 500mL, 1 L and 2L)	Borosil®
4.	Funnel	Borosil®
5.	Measuring cylinder (10 mL, 50 mL, 100 mL, 250 mL)	Borosil®
6.	Pipette (10 mL, 25 mL, 50 mL)	Borosil®
7.	Petriplates	Borosil®
8.	Separating funnel (100 mL, 250 mL)	Borosil®
9.	Test-tubes (10 mL, 100 mL)	Borosil®

Table 3.2: Details of chemicals used in present work

S. No	Chemicals	Make	Use
1.	Agar A	Hi-media®	**Solidifying agent**
2.	Ammonium sulphate ($(NH_4)_2SO_4$)	Merck®	**Minimal salt media (MSM) preparation**
3.	Ammonium chloride (NH_4Cl)	Merck®	
4.	Calcium sulphate ($CaSO_4$)	Merck®	
5.	Di-potassium hydrogen orthophosphate (K_2HPO_4)	Merck®	
6.	Ferrous sulphate heptahydrate ($FeSO_4.7H_2O$)	Merck®	
7.	Magnesium sulphate heptahydrate ($MgSO_4.7H_2O$)	Merck®	
8.	Magnesium chloride hexahydrate ($MgCl_2.6H_2O$)	Merck®	
9.	Potassium dihydrogen phosphate (KH_2PO_4)	Merck®	
10.	Potassium nitrate (KNO_3)	Merck®	
11.	Potassium chloride (KCl)	Merck®	
12.	Sodium chloride (NaCl)	Merck®	
13.	DL-Dithiothreitol (DL-DTT) (Antioxidants and Reducing Agents for Protein Stabilization)	Hi-media®	**Component of cell- lysis buffer**
14.	Lysozyme (Bacterial cell wall lytic enzyme)	Hi-media®	
15.	Phenylmethanesulfonyl fluoride ($C_7H_7FO_2S$) (Protease inhibitor)	Hi-media®	
16.	Tris, Free base (Permeabilizes outer membranes)	Hi-media®	
17.	Tris-Cl (1 M, pH 7.6) (Permeabilizes	Hi-media®	

	outer membranes)		
18.	Triton X-100 (For prevention of aggregation of hydrophobic and membrane proteins)	Hi-media®	
19.	Nutrient Broth	Hi-media®	**Growth media**
20.	Chloroform ($CHCl_3$)	Merck®	**Extractant and solvent**
21.	Methanol (CH_3OH)	Merck®	
22.	Acetone (C_3H_6O)	Merck®	**Cleaning**
23.	Ethanol (C_2H_5OH)	Merck®	
24.	Potassium hydroxide (KOH)	Merck®	**Transestrification reaction**
25.	Sulfuric acid (H_2SO_4)	Merck®	
26.	Sodium thiosulfate ($Na_2S_2O_3$)	Hi-media®	**Energy substrate**
27.	Sodium carbonate (Na_2CO_3)	Merck®	**Buffer**
28.	Sodium bi-carbonate ($NaHCO_3$) (C-source)	Merck®	
29.	Hexane (C_6H_{14})	Merck®	**Solvent**
30.	Dodecanol	Alfa Aesar®	**Standard**
31.	Tetradecanol	Alfa Aesar®	
32.	Pentadecanol	Alfa Aesar®	
33.	Octadecanol	Alfa Aesar®	
34.	FAME mix (C_8-C_{24})	Supelco®	

Table 3.3: Composition of MSM for different microbial culture

S.No.	**Component**	**Iron (Fe[II]) utilizing bacteria from STP and SSL**		**Sulfur oxidizing bacterium from SSL**	
		STP ($g\ L^{-1}$)	**SSL ($g\ L^{-1}$)**	**Isolation medium ($g\ L^{-1}$)**	**MSM ($g\ L^{-1}$)**
1.	K_2HPO_4	0.8	0.5	1	1
2.	KH_2PO_4	0.2	0.2	-	-
3.	$CaSO_4.2H_2O$	0.05	-	-	-
4.	$MgSO_4.7H_2O$	0.5	-	-	-
5.	$(NH_4)_2SO_4$	1	-	-	-
6.	NaCl	-	29.22	16	35
7.	KCl	-	0.2	-	-
8.	KNO_3	-	0.1	1	1
9.	NH_4Cl	-	0.2	3 mM	3 mM
10.	$MgCl_2.6H_2O$	-	0.2	1 mM	-
11.	Na_2CO_3	-	-	95	-
12.	$NaHCO_3$	-	-	15	-

3.2.3 Enrichment, isolation and identification

3.2.3.1 Culture obtained from STP

Selective enrichment culture technique described in literature with modifications was used to obtain the mixed microbial population, which was capable of utilizing CO_2 as carbon source (Raghuvanshi et al., 2009). In a 500 mL beaker, 50 mL of sludge sample was taken and thoroughly mixed with 100 mL of de-ionized water. The resulting mixture was left to settle for 4 h at 37 ^{o}C. After 4 h, 25 mL of supernatant was collected using pipette and mixed with 50 mL of deionized water in separate 100 mL beaker. This mixture was allowed to settle for 2 min at 37 ^{o}C. Later, 10 mL of sample was withdrawn carefully using pipette, and mixed with 100 mL MSM in 500 mL Erlenmeyer flask. 10 mM concentration of $NaHCO_3$ as carbon source and 100 ppm of Fe[II] concentration as energy source were maintained in the flask by adding appropriate amount of $NaHCO_3$ and Fe[II] stock solutions, respectively. Final pH of the solution was obtained as 6.7. Further, the flask was kept in the orbital shaking incubator (MSW-132, Macroscientific Work Pvt. Ltd., India) for the duration of 48 h at 37 ^{o}C and at 120 rpm. After 48 h, 5 mL of grown culture was taken and mixed with 100 mL fresh MSM in a 500 mL flask. $NaHCO_3$ concentration was increased and was kept as 50 mM. The Fe[II] concentration was kept constant as 100 ppm. Further, the flask was kept in an orbital shaking incubator under similar condition for the duration of next 48 h. The same procedure was repeated twice by gradually increasing the $NaHCO_3$ concentration to 100 mM and 150 mM. The culture obtained after eight day was preserved at 4 ^{o}C and was further utilized for the enrichment studies.

Fully grown culture obtained from $NaHCO_3$ as carbon source was further enriched by using CO_2(g) as carbon source. The obtained culture (2 mL) was mixed with 100 mL of MSM in 500 mL volume Erlenmeyer flask for the further enrichment. The appropriate amount of stock

Fe[II] solution was added to maintain 50 ppm of Fe[II] concentration in the 500 mL flask. The flask was sealed from the top using the two port assembly as shown in Fig. 3.1. CO_2-air mixture [2% (v/v)] was then allowed to pass through a capsule air filter at the flow rate of 1 L min^{-1} (Fig. 3.1). The concentration of CO_2 was monitored at the outlet port at regular intervals of time using CO_2(g) analyzer (906, Quantek instruments, USA) in terms of volume percent (% v/v). The ports were closed and the flask was airtight, when the concentration of CO_2 reached 2% (v/v) at the outlet. It ensured the required concentration of CO_2 in the gaseous phase. The flask was kept in an orbital shaking incubator and the culture was grown at 37 ^oC and 120 rpm for 3 days. After 3 days, the 2 mL of grown culture were taken and the same procedure was repeated for another 3 days by increasing the CO_2 concentration from 2 to 5% (v/v). The fully grown 6th day culture at 5% (v/v) CO_2 concentration was used for the species isolation and identification. Five different microbial species (SM1, 2, 3, 4, 5) were present in the culture obtained and were isolated using the streak plate method (Dailey et al., 2014).

Batch experiments were conducted using each isolated species individually by maintaining 5% (v/v) inlet CO_2 concentration to check their CO_2 fixation capability for total period of 4 days. Gaseous and liquid phase samples for all experiments were analyzed on the per-day basis. Out of the five isolated species, the isolates were selected on the basis of their CO_2 fixing ability. A-biotic control flask was kept in each experiment under similar conditions.

3.2.3.2 Culture obtained from SSL

The experimental methodology of enrichment, isolation, identification and abiotic tolerance assay for CO_2 fixing strains obtained from sample of Sambhar salt lake, Rajasthan, India, is discussed below (Raghuvanshi et al., 2009; Dailey et al., 2014).

10 g sediment and 20 mL of water sample obtained from Sambhar lake, Rajasthan, India were mixed thoroughly with 50 mL of autoclaved distilled water and allowed to settle for 4 h. 25 mL of supernatant of this mixture was centrifuged (CPR-24 plus, REMI laboratory instruments, India) at 15,000 rpm for 10 min at 4 ^{o}C. After centrifugation, supernatant was removed and the obtained pellet was used for the enrichment of microbial culture using CO_2(g) as carbon source as per the method described in paragraph 2 of section 3.2.3.1. However, the enrichment was carried in the presence of 100 ppm of Fe[II] concentration and 50 mM $S_2O_3^{2-}$ concentration in two separate flasks. The study was carried out at 37 ^{o}C and 120 rpm in an orbital shaking incubator. The isolates obtained from enrichment process were named as SSL4 for iron utilizing bacterium and SSL5 for $S_2O_3^{2-}$ utilizing bacterium. The glycerol stocks of the pure isolates were prepared and preserved at -20 ^{o}C for the further experimental studies.

3.3 Identification of isolated strains

The slants of the pure strains (SM1, SM3, SM4, SSL4 and SSL5) were prepared and were sent to Xceleris Genomic Labs, Ahmedabad, India for 16S rRNA gene sequencing. The obtained gene sequence was further analyzed by the BLAST-N tool available at the National Center for Biotechnology Information (NCBI) (www.ncbi.nlm.nih.gov). The taxonomic affiliations of the selected isolates were assigned based on the closest match obtained on pair-wise alignment in BLAST results. Pair wise alignment giving closest match was chosen and phylogenetic tree was drawn and aligned using the MEGA 4.0 software for individual strains and were aligned using CLUSTAL-X software (Tamura et al., 2007).

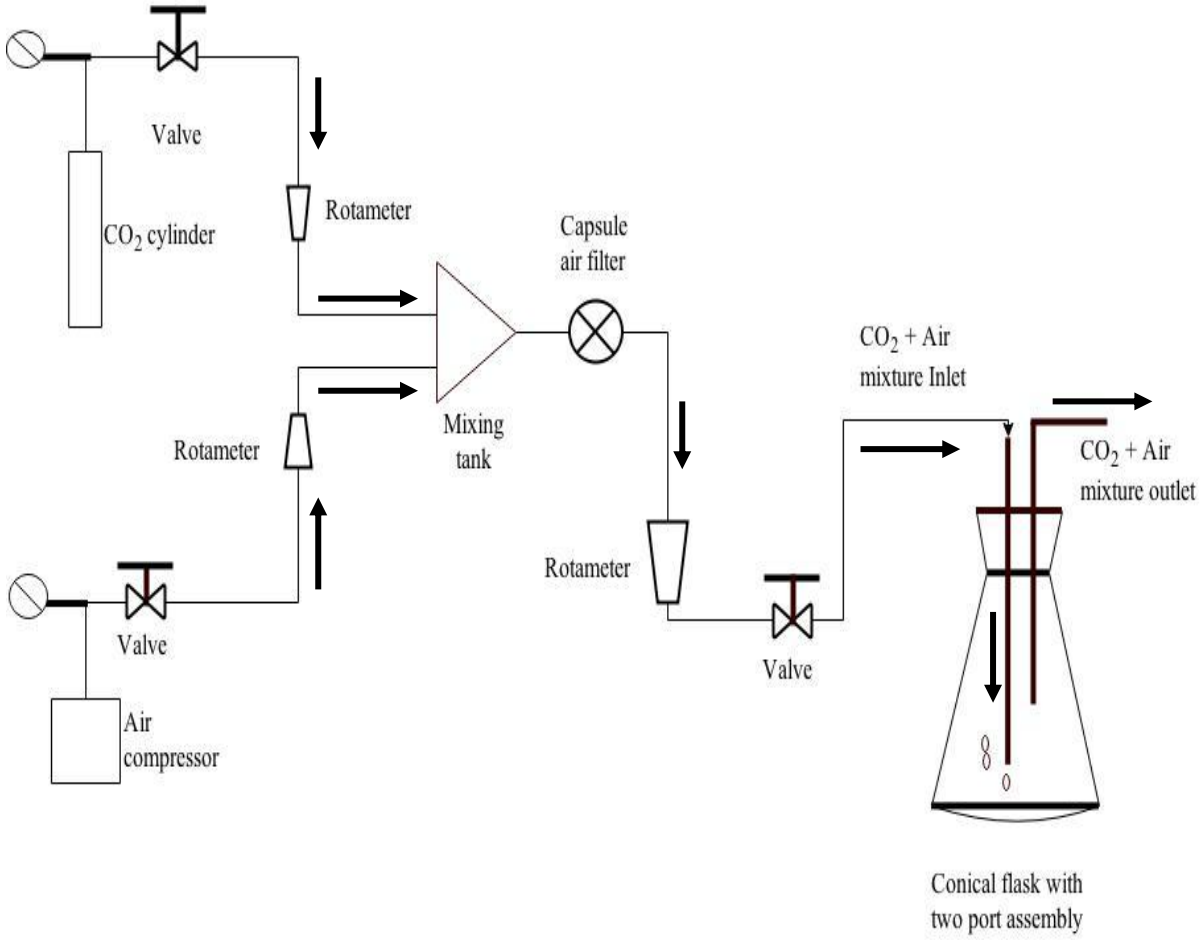

Fig. 3.1 Schematic diagram of experimental setup for batch studies.

3.4 Batch studies

3.4.1 CO_2 utilization ability at varying energy substrate concentration

CO_2(g) bio-mitigation batch studies are one of the most significant studies carried out in present work. The study gives a thorough understanding of CO_2 utilization ability of mixed microbial population and isolated strains (SM1, SM3, SM4, SSL4 and SSL5). Experimental conditions used in different batch studies are summarized in Table 3.4. Each batch study was conducted in 250 mL flasks and number of flasks was selected on the basis of the period of batch study. Flasks were divided into groups (G1, G2, G3 and G4) and an equal number of flasks were present in each group as per details given in Table 3.4. Group G1, G2, G3 and G4 were having the energy substrate concentration of 0 (biotic control), 50, 100 and 200 in their respective units.

Every flask was added with 40 mL of MSM along with 2 mL of fully fresh grown culture which has shown the optical density of 0.80. The required energy substrate concentration was maintained in each flask as per the detail given in Table 3.4. pH value of the solution in each flask was maintained as 7 and 10 for iron utilizing and $S_2O_3^{2-}$ utilizing bacteria, respectively. The flasks were sealed at the top and required CO_2(g) concentration (% v/v) was maintained in the head space of each flask as per method described in Section 3.2.3.1 (paragraph 2). The percentage of initial CO_2(g) concentration was chosen on the basis of percentage of CO_2(g) present in different flue gases (Muradov, 2014). The flasks were kept in orbital shaking incubator programmed at 37 ^oC and at 120 rpm. After every 24 hours, one flask was taken from each group for the analysis of gaseous and liquid samples. The control flask was kept without inoculum to ensure that there was no loss of CO_2 during the study and also the bacterium was responsible for the decrease in CO_2(g) concentration from the head space.

3.4.2 Analytical methods

The analytical techniques used for measuring the CO_2(g) concentration, biomass growth, dissolved CO_2 concentration and product analysis are described in following sections.

3.4.2.1 CO_2 (g) measurement

The concentration of CO_2(g) was measured using CO_2 gas analyzer in terms of % v/v. CO_2(g) removal efficiency (η_{CO2}) is estimated using Eq. (3.1) (Chen et al., 2016).

$$\eta_{CO_2} = \frac{y_{CO2,in} - y_{CO2,final}}{y_{CO2,in}} \times 100\,\% \tag{3.1}$$

Where, $y_{CO2,\,in}$ and $y_{CO2,\,final}$ are the initial (t = 0) and final ($t = t_x$) head space CO_2 concentration (% v/v), respectively.

3.4.2.2 Biomass concentration measurement

Biomass growth was determined in terms of dry weight and optical density (absorbance). Measurement of dry weight in terms of g L^{-1} was carried out on the per day basis by filtration method as reported in the literature (Majumdar et al., 2016). Optical density (OD) was also measured using UV-Vis spectrophotometer (Evolution 201, Thermo scientific, USA) on a per-day basis at a wavelength of 600 nm for the culture obtained from the CO_2 bio-mitigation studies. The relation between OD (y) and dry weight [x (g L^{-1})] was obtained for all isolates and mixed microbial population using calibration plots and the mathematical co-relations are given in Table 3.5.

Biomass productivity (P_{Max}, g L^{-1} d^{-1}) on perday basis is calculated using Eq. (3.2):

$$P_{Max} = \frac{(X_t - X_o)}{t_1 - t_o} \tag{3.2}$$

Where, X_o and X_t are the biomass concentration (g L^{-1}) at the initial (t_o) and at the end of the cultivation period (t_1), respectively.

Specific growth rate (μ, d^{-1}) was calculated using Eq. (3.3) (Chandra et al., 2016).

$$\mu = \frac{\ln X_{t1} - \ln X_o}{t_1 - t_o} \tag{3.3}$$

The maximum biomass concentration obtained for each microbial culture is represented as X_{Max}. Empirical formula for biomass was taken as $C_6H_{12}O_7N$ as described in the literature and fraction of carbon content (C_C) in the biomass was estimated as 0.34. These values are further utilized to calculate CO_2 fixation rate (R_{CO2}) as given by Eq. (3.4) (Ritmann and McCarty, 2012):

$$R_{CO_2} = C_C \times P_{Max} \times \frac{M_{CO_2}}{M_C} \tag{3.4}$$

Where, M_{CO2} is the molecular weight of CO_2 and M_C is the atomic weight of carbon. Actual CO_2(g) utilization efficiency ($R.R_{CO2}$) at varying energy source concentration (Fe[II] and $S_2O_3^{2-}$) is given by Eq. (3.5):

$$R.R_{CO_2} = \frac{\text{Moles } CO_2\text{(g) fixed as C in biomass}}{\text{Moles of } CO_2\text{(g) supplied initially}} \times 100 \tag{3.5}$$

Table 3.4: Strains, associated energy substrate concentration, duration of batch study and conditions employed.

Culture	CO_2(g) concentration (% v/v)	Period of batch study (days)	Number of flask (Groups)	Energy substrate
SM1	13 (±1)	5	20 (4)	Fe [II] (ppm)
Mixed microbial population	15 (±1)	6	18 (3)	
SM3	15 (±1)	6	18 (3)	
SM4	15 (±1)	6	18 (3)	
SSL-4	17 (± 0.8)	8	24 (8)	
SSL-5	15 (±1)	6	18 (3)	$S_2O_3^{2-}$ (mM)

Table 3.5: Mathematical correlations obtained for dry weight vs optical density

S. No.	Bacterial Culture	Mathematical correlations	R^2 value
1.	SM1	y = 0.03928 x + 0.24	0.9787
2.	Mixed microbial population	$y = 0.47\ x + 0.025$	0.9438
3.	SM3	$y = 0.31\ x + 0.062$	0.88
4.	SM4	$y = 0.47\ x - 0.014$	0.964
5.	SSL-4	$y = 0.00119\ x + 0.000494$	0.9393
6.	SSL-5	$y = 0.93343\ x + 0.07911$	0.946

3.4.3 Product analysis

3.4.3.1 Extraction procedure

Cultures of mixed microbial population and isolated species (SM1, SM3, SM4, SSL4 and SSL5) obtained after the CO_2 bio-mitigation studies from group G3 were used to analyze the metabolite (valuable products) formed during CO_2 bio-mitigation studies. Recovery of metabolites from biomass and the supernatant was carried out by following the procedure given in literature (Zheng et al., 2012; Bharti et al., 2014). The culture obtained from CO_2 bio-mitigation batch studies was centrifuged at 10,000 rpm for 20 minutes at 4 ^{o}C and the obtained supernatant was preserved for extracellular (cell free) metabolite extraction. The obtained cell pellet was washed twice with de-ionized water and was centrifuged again. The obtained pellet was re-suspended in cell lysis buffer [50 mM Tris-HCl, pH = 7.5, 1 mM Phenyl methane sulfonyl fluoride (PMSF**)** and 0.2% lysozyme] and the cells were lyzed through sonication for 5 min with 5 s intervals at 15,000 Hz and at 4 ^{o}C. The lysate was centrifuged at 10,000 rpm for 20 min at 4 ^{o}C and supernatant obtained was utilized for the cellular primary metabolite extraction. The obtained extracted samples of cell free supernatant and cell lysate were concentrated on rotary evaporator (R-210, BUCHI, Switzerland).

3.4.3.2 FT-IR analysis

The samples obtained from extraction of cell lysate and cell free supernatant were investigated using FT-IR (Frontier, Perkin Elmer, India) equipped with Attenuated Total Reflectance (ATR) accessory (GladiATR, PIKE Technologies, Inc.). The diamond plate was used as an internal reflection element in ATR (Jiang et al., 2012; Meng et al., 2014).

3.4.3.3 GC-MS procedure

Concentrated samples of cell lysate obtained from rotary evaporator were further analyzed using gas chromatography-mass spectroscopy (GC-MS) (QP-2010 Plus, Shimadzu, Japan) for value added products. The dimension of the column DB-5 MS used was (film thickness = 0.25 µm, i.d. = 0.25 mm, length = 30 m). 1 µL of each concentrated sample (cell lysate and cell free supernatant) was analyzed and helium (He) (head pressure = 86.5 kPa; flow rate = 1.21 mL min^{-1}; split ratio = 10) was used as a carrier gas into the column. The variation of oven temperature with time was programmed. Initially, oven temperature was kept at 80 ^{o}C with holding time of 2 min while starting the characterization. The temperature was set to increase linearly at a rate of 10 ^{o}C min^{-1} with 5 min holding time up to 250 ^{o}C. The temperature was further set to increase from 250 ^{o}C to 280 ^{o}C with linear rate of 15 ^{o}C min^{-1} and was maintained constant for 24 min at 280 ^{o}C. The operational conditions employed for MS were: scan mode, start m/z 40.00, end m/z 650.00 and scan speed of 1250 with event time of 0.5 s. The analysis time started at 3.00 min and ended at 49.99 min. The obtained data were compared with the inbuilt standard mass spectra library system (NIST-05 and Wiley-8) of GC-MS (Bharti et al., 2014).

3.4.4 Product quantification

The products obtained from the cultures of mixed microbial population and isolates (SM1, SM3, SM4, SSL4 and SSL5) were identified and characterized using the analysis of the results obtained during FT-IR and GC-MS analysis. The obtained results indicated the presence of different chemicals as valuable metabolites in the culture of STP and SSL. The quantification procedure of these chemicals is discussed in following sub-sections.

3.4.4.1 Transestrification and quantification of biodiesel

The cultures obtained for mixed microbial population, SM1, SM3, and SM4 from CO_2 mitigation studies of group G3 were converted to fatty acid methyl ester (FAME) via transestrification (O'Fallon et al., 2007). The products of cell lysate (after sonication) and supernatant obtained from the batch study at 100 ppm Fe[II] concentration as per the method described in the section 3.4.3.1, were mixed together for the transesterification reaction. 2 mL of mixed sample was placed in 25 mL conical flask and was mixed with 20 µL of methyl tridecanoate, which was used as an internal standard for this study. 1 mL of 10 N KOH along with 5 mL of methanol were added in the same flask. The conical flask was incubated in a water bath (55 ^{o}C) for 1.5 h at 120 rpm. After incubation, the conical flask was cooled below the room temperature in a cold tap water and it was added with 1 mL of 24 N H_2SO_4. The conical flask was incubated again at 55 ^{o}C in water bath for 1.5 h at 120 rpm in order to complete the FAME synthesis reaction.

The conical flask was cooled in a cold tap water bath after the completion of FAME reaction and mixture was transferred to the 50 mL centrifuge tube. 20 mL of hexane was added to the existing FAME mixture in the centrifuge tube and it was vortex-mixed for 5 min on a multi-tube vortex mixer. The separation of phases was carried out at 1000 rpm and at 4 ^{o}C by centrifugation for 5 min in a centrifuge. The layer of hexane was concentrated on rotary evaporator, which contained the FAME and was placed into a GC vial for the further analysis (section 3.4.3.3).

The final concentrated hexane phase (rich in ester) was utilized to obtain product yield. The yield was calculated in terms of the productivity of FAME, which was quantified using standard FAME mix (C_8-C_{24}) obtained from Supelco (USA) by following the method described

by Van Wychen and Laurens (Wychen and Laurens, 2013). The product yield is estimated by the following Eq. (3.6).

$$Yield\ (\%) = \frac{W_{\text{FAME}}}{W_{\text{Biomass}}} \times 100 \quad (3.6)$$

Where, W_{FAME} and W_{Biomass} are weight of FAME obtained and weight of biomass taken, respectively.

3.4.4.2 Fatty alcohol quantification and product yield of targeted by-products

Products yield estimation for the isolate SSL-4 and SSL-5 are based on the fatty alcohols (C_{12}-C_{18}) as targeted compounds. The quantification was carried out by following the external multipoint calibration method for GC analysis and 0.05 mg of 1-octanol was added as an internal standard. The targeted compounds were procured from Alfa aesar (Hyderabad, Andhra Pradesh, India) of purity > 98% and standard plot (Peak area vs. concentration) was prepared for each compound. The organic phase which was concentrated over rotary evaporator and later re-dissolved in chloroform was subjected to quantification via gas chromatography under similar conditions described in section 3.4.3.3. The product yield is defined by Eq. 3.7:

$$Yield\ (\%) = \frac{W_{(\text{Fatty alcohol obtained})}}{W_{\text{Biomass}}} \times 100 \quad (3.7)$$

Where, $W_{(\text{Fatty alcohol obtained})}$ = weight of Fatty alcohol obtained

3.4.5 Abiotic tolerance assay

As per the characteristics of isolated strains, SSL4 and SSL5, were further tested for different abiotic stress tolerance such as salt concentration (*S*), pH and temperature (*T*). These studies were conducted by considering sodium chloride (NaCl) concentration in medium as total salt

concentration. SSL4 and SSL5 strains were freshly inoculated in the peptone broth (pH = 7) and kept for 24 h at 120 rpm and at 37 ^{o}C in an orbital shaking incubator. 10µL aliquot of the fully grown cultures of SSL4 and SSL5 were inoculated into peptone broth (pH = 7) and were supplemented with various concentrations of salt [1-6% (w/v) for SSL4 & 2-12% (w/v) for SSL5] for the salt tolerance test. Three samples were kept in the shaker for incubation time (*t*) of 48 h at 120 rpm and at 37 ^{o}C. An aliquots of freshly prepared culture of SSL4 and SSL5 were inoculated into the peptone broth (pH = 8) at 3% (w/v) and 6% (w/v) salt concentration for SSL4 and SSl5, respectively and were kept in the orbital shaker for 48 h at different temperatures of 30-60 ^{o}C and10-60 ^{o}C for SSL4 and SSL5, respectively to evaluate temperature tolerance capability. Isolated strain SSL5 was also tested for there pH tolerance by growing it at different pH values in the range of 2-12 for 48 h at 6% (w/v) salt concentration and at 37 ^{o}C. The measurements of the dry weight and absorbance (at 600 nm) were carried out after every 12 h interval for the total incubation period of 48 h. Medium without inoculum was used as a blank during the absorbance measurement.

3.4.6 Growth response, product yield, DIC, and carbon allocation

Among all the isolates and mixed microbial population, SSL5 was found as superior candidate to be employed for the development of the CO_2 bio-mitigation system. Therefore, in order to understand CO_2 utilization mechanism and effect of physicochemical parameters on product yield, additional experiments were carried out for isolate SSL5. The detailed experimental methodology was followed and is discussed in subsequent subsections.

3.4.6.1 Growth response and product yield

The shake flask studies were conducted to observe the effect of different parameters such as initial CO_2 concentration, salt concentration, pH and temperature on CO_2 bio-mitigation ability of SSL5. The values of different parameters taken along with experimental conditions employed are given in Table 3.6. SSL5 was cultivated under different CO_2 environment as given in Table 3.6 for the total duration of 6 days to study the effect of inlet CO_2 concentration. Three flasks of 500 mL were taken and each flask was added with 100 mL of MSM along with 2 mL of culture. The concentration of $S_2O_3^{2-}$ was maintained as 100 mM in each flask. Flasks were sealed at the top using two port assembly and respective CO_2 concentrations were maintained in the head space of each flask by the method described in 2nd paragraph of section 3.2.3.1. Similarly, the influence of pH and temperature on CO_2 bio-mitigation process was studied by cultivating the bacterium SSL5 at different initial pH, temperature and NaCl values as given in Table 3.6 by keeping the other parameters constant. Headspace CO_2 concentration of 15% (v/v) was maintained in each flask for the study of effects of salt concentration, pH and temperature by SSL5 following the procedure described in 2nd paragraph of section 3.2.3.1. Flasks were kept in an orbital shaking incubator at 37 ^{o}C and at 120 rpm for the total duration of 6 days. At the end of 6th day, flasks were withdrawn for the analysis of gaseous and liquid phases. CO_2(g) concentration was measured using CO_2 analyzer in terms of volume percent (% v/v). The biomass obtained from liquid phase was separated and dry weight (g L^{-1}) was measured using filtration method as described in section 3.3.2.2.

The biomass obtained from the batch studies related to the effect of salt concentration, pH and temperature on bacterium growth was studied for obtaining the product yield in terms of primary metabolites. The sixth day culture obtained from the batch studies was utilized for

product extraction and quantification using gas chromatography (GC) as described previously in section 3.4.3.1 and 3.4.4.2.

3.4.6.2 Dissolved Inorganic carbon utilization (DIC)

The culture obtained from CO_2 bio-mitigation batch studies at 50 mM and 100 mM $S_2O_3^{2-}$ ion concentration was utilized for estimating the dissolved CO_2 concentration on per day basis (section 3.4.1). The biomass obtained in the experiment was separated from liquid phase by centrifugation. Obtained supernatant (liquid sample) of each flask was analysed for the estimation of dissolved CO_2 by following the standard procedure as given in the literature (Swarnalatha et al, 2015, APHA).

3.4.6.3 Effect of initial CO_2 concentration on cellular carbon allocation

The biomass obtained from studies of inlet CO_2 concentration [5, 10 and 15% (v/v)] on SSL-5 (section 3.4.6.1) was utilized for the cellular biochemical analysis in terms of protein, carbohydrate and total primary metabolite.

3.4.6.3.1 Semi- quantification using FT-IR

The biochemical composition of the cells cultivated at different CO_2 concentration (5%, 10% and 15%) was investigated using FT-IR by following the methodology described in section 3.4.3.2. Approximately, 10 mg of finely powdered freeze-dried biomass obtained at different CO_2 concentration (5%, 10% and 15%) was loaded onto the ATR crystal and FT-IR signals were collected in the spectral region between 400 and 4000 cm^{-1}, at a resolution of 4 cm^{-1}. The spectra for each sample were acquired in duplicate and obtained peak area was determined and averaged.

The initial spectrum without sample was taken as background and was auto subtracted from the sample spectra. Ethanol was used to clean the diamond ATR between samples. All acquired spectra were subjected to baseline correction algorithm of the software. This was done in order to minimize differences between the recorded spectra due to the baseline shifts and to minimize effect of the absolute amount of sample used for spectra acquisition.

Different functional groups present in the compound on exposure to infrared (IR) radiation gives spectrum having distinct frequency, intensity and bandwidth, which facilitate there identification and quantification. Hence, the bandwidth was attributed to cellular organic pool as given in literature for the identification of functional groups presents in the sample (Jiang et al., 2012; Vasileva et al., 2013). FT-IR spectrum of biomass obtained at different CO_2 concentration has shown the difference in ratios of various organic cellular constituents which can be estimated by semi-quantification. Hence, in the present study, cellular carbohydrate content was semi-quantified according to the Palmucci et al. (2011) and cellular primary metabolite content relative to protein was evaluated as per the methodology given by Meng et al. (2014) using absorption spectrum of FT-IR analysis (Palmucci et al., 2011; Meng et al., 2014).

3.4.6.3.2 Estimation of cellular organic pool

Experimental studies were also carried out to quantify the cellular protein and carbohydrate contents of the biomass obtained at different CO_2 concentration. The pellet was obtained from culture sample collected at the end of 6^{th} day of experiment as described in section 3.4.3.1. It was freeze dried (SCANVAC, Coolsafe, 55-4 pro, Bionics Asia, New Delhi, India) for 24 h. The cellular protein (Lowry protein method) and carbohydrate contents were estimated by phenol assay method as described in literature (Giordano et al., 2001; Palmucci et al., 2011 Memmola et

al., 2014). The total primary metabolite was extracted according to the procedure described in section 3.4.3.1 for the extraction of fatty alcohols. The obtained organic phase was concentrated on rotary evaporator and was further quantified by GC for the estimation of the product yield by following the methodology given in section 3.4.4.2.

3.5 Semi-continuous study

The strain SSL5 was evaluated for its CO_2 utilization capability and profitable extraction of valuable chemicals in a large scale laboratory bioreactor. The detailed experimental procedure was followed which is discussed in present section.

The schematic diagram of the bioreactor is shown in Fig. 3.2 and photograph is shown in Plate 3.1. The bioreactor (Bio-age, Bangluru, India) is jacketed type having a working volume of 3 L and a head space of 2 L. It is made up of stainless steel, equipped with micro control (PLC) system. The accessories associated with bioreactor include: dissolved oxygen (DO) probe, antifoam, aeration, temperature, stirrer and pH. The pH meter (Mettler Toledo, USA) was calibrated using buffer at pH 4 and 7.0 (VWR, Canada). DO probe was calibrated to zero using sodium sulfate and to 100% by purging air in distilled water. The enriched culture of 250 mL volume having an optical density of 0.8 was utilized as bacterium innoculum (Section 3.2.3.2). The bioreactor run was carried out on the semi-continuous mode. CO_2(g) concentration of 15% (v/v) was achieved by premixing the air and pure CO_2. A mixture of CO_2(g) (15%) and air (85%) was supplied continuously at the gas inlet port of the bioreactor with an aeration rate of 1 LPH. The bioreactor was programmed at 120 rpm and at 37 ^{o}C and the study was continued for the total period of 3 days. In the semi-continuous study, pH and dissolved oxygen concentration values were collected at regular time intervals of 12 h. CO_2 mitigation efficiency of SSL5 was

evaluated by observing CO_2(g) concentration at the outlet of bioreactor and by estimating the concentration of dissolved CO_2 in every 12 h as described in section 3.4.2.1 and 3.4.6.2. 50 mL sample was withdrawn aseptically from the reactor at every time intervals of 12 h and out of which 30 mL was utilized for calculating the biomass in terms of dry weight (g L^{-1}) and optical density was calculated as per the method described in section 3.4.2.2.

The biomass growth rate depicted in terms of biomass productivity per day (P, g L^{-1} d^{-1}), specific growth rate (μ, per day), and CO_2 removal rate (R_{CO2}) were calculated as per Eq. 3.2, 3.3, and 3.4.

Table 3.6: Different experimental condition employed on SSL5 during study the effect of different physicochemical parameters

Parameters (units)	**Values**	**Values of other parameters**
Initial CO_2 concentration (% v/v)	5, 10 and 15	T = 37 ^oC, *S* = 0.5 M, $S_2O_3^{2-}$ = 100 mM
pH	6, 8 and 10	T = 37 ^oC, *S* = 0.5 M, $S_2O_3^{2-}$ = 100 mM and CO_2 (g) = 15 % (v/v)
Temperature (^oC)	20, 30 and 50	*S* = 0.5 M, pH=7, $S_2O_3^{2-}$ = 100 mM and CO_2 (g) = 15 % (v/v)
Salt (M)	0, 0.5 and 1	CO_2 (g) = 15 % (v/v), pH =7, $S_2O_3^{2-}$ = 100 mM and T = 37 ^oC

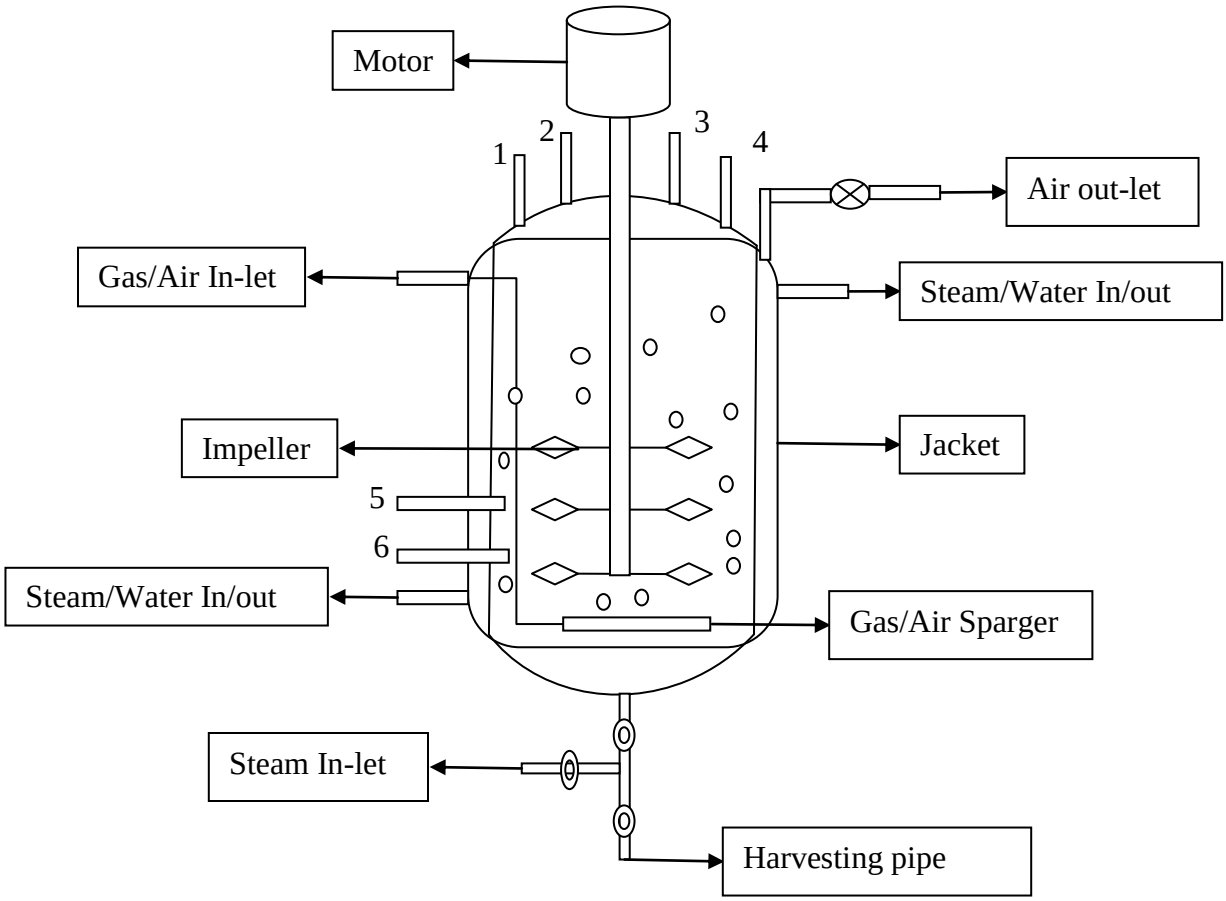

Fig. 3.2 Schematic diagram of bioreactor used for semi-continuous studies.

Plate 3.1 Experimental setup used for semicontinuous studies.

3.5.1 Biomass harvesting and fatty alcohol recovery

Third day culture (~ 2.5 L) obtained from the bioreactor was utilized for harvesting the biomass and for the recovery of fatty alcohols. The experimental methodology followed is given in Fig. 3.3. The culture was divided into two equal parts and one part was subjected to filtration method while other part was subjected to centrifugation method for the biomass recovery. The supernatants obtained from method were preserved at 4 ^{o}C for the recovery of products. The obtained biomass from each method was further divided into two equal parts. One part was subjected to cell lysis and other one was kept as it is, for the extraction of fatty alcohols.

The extraction of fatty alcohols from cell lysate and wet biomass was carried out by both solvent extraction and reactive extraction methods. The recovery of fatty alcohols from wet biomass was carried using chloroform and methanol (2:1) extractant system using the solvent extraction. Solvents were added to wet biomass and the mixture was kept in an orbital shaker for a period of 2 h at 120 rpm and at 37 ^{o}C for phase separation. After reaching equilibrium, mixture was filtered, concentrated on the rotary evaporator and preserved at 4 ^{o}C for GC-MS analysis. The solvent system used for reactive extraction was cyclohexane, decanol and Tri-octyl amine in the ratio of 1:1:1. Solvents were added to wet biomass and were kept in an orbital shaker for the period of 8 h for the separation of phases at 120 rpm and at 37 ^{o}C. The mixture was filtered, concentrated on rotary evaporator and preserved at 4 ^{o}C for GC-MS analysis.

The fatty alcohol recovery from cell lysate was carried out by following the same method adopted for wet biomass using solvent extraction and reactive extraction methods. The obtained supernatant was subjected only for solvent extraction methodology by following the same methodology utilized for wet biomass.

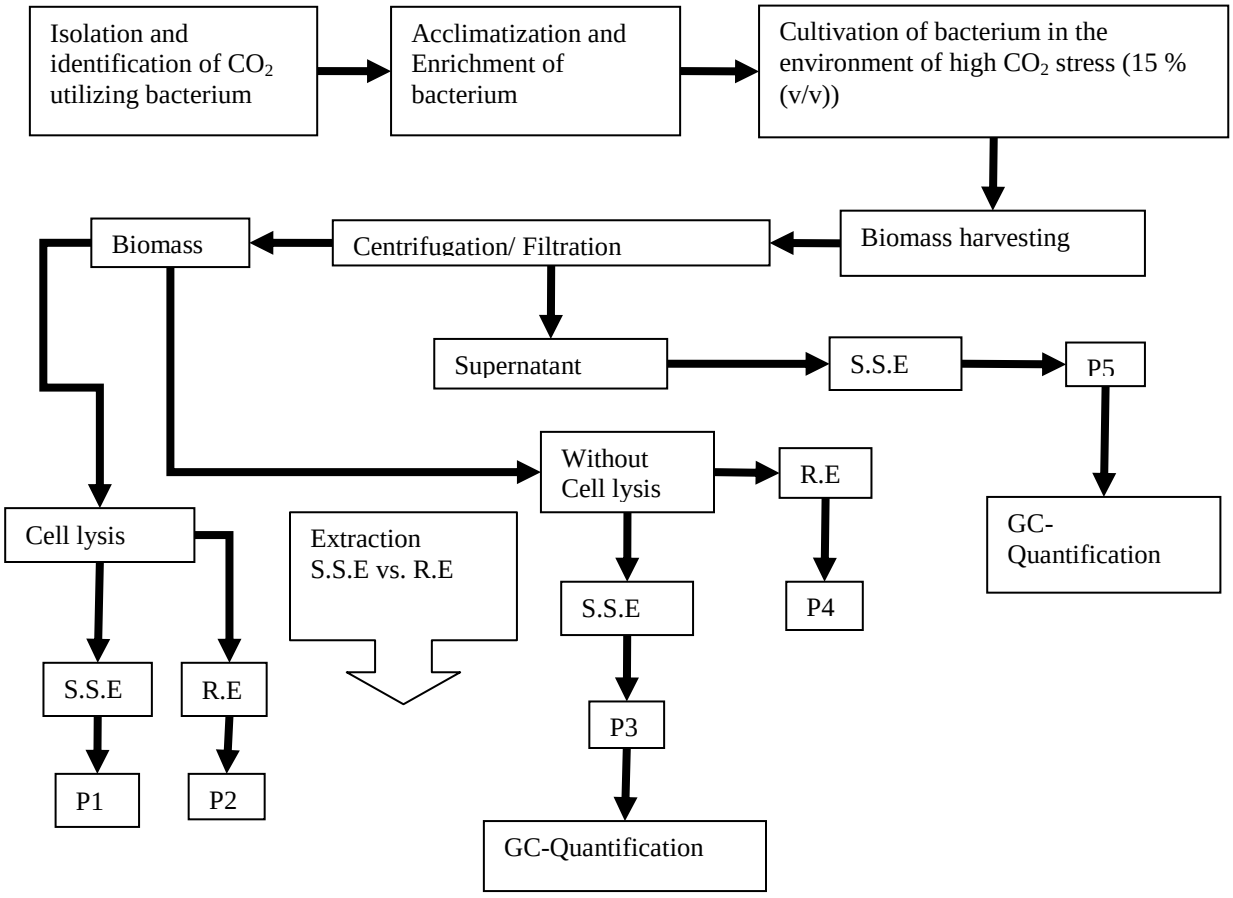

Fig. 3.3 Flow sheet for downstream processing strategy used during semi-continuous studies.

3.5.2 Analysis of primary metabolite recovery via GC-MS

The concentrated samples obtained after extraction processes for wet biomass and cell lysate were analyzed using GC-MS as per the method described in section 3.4.3.3.

3.5.3 Fatty alcohol quantification

The quantification of various fatty alcohols was carried out by following the procedure described in section 3.4.4.2. The actual product recovery was estimated using Eq. 3.8:

$$Actual\ \ product\ Yield\ (\%) = \frac{Fatty\ alcohols\ recovered}{Total\ cellular\ \ fatty\ alcohols\ content} \times 100 \qquad (3.8)$$

3.6 Continuous study

3.6.1 Packed bed bioreactor setup

In the present study, the packed bed bioreactor was developed and utilized for the CO_2 bio-mitigation studies. The schematic diagram of the experimental setup is given in Fig. 3.4. A snapshot of laboratory experimental setup is shown in Plate 3.2. The packed bed bioreactor is made of stainless steel of 0.3 m inner diameter and 1.6 m length.

The column was packed with the mixture of compost and coal taken in the weight ratio of (4:1). Coal was procured from the local market of Pilani, India. It was crushed and sieved through 8-10 mm mesh screen. The particle size of coal was obtained as approximately 3 mm. The coal particles were washed with deionized water to remove impurities and after that it were dried in hot air oven at 100 ^{o}C for duration of 24 h. The matured compost was obtained from the Amrit Dairy farm, Jhunjhunu, Rajasthan, India. The moisture content of the packing material was analyzed and found as 58%. The column was packed with this mixture. The total amount of coal and compost utilized in present study was 0.88 kg and 3.52 kg, respectively. The

macronutrients (nitrogen, phosphorus, potassium) and organic matters are present in the compost, which supports the microbial growth (Delhomenie ans Heitz, 2005). Due to this reason the mixture of coal and compost was utilized in present study. The bed was supported by two stainless steel meshes fixed at the top and bottom of the column. The height of the packing was 90 cm. The liquid distributer was attached at 15 cm from bottom of the bio-reactor.

CO_2(g) at desired concentration was prepared by diluting pure CO_2(g) with air. The flow rates of CO_2(g) and air were measured using rotameters. The air flow rate was maintained at 1 LPM and CO_2 flow rate was varied from 0.05-0.2 LPM to maintain the CO_2(g) concentration in the range of 5 - 20% (v/v) at normal room temperature and pressure. CO_2(g) + air mixture is fed at the bottom of the column through ring type gas sparger having inner diameter of 1 mm. The gas sparger was placed 15 cm from the bottom of the column. The MSM was supplied to the column from the top at the rate of 5 mL min^{-1} for the duration of 15-30 minutes on daily basis to provide necessary nutrient supply for the growth of the microorganism. The column has six sampling ports along the length of the packed bed and placed at an interval of 15 cm from the bottom of the packing.

3.6.2 Culture preparation and column development

The mixed microbial culture obtained from STP along with SSL4 and SSL5 were used as a seeding culture for packed bed bioreactor. Seeding culture was grown in bulk in a fermenter. The enriched fully grown mixed microbial population was fed into the column from the top and the leachate was collected from the bottom after 2 h. The obtained leachate was re-circulated manually into the bioreactor. The procedure was carried out twice in a day and was continued for the total period of 15 days. MSM was inducted into the bioreactor from the top at 5 mL min^{-1}

flow rate for the duration of 30 minutes once in a day to provide necessary nutrient supply for the growth of the microorganism. After 15 days, the investigation of packing material was carried out for ensuring the development of bio-film using biomass concentration.

3.6.3 Biomass concentration

Biomass concentration was measured in terms of colony forming of units (CFU) g^{-1} of packing material. At the end of acclimation period one gram of moist packing material was collected from the first sampling port (numbering bottom to top). Similarly, at the end of the packed bed bioreactor operation same amount of moist packing material was collected from different sampling ports (i.e. first, second, third, fourth, fifth and sixth or 15, 30, 45, 60, 75 and 90 cm from bottom of packd bed) located along the length of packed bed to analyze the variation of biomass concentration with height of packed bed. Moist packing material was added with 0.8% of NaCl solution and kept in a shaker for 15 min and then serially diluted with sterilized water to isolate the bacteria from packing material. Spread plating technique was used to estimate the CFU values (CFU g^{-1} of packing material).

3.6.4 Column operating conditions

The entire continuous study is divided into three phases based upon the acclimatization period and inlet CO_2(g) concentration to the column. The first phase of the bioreactor operation is acclimatization period, which was continued for the total period of 31 days. The CO_2(g) and air mixture at concentration of 5% (v/v) is fed through the bottom of column with a flow rate of 1.05 LPM. The CO_2 concentration was monitored at the outlet of column on perday basis using CO_2 gas analyzer. The sample from each port was collected for estimating the biomass growth as

described in section 3.6.3 at the end of 31 days. The inlet CO_2 load to the column was increased to 10% (v/v) and 20% (v/v) for the next 26 days and 20 days, respectively. The CO_2(g) and air stream were fed to the column at flow rate of 1.1 LPM. The outlet CO_2 concentration was measured on perday basis by following the procedure described above. The biomass growth was estimated from each sample port after 26 and 20 days by following the similar methodology described in section 3.6.3. The column was operated for total duration of 77 days.

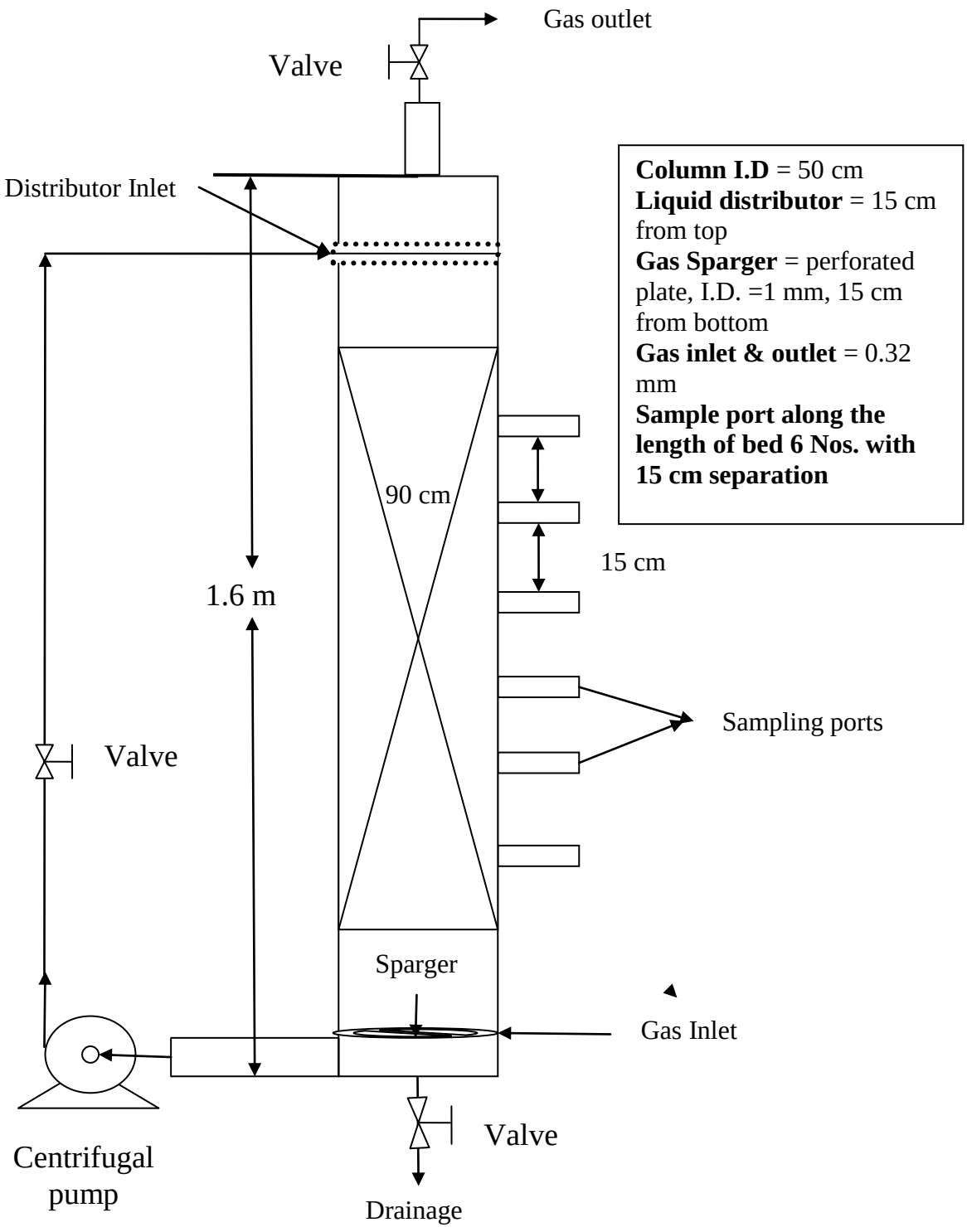

Fig. 3.4 Schematic diagram of packed bed bioreactor used for continuous studies.

Plate 3.2 Experimental setup used for continuous studies.

Chapter 4

Theoretical Studies

The material balance and thermodynamic assessment of the overall CO_2 fixation, development of downstream methodology for the production of fatty alcohols, having carbon chain length in the range of C_{12}-C_{18}, utilizing bacterium having highest CO_2 utilization efficiency and economic analysis of the product recovery are described in this chapter.

This chapter provides the detailed strategy adopted to carry out approximate material balance and thermodynamic analysis for the CO_2 fixation using microbial species used in the present study. The development of downstream processing strategy for the recovery of valuable chemicals using the bacterium having highest CO_2 utilization efficiency is illustrated in the present chapter of this thesis. The chapter also includes the economic assessment of developed downstream processing strategy in comparison to existing processes.

4.1 Approximate Material balance

The general material balance equation for any system includes the terms such as input, output, accumulation and generation of material. The material balance in the present CO_2 bio-mitigation system would be helpful in estimating the actual amount of CO_2 assimilated as carbon into the biomass. This would also help in the calculation of actual CO_2(g) utilization efficiency of the microorganisms. The experimental system under investigation is 250 mL conical flask containing 40 mL of MSM along with 2 mL of fully grown enriched microbial culture at particular concentration of energy substrate (Fig. 3.1). In the present system, carbon (C) supplied to the system as CO_2(g) was utilized by microorganisms and assimilated as biomass. At the end of experiment, unutilized CO_2 was present as CO_2 in gaseous form and dissolved CO_2 in liquid. Hence, the total elemental carbon balance is given by Eq. 4.1:

$$M_{C,\text{in}} = M_{C,\text{go}} + M_{C,bo} + M_{C,CO_2(l)} \quad (4.1)$$

Where, $M_{C,\text{in}}$ = mass of C supplied as CO_2(g) , $M_{C,\text{go}}$ = C left in gaseous phase as CO_2 at the end of batch study, $M_{C,\text{bo}}$ = C assimilated as biomass and $M_{C,CO2(l)}$ = dissolved CO_2 in aqueous phase.

$M_{C,\text{in}}$ is calculated using Eq. 4.2:

$$M_{C,\,in} = M_{Cin,CO2(g)} + M_{Cin,CO2(l)} \quad (4.2)$$

Where, $M_{Cin,CO2(g)}$ is the mass of CO_2(g) present in the head space of flask and $M_{Cin,CO2(l)}$ is the CO_2 present in dissolved form in the liquid media.

$M_{Cin,CO2(g)}$ was calculated using ideal gas law given by Eq. 4.3

$$M_{C_{in},CO_2(g)} = \frac{y_{in} \times P \times M.wt_{CO_2} \times V_{CO_2}}{RT} \quad (4.3)$$

Where, y_{in} is the initial concentration of CO_2 and P is the total pressure assumed as 1 atm.

The final CO_2 concentrations in gaseous and liquid phases were assumed in equilibrium. Final dissolved CO_2(l) is calculated using Henry's law for all microbial cultures. However, titration method was used to estimate the initial and final CO_2(l) concentration in case of SSL5 (*H. stevensii*) as the pH of the solution was changing with CO_2 concentration (Swarnalatha et al, 2015, APHA). Henry's constant for CO_2 is 29.41 atm L Mole^{-1} as given in the literature (McCollom and Amend, 2005). $M_{C,bo}$ was calculated using the empirical formula of biomass given in the literature (Rittman and Mccarty, 2012). It was taken as $C_6H_{12}O_7N$ and the fraction of carbon content (C_C) in the biomass was estimated as 0.34. Thus, $M_{C,bo}$ is given by Eq. 4.4:

$$M_{C,bo} = 0.34 \times \text{biomass obtained} \quad (4.4)$$

$M_{C,go}$ was estimated as per the final concentration (y_{CO2out}) of CO_2(g) by utilizing the Eq. 4.3.

4.2 Thermodynamic assessment

Considering constant temperature and pressure for a biological system, it is possible to predict the fate of bio-chemical reaction by estimating the change in Gibb's free energy (ΔG). The chemical reaction is thermodynamically unfavorable, if $\Delta G > 0$. In such cases, cells are able to carry out reaction by coupling it to a reaction which has a negative ΔG of larger magnitude, so

that the sum of the ΔG values for two reactions would have a negative ΔG. This way thermodynamic assessment of the microbial system w.r.t electron acceptor/donor component helps in the development of an appropriate mitigation strategy (Inskeep et al., 2005). The information w.r.t electron donor/electron acceptor scheme may be helpful in quantifying the products being formed during biological reactions (McCollom and Amend, 2005). Hence, in the present study, ΔG was estimated for all biological reactions involved in CO_2 fixation using the cultures obtained from STP and SSL. Hence, the present work was focused on the thermodynamic assessment of the biological systems by varying the concentration of an electron donor (Fe[II] or $S_2O_3^{2-}$).

The metabolic energy is obtained from the aerobic oxidation of Fe[II] to Fe[III] and the reduction of Fe[III] to Fe[II] with H_2 for isolates of STP and SSL4. The reaction scheme for oxidation and reduction reaction is given by Eq. 4.5 and 4.6.

$$3Fe^{2+} + 0.5\,O_2 + 3\,H_2O \rightarrow 3Fe^{3+} + 6\,H^+ \quad (4.5)$$

$$3Fe^{3+} + H_2 + 6\,H^+ \rightarrow 3Fe^{2+} + 4H_2O \quad (4.6)$$

Overall reaction for the reduction of CO_2 into cellular biomass as hexadecanoic acid is given by Eq. 4.7 for the cultures obtained from STP.

$$16\,CO_2 + Fe^{2+} + 90\,e^- + 91\,H^+ \rightarrow C_{16}H_{30}OOH + Fe^{3+} + 30\,H_2O \quad (4.7)$$

The reduction of CO_2 into cellular biomass as dodecanol for SSL4 is represented by the following overall reaction (Eq. 4.8):

$$12\,CO_2 + Fe^{2+} + 71\,e^- + 72\,H^+ \rightarrow C_{12}H_{26}O + Fe^{3+} + 23\,H_2O \quad (4.8)$$

Overall reaction for the reduction of CO_2 into cellular biomass using $S_2O_3^{2-}$ as an energy source by considering dodecanol as major product is given by Eqs. 4.9 for isolate SSL5.

$$12CO_2 + S_2O_3^{2-} + 64e^- + 62H^+ \rightarrow C_{12}H_{26}O + 2SO_4^{2-} + 18H_2O \quad (4.9)$$

Furthermore, in terms of adenosine triphosphate (ATP) generation, the thermodynamic assessment of the overall mechanism of autotrophic assimilation of CO_2 into the cellular biomass up to the level of carbohydrate (fructose) by sulfur oxidizing bacterium was studied and is given by Eq. 4.10 (Kelly, 1999):

$$6CO_2 + 18\,ATP + 12\,NADH + 12\,H^+ + 12\,H_2O \rightarrow C_6H_{12}O_6 + 18\,ADP + 12\,NAD^+ + 18\,P_i \quad (4.10)$$

Where, P_i is H_3PO_4. The free energy change (ΔG^o) for the Eq. 4.10 was calculated as +114 kJ (mol of CO_2 fixed)$^{-1}$.

Considering the $S_2O_3^{2-}$ oxidation reaction, the coupled overall reaction using $S_2O_3^{2-}$ as an electron donor and CO_2 as electron acceptor is given by Eq. 4.11:

$$6\,CO_2 + 3\,S_2O_3^{2-} + 9\,H_2O \rightarrow C_6H_{12}O_6 + 6\,SO_4^{2-} + 6\,H^+ \quad (4.11)$$

ΔG^o value for the Eq. 4.11 was calculated as + 101.3 kJ (mol of CO_2 fixed)$^{-1}$ (Kelly, 1999).

During semi-contineous studies the GC-MS analysis and the product yield calculations have revealed the tetradecanol as primary metabolite. Hence, tetradecanol was considered as one of the main products for the estimation of Gibb`s free energy for the fixation of CO_2 into the cellular biomass. Overall reaction of reduction of CO_2 into cellular biomass such as tetradecanol (major product obtained in this study) is given by Eq. 4.12

$$14CO_2 + S_2O_3^{2-} + 76e^- + 74H^+ \rightarrow C_{14}H_{30}O + 2SO_4^{2-} + 22H_2O \quad (4.12)$$

The emphasis is given on the overall reaction rather than the stepwise reactions of CO_2 metabolic process. The general equation of thermodynamic evaluation is given by Eq. 4.13.

$$\Delta G^o_{Reaction} = \Delta G^o_{Product} - \Delta G^o_{Reactant} \quad (4.13)$$

Where, $\Delta G^o_{Reaction}$ = Gibb's free energy change of the reaction, $\Delta G^o_{Product}$ = standard Gibb's free energy of formation of products and $\Delta G^o_{Reactant}$ = standard Gibb's free energy of

formation of reactant. The values of standard Gibb's free energy of formation ($\Delta G^{o}_{Formation}$) were taken from the literature (Ritmann and McCarty, 2012). Thermodynamic assessment was carried out by considering the system temperature at 25 ^{o}C. Gibb's free energy change of product and reactant was calculated using the standard Gibb's free energy of formation values of various compounds as reported in literature (Ritmann and McCarty, 2012).

4.3 Economic feasibility of downstream processing

The biomass obtained from semi-continuous studies (section 3.6) can be utilized for the recovery of products by downstream bio-processing. The major challenges in the development of downstream bio-processing strategy include: (1) efficient separation of biomass from the broth and (2) higher yield of targeted compounds from the obtained biomass. Therefore, there is a need for the development of efficient downstream bio-process methodology for the recovery of valuable compounds. The developed downstream bio-processing strategy involves five major steps:

- Chemoautotrophic growth of isolate SSL5 in bioreactor at 15% (v/v) inlet CO_2 concentration.
- Identification and characterization of bio-molecules.
- Investigation of the product recovery options from biomass: with/without cell disruption.
- Identification of the suitable option available for product extraction: reactive/solvent-solvent extraction.
- Quantification of yield by identified extraction strategy.

Hence, in the present work, the economic feasibility of the developed downstream processing method (section 3.5) was carried out and is discussed in following sections.

The economic analysis was carried out for the production of fatty alcohols without cell lysis as per the process scheme illustrated in Fig. 3.3. The proposed downstream process methodology will be acceptable only if the product recovery cost for the present case would fall within the range of cost of existing bio-based processes. The total cost of any process for fatty alcohol production is mainly comprised of the cost of raw material and cost of downstream processing. In order to compete with the existing bio-based processes of fatty alcohol production (coconut oil), the cost of proposed methodology should be lower or comparable to total cost of existing processes (coconut oil). Production of 1 kg of fatty alcohols having carbon chain length in range of C_{12} and C_{14} was taken as basis for total cost estimation. The total cost (P_T) for the production of fatty alcohols from coconut oil is calculated as procedure described by Belrabi et al. (2000) and is given by Eq. 4.14:

$$P_T = P_R + f \times P_T \tag{4.14}$$

Where, P_R is the cost of raw material (coconut oil) and f is the fraction of cost which represents the downstream processing costs. The f is typically in the range of 0 to 1 for all processes. However, it is taken in between 0.7 to 0.8 for bio-processes (Belrabi et al., 2000). Thus, the total cost for the recovery of 1 kg of fatty alcohol from coconut oil is calculated by using the Eq. 4.15:

$$P_T = \frac{P_R}{1 - f} \tag{4.15}$$

In order to produce 1 kg fatty alcohol from bacterium biomass, the total production cost is calculated from Eq. 4.16:

$$P_M = P_R + y \times f \times P_T \tag{4.16}$$

Where, P_M is the total cost for the process using biomass as raw material, y is factor correcting for the differences in the solvent recovery costs and was taken as 0.325 (Belrabi et al., 2000).

The biomass required to produce 1 kg of fatty alcohol may not be available at the same cost of P_R. Hence, the maximum acceptable price for biomass is necessary to calculate for proposed process. The total cost difference between the proposed process and existing process for producing 1 kg of fatty alcohol from coconut oil is added to the P_R and resulting value is divided by the amount of biomass required (M_A). Thus, the cost of biomass (C) is given by Eq. 4.17:

$$C = \frac{P_T - P_M + P_R}{M_A} \tag{4.17}$$

From Eq. 4.16, the value of P_M was substituted in Eq. 4.17 and resulting equation is given by Eq. 4.18:

$$C = \frac{P_T \times [1 - (y \times f)]}{M_A} \tag{4.18}$$

The maximum acceptable biomass cost (C_M) is given by Eq. 4.19:

$$C_M = RzP[1 - (y \times f)] \tag{4.19}$$

Where, R = experimentally obtained product recovery, z = mass fraction of fatty alcohol in the biomass (Belrabi et al., 2000).

Chapter 5

Results and Discussion

In this chapter, the results of strain identification and the CO_2 mitigation batch studies results using mixed microbial population and isolates (SM1. SM3, SM4, SSL4 and SSL5) at different concentrations of energy source are discussed. The by-products formed during CO_2 bio-mitigation shake flasks studies were analyzed using FT-IR and GC-MS and are illustrated. The present chapter also describe the product yield of valuable chemicals. The strain is chosen on the basis of its CO_2(g) removal efficiency and was investigated further for better CO_2 fixing ability and development of economic downstream processing strategy. The results of these experiments are presented in this chapter of the thesis. The outcome of the CO_2 mitigation studies using packed bed column is also discussed in this chapter.

The results from this work have been published and accepted in **Bioprocess and Biosystems Engineering Journal** -: DOI:10.1007/s00449-016-1603-z, **Process Biochemistry Journal** -: DOI:10.1016/j.procbio.2017.01.019, **Process Safety and Environmental Protection -: Available Online & in Press**

This chapter deals with the detailed analysis and discussion of the results obtained from experimental studies of CO_2 bio-mitigation using microorganisms isolated from different habitats (STP and SSL).

5.1 Isolation and identification of CO_2 utilizing bacterium

5.1.1 Culture obtained from STP

Total five strains namely SM1, SM2, SM3, SM4 and SM5 were isolated from the mixed microbial population (Plate 5.1) obtained from STP and were enriched under head space CO_2 concentration of 5% (v/v). Out of five strains, isolates SM1, SM3 and SM4 were found better as compared to other strains (SM2 and SM5) for CO_2 utilization and have shown the stable growth. Hence, isolates SM1, SM3 and SM4 were selected for further experimental batch studies. The molecular analysis based on 16S rRNA gene homology has shown 99% similarity which belonged to the group of *γ-Proteobacteria* with the existing sequences of *Bacillus cereus*, *Enterobacter cloacae* and *Pseudomonas putida* for SM1, SM3 and SM4, respectively in NCBI database. The nucleotide sequences have been submitted to NCBI GenBank database for *Bacillus cereus* SM1, *Enterobacter cloacae* PP1 and *Pseudomonas putida* SM2 under the accession no. of KJ755083, KJ55082 and KJ55084, respectively. Phylogenetic tree for each isolate was constructed using the gene sequence of the isolate and the representative bacteria of related taxonomy are shown in Figs. 5.1 - 5.3. The isolates SM1, SM3 and SM4 have shown their closest match on the basis of their phylogenetic analysis with *B. cereus* OKF01, *E. sp.* SCU-B225 *and P. monteilii* CSR2, respectively.

5.1.2 Culture obtained from SSL

Two strains namely SSL4 and SSL5 have been isolated from the culture obtained from SSL. The streak plate of SSL4 and SSL5 were shown in Plate 5.2. Phylogenetic analysis based on 16S rRNA gene sequence comparisons revealed the strains SSL4 and SSL5 are belonged to the genus of *Pseudomonas* and *Halomonas* and were most close to *Pseudomonas aeruginosa* and *Halomonas stevensii* (99% 16S rRNA gene sequence similarity). *P. aeruginosa* SSL4 and *H. stevensii* SSL5 were deposited in NCBI GenBank database under the accession number KP163922 and KP163920, respectively. The phylogenetic relationship among different bacterial species for *P. aeruginosa* and *H. stevensii* are shown in Figs. 5.4 - 5.5, respectively.

P. aeruginosa and *H. stevensii* are gram negative bacteria and belongs to the class γ-proteobacteria. *P. aeruginosa* is found in a wide variety of habitats (soil, marshes, marine habitats, plants and animal tissues) and has evolved a mechanism for thriving in environments at different CO_2 concentrations. *Halomonas* was initially found in hypersaline environments such as the Dead Sea, hypersaline lakes, hypersaline soils and solar salterns. However, later studies confirmed that the members of the genus *Halomonas* are widespread in the biosphere and they colonized themselves in extreme environments (Stover et al., 2000; Gaboyer et al., 2014; Aggarwal et al., 2015). This widespread distribution of the species *Pseudomonas* and *Halomonas* suggested that the bacteria are exhibited a varied physiological flexibility and metabolic versatility. Thus, they have developed a specific adaptation technique which allowed them to grow under extreme habitat. The versatility in bacteria towards changing environmental conditions has made it an attractive choice for their utilization in the real scenario.

Plate 5.1 Mixed microbial population (STP) on petriplates

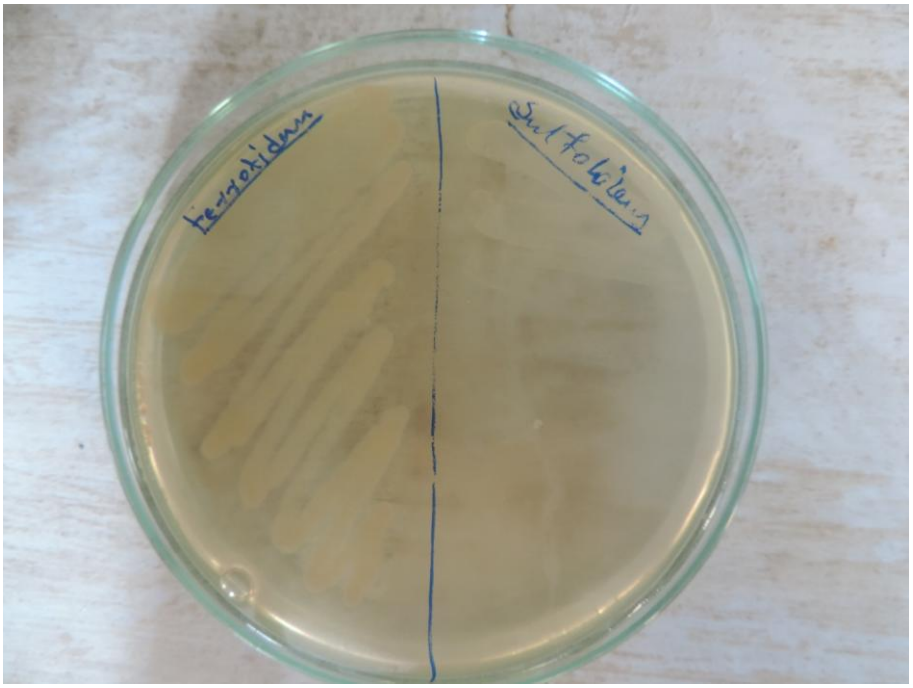

Plate 5.2 Streak Plate of SSL4 and SSL5

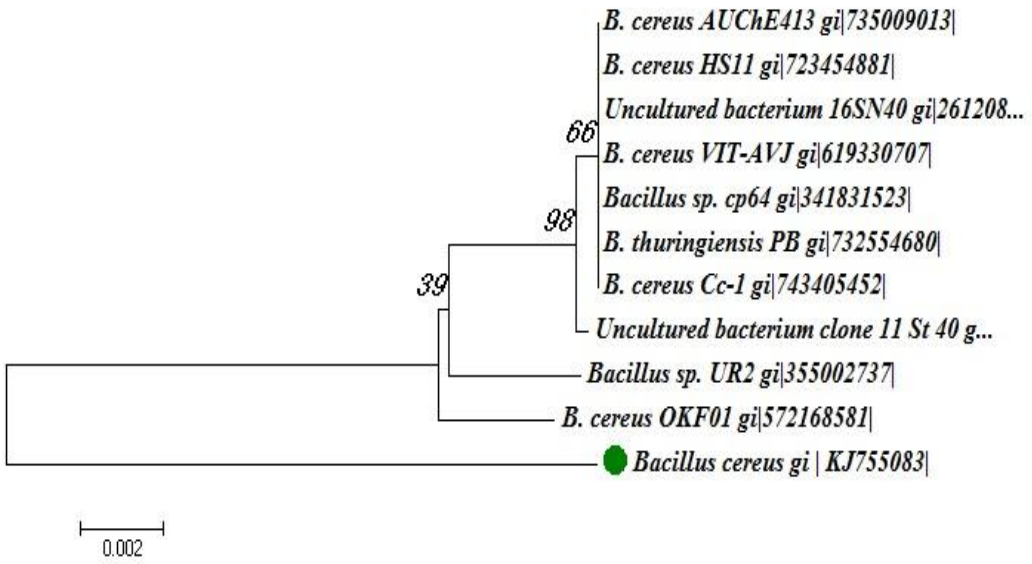

Fig. 5.1 Phylogenetic tree of isolate SM1 based on 16S rRNA gene sequences comparison.

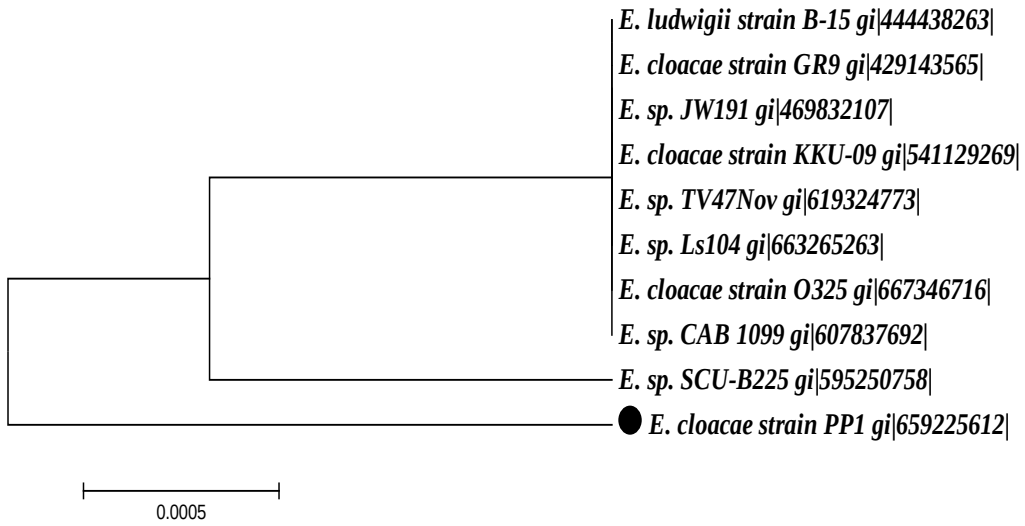

Fig. 5.2 Phylogenetic tree of isolate SM3 based on 16S rRNA gene sequences comparison.

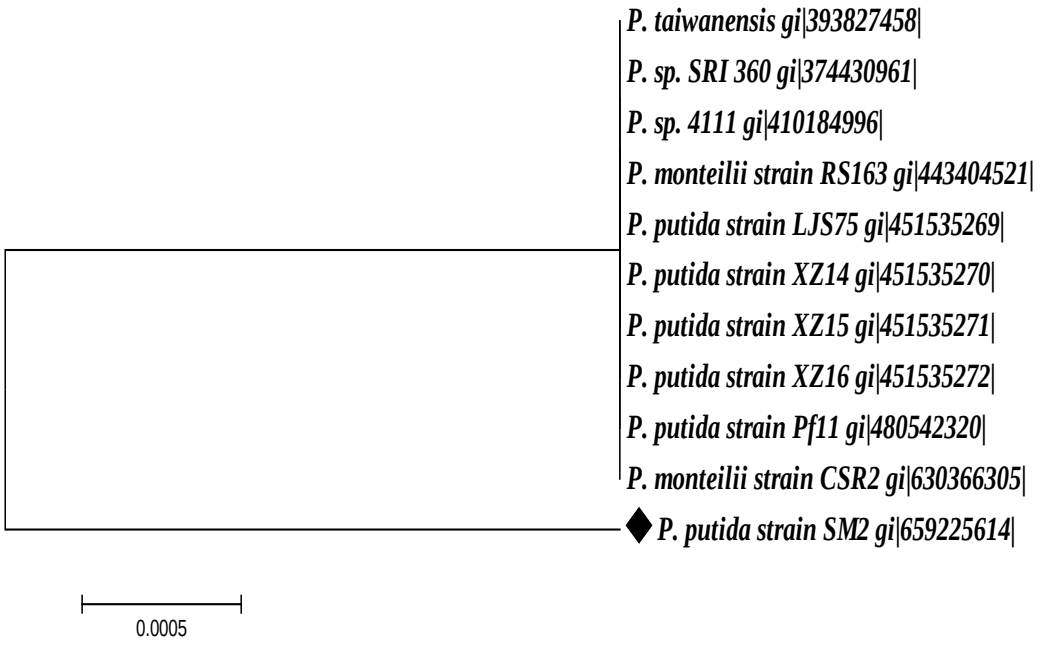

Fig. 5.3 Phylogenetic tree of isolate SM2 based on 16S rRNA gene sequences comparison.

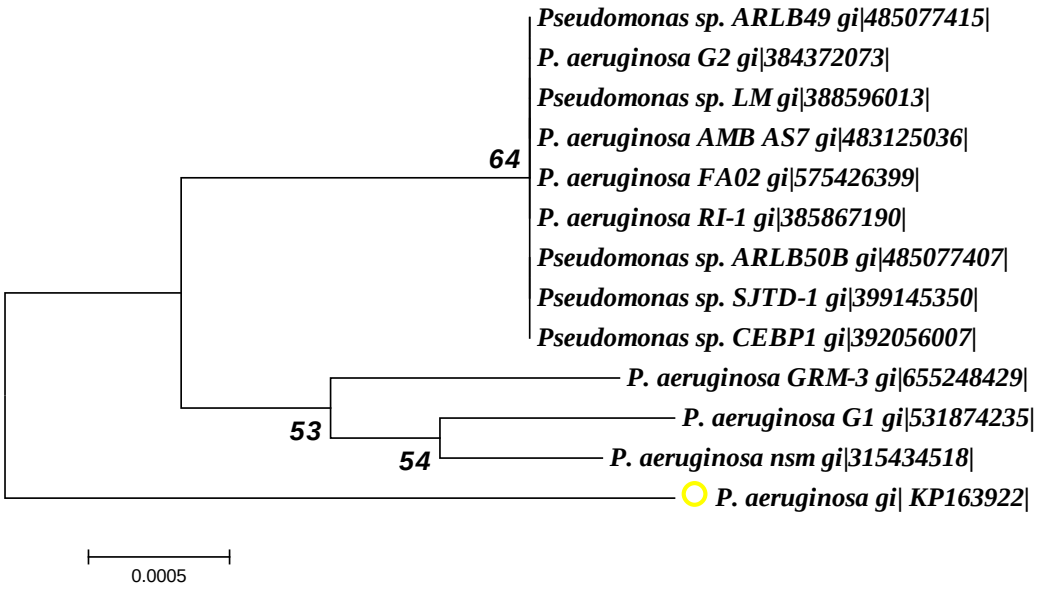

Fig. 5.4 Phylogenetic tree of isolate SSL4 based on 16S rRNA gene sequences comparison.

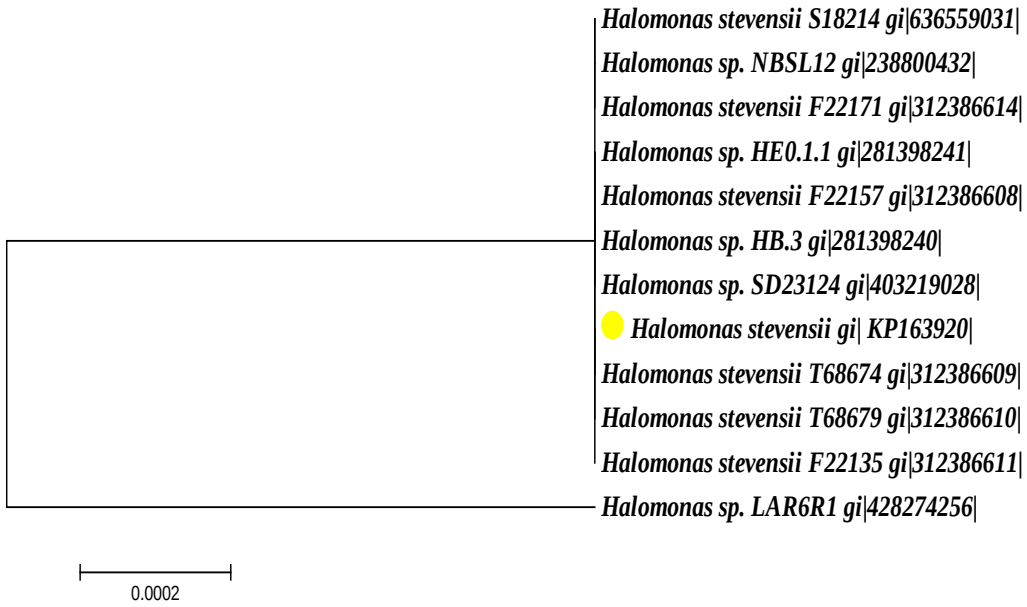

Fig. 5.5 Phylogenetic tree of isolate SSL5 based on 16S rRNA gene sequences comparison.

5.2 CO_2 bio-mitigation studies

5.2.1 Iron utilizing strains from STP and SSL

Results obtained for CO_2 bio-mitigation studies using *B. cereus*, mixed microbial population, *E. cloacae*, *P. putida* and *P. aeruginosa* are shown in Figs. 5.6 - 5.10. All the data was reported everywhere as mean ± standard deviation (SD). In the Figures statistically significant differences among duplicate groups, analyzed using t - test, are represented as $p < 0.05$ denoted by (*). Figures represent the effect of time on final CO_2(g) concentration. The corresponding CO_2(g) removal efficiency (η_{CO2}) was estimated and was reported in Table 5.1. There was no significant change in CO_2(g) concentration observed for abiotic control and at 0 ppm Fe[II] concentration for all five studies (Figs. 5.6 - 5.10).

CO_2 bio-mitigation results of *B. cereus* indicated a significant decrease in CO_2(g) concentration from 13 (±1) to 0.5 (±0.84)% and 1.5 (±1.4)% (v/v) for 100 and 200 ppm of Fe[II] concentration, respectively for the first 3 days and thereafter it became almost constant (Fig. 5.6). This may be due to the availability of more CO_2 to be fixed by *B. cereus* and higher Fe[II] concentration (energy source) in the initial period of CO_2 fixation. The results obtained for mixed microbial population, *E. cloacae* and *P. putida* showed continuous decrease in CO_2(g) concentration on the perday basis at 50 ppm and 100 ppm of Fe[II] concentration (Figs. 5.7- 5.9). Fixation of CO_2 using *P. aeruginosa* was obtained at different Fe[II] concentration (0, 50 and 100 ppm) on a perday basis and is shown in Fig. 5.10. CO_2(g) concentration was found to decrease for first 5 days at 50 and 100 ppm Fe[II] concentration and later it became constant (Fig. 5.10). These results confirmed that Fe[II] (energy substrate) plays a major role in CO_2 fixation.

The η_{CO2}(g) values for *B. cereus* were obtained as 10.66 (±1.23), 29.76 (±0.44), 84.6 (±5.76) and 80 (±9.45)% at 0, 50, 100 and 200 ppm Fe[II] concentration, respectively. There was no significant increase in η_{CO2}(g) value as observed with increase in Fe[II] concentration from 100 to 200 ppm. Hence, Fe[II] concentration was kept upto 100 ppm for CO_2 bio-mitigation studies using other species. η_{CO2}(g) at 0, 50 and 100 ppm of Fe[II] concentration, for mixed microbial population, *E. cloacae* and *P. putida* indicated that the η_{CO2}(g) increased with increase in energy substrate concentration (Table 5.1). However, at 50 ppm Fe[II] concentration, approximately similar η_{CO2}(g) values were observed for mixed microbial population, *E. cloacae* and *P. putida*. *P. aeruginosa* showed the maximum η_{CO2}(g) of 92.37 (±2.46)% at 100 ppm Fe[II] concentration on the 5^{th} day of the experiment. η_{CO2}(g) of 55.66 (±3.6)% was obtained at 50 ppm of Fe[II] concentration which was significantly lower than the removal efficiency obtained for 100 ppm Fe[II] concentration. This may be due to the fact that more amount of energy substrate was available at 100 ppm Fe[II] concentration as compared to 50 ppm Fe[II] concentration which lead to more amount of CO_2 fixation. Among all the iron oxidizing microbial cultures, *P. aeruginosa* isolated from SSL has shown the maximum η_{CO2}(g). Hence, *P. aeruginosa*, a robust strain obtained from extreme habitat is proved to be a superior candidate for CO_2(g) mitigation.

The obtained results can be understood by the chemistry of the available CO_2 and Fe[II] in bio-usable form. The solubility of CO_2(g) in aqueous phase is governed by Henry's law. Solubility of CO_2(g) is found to decrease with increase in temperature and with decrease in pH and pressure. Bio-availability of CO_2 as a carbon source depends on the equilibrium between CO_2(g) concentration and dissolved CO_2(l) concentration. The portion of dissolved CO_2 in aqueous phase reacts to form weak carbonic acid (H_2CO_3) which further dissociates to give biocarbonate (HCO_3^-) ion (Eq. 5.1).

$$H_2CO_3 \leftrightarrow HCO_3^- + H^+ \quad (5.1)$$

This HCO_3^- ion was utilized by the micro-organisms as an inorganic carbon source and its accumulation into cytosole and carboxyzome is facilitated by the enzyme known as CA (Eq. 5.2) (Supuran, 2016).

$$CO_2 + H_2O \xleftrightarrow{CA} HCO_3^- + H^+ \quad (5.2)$$

The bacteria belong to the genera *Bacillus*, *Enterobacter* and *Pseudomonas* are already known for the presence of carboxylating enzyme CA (Santini et al., 2000; Sharma et al., 2008; Prabhu et al., 2011; Lotlikar et al., 2013; Sundaram et al., 2015; Eminoglu et al., 2015; Aggarwal et al., 2015). The initial CO_2 partial pressure of 0.13 atm was used for *Bacillus*, 0.15 atm was used for mixed microbial population, *Enterobacter* & *Pseudomonas* and 0.17 atm was used for *P. aerugonisa*. CO_2(g) from the head space of the flask gets dissolved in water to give HCO_3^-. The equilibrium was attained between gas phase and liquid phase CO_2 concentrations. The microbial utilization of HCO_3^- resulted in the reduction of liquid phase CO_2 concentration at equilibrium. More amount of CO_2(g) would dissolve to increase CO_2(l) concentration due to the shift in equilibrium. This may be one of the possible reasons for the decrease in head space CO_2 concentration on the per day basis (Alonso-Sa´ez et al., 2010; Swarnalatha, 2015).

The principal and necessary requirement for the survival of the non-photosynthetic microorganisms in dark is the presence of inorganic molecules in bio-usable form as an energy substrate and that too in an adequate amount. Non-photosynthetic microbes microorganisms gain energy by catalyzing redox reactions of the reduced inorganic molecules such as Fe[II], $S_2O_3^{2-}$, S_8 etc (Amend and Shock, 2001). Energy gained by catalyzing a particular redox reaction is governed by the type of reactants participating in the reaction, which in turns decides the redox potential of the system. Also, the cultivation environments (aerobic or anaerobic) will decide the

amount of energy that can be harnessed by redox reaction (Amend and Shock, 2001; McCollom and Amend, 2005). Generally, in an aerobic environment, oxygen (O_2) acts as an electron acceptor species (Hedrich et al., 2011). The loss of electron by Fe[II] was gained by O_2 and the energy gained in this process was utilized for the reduction of CO_2 into the cellular biomass. Different studies have reported the utilization of Fe[II] by Bacillus, Pseudomonas and Enterobacter (Tiel-Menkveld et al., 1982; Segond et al., 2014; Molina et al., 2016; Daas et al., 2017). The less amount of energy substrate (Fe[II]) concentration, i.e. 50 ppm has signified the availability of less amount of energy that can be harnessed for the reduction of CO_2 into the cellular biomass. Fe[II] form was susceptible to oxidize chemically in the presence of O_2 and was stable only at solution pH value < 5. Fe[III] was stable in the aerobic environment and it hydrolyzed in the aqueous solution to form insoluble compounds at pH 7. Thus, in order to meet the energy requirement under inadequate supply of iron, microbes have developed certain strategies such as (1) production of siderophores for iron solubilization, (2) surface reduction, (3) lowering of pH and (4) reduction of Fe[III] to Fe[II] by enzyme reductases followed by cellular transportation (Andrews and Robinson, 2003; Miethke et al., 2013).

In the present system, the pH was near to neutral and throughout the period of study, on an average 15% CO_2 concentration was maintained in the headspace of each flask which eventually make the system micro-aerobic. Thus, system conditions signify the less availability of the bio-usable form of iron (Fe[II], Fe[III]) which decreases with decrease in iron concentrations (Fe[II]). Hence, the lesser availability and inadequate supply of iron in bio-usable form may be the possible reason for the lower CO_2(g) removal efficiency at lower Fe[II] concentration. Fe[II] may be present in the form of Fe[II] (unutilized) and Fe [III] (produced by redox reaction) at the end of the CO_2 bio-mitigation studies.

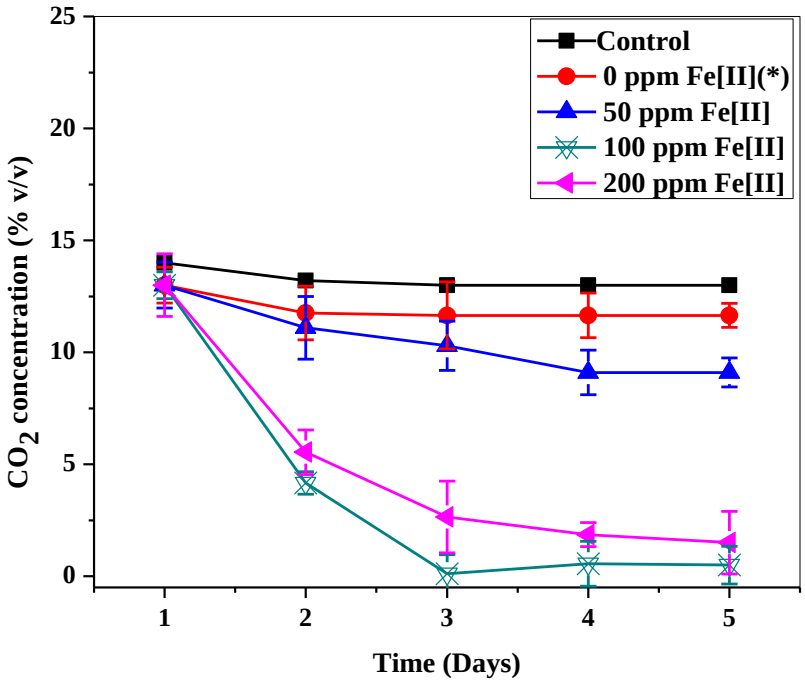

Fig. 5.6 CO_2 fixation by *B. cereus* SM1 on per day basis at different Fe[II] concentration.

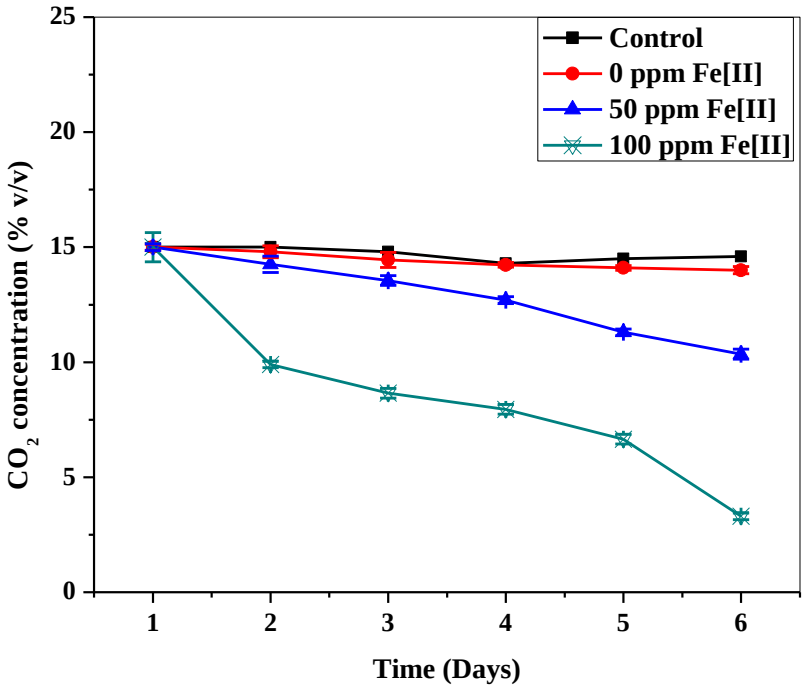

Fig. 5.7 CO_2 fixation per day basis of mixed microbial population at different Fe[II] concentration.

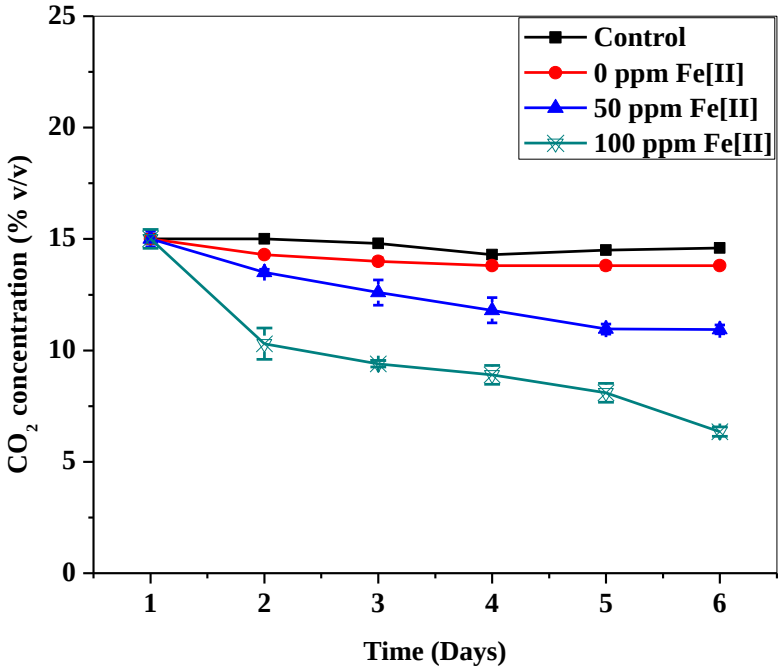

Fig. 5.8 CO_2 fixation per day basis of *E. cloacae* at different Fe[II concentration.

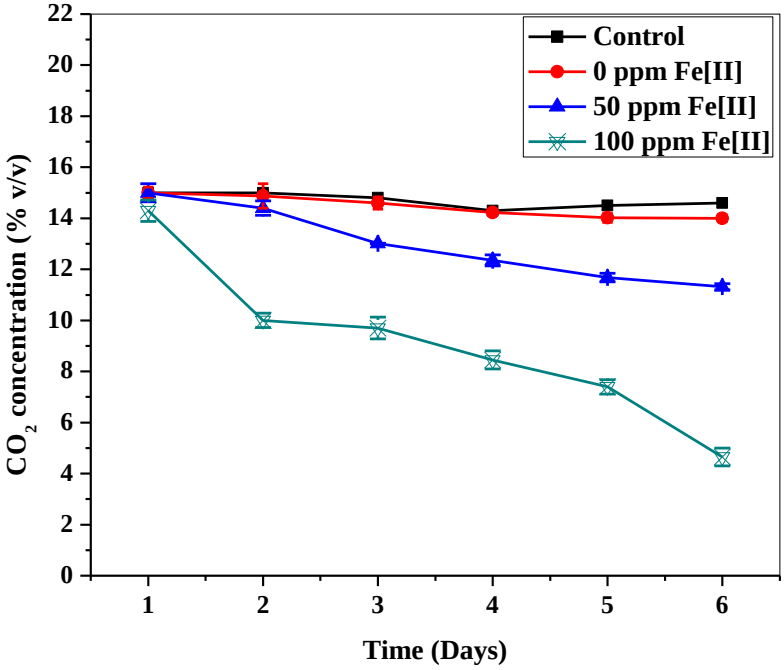

Fig. 5.9 CO_2 fixation per day basis of *P. putida* at different Fe[II] concentration.

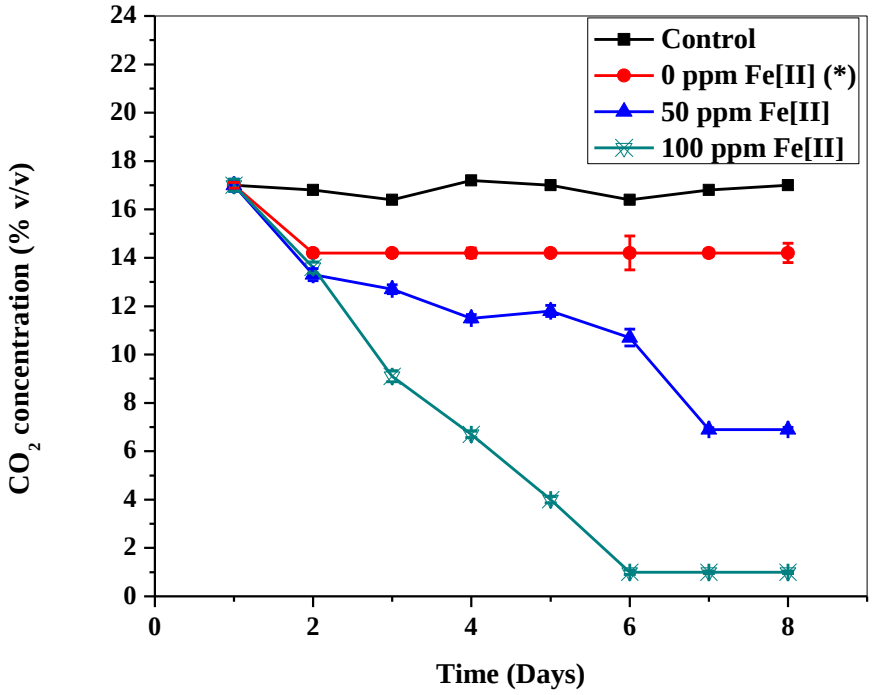

Fig. 5.10 CO_2 fixation by *P. aerugonisa* on per day basis at different Fe[II] concentration.

5.2.2 Sulfur oxidizing strain from SSL

Sulfur oxidizing strain obtained from SSL was *H. stevensii* which was cultivated using $S_2O_3^{2-}$ as an energy substrate. Out of different reduced sulfur compounds the oxidation of thiosulfates was the most energetically favored and thus it is a most important substrate for sulfur oxidizing bacteria (SOB) (Sorokin et al., 2005). When thiosulphate is used as electron donor, it is split into elemental sulphur and sulphite, both of which are then oxidized to sulphate. In different studies, researchers have utilized thiosulfate to isolate SOB's from haloalkalophilic environment (Teske et al., 2000; Sorokin et al., 2003; Sorokin et al., 2005). Based on the literature, thiosulfate was utilized as energy substrate in present work.

H. stevensii was examined for its CO_2 fixation capability on the perday basis at 0, 50 and 100 mM $S_2O_3^{2-}$ concentrations. The cells were grown in the absence of light under CO_2 as a sole carbon source. Abiotic control flask was also kept without the inoculum by maintaining the same CO_2 concentration (%v/v) and 100 mM of $S_2O_3^{2-}$ concentration. The obtained results indicated that there was a decrease in the CO_2(g) concentration in G1, G2 and G3 (Fig. 5.11). At the end of 6^{th} day of batch study, minimum CO_2(g) concentrations of 14.3 (±0.14), 0.15 (±0.07) and 0.16 (±0.09)% (v/v) were observed in G1, G2 and G3, respectively (Table 5.1). Continuous decrease in CO_2(g) concentration was observed in G2 and G3 (Fig. 5.11). However, in G1, the CO_2(g) concentration was decreases from 15 (±1) to 14.3 (±0.14)% up to day 3 and became constant afterwards. This indicated that the concentration of $S_2O_3^{2-}$ has a significant effect on the CO_2 utilization capability of *H. stevensii*. CO_2(g) concentration (%v/v) in the control flask was found to be unchanged with time which revealed that the removal of CO_2(g) was due to the presence of *H. stevensii*. Higher removal of CO_2 was observed at 50 and 100 mM $S_2O_3^{2-}$ concentrations as compared to 0 mM $S_2O_3^{2-}$ concentration. This may be due to the availability of adequate amount

of $S_2O_3^{2-}$ ion as an energy source which was required for the fixation of given amount of bio-available CO_2. Bio-availability of CO_2 can be understood by the transfer of CO_2 from gaseous phase to liquid phase and its pH dependency as discussed in section 5.2.1, paragraph 4.

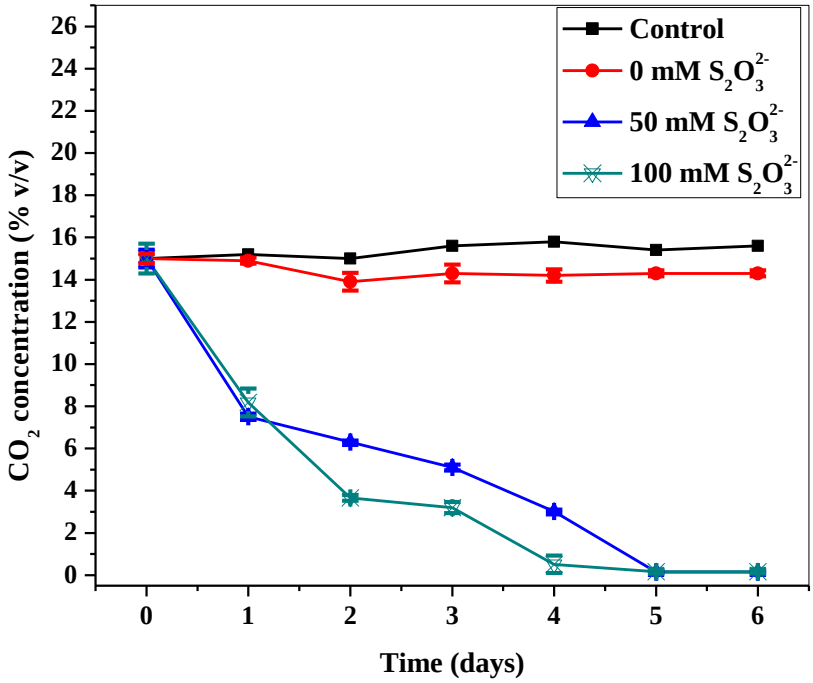

Fig. 5.11 CO_2 fixation per day basis of *Halomonas stevensii* at different $S_2O_3^{2-}$ concentration.

Table 5.1: Final headspace CO_2 concentration (% v/v) and CO_2 removal efficiency (η_{CO2}) values obtained for *B. cereus*, mixed microbial population, *E. cloacae*, *P. putida*, *P. aeruginosa* and *H. stevensii* at different energy substrate concentrations (Fe[II] or $S_2O_3^{2-}$).

Species	Initial CO_2(g) concentration (% v/v)	CO_2(g) concentration (% v/v)			CO_2(g) removal efficiency (η_{CO2})		
		Fe[II] (ppm) or $S_2O_3^{2-}$ (mM) concentration					
		0	**50**	**100**	**0**	**50**	**100**
B. Cereus	13 (±1)	11.65 (±0.54)	9.1 (±0.65)	0.5 (±0.84)	10.66 (±1.23)	29.76 (±0.44)	84.6 (±5.76)
Mixed Microbial population	15 (±1)	14 (±0.16)	10.35 (±0.21)	3.3 (±0.14)	6.66 (±0.16)	31.445 (±2.04)	78.07 (±0.014)
E. cloacae	15 (±1)	13.8 (±0.1)	10.94 (±0.19)	6.35 (±0.21)	8.0 (±0.1)	25.79 (±3.12)	56.44 (±2.68)
P. putida	15 (±1)	14 (±0.14)	11.32 (±0.12)	4.65 (±0.35)	6.66 (±0.14)	26.2 (±1.55)	67.44 (±2.44)
P. aeruginosa	17 (±1)	14.2 (±0.3)	6.9 (±0.09)	1 (±0.13)	11.26 (±0.74)	55.66 (±0.35)	92.37 (±2.47)
H. stevensii	15 (±1)	14.3 (±0.14)	0.15 (±0.072)	0.16 (±0.09)	6.82 (±0.2)	98.97 (±0.53)	98.59 (±0.59)

5.3 Biomass concentration, CO_2(g) fixation rate (R_{CO2}) and CO_2(g) removal rate ($R.R_{CO2}$)

5.3.1 Growth response of iron utilizing bacterium

After determining the head space CO_2 concentration, the estimation of biomass growth in terms of dry weight (g L^{-1}) and absorbance (600 nm) was carried out on the perday basis. The dry weight values of *B. cereus*, mixed microbial population, *E. cloacae*, *P. putida* and *P. aeruginosa* at different time intervals are shown in Figs. 5.12 - 5.16, respectively.

The obtained results indicated that the biomass concentration of *B. cereus*, mixed microbial population, *E. cloacae*, *P. putida* and *P. aeruginosa* were found to increase with time for all concentrations of Fe[II] (Figs. 5.12 - 5.16). X_{Max} value of *B. cereus* was estimated as 0.187 (±0.003), 0.256 (±0.008), and 0.386 (±0.002) g L^{-1} at 50, 100, and 200 ppm of Fe[II] concentration, respectively (Table 5.2). X_{Max} obtained for 50 ppm Fe[II] concentration was nearly 73% and 48.33% as compared to the X_{Max} values obtained at 100 ppm and 200 ppm of Fe[II] concentration, respectively.

X_{Max} values of mixed microbial population, *E. cloacae* and *P. putida* were observed as 0.48 (±0.02) g L^{-1}, 0.248 (±0.022) g L^{-1} and 0.355 (±0.03) g L^{-1}, respectively at 100 ppm Fe[II] ion concentration (Table 5.2). X_{Max} values, for 50 ppm Fe[II] concentration, of mixed microbial population, *E. cloacae* and *P. putida* were found to be 70%, 92.74% and 64.78%, respectively of the X_{Max} values obtained at 100 ppm of Fe[II] concentration (Table 5.2). The growth of *P. aeruginosa* was found to increase till 8^{th} day and corresponding X_{Max} value was obtained as 0.21 g L^{-1} at 100 ppm Fe[II] concentration. X_{Max} value was observed as 0.1306 g L^{-1} for 50 ppm Fe[II] concentration which was 62.19% of the X_{Max} value obtained at 100 ppm of Fe[II] concentration (Table 5.2).

The more realistic growth response of microorganisms can be understood by estimating the biological parameters such as biomass productivity per day (P, g $L^{-1}d^{-1}$), CO_2(g) fixation rate (R_{CO2}) and CO_2 removal rate ($R.R_{CO2}$). These parameters were estimated at different energy substrate concentrations for all the iron oxidizing species and are reported in Table 5.2. The obtained results indicated that increase in concentration of Fe[II] resulted in the improved values of P, R_{CO2} and $R.R_{CO2}$. There was no significant difference in η_{CO2} as observed at 100 and 200 ppm Fe[II] concentration. However, the highest values of P, R_{CO2} and $R.R_{CO2}$ of *B. cereus* were observed as 0.0772 (±0.00056), 0.0638 (±0.003) and 66.6 (±0.0014)%, respectively at 200 ppm of Fe[II] concentration. The increase in dry weight values of biomass may be due to the possible precipitation of excess Fe[III] at neutral pH. This may be the reason for obtaining the higher values of P, R_{CO2} and $R.R_{CO2}$ at 200 ppm Fe[II] concentration as compared to 100 ppm Fe[II] concentration.

The maximum values of P, R_{CO2} and $R.R_{CO2}$ for mixed microbial population were obtained as 0.078 (±0.004)%, 0.107 (±0.018)% and 57.67 (±0.04)%, respectively at 100 ppm of Fe[II] ion concentration (Table 5.2). These respective parameters for mixed microbial population were found to be better when compared with the isolated pure strains of *B. cereus*, *E. cloacae*, *P. putida* and *P. aeruginosa* in terms of CO_2 utilization ability (Table 5.2). Hence, the superior performance of mixed microbial population for CO_2 bio-mitigation has paved a pathway which could lead to the development of sustainable and economic CO_2 bio-mitigation system.

The obtained results revealed that the increased Fe[II] concentration from 50 to 100 ppm has not only increased the CO_2 removal efficiency but also has approximately doubled the biomass obtained. As discussed in section 5.2, amount of CO_2 that can be reduced into the cellular biomass was relied upon the adequate supply of energy substrate Fe[II] in bio-usable

form. The lower value of energy substrate concentration (50 ppm) resulted in lesser amount of CO_2 fixation into the cellular biomass. Due to this reason, obtained values of P, R_{CO2} and $R.R_{CO2}$ at 50 ppm Fe[II] concentration were found to be lower in comparison to the values obtained at 100 ppm Fe[II] concentration. Various studies reported the presence of minerals like pyrites, greigite, goethite, chlorite which are rich in Fe[III] (Sinha and Raymahashay, 2004; McBeth et al., 2011). Therefore, the possibility of metabolization of iron is quite high in haloalkalophilic environment. Hence, *P. aeruginosa*, obtained from Sambhar lake has a capability to utilize Fe[II] as energy source for assimilating CO_2 which is also confirmed by the results obtained in the present study.

5.3.2 Growth response of $S_2O_3^{2-}$ utilizing bacterium

Biomass growth in terms of dry weight (g L^{-1}) at respective $S_2O_3^{2-}$ concentration is shown in Fig. 5.17. Growth of *H. stevensii* was found to increase up to day 5 and it became nearly constant afterwards. Maximum biomass was obtained as 0.845 (±0.025) g L^{-1} and 1.05 (±0.07) g L^{-1} for 50 and 100 mM $S_2O_3^{2-}$ concentration, respectively (Table 5.2). It was also observed that the increase in $S_2O_3^{2-}$ concentration from 50 to 100 mM resulted in the increased biomass concentration by approximately 20%. However, no significant change was observed in the removal efficiency of CO_2 with the increase in $S_2O_3^{2-}$ from 50 mM [98.97 (±0.53)%] to 100 mM [98.59 (±0.59)%] (Table 5.1). The removal of CO_2 from the gaseous phase depends on the solubility of CO_2 in liquid media and also on the equilibrium which existed between gaseous and liquid phase CO_2 concentrations.

The values of $P_{Max,}$ μ_{Max} and X_{Max} for *H. stevensii* were obtained as 0.14 g L^{-1} d^{-1}, 0.21 d^{-1} and 0.845 g L^{-1}, respectively for 50 mM $S_2O_3^{2-}$ concentration and 0.175 g L^{-1} d^{-1}, 0.25 d^{-1} and

1.05 g L^{-1}, respectively for 100 mM $S_2O_3^{2-}$ concentration. R_{CO2} values of 0.174 g L^{-1} d^{-1} and 0.218 g L^{-1} d^{-1} were obtained at 50 and 100 mM $S_2O_3^{2-}$ concentrations, respectively. This also indicated that increase in $S_2O_3^{2-}$ concentration resulted in the increased CO_2 fixation rate.

It is a well known fact that the energy required for the reduction of CO_2 into cellular biomass was exploited either from light or inorganic compounds depending on the type of organisms. As discussed earlier in section 5.2.1, $S_2O_3^{2-}$ is one such inorganic compound in which sulfur is present in its reduced state and was oxidized by bacterium for CO_2 fixation. Sambhar salt lake represents the natural habitat for haloalkalophilic prokaryotes. Sulfide reacts with the insoluble sulfur present in the lake to form soluble polysulfide which is rapidly oxidized to $S_2O_3^{2-}$ under aerobic conditions (Gosh and Dam, 2009; Sorokin et al., 2011). Also, the dominance of $NaHCO_3$ over Na_2CO_3 in the lake as pH value of the lake is below 10. This has shown more probability for the presence of micro-organisms capable of fixing CO_2 (Gosh and Dam, 2009; Sorokin et al., 2011). Therefore, *H. stevensii* which was isolated from Sambhar salt lake, was found capable of fixing CO_2 as cellular biomass by oxidizing $S_2O_3^{2-}$ ion to SO_4^{2-} (Sulfate) ion.

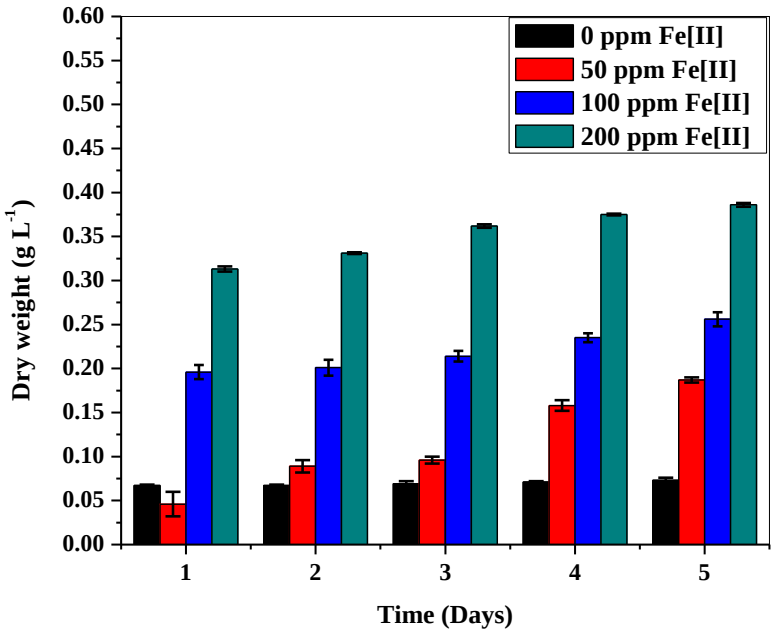

Fig. 5.12 Biomass growth (g L^{-1}) of *Bacillus cereus* at different Fe[II] concentration.

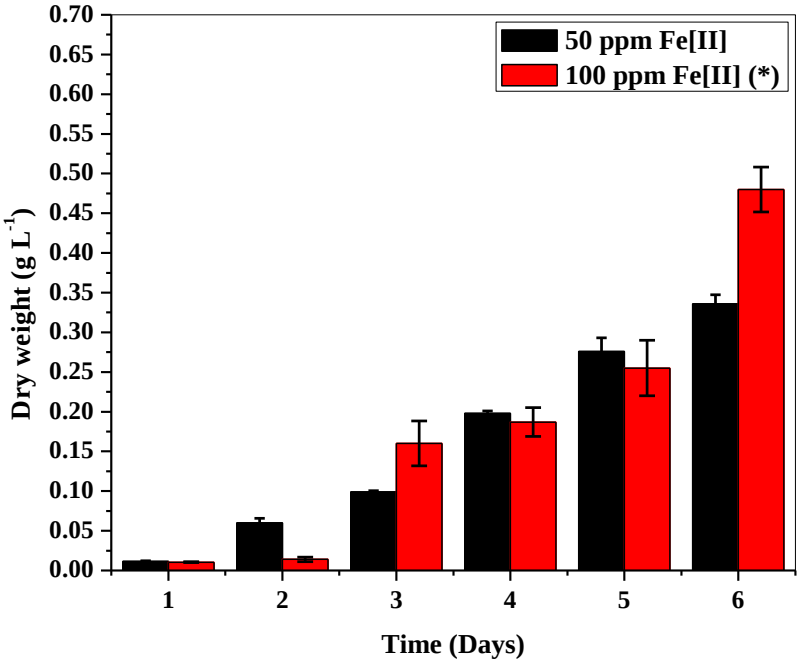

Fig. 5.13 Biomass growth (g L^{-1}) of mixed microbial population at different Fe[II] concentration.[1]

[1] "*" -: Denotes statistically significant differences for duplicates (t - test, $P < 0.05$)

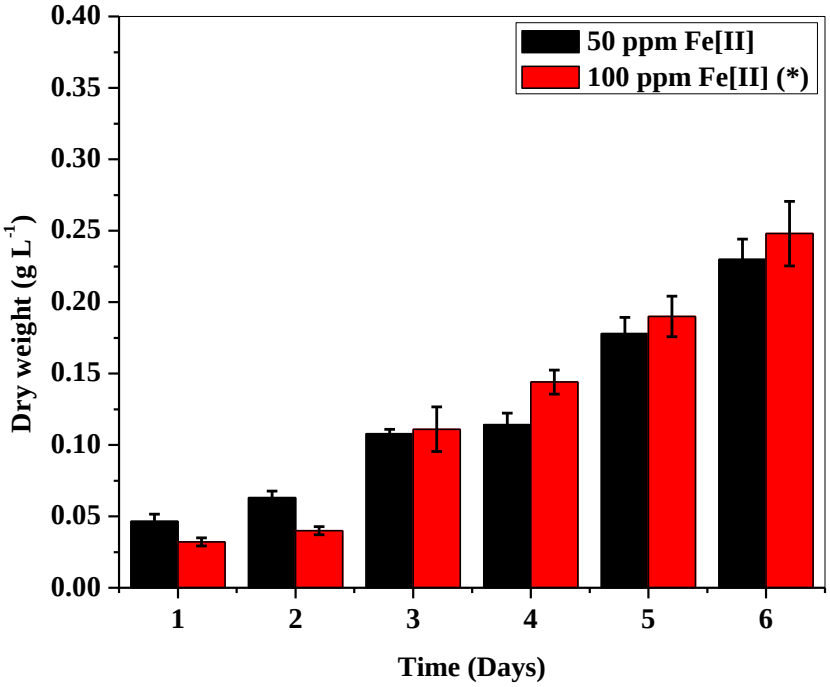

Fig. 5.14 Biomass growth of *E. cloacae* at different Fe[II] concentration.[1]

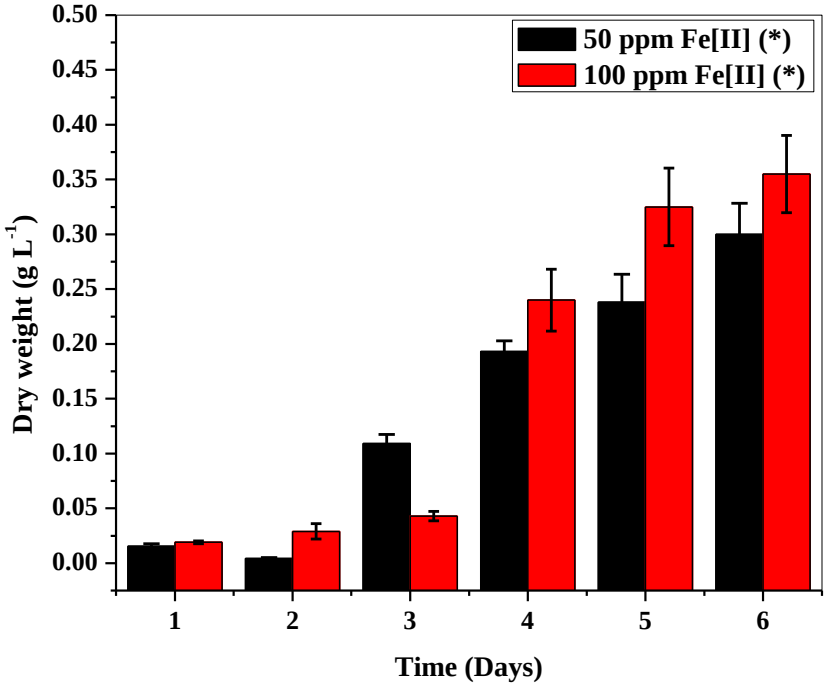

Fig. 5.15 Biomass growth (g L^{-1}) of *P. putida* at different Fe[II] concentration.[1]

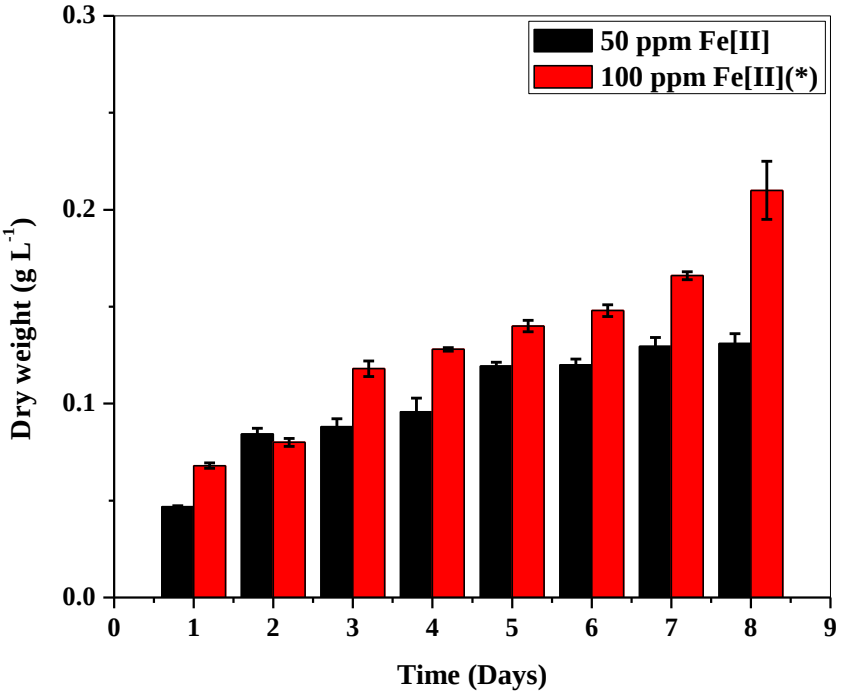

Fig. 5.16 Biomass growth (g L^{-1}) of *P. aeruginosa* at different Fe[II] concentration.[1]

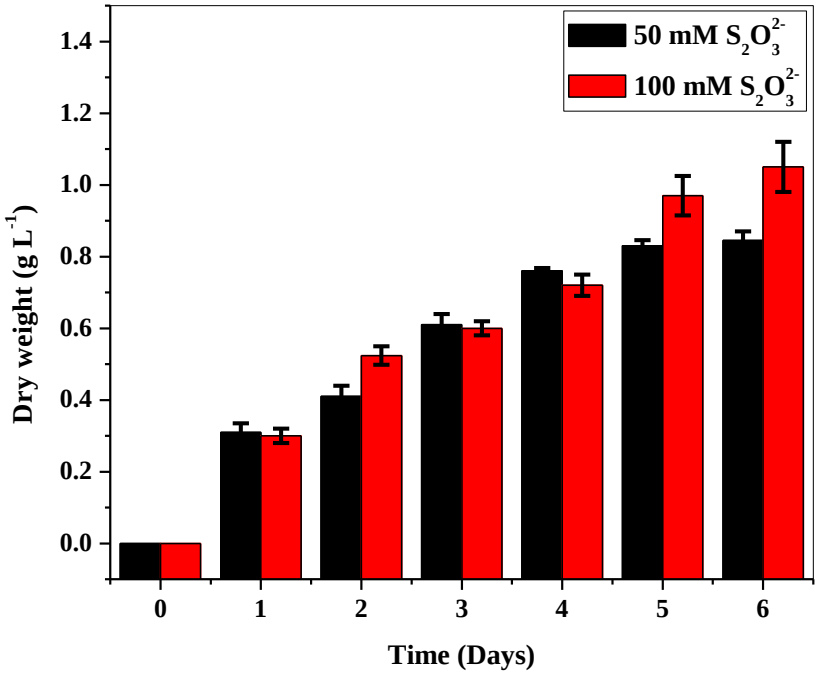

Fig. 5.17 Biomass growth (g L^{-1}) of *H. stevensii* at different $S_2O_3^{2-}$ concentration.[1]

Table 5.2: P (g L^{-1} d^{-1}), X_{Max} (g L^{-1}), R_{CO2} (g_{CO2} L^{-1} d^{-1}) and $R.R_{CO2}$ values estimated for *B. cereus*, mixed microbial population, *E. cloacae*, *P. putida*, *P. aeruginosa* and *H. stevensii* at different energy substrate concentrations (Fe[II] or $S_2O_3^{2-}$).

Species	Fe[II] (ppm) or $S_2O_3^{2-}$ concentration (mM)	P (g L^{-1} d^{-1})	X_{Max} (g L^{-1})	R_{CO2} (g_{CO2} L^{-1} d^{-1})	$R.R_{CO2}$ (%)
B. cereus	50	0.0374 (±0.0006)	0.187 (±0.003)	0.0466 (±0.0003)	32.3 (±0.0071)
	100	0.0512 (±0.002)	0.256 (±0.008)	0.0638 (±0.003)	44 (±0.02)
	200	0.0772 (±0.00056)	0.386 (±0.002)	0.0962 (±0.00071)	66.6 (±0.0014)
Mixed microbial population	50	0.054 (±0.0014)	0.336 (±0.01)	0.0675 (±0.0021)	40.13 (±0.101)
	100	0.078 (±0.004)	0.48 (±0.02)	0.107 (±0.018)	57.67 (±0.04)
E. cloacae	50	0.0305 (±0.0035)	0.23 (±0.014)	0.038 (±0.004)	27.64 (±0.17)
	100	0.036 (±0.0042)	0.248 (±0.022)	0.0445 (±0.005)	29.77 (±0.28)
P. putida	50	0.0495 (±0.004)	0.3 (±0.028)	0.0617 (±0.006)	36.47 (±0.7)
	100	0.056 (±0.0056)	0.355 (±0.03)	0.07 (±0.007)	42.66 (±0.54)
P. aeruginosa	50	0.0172 (±0.001)	0.131 (±0.005)	0.0214 (±0.001)	13.8 (±0.7)
	100	0.024 (±0.0025)	0.21 (±0.015)	0.0302 (±0.0031)	22.16 (±1.14)
H. stevensii	50	0.14 (±0.006)	0.845 (±0.025)	0.174 (±0.007)	67.79 (±1.2)
	100	0.174 (±0.016)	1.05 (±0.07)	0.215 (±0.02)	84.18 (±2.1)

5.3.3 Screening of best CO_2 utilizing strain

The results obtained for the CO_2 bio-mitigation batch studies of different microbial species isolated from STP and SSL using different energy substrate concentrations are summarized in Tables 5.1 and 5.2. It was observed that the η_{CO2} value was found to decrease in the order of microorganisms *H. stevensii* > *P.* aeruginosa > *B. Cereus* > Mixed Microbial population > *P. putida* > *E.* cloacae at approximately similar initial head space CO_2(g) concentration (Table 5.1). The growth response of *H. stevensii* in terms of *P*, X_{Max}, R_{CO2} and $R.R_{CO2}$ was found to be better than the growth response of other microbial species used in the present study (Table 5.2). The net energy gained by oxidizing $S_2O_3^{2-}$ was found to be many times higher than the energy gained by oxidizing Fe[II]. This may be one of the reasons for the higher values of η_{CO2}(g) in case of *H. stevensii* (Ritmann and McCarty, 2012).

Thus, *H. stevensii* emerged as a superior candidate than mixed microbial population and other isolates on the basis of CO_2(g) utilization. Hence, *H. stevensii* can be employed for the development of sustainable and cost effective CO_2 bio-mitigation system.

5.4 Product analysis

Preliminary identification and characterization of the substances present in the cell lysate and supernatant obtained from CO_2 fixation batch studies were carried out using FT-IR and GC-MS.

5.4.1 Culture obtained from STP

5.4.1.1 FT-IR analysis

The knowledge of functional group present in the compound is sufficient to confirm that the compound belongs to a particular group and hence, helps in identification and characterization.

Thus, peak attribution was carried out according to the available literature for the identification of functional group (Jiang et al., 2012; Meng et al., 2014; Basu et al., 2015).

FT-IR spectra observed for the cell lysate extract and cell free supernatant extract of *B. cereus*, mixed microbial population, *E. cloacae* and *P. putida* obtained from CO_2 bio-mitigation shake flask studies at 100 ppm Fe[II] concentration have shown distinct peaks in the region of 4000 - 500 cm^{-1} (Figs.5.18 - 5.25). The specific values of the wave number related to different peaks for cell lysate extract and cell free supernatant extract of respective species are given in Table 5.3.

In the spectra obtained for all species, the major peaks were found in the region of 3600 - 3000 cm^{-1}, 3000 - 2800 cm^{-1}, 1700 -1600 cm^{-1}, 1500 -1400 cm^{-1}, 1300 -1000 cm^{-1} and 800 - 600 cm^{-1} (Table 5.3). The spectra obtained for cell lysate extract and cell free supernatant extract of *B. cereus*, mixed microbial population, *E. cloacae* and *P. putida* have shown the wide and strong peak in the region of 3600 - 3000 cm^{-1} which refers to the hydroxyl group (-OH) of carboxylic acid (Table 5.3). The peaks obtained in region 3000 - 2800 cm^{-1} indicated the -CH stretching of long chain fatty acids. Sometimes, the wider peak of -OH group would superimpose the peaks of sharp -CH stretching and hence they are difficult to differentiate. In the case of mixed microbial culture and *E. cloacae* cell lysate, it was difficult to differentiate –OH and –CH groups (Figs. 5.20 and 5.22). The characteristic peak of –C=O group, represents either the cell bound fatty acids or the amide (I) band of proteins and was confirmed by the peaks obtained in the region of 1700 - 1600 cm^{-1}. The presence of peak in the region of wave number 1500 - 1400 cm^{-1} has indicated either the -C=O group of carbonate ion formed due to the CO_2 fixation or due to the bending of -CH present in aliphatic group and -OH bending of COOH group (Table 5.3). The occurrences of peaks in the region of wave number 1300 - 1100 cm^{-1} have represented CN group

and -C-O group of proteins. The C-O-C and C-O Stretching of COOH group from lipids or polysaccharides was confirmed by the presence of peaks obtained in the region of wave number 1100 - 1000 cm^{-1}. The presence of compounds having un-saturation (double bond) and C-H rock of long chain alkanes were observed by the peaks obtained in the region of wave number 800 - 600 cm^{-1}. Thus, FT-IR analysis of the cell lysate and cell free supernatant extract obtained from *B. cereus*, mixed microbial population, *E. cloacae* and *P. putida* have revealed the presence of organic compounds having functional groups such as C=O, -OH, C-O, C=C.

FT-IR spectrum alone was not sufficient to provide the qualitative and quantitative information of organic compounds present in the sample. Hence, the cell lysate extract and cell free supernatant extract of all species were further characterized using GC-MS and the results obtained are given in subsequent subsection.

5.4.1.2 GC-MS analysis

GC-MS analysis of the cell lysate extracts obtained from *B. cereus*, mixed microbial population, *E. cloacae* and *P. putida* has revealed the presence of fatty acids and hydrocarbons (Tables 5.4 - 5.7). The carbon chain lengths present in the fatty acids were found in the range of C_{11} to C_{19}. Benzoic acid, tetradecanoic acid, hexadecanoic acid, octadecanoic acid and 9-octadecanoic acid are the major fatty acids present in the cell lysate extract of all four species (Tables 5.4 - 5.7). The cell lysate extracts of *B. cereus* and mixed microbial population have shown the presence of aromatic and unsaturated fatty acids (Tables 5.4 and 5.5). The total fatty acids contents of the cell lysate extracts for *B. cereus*, mixed microbial population, *E. cloacae* and *P. putida* were obtained as 3.74%, 2.76%, 1% and 0.54%, respectively. The smaller size of the prokaryotic cell in comparison to eukaryotic cell may be the possible reason for lesser cellular fatty acid content

(Bharti et al., 2014). Most of the fatty acids present in the cell lysate extract falls in the range of carbon chain length C_{14}-C_{18} (Tables 5.4 - 5.7). The obtained fatty acids can be suitably converted into biodiesel via transestrification reaction (Bharti et al., 2014).

The cell lysate extracts of all four species have shown the presence of hydrocarbons having carbon chain length in the range of C_{10}-C_{24} (Tables 5.4 - 5.7). The hydrocarbon content of cell lysate extracts of mixed microbial population and *E. cloacae* are comprised of saturated, unsaturated and branched hydrocarbons (Tables 5.5 and 5.6). However, the cell lysate extracts of *B. cereus* and *P. putida* were found to contain only saturated hydrocarbons (Tables 5.4 and 5.7). The total hydrocarbon content for the cell lysate extracts of *B. cereus*, mixed microbial population, *E. cloacae* and *P. putida* were observed as 2.55%, 10.71%, 10.64% and 2.1%, respectively (Tables 5.4 - 5.7). These hydrocarbons are having compositions equivalent to light oil or kerosene and hence, can be utilized as a fuel. The cell lysate extracts of mixed microbial population and *E. cloacae* have shown the presence of unsaturated hydrocarbons in considerable amount. This can be used as a precursor for the production of compounds such as higher alcohols, alkanes, halides, polymer products, etc.

The cell free supernatant extracts obtained from CO_2 bio-mitigation studies of all four species were analyzed using GC-MS. This analysis confirmed the presence of fatty acids and hydrocarbon in extractable form (Tables 5.4 - 5.7). The fatty acids were found to have carbon chain length in the range of C_5-C_{19} which mainly comprised of saturated, unsaturated and branched hydrocarbons (Tables 5.4 - 5.7). Analysis of cell free supernatant of *B. cereus* and mixed microbial population revealed the presence of 16.24% and 22.17% fatty acids of the total supernatant extract, respectively (Tables 5.4 - 5.7). *B. cereus* extract has revealed the presence of maximum amount of unsaturated fatty acids (Table 5.4). The fatty acids contents of cell free

supernatant extracts of *E. cloacae* and *P. putida* were found to be 0.93% and 6.32%, respectively which was less in comparison to fatty acid content of *B. cereus* and mixed microbial population (Tables 5.4 - 5.7). The obtained results indicated that the fatty acids composition of the cell free supernatant extract of all four species can be utilized for the biodiesel production via transestrification.

GC-MS analysis of cell free supernatant extract also revealed the presence of hydrocarbons having carbon chain length in the range of C_{10}-C_{24}. The hydrocarbons content of the cell free supernatant extracts for *B. cereus*, mixed microbial population, *E. cloacae* and *P. putida* were found as 6.78%, 22.38% (4.35% unsaturated & branched), 24.62% (23.86% unsaturated & branched) and 6.9% (1.15% unsaturated & branched), respectively (Tables 5.4 - 5.7). The composition of hydrocarbons was found to be similar to that of light oil or kerosene oil and hence, it can be utilized as fuels. Presence of higher unsaturated hydrocarbons in cell free supernatant extract of *E. cloacae* makes it an excellent candidate for the production of chemicals such as higher alcohols, alkanes, halides, polymer products, etc.

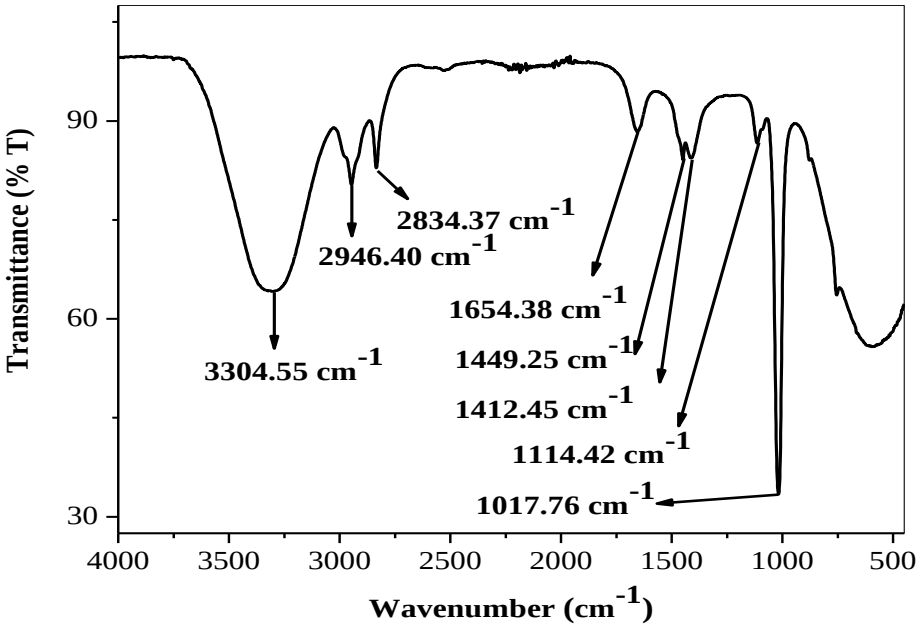

Fig. 5.18 FT-IR spectrum of cell lysate extract of *B. cereus* SM1.

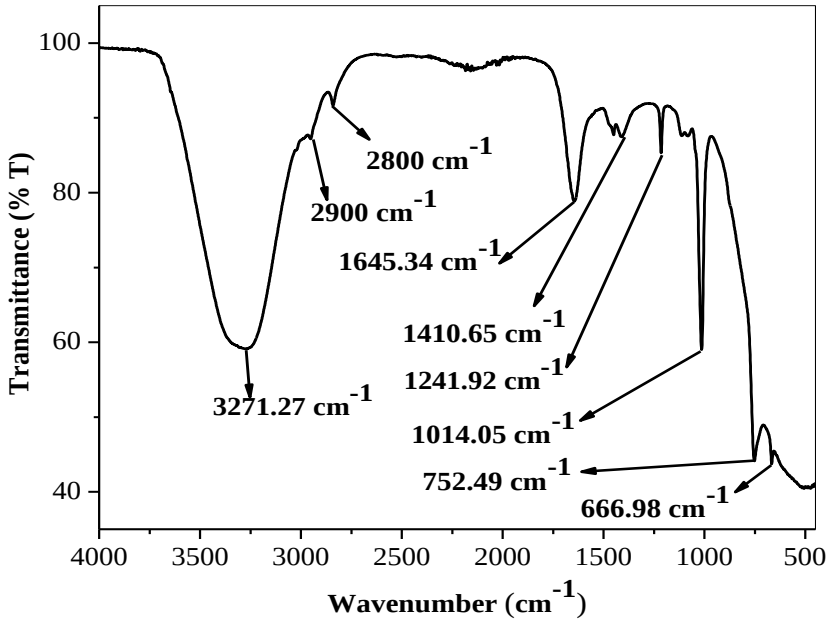

Fig. 5.19 FT-IR spectrum of cell free supernatant extract of *B. cereus* SM1.

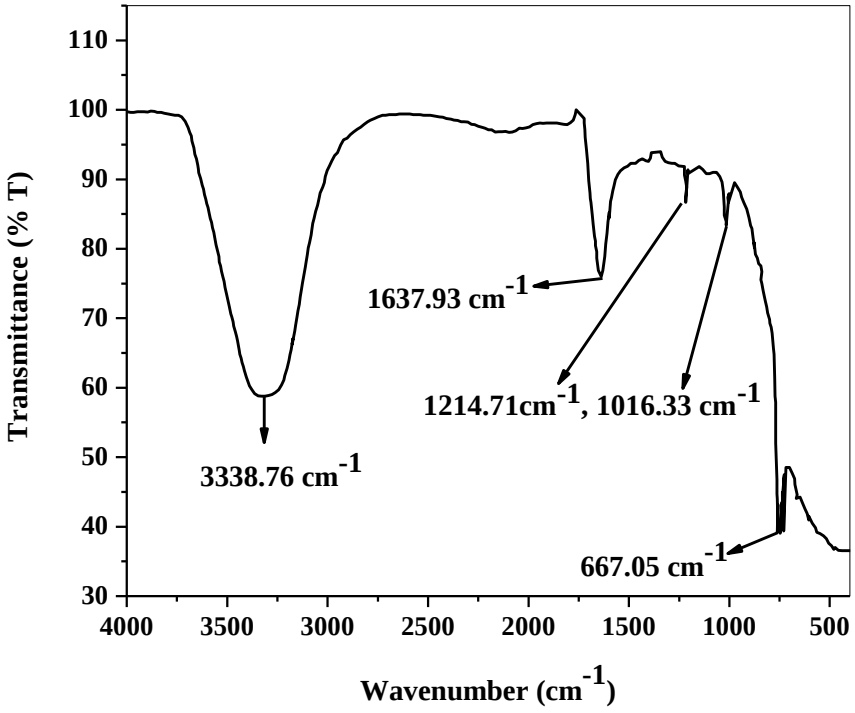

Fig. 5.20 FT-IR spectrum of cell lysate extract of mixed microbial population.

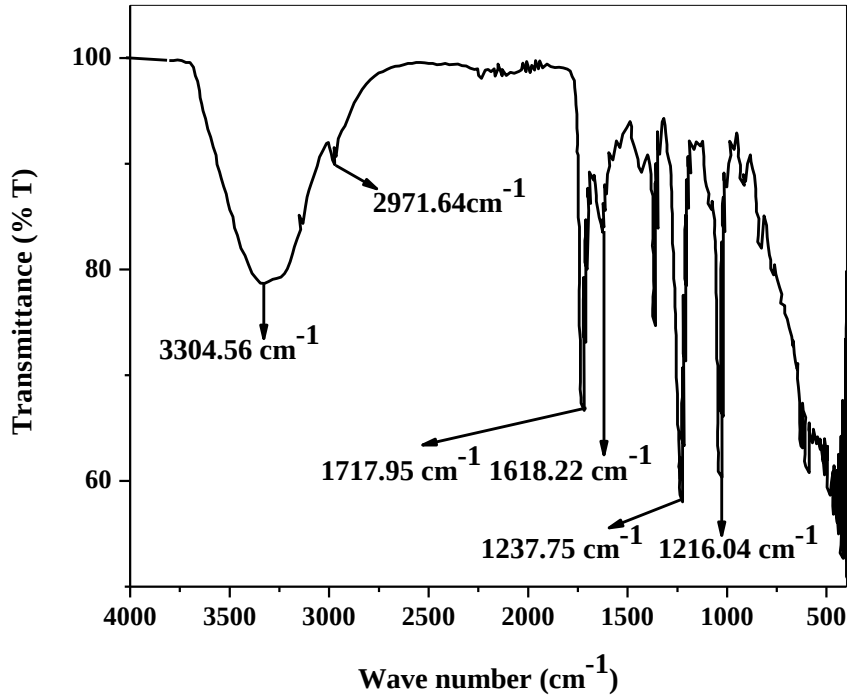

Fig. 5.21 FT-IR spectrum of cell free supernatant extract of mixed microbial population.

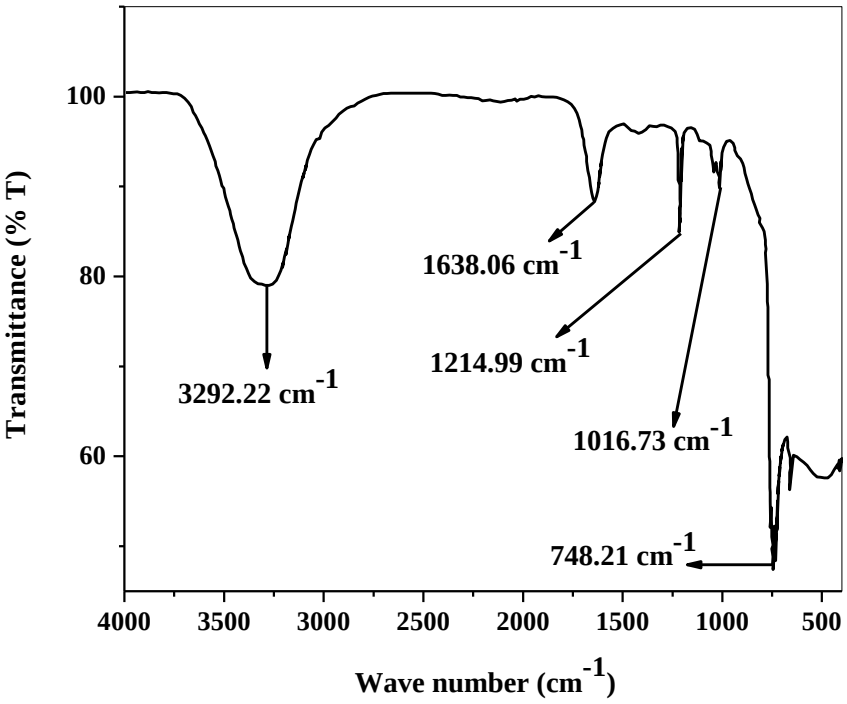

Fig. 5.22 FT-IR spectrum of cell lysate extract of *E. cloacae*.

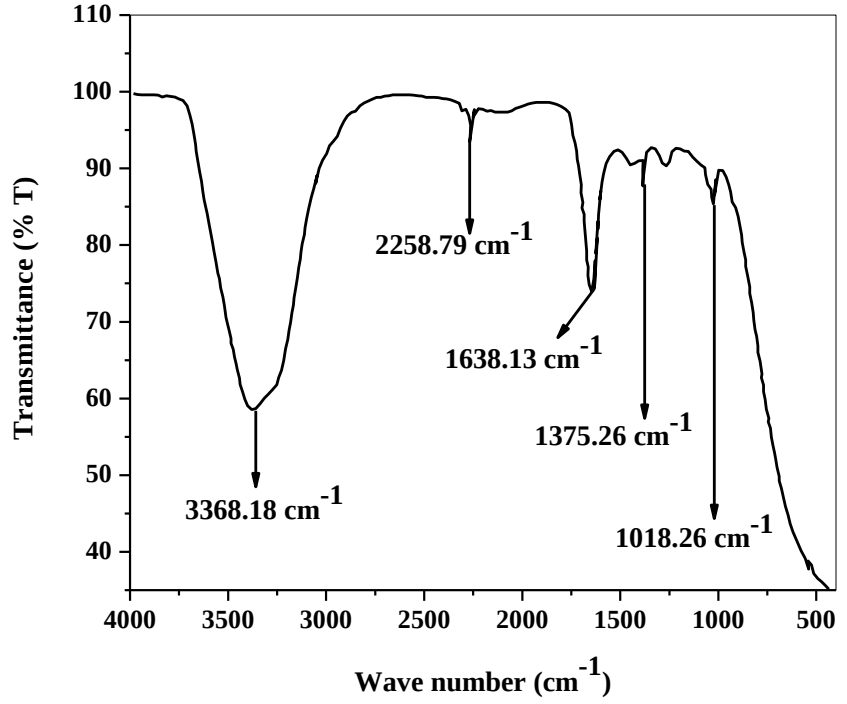

Fig. 5.23 FT-IR spectrum of cell free supernatant extract of *E. cloacae*.

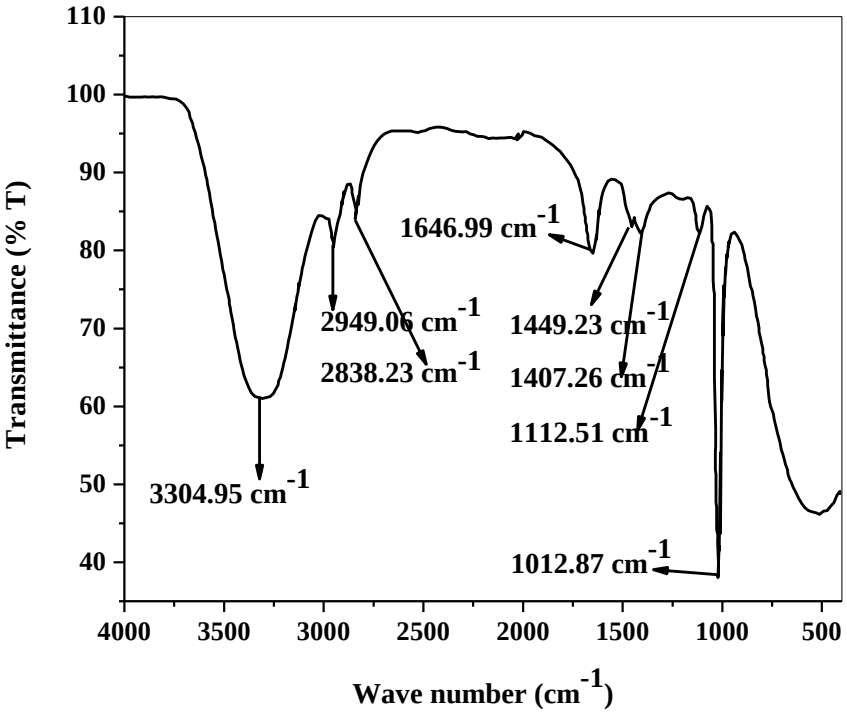

Fig. 5.24 FT-IR spectrum of cell lysate extract of *P. putida*.

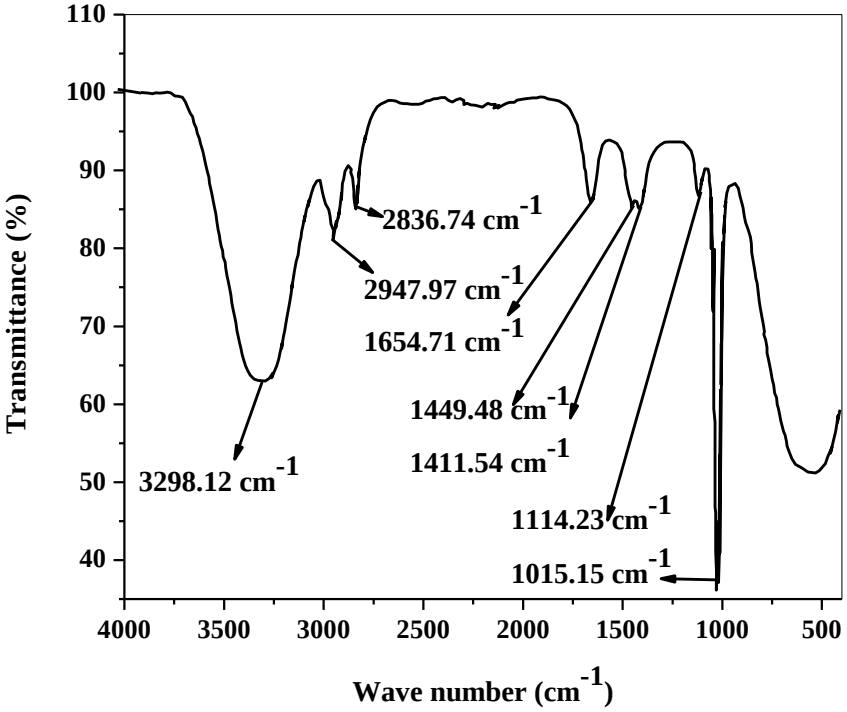

Fig. 5.25 FT-IR spectrum of cell free supernatant extract of *P. putida*.

Table 5.3: Band assignments to peaks obtained for cell lysate extract and cell free supernatant extract of *B. cereus*, mixed microbial population, *P. putida* and *E. cloacae*

	B. cereus **(cm^{-1})**	**Mixed Microbial Population (cm^{-1})**	***E.*** **cloacae (cm^{-1})**	***P. putida*** **(cm^{-1})**	**Group attribution**	**Bio-molecule representation**
Cell lysate extract	3304.55	3338.76	3292.22	3304.95	OH stretching	Carbohydrates, proteins, lipids (sterols and fatty acids), nucleic acids
	2946.40, 2834.37	3000-2800	3000-2800	2949.06, 2838.23	CH stretching	Long chain hydrocarbons
	1654.38	1637.93	1638.06	1646.99	C=O stretch	Lipids, proteins
	1449.25, 1412.45	1500-1400	1500-1400	1449.23, 1407.26	C=O, CH bending , OH bending	Carbonate ion, Aliphatic group, COOH group
	1114.42	1248.17, 1214.71	1214.99	1300-1100	C-N, C-O	Protein
	1017.76	1016.33	1016.73	1112.51, 1012.87	C-O-C, C-O Stretching of COOH	Lipids, polysaccharides
	595.04	751.16, 667.05	748.21, 666.63	-	C=C bending	Alkenes
Cell free supernatant extract	3271.27	3250	3199.99	3298.12	OH stretching	Carbohydrates, proteins, lipids (sterols and fatty acids), nucleic acids
	2900, 2800	3000-2800	3000-2800	2947.97, 2836.74	CH stretching	Long chain hydrocarbons
	1645.34	1750, 1600	1638.06	1654.71	C=O stretch	Lipids, proteins
	1410.65	1500 -1400	1500 - 1400	1449.48, 1411.64	C=O, CH bending , OH bending	Carbonate ion, Aliphatic group, COOH group
	1241.92	1237.75	1155.80	1114.23	C-N, C-O	Protein
	1014.05	1100-1000	1015.69	1015.15, 1086.50	C-O-C, C-O Stretching of COOH	Lipids, polysaccharides

Table 5.4: GC-MS analysis of cell lysate extract and cell free supernatant extract of *Bacillus cereus*

	Run time (min)	Formulae	Compound	% Area	Relative molecular mass	Match quality (%)
Cell lysate extract	14.6	$C_{11}H_{14}O_3$	benzoic acid	0.76	194	89
	19.017	$C_{17}H_{34}O_2$	hexadecanoic acid	0.29	270	89
	20.717	$C_{19}H_{36}O_2$	9-octadecanoic acid (z)-	0.97	296	86
	20.9	$C_{18}H_{36}O_2$	heptadecanoic acid	0.22	284	86
	12.979	$C_{15}H_{32}$	pentadecane	1.76	212	95
	14.2	$C_{17}H_{36}$	heptadecande	0.66	240	92
	15.4	$C_{11}H_{24}$	nonane	0.13	156	87
Cell free supernatant extract	4.429	$C_5H_{10}O_2$	butanoic acid	4.03	102	95
	14.698	$C_{11}H_{14}O_3$	benzoic acid	5.53	194	94
	17.303	$C_{14}H_{28}O_2$	tetradecanoic acid	3.45	228	94
	19.015	$C_{18}H_{36}O_2$	hexadecanoic acid	2.00	284	90
	27.2	$C_{21}H_{42}O_2$	ecosanoic acid	0.41	326	73
	27.483	$C_{21}H_{30}O_2$	dehydroabietic acid	0.35	314	67
	7.359	$C_{10}H_{22}$	decane	0.31	142	86
	7.942	$C_{22}H_{46}$	docosane	0.35	310	89
	12.982	$C_{14}H_{30}$	tetradecane	4.24	198	94
	14.259	$C_{15}H_{32}$	pentadecane	1.62	212	92
	15.467	$C_{11}H_{24}$	nonane	0.26	156	88
Total saturated fatty acid				**10.4 %**		
Total unsaturated fatty acid				**7.61 %**		
Total fatty acid				**18.01 %**		

Table 5.5: GC-MS analysis of cell lysate and cell free supernatant extract obtained from mixed microbial population

	Run Time (min)	Formula	Compound	% Area	Relative molecular mass	Match quality (%)
Cell lysate extract	8.249	$C_{16}H_{34}$	n-hexadecane	0.12	226	92
	8.631	$C_{12}H_{24}$	7-methyl-1-undecene	0.12	168	89
	8.869	$C_{12}H_{24}$	7-methyl-1-undecene	0.14	168	87
	9.882	$C_{12}H_{26}$	n-dodecane	0.12	170	94
	10.893	$C_{13}H_{26}$	1-tridecene	4.36	182	95
	11.618	$C_9H_{10}O_3$	4-ethoxybenzoic acid	0.15	166	80
	12.372	$C_{15}H_{32}$	pentadecane	0.18	212	95
	13.311	$C_{18}H_{36}$	3-octadecene	3.64	252	95
	13.646	$C_{18}H_{38}$	octadecane	0.17	254	92
	14.276	$C_{14}H_{28}O_2$	tetradecanoic acid	1.69	228	96

	14.602	$C_{21}H_{44}$	heptadecane	0.19	296	94
	15.031	$C_{11}H_{22}$	3-methyl-2-decene	0.11	154	79
	15.420	$C_{18}H_{36}$	9-octadecene	0.26	252	95
	15.493	$C_{20}H_{40}$	9-eicosene	0.52	280	94
	16.312	$C_{16}H_{32}O_2$	n-hexadecanoic acid	0.92	256	94
Cell free supernatant extract	4.170	$C_{10}H_{22}$	decane	0.46	142	96
	4.991	$C_{16}H_{34}$	n-hexadecane	0.34	226	94
	7.090	$C_{12}H_{26}$	dodecane	0.86	170	97
	8.015	$C_{14}H_{30}$	tetradecane	0.31	198	92
	8.250	$C_{13}H_{28}$	5-isobutylnonane	0.71	184	94
	8.366	$C_{19}H_{40}$	nonadecane	0.28	268	93
	8.632	$C_{12}H_{24}$	7-methyl-1-undecene	0.6	168	91
	9.884	$C_{14}H_{30}$	tetradecane	1.39	198	97
	10.685	$C_{15}H_{32}$	2,6,10-trimethyldodecane	0.55	212	94
	11.047	$C_{18}H_{38}$	octadecane	0.54	254	92
	11.125	$C_{17}H_{36}$	heptadecane	1.39	240	94
	11.243	$C_{14}H_{30}$	2,3,5,8-tetramethyl-decane	0.27	198	74
	12.374	$C_{24}H_{50}$	tetracosane	1.74	338	96
	12.933	$C_{18}H_{38}$	2,6,10-trimethylpentadecane	0.47	254	93
	13.058	$C_{21}H_{44}$	2,6,10,15-tetramethylheptadecane	0.37	296	91
	13.514	$C_{23}H_{48}$	tricosane	1.29	324	78
	13.932	$C_{10}H_{19}$	2-methyl-2-nonene	3.53	141	77
	14.321	$C_{14}H_{28}O_2$	tetradecanoic acid	10.23	228	97
	14.605	$C_{21}H_{44}$	n-heneicosane	1.82	296	96
	15.636	$C_{20}H_{42}$	eicosane	0.46	282	94
	15.902	$C_{29}H_{60}$	n-nonacosane	0.93	408	91
	16.348	$C_{16}H_{32}O_2$	n-hexadecanoic acid	7.12	256	87
	16.624	$C_{20}H_{42}$	2,6,10,14-tetramethylhexadecane	0.92	282	95
	17.470	$C_{20}H_{40}$	3-eicosene	0.22	280	92
	17.808	$C_{34}H_{70}$	tetratriacontane	0.25	478	90
	17.933	$C_{18}H_{38}$	8-methylheptadecane	0.70	254	91
	18.209	$C_{18}H_{36}O_2$	octadecanoic acid	2.06	284	93
	18.467	$C_{21}H_{44}$	n-heneicosane	0.77	296	96
	19.859	$C_{44}H_{90}$	tetratetracontane	0.65	618	90
	25.551	$C_{32}H_{66}$	n-dotriacontane	0.19	450	87
	25.914	$C_{27}H_{56}$	n-heptacosane	0.37	380	90

	4.170	$C_{10}H_{22}$	decane	0.46	142	96
Total saturated fatty acid				**22.02 %**		
Total unsaturated fatty acid				**0.15 %**		
Total fatty acid				**22.17 %**		

Table 5.6: GC-MS analysis of *E. cloacae* cell lysate and cell free supernatant extract

	Run Time (min)	**Formula**	**Compound**	**% Area**	**Relative molecular mass**	**Match quality (%)**
Cell lysate extract	8.015	$C_{12}H_{26}$	dodecane	0.08	170	90
	8.250	$C_{14}H_{30}$	tetradecane	0.17	198	92
	8.632	$C_{12}H_{24}$	1-undecene	0.17	168	89
	8.749	$C_{12}H_{24}$	2-undecen	0.08	168	87
	10.894	$C_{13}H_{26}$	1-tridecene	4.65	182	94
	13.314	$C_{18}H_{36}$	3-octadecene	3.99	252	94
	13.509	$C_{23}H_{48}$	tricosane	0.15	324	74
	14.268	$C_{18}H_{34}O_2$	9-octadecenoic acid	0.42	282	94
	15.027	$C_{11}H_{22}$	3-methyl-2-decene	0.43	154	77
	15.502	$C_{22}H_{44}$	1-docosene	0.60	308	92
	15.900	$C_{20}H_{42}$	eicosane	0.14	282	91
	16.314	$C_{18}H_{34}O_2$	octadecenoic acid	0.58	282	90
Cell free supernatant extract	9.878	$C_{17}H_{36}$	heptadecane	0.12	240	89
	10.899	$C_{17}H_{34}$	heptadec-8-ene	0.43	238	89
	12.370	$C_{14}H_{30}$	n-tetradecane	0.30	198	93
	13.316	$C_{19}H_{38}$	1-nonadecene	0.40	266	89
	13.945	$C_{12}H_{24}$	2-undecene	5.51	168	77
	14.228	$C_{10}H_{19}$	2-methyl-2-nonene	0.53	141	75
	15.108	$C_{11}H_{22}$	3-methyl-2-decene	16.88	154	76
	16.567	$C_{20}H_{40}$	9-eicosene	0.11	280	88
	16.622	$C_{24}H_{50}$	n-tetracosane	0.22	338	94
	21.836	$C_{19}H_{38}O_4$	hexadecanoic acid	0.37	330	87
	22.379	$C_{24}H_{38}O_4$	1,2-benzenedicarboxylic acid	0.56	390	93
	9.878	$C_{17}H_{36}$	heptadecane	0.12	240	89
Total saturated fatty acid				**0.95 %**		
Total unsaturated fatty acid				**1.01 %**		
Total fatty acid				**1.96 %**		

Table 5.7: GC-MS analysis of *P. putida* cell lysate and cell free supernatant extract

	Run Time (min)	Formula	Compound	% Area	Relative molecular mass	Match quality (%)
Cell lysate extract	12.979	$C_{15}H_{32}$	pentadecane	1.45	212	94
	14.257	$C_{17}H_{36}$	heptadecane	0.54	240	91
	15.467	$C_{11}H_{24}$	3-methyldecane	0.11	156	84
	17.348	$C_{16}H_{32}O_2$	hexadecanoic acid	0.54	256	84
Cell free supernatant extract	7.360	C_9H_{20}	2,2,3-trimethylhexane	0.43	128	87
	12.984	$C_{13}H_{28}$	n-tridecane	4.07	184	93
	14.259	$C_{17}H_{36}$	heptadecane	1.68	240	93
	15.467	$C_{11}H_{24}$	3,7-dimethylnonane	0.29	156	88
	17.306	$C_{14}H_{28}O_2$	n-tetradecanoic acid	2.85	228	92
	19.367	$C_{16}H_{32}O_2$	n-hexadecanoic acid	3.47	256	85
	7.360	C_9H_{20}	2,2,3-trimethylhexane	0.43	128	87
Total saturated fatty acid				**6.86 %**		
Total unsaturated fatty acid				**-**		
Total fatty acid				**6.86 %**		

5.4.2. Culture obtained from SSL

5.4.2.1 FT-IR analysis

Preliminary identification and characterization of substances present in the cell lysate and cell free supernatant extracts of *P. aeruginosa* and *H. stevensii* obtained from CO_2 fixation batch studies were carried out using FT-IR spectroscopy. The specific values of the wave numbers related to different peaks for cell lysate extracts and cell free supernatant extracts of *P. aeruginosa* and *H. stevensii* were observed in the specific region of the spectrum and are given in Table 5.8.

FT-IR spectra of cell lysate extracts of *P. aeruginosa* and *H. stevensii* obtained after CO_2 mitigation batch studies displayed absorption spectrum in the range of 3700 - 2800 cm^{-1}, 2000 - 1300 cm^{-1} and 1200 - 1000 cm^{-1} (Figs. 5.26 and 5.27). Peaks obtained at 3280.27 cm^{-1} for *P. aeruginosa* and at 3257.62 cm^{-1} for *H. stevensii* indicated the presence of -OH stretching. This belongs to the alcoholic compounds which are having free or intermolecular hydrogen bonding (Kalsi, 2004). Peaks obtained between 3000 cm^{-1} and 2800 cm^{-1} represented the -CH stretching of long chain hydrocarbons (Table 5.8). Peaks observed at 1647.12 cm^{-1} and 1654.18 cm^{-1} for cell lysate extracts of *P. aeruginosa* and *H. stevensii*, respectively indicated the characteristic peak of –C=O group due to the cell bound fatty acids or the amide (I) band of proteins or the C=C stretching of alkenes (Kalsi, 2004). Peaks observed between 1500 and 1400 cm^{-1} revealed the presence of C=O group of carbonate ion. The presence of carbonate ion may be due to the CO_2 fixation or -CH bend of aliphatic group or C-O-H bend and O-H bend in the same plane (Table 5.8). Occurrence of peak between 1200 cm^{-1} and 1100 cm^{-1} represented C-C-C bending in the long chain hydrocarbons and has confirmed the presence of C-O stretch of alcoholic compounds (Table 5.8) (Kalsi, 2004).

FT-IR spectra for the cell free supernatant extracts of *P. aeruginosa* and *H. stevensii* obtained from the batch studies are also shown in Figs. 5.28 and 5.29, respectively and reported in Table 5.8. The spectra can be divided into two ranges as 3700 - 2800 cm^{-1} and 2000 - 1000 cm^{-1}. The peaks obtained at 3252.23 cm^{-1} for *P. aeruginosa* and at 3323.97 cm^{-1} for *H. stevensii* represented the -OH stretching of alcoholic compounds which were free of hydrogen bonding. The presence of peak at 1634.22 cm^{-1} and 1637.71 cm^{-1} in the spectra of *P. aeruginosa* and *H. stevensii*, respectively indicated the presence of C=C stretching of alkenes. The occurrence of peak between 1100 cm^{-1} and 1000 cm^{-1} in the spectra of *P. aeruginosa* and *H. stevensii*, represented the -C-O stretch of alcoholic compounds (Fig. 5.28 and 5.29). Absence of -CH stretch of long chain hydrocarbons may be due to the overlapping of strong -OH stretch (Kalsi, 2004). Thus, the FT-IR spectra of cell lysate and supernatant extracts have revealed the presence of compounds having -OH, -CH, C=C and C-O as major functional groups (Kalsi, 2004). Hence, the cell lysate and supernatant extract obtained from CO_2 bio-mitigation studies were consist of different organic compounds such as fatty alcohols and hydrocarbons.

5.4.2.2 GC-MS analysis

The obtained cell lysate extracts and cell free supernatant extracts from CO_2 fixation batch studies were further analyzed using GC-MS for the identification and confirmation of different compounds. Identification of an individual compound present in the sample to its closest match is helpful in developing the strategy for the recovery of the same compound.

GC-MS analysis of the cell lysate extracts obtained from *P. aeruginosa* and *H. stevensii* have revealed the presence of fatty alcohols in considerable amount with match quality ranging from 89% to 98% (Tables 5.9 and 5.10). GC spectrum area obtained for *P. aeruginosa* and *H.*

stevensii was comprised of approximately 40% and 27.84% fatty alcohols, respectively. The fatty alcohols were found to have carbon chain length in the range of C_{12}-C_{18}.

The fatty alcohols mainly present in the cell lysate extract of *P. aeruginosa* were dodecanol (24.90%), tetradecanol (13.0%), pentadecanol (2.26%) and octadecanol (0.52%). The results for *P. aeruginosa* have also shown the presence of fatty acids such as tetradecanoic acid, hexadecanoic acid and fatty aldehyde cis-9-hexadecenal (match quality 89%) in trace amounts (Table 5.9).

The fatty alcohols present in the cell lysate extract of *H. stevensii* were mainly comprised of compounds such as dodecanol (17.76%), tetradecanol (8.66%), pentadecanol (1.08%), octadecanol (0.34%), etc. Other compounds such as fatty aldehyde, cis-9-hexadecenal (match quality of 90%), myristic acid (match quality 95%), n-hexadecanoic acid (match quality 95%), etc. were also found in trace amount in the cell lysate extract of *H. stevensii* (Table 5.10).

The cell free supernatant extracts of *P. aeruginosa* and *H. stevensii* have confirmed the presence of alkanes, alkenes and fatty alcohols with the match quality ranging from 78% to 98% (Tables 5.9 and 5.10). Fatty alcohols obtained from *P. aeruginosa* and *H. stevensii* were accounted for 39.68% and 10.16% of total area of the supernatant extracts, respectively.

The major compound of fatty alcohols obtained from *P. aeruginosa* cell free supernatant extract were dodecanol (19.60%), 2,4-di-tert-butylphenol (1.69%), tetradecanol (10.36%), octadecanol (2.51%), heneicosanol (2.21%), lignoceric alcohol (1.89%) and octacosanol (1.42%). Saturated, unsaturated and branched hydrocarbons were comprise of 7.36% of the total supernatant extract. Trace amounts of fatty acids such as myristic acid (1.04%), cis-vaccenic acid (0.21%), etc. were also present in the supernatant extract (Table 5.9).

The fatty alcohol obtained from cell free supernatant extract of *H. stevensii* comprised of 3, 5-di-t-butylphenol (3.12%), heneicosanol (3.45%), octacosanol (3.45%), etc. The obtained results indicated the presence of saturated, unsaturated and branched hydrocarbons which consist of 20.9% of the total area of the cell free supernatant extract. Fatty acids such as stearic acid (3.07 %) and cis-vaccenic acid (0.35%) were also present in the cell free supernatant extract in trace amount (Table 5.10).

Thus, the total cell extract (cell lysate & supernatant) obtained from *P. aeruginosa* and *H. stevensii* was found to be composed of approximately 80% and 38% fatty alcohols, respectively. This included the compounds having carbon chain length in the range of C_{12}-C_{28}. The obtained fatty alcohols were mainly composed of dodecanol (51.86%) and tetradecanol (23.36%) for *P. aeruginosa* and dodecanol (17.76%) for *H. stevensii*. Hence, the results of GC-MS analysis confirmed that *P. aeruginosa* and *H. stevensii* have assimilated CO_2 as fatty alcohols.

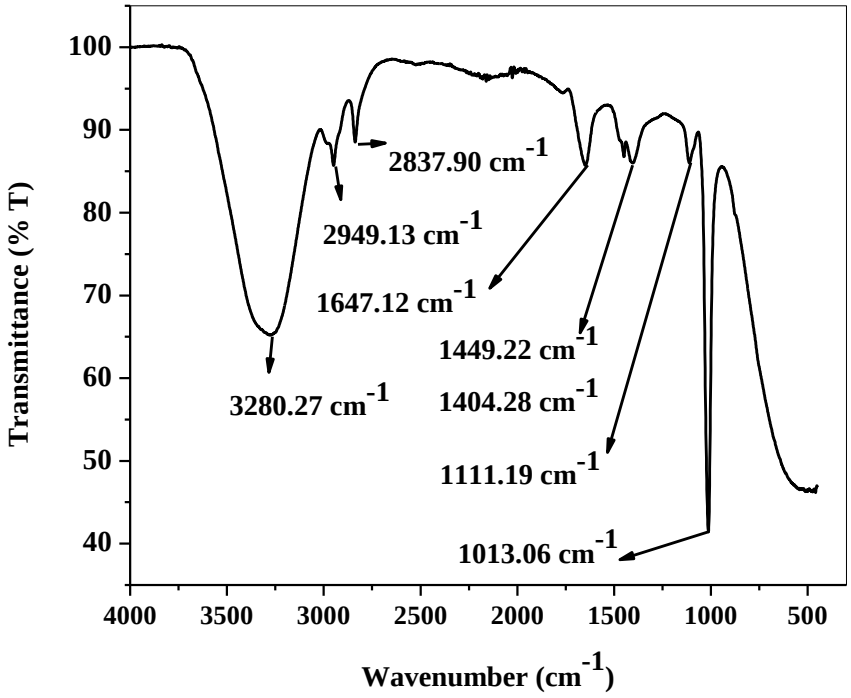

Fig. 5.26 FT-IR spectrum of cell lysate extract of *P. aeruginosa*.

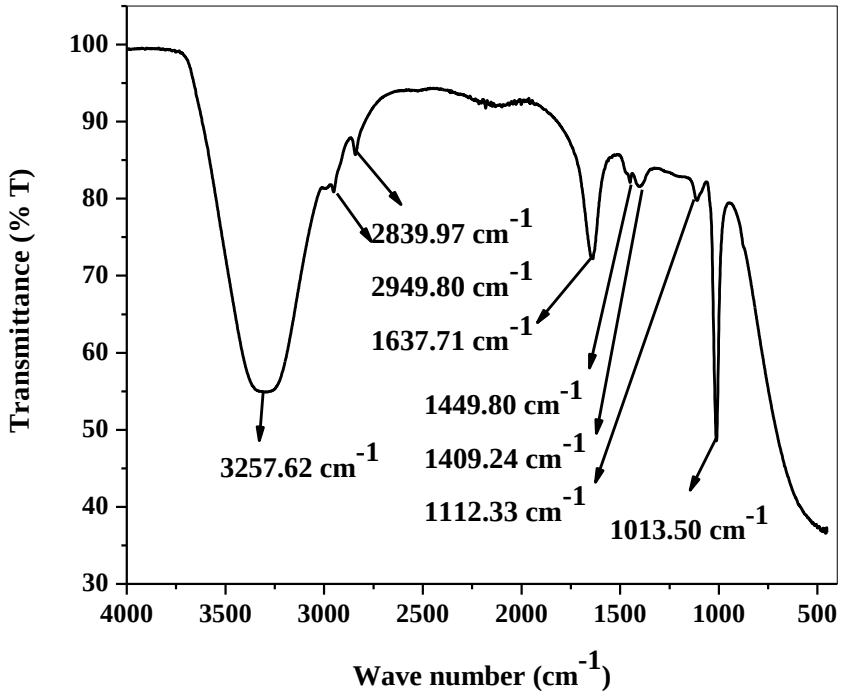

Fig. 5.27 FT-IR spectrum of cell lysate extract of *H. stevensii*.

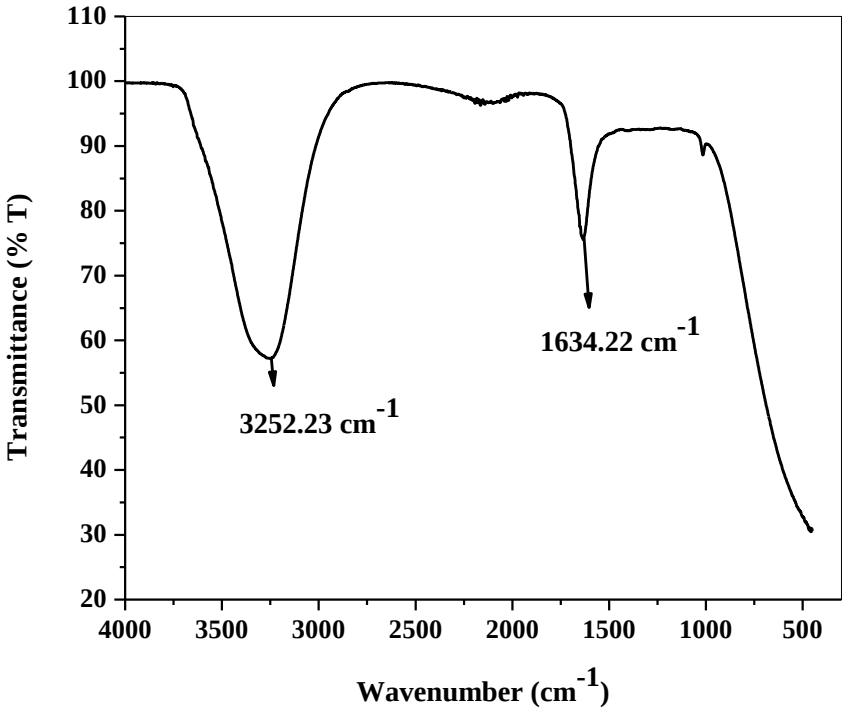

Fig. 5.28 FT-IR spectrum of cell free supernatant extract of *P. aeruginosa*.

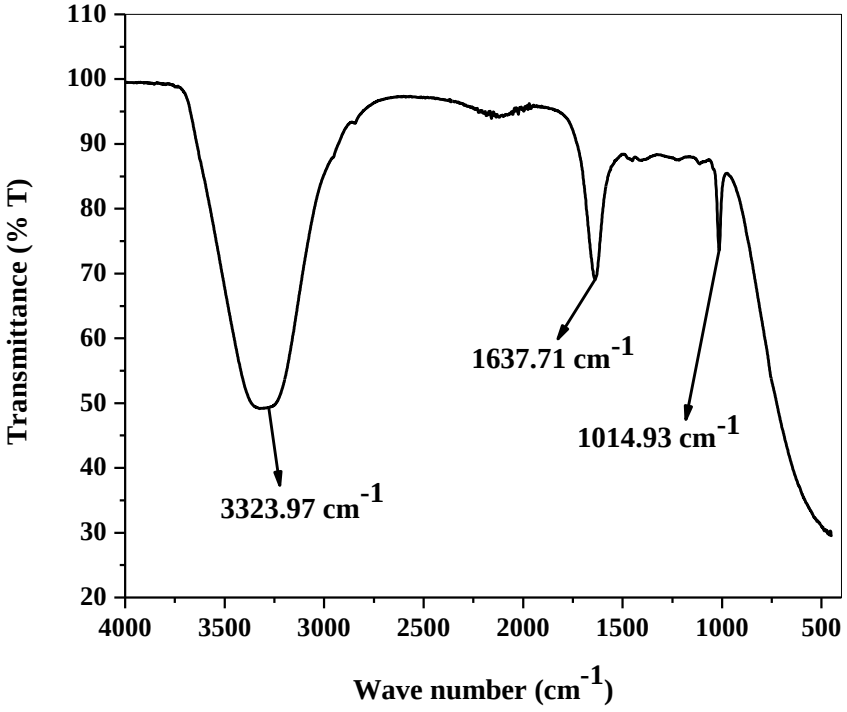

Fig. 5.29 FT-IR spectrum of cell free supernatant extract of *H. stevensii*.

Table 5.8 Band assignments to peaks obtained for cell lysate extracts and cell free supernatant extracts of *P. aeruginosa* and *H. stevensii*

	P. aeruginosa **(cm^{-1})**	***H. Stevensii*** **(cm^{-1})**	**Group attribution**	**Compounds**
Cell lysate extract	3280.27	3257.62	OH stretching	Fatty alcohols, Carbohydrates, proteins, lipids and nucleic acids
	2949.13, 2837.90	2949.80, 2839.97	-CH stretching	Long chain hydrocarbons
	1647.12	1637.71, 1654.18	C=O stretch C=C stretching	Proteins, lipids and alkenes
	1449.22, 1404.28	1409.24	C-O-H bending or O-H bending	Carbonate ion, fatty alcohol
	1111.19	1112.33	C-C-C bending	Long chain hydrocarbons
	1013.06	1014.93, 1013.50	C-O stretch of alcoholic products	Fatty alcohol
Cell free supernatant extract	3252.23	3323.97	OH stretching	Fatty alcohols, Carbohydrates, and lipids
	1634.22	1637.71	C=C stretching	Alkenes
	Around 1100	1014.93	C-O stretch of alcoholic products	Fatty alcohol

Table 5.9: GC-MS analysis of cell lysate extract products and of cell free supernatant extract products extracted in chloroform-methanol of *P. aeruginosa*

	Run Time (min)	**Formula**	**Compound**	**% Area**	**Relative Molecular mass**	**Match quality**
Cell lysate extract	8.204	$C_{10}H_{22}O$	decanol	0.08	158	94
	11.014	$C_{12}H_{26}O$	dodecanol	24.90	186	98
	13.383	$C_{14}H_{30}O$	tetradecanol	13.00	214	98
	14.282	$C_{14}H_{28}O_2$	tetradecanoic acid	0.07	228	92
	15.499	$C_{15}H_{32}O$	pentadecanol	2.26	228	97
	16.329	$C_{16}H_{32}O_2$	hexadecanoic acid	0.21	256	95
	17.472	$C_{18}H_{38}O$	octadecanol	0.52	270	97
	18.055	$C_{18}H_{34}O_2$	cis-9-hexadecenal	0.25	282	89
	4.151	$C_{11}H_{24}$	undecane	0.13	156	95
	4.607	$C_8H_{18}O$	2-ethylhexan-1-ol	0.30	130	95
	6.953	$C_{11}H_{22}$	n-1-undecene	0.57	154	97
	7.068	$C_{13}H_{28}$	n-tridecane	0.30	184	97
	8.227	$C_{14}H_{30}$	4,6-	0.19	198	94

			dimethyldodecane			
	9.772	$C_{14}H_{28}$	1-tetradecene	1.27	196	98
	9.867	$C_{17}H_{36}$	heptadecane	0.17	240	97
	10.670	$C_{13}H_{28}$	3,8-dimethylundecane	0.14	184	92
	10.950	$C_{12}H_{26}O$	dodecanol	19.60	186	98
	12.288	$C_{16}H_{32}$	hexadecene	1.99	224	98
	13.346	$C_{14}H_{30}O$	tetradecanol	10.36	214	98
	13.636	$C_{17}H_{36}$	n-heptadecane	0.25	240	93
	14.326	$C_{14}H_{28}O_2$	tetradecanoic acid	1.04	228	96
	14.537	$C_{18}H_{36}$	octadecene	2.60	252	97
	15.507	$C_{18}H_{38}O$	octadecanol	2.51	270	96
	16.574	$C_{21}H_{44}O$	heneicosanol	2.21	312	97
	17.488	$C_{19}H_{40}O$	nonadecanol	0.26	284	96
	18.078	$C_{18}H_{34}O_2$	cis- octadec-11-enoic acid	0.21	282	88
	18.428	$C_{24}H_{50}O$	tetracosanol	1.89	354	96
	20.295	$C_{28}H_{58}O$	octacosanol	1.42	410	97

Table 5.10: GC-MS analysis of cell lysate extract products and of cell free supernatant extract products extracted in chloroform-methanol of *H. stevensii*

	Run time (min)	**Formula**	**Compound**	**% Area**	**Relative molecular mass**	**Match quality (%)**
Cell lysate extract	11.014	$C_{12}H_{26}O$	dodecanol	17.76	186	98
	13.377	$C_{14}H_{30}O$	tetradecanol	8.66	214	97
	14.290	$C_{14}H_{28}O_2$	myristic acid	0.1	228	95
	15.498	$C_{15}H_{32}O$	pentadecanol	1.08	228	97
	16.334	$C_{16}H_{32}O_2$	n-hexadecanoic acid	0.17	256	95
	17.471	$C_{18}H_{38}O$	octadecanol	0.34	270	97
	18.096	$C_{16}H_{30}O$	cis-9-hexadecenal	0.14	238	90
Cell free supernatant extract	6.951	$C_{12}H_{24}$	1-dodecene	0.64	168	96
	8.227	$C_{14}H_{30}$	4,6-dimethyldodecane	0.28	198	93
	8.869	$C_{12}H_{26}$	3,7-dimethyldecane	0.22	170	91
	9.772	$C_{13}H_{26}$	1-tridecene	1.63	182	97
	9.868	$C_{17}H_{36}$	n-heptadecane	0.20	240	96
	11.487	$C_{14}H_{22}O$	3,5-di-t-butylphenol	3.12	206	94
	12.285	$C_{15}H_{30}$	1-pentadecene	3.05	210	97
	12.363	$C_{15}H_{32}$	pentadecane	0.27	212	96
	14.323	$C_{18}H_{36}O_2$	stearic acid	3.07	284	78

	14.534	$C_{19}H_{38}$	1-nonadecene	3.37	266	97
	15.631	$C_{19}H_{40}$	n-nonadecane	0.25	268	94
	15.890	$C_{20}H_{42}$	n-eicosane	0.54	282	92
	16.572	$C_{21}H_{44}O$	henicosan-1-ol	3.45	312	97
	18.050	$C_{18}H_{34}O_2$	cis-vaccenic acid	0.35	282	87
	18.427	$C_{28}H_{58}O$	octacosanol	3.59	410	96

5.5 Transestrification of fatty acids obtained from STP culture

Product analysis of the cultures obtained from CO_2 bio-mitigation batch studies for *B. cereus*, mixed microbial population, *E. cloacae* and *P. putida* have shown the presence of fatty acids in the extractable amount (section 5.4.1). These acids were further converted to biodiesel via transestrification by following the methodology described in literature (O'Fallon et al., 2007). The fatty acids present in extracts having carbon chain length in the range of C_{14}-C_{18} were found suitable for the biodiesel production. Therefore, the fatty acids having carbon chain length in the range of C_{14}-C_{18} were considered as targeted compounds for determining the product yield. The FAME standard (FAME mix from C_8-C_{24}, Supelco, Sigma Aldrich, Bangluru, India) was acquired and external point calibration methodology was followed to quantify the biodiesel product yield (Cuadros-Rodrìguez et al., 2007). Different concentrations of FAME were prepared using the FAME standard and at each concentration, peak area was acquired in duplicates, averaged and calibration plots were generated. The obtained mathematical best fit equations for tetradecanoic methyl ester, hexadecanoic acid methyl ester, octadecanoic acid methyl ester and cis-9-oleic methyl ester calibration curves along with their R^2 values are given by Eqs. 5.3 - 5.6:

$$Y = 12.83x - 0.6 \qquad R^2 = 0.922 \qquad (5.3)$$

$$Y = 9.11x - 0.56 \qquad R^2 = 0.803 \qquad (5.4)$$

$$Y = 6.3817x - 0.466 \qquad R^2 = 0.77 \qquad (5.5)$$

$$Y = 17.55x - 1.067 \qquad R^2 = 0.81 \qquad (5.6)$$

The identification of the FAME present in the sample was carried out using FAME standard by following retention time comparison methodology (Lee at el., 2010). The individual

and total quantified values of FAME obtained from *B. cereus*, mixed microbial population, *E. cloacae* and *P. putida* are reported in Table 5.11.

The results revealed that the FAME obtained from all the extracts has shown the presence of both saturated and unsaturated FAMEs. The highest concentration of unsaturated FAME was observed in the extract of mixed microbial population followed by *B. cereus* and then *E. cloacae* (Table 5.11). Saturated FAME has high cetane number and oxidative stability, however it possesses poor flow quality at low temperature. On the other hand, unsaturated FAME has better flow quality at low temperature but has low cetane numbers and oxidative stability. Thus, the presence of monounsaturated fatty acid esters along with saturated fatty acid esters was necessary for quality of FAME to be utilized as fuel (Knothe, 2008). Hence, due to the presence of saturation and unsaturation in definite proportion, the FAME obtained from mixed microbial population, *B. cereus* and *E. cloacae* was qualified to be utilized as fuel. The quality of FAME obtained from mixed microbial population was superior as compared to FAME obtained from other species. The product yield in terms of biodiesel production was found highest for mixed microbial population (Table 5.11). It may be due to the higher fatty acid content for mixed microbial population as revealed by GC-MS analysis (Table 5.5).

5.6 Fatty alcohol production obtained from SSL culture

GC-MS analysis of total cell extracts of *P. aeruginosa* and *H. stevensii* has confirmed the presence of fatty alcohols. The major fatty alcohols found in the GC-MS analysis were dodecanol, tetradecanol, pentadecanol in both species and octadecanol in only *P. aeruginosa*.

The obtained leachates of *P. aeruginosa* at 17% (v/v) CO_2 concentration and of *H. stevensii* at 5, 10 and 15% (v/v) CO_2 concentrations were analyzed using GC for the

quantification of fatty alcohols. This quantification was limited to the four products as per the results suggested by GC-MS analysis. The quantification was carried out by following the procedure of multipoint external standard method for GC quantification. Pure compounds were procured and calibration plots for all the analytes were prepared in the range of 0.001 - 0.008 mg, by dissolving 0.1 g of each analyte in 10 mL of chloroform and diluting the mixture to their respective concentrations. The calibration plots of dodecanol, tetradecanol, pentadecanol and octadecanol were fitted linearly and are given by Eqs. 5.7 - 5.10, respectively. The samples were analyzed in triplicates and an average value of peak area is used to generate the calibration plot.

Dodecanol $Y = 4.4\times10^{7} X - 50860.5$ $R^2 = 0.86$ (5.7)

Tetradecanol $Y = 4.7\times10^{7} X - 53741.9$ $R^2 = 0.87$ (5.8)

Pentadecanol $Y = 4.5\times10^{7} X - 51139.2$ $R^2 = 0.87$ (5.9)

Octadecanol $Y = 4.3\times10^{7} X - 49752.05$ $R^2 = 0.87$ (5.10)

The fatty alcohols obtained from the biomass of *P. aeruginosa* were found to be comprised of 2.62 (±0.024) mg dodecanol, 4.00 (±0.04) mg tetradecanol, 2.62 (±0.085) mg pentadecanol and 2.56 (±0.046) mg octadecanol. Hence, total fatty alcohols in terms of product yield were calculated as 0.392 (±0.14) g g^{-1} (biomass). The study revealed that *P. aeruginosa* has shown the potential to be used as a source for the production of fatty alcohols via CO_2 fixation.

GC analysis for the quantification of dodecanol, tetradecanol and pentadecanol in leachate of *H. stevensii* obtained at different CO_2 concentrations is reported in Table 5.12. The analysis has revealed the presence of dodecanol, tetradecanol and pentadecanol as primary metabolites. As the CO_2 concentration was increased from 5% to 15% (v/v), concentrations of dodecanol and tetradecanol have also increased from 2.5 (±0.1) mg to 3.43 (±0.05) mg and 2.28 (±0.15) mg to 2.96 (±0.18) mg, respectively (Table 5.12). However, the concentration of

pentadecanol was found to be approximately same at 5% and 10% CO_2 concentrations (v/v). Presence of pentadecanol was not observed at 15% (v/v) inlet CO_2 concentration. It was observed, that with the increase in CO_2 inlet concentration from 5% to 15%, formation of fatty alcohols having odd chain length decreased and those of even chain length increased. Total fatty alcohols in terms of product yield were obtained as 0.355 (±0.01), 0.377 (±0.06) and 0.32 (±0.016) g g^{-1} of biomass at 5%, 10% and 15% CO_2 concentration (v/v), respectively (Table 5.13). At 15% CO_2 concentration, the obtained values of total fatty alcohols [0.32 (± 0.016) g g^{-1} (biomass)] were lower than the value [0.377 (± 0.06) g g^{-1} (biomass)] obtained at 10% CO_2 concentration (v/v). The possible reason for this was the limitation of the availability of pure compounds for GC quantification as GC-MS results showed the presence of higher fatty alcohols (Table 5.12).

Table 5.11: Individual FAME concentration (mg per 100 mg of biomass) obtained from the extracts of *B. cereus*, mixed microbial population, *E. cloacae* and *P. putida.* Data are shown as mean ± SD (mean ± standard deviation)

Species	Tetradecanoic methyl ester	Hexadecanoic acid methyl ester	Octadecanoic acid methyl ester	cis-9-Oleic methyl ester	Total yield of biodiesel production
B. cereus	13.95 (±0.002)	38.36 (±0.04)	18.7 (±0.02)	15.49 (±0.01)	86.5 (±0.048)
Mixed microbial population	17.79 (±0.94)	31.44 (±0.91)	23.22 (±0.0.64)	19.1 (±0.51)	91.55 (±0.198)
E. cloacae	16.2 (±0.67)	17.05 (±0.168)	22.48 (±0.105)	14.1 (±0.51)	77.49 (±0.1)
P. putida	8.68 (±0.34)	12.97 (±1.09)	17.03 (±0.24)	-	38.69 (±1.66)

Table 5.12: Dodecanol, tetradecanol and pentadecanol contents and total product yield of *P. aeruginosa* and *H. stevensii* under different CO_2 concentrations. Values are represented with the mean (±) standard deviation (mean ± SD)

S.No.	Compounds	Product recovery (mg per 50 mL)			
		P. aeruginosa	*H. stevensii*		
		15% CO_2 (%v/v)	**5%** CO_2 (%v/v)	**10%** CO_2 (%v/v)	**15%** CO_2 (%v/v)
1.	Dodecanol	2.62 (±0.024)	2.5 (±0.1)	2.78 (±0.2)	3.43 (±0.05)
2.	Tetradecanol	4.00 (±0.04)	2.28 (±0.15)	2.44 (±0.06)	2.96 (±0.18)
3.	Pentadecanol	2.62 (±0.085)	2.31 (±0.03)	2.32 (±1.6)	-
4.	Octadecanol	2.56 (±0.046)	-	-	-
Total fatty alcohol content		**11.82 (±0.15)**	**7.09 (±0.18)**	**7.54 (±1.27)**	**6.39 (±0.33)**
Total Product yield (g $g^{-1}$of biomass)		**0.392 (±0.14)**	**0.3545 (±0.01)**	**0.377 (±0.06)**	**0.3195 (±0.016)**

5.7 Aboitic stress tolerance of SSL cultures

The growth of the microorganisms was governed by different physicochemical parameters such as salt, pH and temperature. These parameters not only regulate the transport of nutrient across cells but also determine cellular organic pool compositions. Therefore, the response of *P. aeruginosa* for varying salt and temperature stress and *H. stevensii* for varying salt, pH and temperature stress are studied. The maximum specific growth rate (μ_{Max}, h^{-1}) of the isolate *P. aeruginosa* and *H. stevensii* was calculated at different physicochemical stresses. The obtained results of *P. aeruginosa* and *H. stevensii* are shown in Fig. 5.30 and 5.31, respectively.

The effect of varying salt concentration and temperature on growth of *P. aeruginosa* is shown in Fig. 5.30(a) and (b), respectively. It was observed that the *P. aeruginosa* was able to tolerate the salt concentration up to 6% (w/v). The maximum specific growth (μ_{Max}, h^{-1}) of *P. aeruginosa* was found to be 0.425 (±0.0025) h^{-1} at 3% (w/v) salt concentration [Fig. 5.30(a)]. The obtained result revealed that the *P. aeruginosa* was able to tolerate the temperature up to 60 ^{o}C. The μ_{Max} was observed as 0.34 (±0.0063) h^{-1} at 35 ^{o}C for *P. aeruginosa* [Fig. 5.30(b)]. Thus, *P. aeruginosa* was able to adopt to varying environmental conditions of salinity and temperature. Hence, *P. aeruginosa* was found to be one of the suitable candidates for the development of CO_2 mitigation system which can be utilized at extreme environment conditions.

The effects of salt concentration, pH and temperature on the growth of *H. stevensii* in terms of maximum specific growth are shown in Fig. 5.31 (a), (b) and (c), respectively. A significant growth of *H. stevensii* was observed under various salt concentrations in the range of 2-12% (w/v). Maximum specific growth rate has substantially decreased with the increase in salt concentration beyond 11% (w/v). At 6% (w/v) salt concentration, highest μ_{Max} value of 0.42 (±0.001) d^{-1} was observed [Fig. 5.31(a)]. *H. stevensii* was able to grow in the pH range of 6.0-12.0 and μ_{Max} was obtained as 0.42 (±0.014) d^{-1} at pH 8 [Fig. 5.31(b)]. The temperature tolerance

results have revealed that *H. stevensii* was growing in a temperature range of 25-60 ^{o}C. The value of μ_{Max} was found to increase from 0.07 (±0.02) d^{-1} to 0.625 (±0.03) d^{-1} with increase in temperature from 10 to 50 ^{o}C, respectively and was further decreased to 0.305 (± 0.023) d^{-1} with increase in temperature up to 60 ^{o}C [Fig. 5.31(c)]. Thus, *H. stevensii* has shown the capability to grow at temperature greater than 45 ^{o}C while other bacterial species of same genera (closest relatives) were not able to grow (Gaboyer et al., 2014). Hence, the isolate was found to be thermophilic euryhaline phenotype and the traits suggested that it has an ability to withstand the changes in various operational conditions in industrial systems.

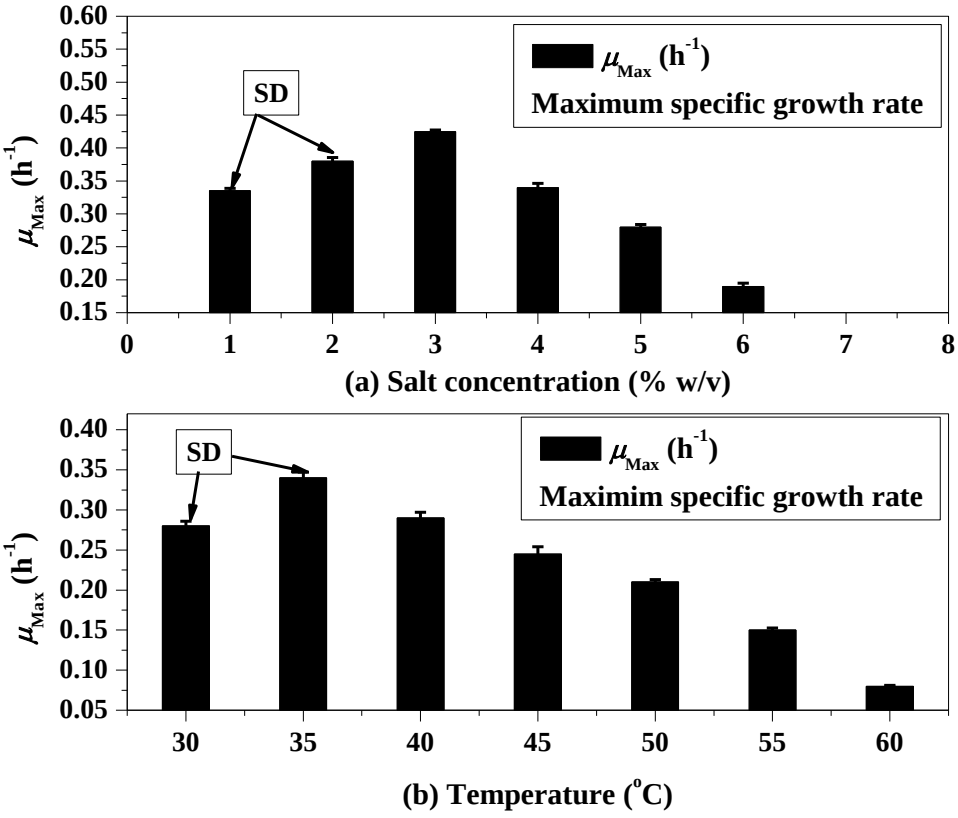

Fig. 5.30 (a) Salt and (b) Temperature tolerance of *P. aeruginosa*.

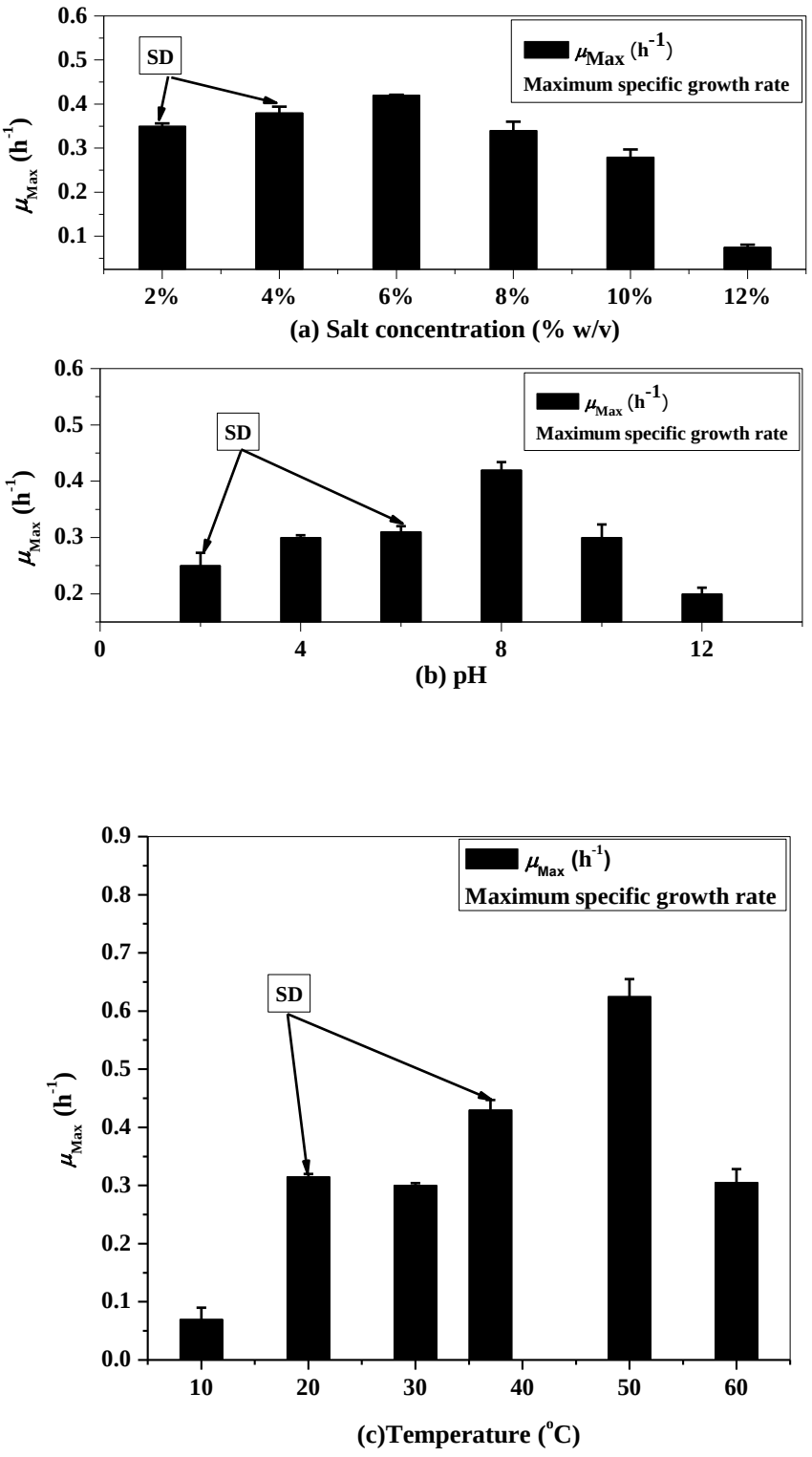

Fig. 5.31 Tolerance of *H. stevensii* towards different parameters including (a) Salt concentration (% w/v) ((b) pH and (c) Temperature (^{o}C).

5.8 Detailed study using *H. stevensii* for CO_2 utilization

5.8.1 Effect of physicochemical parameters

The bacterium was cultivated at different CO_2(g) concentration (%v/v) of 5%, 10% and 15%. The effect of inlet CO_2(g) concentration on the growth of *H. stevensii* was studied. The percentage removal of CO_2(g) was obtained as 98.6 (±0.02)%, 97.8 (±0.014)% and 98.59 (±0.59)% (v/v) for 5, 10 and 15% (v/v) initial CO_2(g) concentrations. As approximately same CO_2(g) removal efficiency was observed, the optimum concentration for further studies was selected based on maximum biomass obtained. The maximum biomass (in terms of dry weight) of 1.12 (± 0.036) g L^{-1} was observed at 15% (v/v) CO_2(g) concentration. The obtained result was obvious as more carbon was supplied at 15% CO_2(g) concentration which eventually got assimilated into the cellular biomass. Hence, further studies were carried out at 15% initial CO_2(g) concentration.

The growth of *H. stevensii* was carried out for the total duration of 6 days at different salt concentration of 0 M, 0.5 M and 1 M by maintaining the initial CO_2(g) concentration of 15% (v/v). The maximum growth was obtained as 0.82 (±0.14), 1.02 (±0.02) and 0.58 (±0.014) at 0, 0.5 and 1 M salt concentration, respectively. The maximum growth in terms of dry weight [1.02 (±0.02) g L^{-1}] was observed at 0.5 M salt concentration. In order to survive under higher or lower salt concentrations, cells have to pay extra energy penalty which is referred as osmotic stress. Therefore, for microorganisms isolated from halophilic environment, an optimum osmotic stress was necessary for their cellular growth (Oren, 2002). Thus, the excessive osmotic stress and related energy penalty are the reasons for the lower growth observed for *H. stevensii* at 0 M and 1 M salt concentrations.

The effect of pH on the growth of *H. stevensii* was studied by growing the bacterium under different pH values of 6, 8 and 10. The initial headspace CO_2 concentration and $S_2O_3^{2-}$ concentration were maintained as 15% (v/v) and 100 mM, respectively. The results have shown that the maximum dry weight of 0.96 (±0.006) g L^{-1} was observed for *H. stevensii* at pH value of 8 as compared to the dry weight values of 0.78 (±0.022) and 0.88(±0.028) g L^{-1} at 6 and 10 pH, respectively. HCO_3^- is the bio-usable form as inorganic carbon source and its concentration was found dominating in the pH range of 7 - 10 in the present study. Hence, this may be the reason for obtaining maximum biomass at pH value of 8 (Prabhu et al., 2011).

H. stvensii was grown at different temperatures of 20 ^oC, 30 ^oC, 37 ^oC and 50 ^oC for investigating the temperature effect on bacterium growth. The maximum dry weight values of 0.3 (±0.002), 0.85 (±0.03), 1.21 (±0.04) and 0.54 (±0.028) g L^{-1} were observed at temperature values of 20 ^oC, 30 ^oC, 37 ^oC and 50 ^oC, respectively. Maximum growth in terms of dry weight was found as 1.21 (±0.04) g L^{-1} at temperature of 37 ^oC. Temperature is one of the important parameter which is responsible for the cellular growth and also decides the availability of CO_2 in the growth medium. A decrease in solubility of CO_2 was observed with increase in temperature and hence its bio-availability follows the same trend (Lower, 1999). Thus, in the present study, lower biomass growth was observed at 50 ^oC. The values of biomass concentrations are summarized in terms of dry weight in Table 5.13 for various parameters. The optimum values of salt concentration, pH and temperature obtained in the present study were 0.5 M, 8 and 37 ^oC, respectively for the growth of *H. stevensii*.

Table 5.13: Maximum biomass productivity values at different physicochemical parameters

Parameters studied	Values	Maximum Biomass Productivity (g L^{-1})
CO_2 concentration (%v/v)	5	0.7 (±0.014)
	10	0.86 (±0.02)
	15	1.12 (±0.036)
Salt concentration (NaCl) (M)	0	0.82 (±0.14)
	0.5	1.02 (±0.02)
	1	0.58 (±0.014)
pH	6	0.78 (±0.022)
	8	0.96 (±0.006)
	10	0.88 (±0.028)
Temperature (^oC)	20	0.3 (±0.002)
	30	0.85 (±0.03)
	37	1.21 (±0.04)
	50	0.54 (±0.028)

5.8.2 Product yield at different physicochemical parameters

The product yield in terms of fatty alcohols (dodecanol, tetradecanol and pentadecanol) was estimated from biomass obtained at different values of salt concentration (0 M, 0.5 M and 1 M NaCl), pH (6, 8 and 10) and Temperature (20 ^{o}C, 30 ^{o}C, 37 ^{o}C and 50 ^{o}C) and the results obtained are reported in Table 5.14.

Total fatty alcohol content and total product yield (g of fatty alcohol per g of biomass) were found as 0.14 (±0.014), 0.143 (±1.13) & 0.144 (±0.11) g L^{-1} and 0.35 (±0.014), 0.396 (±0.056) & 0.358 (±0.11) g g^{-1} of biomass at 0, 0.5 and 1 M salt concentrations, respectively. The product yield was found to increase with increasing salt concentration from 0 M to 0.5 M and was found to decrease with further increase in salt concentration up to 1 M. This may be due to the fact that the results obtained from GC-MS analysis (section 5.4.2.2) have shown the possibility of the synthesis of higher chain fatty alcohols (>C_{15}) by *H. stevensii* at higher salt concentration. The possible reason for this was the limitation of availability of higher fatty alcohols pure compounds for GC quantification as GC-MS results showed the presence of higher fatty alcohols.

The higher salt concentration habitat imposes extra energetic constraints on microorganisms for their survival. These energetic constraints were referred as osmotic stress present in the immediate cellular surrounding. Thus, in order to prevent osmotic stress, cells start synthesizing or accumulating organic osmotic solute such as derivatives of amino acid, carbohydrates, or fatty alcohols (Mudge, 2005; Gosh and Dam, 2009). Therefore, increased total cellular fatty alcohol content with increased salt concentration indicated that *H. stevensii* was synthesizing and accumulating fatty alcohols in order to regulate osmotic stress. Dodecanol concentration was observed to be approximately same at 0 M [0.0472 (±0.014) g L^{-1}] and 0.5 M

[0.0472 (±0.014) g L^{-1}] salt concentration and was found to increase with further increase in salt concentration up to 1 M [0.0488 (±0.028) g L^{-1}] (Table 5.14). The product yields of tetradecanol and pentadecaonol were found to increase with increasing salt concentration from 0 M to 0.5 M. Afterwards, approximately the same value of product yield was observed at 1 M salt concentration for tetradecanol and further decrease was observed as salt concentration increased up to 1 M for pentadecanol (Table 5.14).

Bacteria were capable of synthesizing and accumulating mostly even chain length fatty acids with trace amount of odd chain length fatty acids into their cellular organic pool (Bharti et al.,, 2014). The mechanism for the conversion of fatty acids into fatty alcohols was also reported for bacteria (Hofvander et al., 2011; Willis et al., 2011). Since, the bacterium synthesizes the fatty alcohol at the expense of fatty acids and therefore, in the present study, the formation of fatty alcohols having even number of carbon chain length was found to increase with increase in salt concentration. Thus, salt concentration not only regulates the fatty alcohols product yield but also determines the constituents of cellular organic pool.

H. stevensii was cultivated at three different initial pH values of 6, 8 and 10 and the obtained results for the product recovery at different pH are reported in Table 5.14. The product recovery was estimated as 0.146 (±0.042), 0.147 (±0.014) and 0.1426 (0.046) g L^{-1} for pH values of 6, 8 and 10, respectively. Total fatty alcohol recovery was found to be approximately same at all pH values. Individual product recovery was found to increase when pH was increased from 6 to 8. There was a slight increase in tetradecanol content of total fatty alcohols but a decrease in content was observed with further increase in pH up to 10. Dodecanol and pentadecanol contents were found to decrease continuously with increase in pH values from 6 - 10 (Table 5.15). The accumulation of fatty alcohols was also observed at lower pH value of 6. However, the highest

product yield in terms of dodecanol, tetradecanol and pentadecanol was observed at pH value of 8, though the holding capacity of medium for CO_2 was higher at higher pH. However, this has no significant effect on the yield of fatty alcohols. Thus, from the obtained results it was concluded that the pH had no significant effect on the production of fatty alcohols.

The product yield was obtained as 0.236 (±0.007), 0.2404 (±0.0034), 0.396 (± 0.056) and 0.128 (±0.0028) g g^{-1} of biomass at different temperature of 20 ^{o}C, 30 ^{o}C, 37 ^{o}C and 50 ^{o}C, respectively. Total product yield (g L^{-1}) was found to increase with increase in temperature from 20 ^{o}C to 37 ^{o}C and the highest product yield of fatty alcohols was observed at 37 ^{o}C. One such study has suggested that the role of fatty alcohol in bacterium can also be considered as thermal insulators that give them protection from fluctuating temperature environment (Mudge, 2005). Thus, the accumulation of fatty alcohols into cellular biomass can be considered as the outcome of the changing temperature conditions. However, the product yield was found to decrease with a further rise in temperature from 37 ^{o}C to 50 ^{o}C (Table 5.14).

The same value of dodecanol was observed as temperature was increased from 20 ^{o}C to 37 ^{o}C. As temperature increased from 37 ^{o}C to 50 ^{o}C, dodecanol concentration was also found to increase from 0.0472 (±0.0014) g L^{-1} to 0.0512 (±0.05656) g L^{-1}, respectively. Tetradecanol content of the total fatty alcohols was only observed at temperature 30 ^{o}C and 37 ^{o}C (Table 5.14). Pentadecanol was observed only at temperature of 20 ^{o}C and 37 ^{o}C. Hence, increasing temperature supported the formation of fatty alcohols having higher even number chain length (Table 5.14).

This study suggested that the production of fatty alcohols having carbon chain length of C_{12}, C_{14} and C_{15} via CO_2 fixation route would be higher for the temperature in the range of 30 ^{o}C to 40 ^{o}C. At higher temperature of 50 ^{o}C, inhibition was observed in the synthesis of fatty

alcohols having chain length of C_{14} and C_{15}. This implies that the cell has started the formation of higher chain length fatty alcohols at higher temperature as suggested by GC-MS analysis in section 5.4.2.2. Therefore, from the above discussion, it was concluded that the temperature was not only controlling the fatty alcohol synthesis but also played a significant role in deciding the constituents of total pool of fatty alcohols produced.

5.8.3 Dissolved CO_2 concentration at different $S_2O_3^{2-}$ concentration

pH and the dissolved inorganic carbon of the cultured media (batch studies for G2 and G3 as described in Section (3.5.1) were monitored on the per-day basis and the obtained results are shown in Fig. 5.32. It was difficult to measure the free CO_2 concentration by titration method as pH value has increased above 8 after 24 h. Hence, in the present study, the dissolved inorganic carbon was monitored in terms of carbonate and bicarbonate alkalinities. It was found that the bicarbonate alkalinity decreased from 113.5 (±0.5) mg L^{-1} to 51 (±0.005) mg L^{-1} and 144 (±0. 4) mg L^{-1} to 20 (±0.1) mg L^{-1} for 50 and 100 mM $S_2O_3^{2-}$ concentrations, respectively (Fig. 5.32). Carbonate alkalinity at 50 mM and 100 mM $S_2O_3^{2-}$ concentrations was found to increase from 11 (±0.1) to 35.5 (±0.5) mg L^{-1} and 7 (±0.1) to 38 (±0.2) mg L^{-1}, respectively (Fig. 5.32). Also, the pH value on the per day basis of the liquid medium was found to increase from 6 to 8 in 24 h (up to day 1). Later, it increased gradually and reached to 9.18 (±0.2) and 9.45 (±0.04) at 50 mM and 100 mM $S_2O_3^{2-}$ concentrations at the end of 6 days batch period (Fig. 5.32).

In the present study, dissolved inorganic carbon (DIC) was well correlated to pH profile of the liquid medium. An initial decrease in pH due to the increase in concentration of bicarbonate ions was observed for the samples obtained from G2 & G3. After 24 h, pH remained high (>8) and bicarbonate levels remained low throughout the course of the batch study. This has

ensured the utilization of DIC as HCO_3^- by isolated bacterium *H. stevensii*. Therefore, the gaseous phase removal of CO_2 and utilization of DIC were interdependent and *H. stevensii* has utilized $S_2O_3^{2-}$ ion (an electron donor) as an energy source for the assimilation of CO_2 into the cellular biomass.

Table 5.14: Product yield of *H. stevensii* cultivated under different physiochemical stress of salt concentration (NaCl), pH and temperature.

Metabolites → / **Physicochemical Parameters ↓**	**Dodecanol (g L^{-1})**	**Tetradecanol (g L^{-1})**	**Pentadecanol (g L^{-1})**	**Product Recovery (g L^{-1}) ↓**	**Total Product yield (g $g^{-1}$of biomass) ↓**
Salt concentration (NaCl) (M, Molar) [T= 37 ^{o}C, pH = 7, CO_2 = 15% (v/v)]					
0	0.0472 (±0.014)	0.0464 (±0.042)	0.046 (±0.07)	0.14 (±0.014)	0.35 (±0.014)
0.5	0.0472 (±0.014)	0.0478 (±1.13)	0.0476 (±0.014)	0.143 (±1.13)	0.396 (±0.056)
1.0	0.0488 (±0.028)	0.0476 (±0.028)	0.0472 (±0.056)	0.144 (±0.11)	0.358 (±0.11)
pH [T= 37 ^{o}C, Salt concentration = 0.5 M, CO_2 = 15% (v/v)]					
6	0.0488 (±0.014)	0.0476 (±0.014)	0.05 (±0.042)	0.146 (±0.042)	0.3645 (±0.0021)
8	0.0476 (±0.028)	0.0492 (±0.014)	0.05 (±0.028)	0.147 (±0.014)	0.3665 (±0.0007)
10	0.04776 (±0.004)	0.0472 (±0.028)	0.0476 (±0.014)	0.1426 (±0.046)	0.35 (±0.002)
Temperature (^{o}C) [pH = 7, Salt concentration = 0.5 M, CO_2 = 15% (v/v)]					
20 ^{o}C	0.0472 (±0.0014)	-	0.04728 (±0.0028)	0.0944 (±0.0014)	0.236 (±0.007)
30 ^{o}C	0.0472 (±0.003)	0.0492 (±0.07)	-	0.0964 (±0.068)	0.2404 (±0.0034)
37 ^{o}C	0.0472 (± 0.014)	0.0478 (± 1.13)	0.0476 (± 0.014)	0.143 (± 1.13)	0.396 (± 0.056)
50 ^{o}C	0.0512 (±0.05656)	-	-	0.0512 (±0.05656)	0.128 (±0.0028)

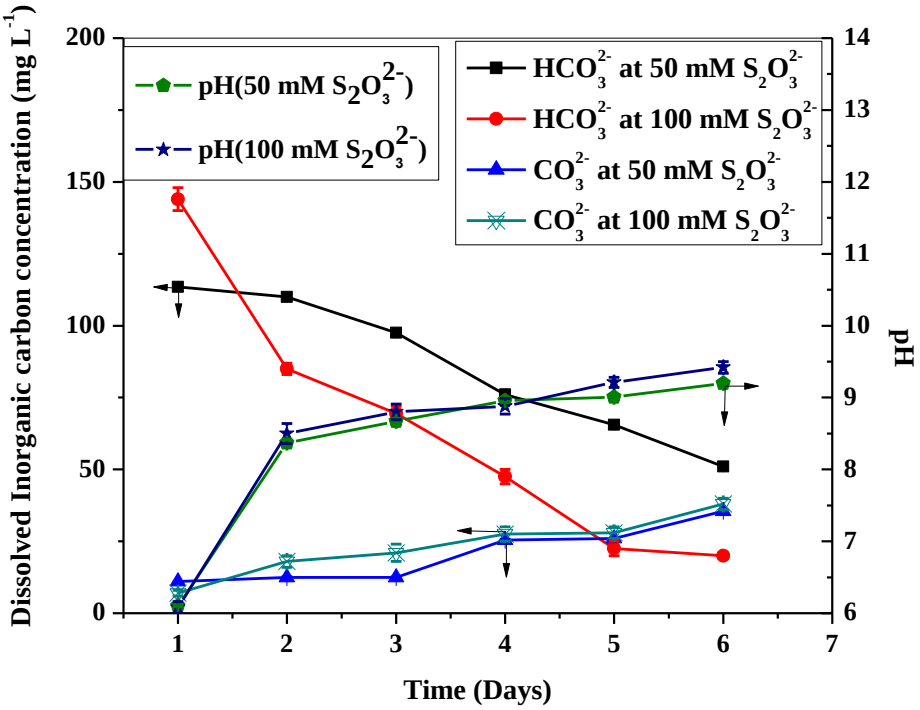

Fig. 5.32 Time course profile of dissolved inorganic carbon (DIC) and pH at different $S_2O_3^{2-}$ concentration (50 mM, 100 mM).

5.8.4 Cellular carbon allocation

The biomass obtained at different inlet CO_2 load of 5%, 10% and 15% (v/v) (section 3.5.6.1) was studied for the allocation of assimilated CO_2 as cellular organic carbon of *H. stevensii*. The estimation of the cellular organic pool (carbohydrates, proteins and fatty alcohols) was carried out by following both chemical and analytical techniques (semi-quantification using FT-IR). The study was intended to give more insight on the assimilation of CO_2 by *H. stevensii* into its cellular biomass and its allocation as carbon among different cellular organic pool of carbohydrates, proteins and fatty alcohols.

The biomass obtained at different CO_2 concentration was analyzed using FT-IR spectrum acquired via ATR. The spectrum analysis of the biomass obtained under various CO_2 stress indicated that the absorption strengths of the peaks were in the range of 3500 to 3000 cm^{-1} for fatty alcohols, 1724 to1585 cm^{-1} for proteins [amide (I), as reference] and 1200 to 950 cm^{-1} for carbohydrates and were quantified relative to proteins [amide (I)] by following the methadology given in literature (Palmucci et al., 2011, Meng et al., 2014). Fatty alcohols were relatively quantified as the ratio of the respective peak area obtained at various CO_2 stresses to the corresponding peak area of protein (amide I). The obtained values of carbohydrates were 6.325 (±0.1) mg L^{-1}, 5.93 (±0.18) mg L^{-1} and 3.665 (±0.26) mg L^{-1} and the relative quantified values for fatty alcohols were calculated as 2.19 (±0.01), 2.24 (±0.07) and 2.98 (±0.32) at 5, 10 and 15% CO_2 concentration (v/v), respectively. Thus, the analysis of the FT-IR spectrum revealed that the increase in CO_2 concentration resulted in the increase in cellular fatty alcohol content. Also, the decreased carbohydrates and protein concentrations were observed under increased CO_2 stress.

Semi-quantified results obtained from FT-IR spectrum analysis were further validated by the chemical quantification of the cellular organic pool (carbohydrates and proteins) at different

CO_2 stress. The carbohydrate content was found to be 0.62 (±0.014) g g^{-1} (biomass), 0.4(±0.007) g g^{-1}(biomass) and 0.168 (±0.007) g g^{-1} (biomass) at 5, 10 and 15% (v/v) CO_2 concentration, respectively. The value of protein concentration was found as 0.85 (±0.02) mg L^{-1}, 0.831 (±0.03) mg L^{-1} and 0.485 (±0.053) mg L^{-1} at 5, 10 and 15% CO_2 concentration (v/v), respectively. Hence, chemical quantification also confirmed that the cellular carbohydrates and protein concentrations were decreased as the CO_2 concentration increased from 5 to 15 % (v/v).

5.9 Approximate material balance and thermodynamic analysis

In the present work, the actual CO_2 utilization efficiency and CO_2 fixation mechanism of all microbial culture are demonstrated by approximate material balance and thermodynamic analysis which are discussed in following sections.

5.9.1 Approximate material balance

Approximate material balance for *B. cereus* was carried out as per Eq. 4.1 and is discussed below in detail. The mass of C in the form of CO_2 supplied to the system was calculated by ideal gas law and was obtained as 0.0123 g. By considering 84.6 % fixation, the amount of C present in gaseous phase after fixation was obtained as 0.00189 g. The biomass obtained for 84.6% removal at 100 ppm of Fe[II] concentration was 0.0132 g. Mass of C in biomass was estimated based on the molecular formula of biomass ($C_6H_{12}O_7N$) (Rittman and McCarty, 2012). Based on the molecular formula of biomass, the mass of C in biomass was estimated as 7.26×10^{-3} g. The dissolved C in aqueous phase was calculated using Henry's law at the end of 5^{th} day. The dissolved C was obtained as 2.65×10^{-3} g at 0.13 atm partial pressure using Henry's law. The values were substituted in Eq. 4.1. L.H.S. and R.H.S. of Eq. 4.1 were calculated and are obtained

as 0.0123 g and 0.0118 g, respectively. These values of $M_{C,in}$ and $M_{C,out}$ were approximately same which indicated that the gaseous phase CO_2 was mainly fixed by the biological activity of *B. cereus* SM1. Similar material balance calculations were carried out for other isolates and mixed microbial culture and the obtained results are given in Table 5.15. For all the species, M_{in} and M_{out} are found approximately same. Hence, approximate material balance calculations confirmed the fixation of CO_2(g) into cellular biomass.

In terms of molar units, total moles of CO_2 supplied to the system of *B. cereus* were 1.025 × 10^{-3} moles. Out of which 4.51 x 10^{-4} was assimilated by *B. cereus* as per carbon balance calculations. Therefore, the actual CO_2 utilization efficiency ($R.R_{CO2}$) was observed as 44.00 (±0.02)% using Eq. 3.5. Similar calculations were carried out for mixed microbial population and other isolates and the obtained results are reported in Table 5.15. The obtained results revealed that the value of $R.R_{CO2}$ was found to decrease in order of *H. stevensii* > mixed microbial population > *B. cereus* > *P. putida* > *E. cloacae* > *P. aeruginosa* (Table 5.15). This implies that *H. stevensii* utilized more CO_2 in comparison to other isolates and hence, has shown better CO_2 utilization performance. Hence, it can be said that the $R.R_{CO2}$ value estimated using approximate material balance is in agreement with value obtained from experiments.

5.9.2 Thermodynamic analysis

Energy required to fix available CO_2 in the batch system was estimated and compared with the available energy in terms of energy substrate (Fe[II] or $S_2O_3^{2-}$). The thermodynamic feasibility study was carried out for all microbial cultures used in the present study and are described in following sections.

5.9.2.1 Cultures obtained from STP

GC-MS analysis result suggested that CO_2(g) was assimilated mainly in the form of fatty acids in the biomass of STP cultures (section 5.4.1). As per GC-MS spectrum, hexadecanoic acid is found to have maximum area as compared to the area obtained for other fatty acids. Thus, it was assumed that CO_2(g) was assimilated into the biomass and metabolizes to form hexadecanoic acid for ΔG calculations. The Gibb's free energy of reaction ($\Delta G_{reaction}$) of CO_2 assimilation reaction for *B. cereus* was calculated using Eqs. 4.5 - 4.7 and is discussed below.

The Gibb's free energy estimated for product and reactant was obtained as -7425.6 kJ mol^{-1} and -6255.19 kJ mol^{-1} respectively. These values were substituted in Eq. 4.13 and the value of Gibb's free energy of reaction calculated was -1170.41 kJ mol^{-1}. Therefore, the energy required to fix 4.51 x 10^{-4} mole of CO_2 as hexadecanoic acid was estimated as 0.033 kJ which was less as compared to the energy available (0.133 kJ for 100 ppm of Fe[II]) in form of Fe[II]. Thus, energy supplied to the system at 100 ppm Fe[II] concentration was sufficient for the fixation of respective CO_2 concentration. The calculation of $\Delta G_{reaction}$ values for Eqs. 4.5 and 4.6 revealed that the energy supplied to the system was only 0.066 kJ at 50 ppm of Fe[II] concentration. This was insufficient to meet the energy requirement for corresponding CO_2 fixation.

The similar thermodynamic assessment calculations were carried out for mixed microbial population, *P. putida* and *E. cloacae* and the obtained result are given in Table 5.16. It indicates that the energy supplied to the system was adequate to meet the energy requirement for the fixation of CO_2 as hexadecanoic acid into the cellular biomass.

Therefore, the thermodynamic assessment of the CO_2 assimilation process has established the fact that the experimental values of X_{Max}, P, η_{CO2}, R_{CO2} and $R.R_{CO2}$ obtained at 50

ppm Fe[II] concentration were less in comparison to the values obtained at 100 ppm Fe[II] concentration.

Hence, the results obtained from approximate material balance and thermodynamic assessments of the CO2 bio-mitigation system have confirmed the assimilation of CO_2 as cellular biomass. Fe[II] concentration have played a major role in CO_2 fixation and governs the biomass productivity that eventually decides the product yield and hence, the profitability of the CO_2 bio-mitigation system.

5.9.2.2 Cultures obtained from SSL

GC-MS analysis of the obtained cell lysate and supernatant, after CO_2 fixation studies, revealed the presence of fatty alcohols having carbon chain length ranging from C_{12}-C_{28}. The analysis also revealed that 80% and 38% area of GC spectrum obtained for *P. aeruginosa* and *H. stevensii*, respectively is represented by fatty alcohols. Out of which, 44.5% and 17.76% of spectrum area obtained for *P. aeruginosa* and *H. stevensii*, respectively is characterized by dodecanol (Tables 5.9 and 5.10). Hence, dodecanol was considered as one of the main products for the estimation of Gibb`s free energy for the fixation of CO_2 into the cellular biomass.

Gibb`s free energy calculations were carried out to obtain the Gibbs free energy of products and reactants for *P. aeruginosa*. These values were obtained as -6463.14 kJ mol^{-1} and -4711.11 kJ mol^{-1} for products and reactants, respectively (Eq. 4.8). Thus, the Gibbs free energy change was obtained as -1752.03 kJ mol^{-1} using Eq. 4.8. These calculations show that, 0.043 kJ of energy was required to fix 2.97×10^{-4} moles of CO_2 as dodecanol. At 100 ppm Fe[II], energy present in the system for complete Fe[II] oxidation was 0.133 kJ but, the energy required for fixation of given amount of CO_2 was 0.043 kJ. Hence energy supplied was greater than energy

required for the fixation. The calculation at 50 ppm Fe[II] concentration revealed that the energy supplied to the system was only 0.065 kJ which is at the thermodynamics limit and thus, inadequate to meet the requirement (0.043 kJ). Therefore, the removal efficiency at 50 ppm Fe[II] concentration was less as compared to 100 ppm fe[II] concentration which was also supported by experimental results.

Gibb`s free energy calculations were carried out to obtain the Gibb's free energy of products and reactants and were obtained as - 6760.86 kJ mol^{-1} and - 5145.64 kJ mol^{-1}, respectively. Thus, for the fixation of 12 moles of CO_2 into dodecanol, the change in Gibb's free energy was obtained as - 1615.22 kJ mol^{-1} (Eq. 4.9). Hence, 0.2 kJ of energy was required to fix 0.00149 moles of CO_2 as dodecanol. In the present study, for 100 mM $S_2O_3^{2-}$, energy available in the system was obtained as -200.266 kJ due to complete $S_2O_3^{2-}$ oxidation. This was much higher than the energy requirement for the fixation of given amount of CO_2 (0.2 kJ). The energy supplied to the system was sufficient to meet the energy demand of Eqs. (4.9 - 4.11). Similar energy assessment was performed for 50 mM $S_2O_3^{2-}$ concentration. The obtained result suggested that the energy supplied to the system was 100.133 kJ which was also adequate to meet the energy requirements of 0.2 kJ Eqs. (4.9 - 4.11). Therefore, the energy available at 100 mM and 50 mM $S_2O_3^{2-}$ concentration was sufficient to meet the requirements of CO_2 fixation and its further metabolism into cellular biomass as fatty alcohols. Energy assessment calculations supported the experimentally obtained higher removal efficiency (≈ 98%) of CO_2 (g) at 50 mM and 100 mM $S_2O_3^{2-}$ concentrations. Hence, the thermodynamic analysis also confirmed the gaseous phase CO_2 fixation in the presence of $S_2O_3^{2-}$ as an energy source and its conversion into the value added products.

Table: 5.15 Values of different parameters estimated for material balance equation

Species	$M_{C,\ in}$ (g)	$M_{C,\ go}$ (g)	$M_{C,bo}$ (g)	$M_{C,CO2(l)}$	$M_{C,\ out}$ (g)	$R.R_{CO2}$ (%)
B. cereus	0.0123	0.00189	0.0054	0.00265	0.0118	44.00 (±0.02)
Mixed microbial population	0.014	0.00312	0.00816	0.00316	0.014	57.67 (±0.04)
E. cloacae	0.014	0.0062	0.004216	0.00316	0.0135	29.77 (±0.28)
P. putida	0.014	0.0046	0.006035	0.00316	0.0137	42.66 (±0.54)
P. aeruginosa	0.016	0.001	0.0036	0.00922	0.014	22.16 (±1.14)
H. stevensii	0.0215	0.0001	0.0178	0.00295	0.021	84.18 (±2.1)

Table 5.16 Δ*G* values of products and reactants

Species	$\Delta G_{Products}$ (kJ mol^{-1})	$\Delta G_{Reactant}$ (kJ mol^{-1})	$\Delta G_{Reaction}$ (kJ mol^{-1})	Energy Required (kJ)	Energy supplied (kJ)
B. cereus	-7425.6	-6255.19	-1170.41	0.033 kJ	0.133 kJ
Mixed microbial population	-7425.6	-6255.19	-1170.41	0.0497	0.133 kJ
E. cloacae	-7425.6	-6255.19	-1170.41	0.0256	0.133 kJ
P. putida	-7425.6	-6255.19	-1170.41	0.0367	0.133 kJ
P. aeruginosa	-6463.14	-4711.11	-1752.03	0.043	0.133 kJ
H. stevensii	- 6760.86	-5145.64	-1615.22	0.2	200.266

5.10 Comparison with existing literature

In the recent years, CO_2 bio-mitigation studies within the framework of carbon capture utilization (CCU) have mostly employed the phototrophic microorganisms. Therefore, in order to authenticate the implementation of present work for the development of CO_2 bio-mitigation system, the work was compared with some existing CO_2 bio-mitigation studies using photoautotrophs. The comparison of present work with other studies is tabulated in Tables 5. 17, 5.18, 5.19 and 5.20.

5.10.1 CO_2 (g) removal efficiency (η_{CO2}) and biomass productivity

CO_2 bio-mitigation potential of different isolates and mixed microbial population used in present work was compared in terms of CO_2 removal efficiency (η_{CO2}) with some reported literature and is given in Table 5.17. The η_{CO2} values of *H. stevensii* [98.59 (±0.59) %], *P. aeruginosa* [92.37(±2.47) %], *B. cereus* [84.6 (±5.76) %] and mixed microbial population [78.07 (±0.014) %] were found to be superior to the reported microalgal strains which were utilized for the development of CO_2 bio-mitigation system [Table 5.17]. The η_{CO2} values of *E. cloacae* and *P. putida* were observed as 56.44 (±2.68) and 67.44 (±2.44) %, respectively and fell well within the range of reported species for CO_2 mitigation. The present bio-mitigation experiment was carried out for CO_2 concentration of 15 % (v/v). This was higher than the CO_2 concentrations used in the reported studies. Therefore, the microorganisms used in the present work were able to survive under higher CO_2 concentration and have more η_{CO2} values. Hence, these microorganisms can be utilized for the development of cost effective and sustainable CO_2 bio-mitigation system.

It can be observed that the CO_2 fixation rate (R_{CO2}) and biomass productivity (P_{Max}) of microorganisms used in the present study were found competitive to those from the other

reported studies (Table 5.18). R_{CO2} and P_{Max} values obtained for mixed microbial population [0.078 (±0.004), 0.107 (±0.018)] and *P. aeruginosa* [0.195 (±0.0025), 0.0302 (±0.0031)] were found comparable to the species reported for CO_2 bio-mitigation. R_{CO2} and P_{Max} values of *H. stevensii* [0.174 (±0.016), 0.218(±0.021)] were found superior to most of isolates reported in Table 5.18 except *Chlorella sp.* [0.171, 0.857] and *Isochrysis galbana* [0.51, 0.933]. Thus, *H. stevensii* showed a promising growth in the environment of higher CO_2 concentration [15% (v/v)] which was found to be much higher than the reported studies (Tables 5.17 and 5.18). Hence, the isolate *H. stevensii* can be seen as a promising candidate for CO_2 mitigation in the absence of light.

5.10.2 Bio-diesel and fatty alcohol production yield

The product yield obtained for bio-diesel and fatty alcohols was compared with few available reported studies and are given in Tables 5.19 and 5.20. The total FAME obtained per g biomass of *B. cereus*, mixed microbial population and *E. cloacae* was 86.5 (±0.048), 91.55 (±0.198) and 77.49 (±0.1) mg, respectively. These values were higher than the reported values of total FAME for microalgae except *Scenedesmus sp.* ISTGA1 (179.86 mg g^{-1} biomass) (Table 5.19). The total FAME obtained per g biomass of *P. putida* was 38.69 (±1.66) which was comparable with the reported FAME yield except for *Tetraselmis elliptica* (77.36 mg g^{-1} biomass) and *Scenedesmus sp.* ISTGA1 (179.86 mg g^{-1} biomass) (Table 5.19).

Total fatty alcohols obtained from the biomass of *P. aeruginosa* and *H. stevensii* were 392 mg and 310 mg, respectively. Thus, the product yield of 39.2 (±0.14) % and 31(±0.28)% was observed for *P. aeruginosa* and *H. stevensii*, respectively from fixation of CO_2 (Table 5.20). The total fatty alcohol production yield of 540 mg of fatty alcohol per g biomass was observed

for *Chelorella sorokinianna* 21 (Table 5.20). *Synechocystis sp.* PCC has shown the total fatty alcohol production of 0.00287 mg of fatty alcohol per g of biomass (Table 5.20). *E. coli* was engineered for the production of fatty alcohols and the product yield was obtained as 0.067, 0.5986 and 0.75 g L^{-1} in different studies (Table 5.20). Thus, it can be seen from the reported studies in Table 5.20 that product yield obtained for fatty alcohols production from CO_2 utilizing bacteria *P. aeruginosa* and *H. stevensii* was equivalent to those of the reported studies.

Hence, it can be seen from the reported studies that product yield obtained for bio-diesel and fatty alcohols production from cultures of STP and SSL is comparable to those of the reported studies. The production of biodiesel was mainly focused on the photoautotrophs and few or almost no study has reported the production of biodiesel from CO_2 utilizing bacterium (Bharti et al., 2014). The reported studies for enhanced fatty alcohol production were mainly focused on the engineered bacterial strain.

Present study has demonstrated that the microorganisms utilizing CO_2 were found to produce biodiesel and fatty alcohols in extractable amount in the absence of light. The isolates from SSL were found to produce fatty alcohols naturally and hence, ease the complications associated with experiments using genetically engineered microorganism. Thus, the microorganisms have shown the potential to be used as a source for production of valuable products such as biodiesel and fatty alcohols via CO_2 fixation which can give commercial value to the CO_2 bio-mitigation system.

Table 5.17: Comparison of CO_2(g) removal efficiency [η_{CO2}(g)] obtained from STP and SSL cultures among reported studies

Species	**Initial CO_2 concentration (%v/v)**	**Cultivation Mode**	**Gas phase CO_2 removal efficiency [η_{CO2}(g), % v/v]**	**References**
Chlorella sp.	1, 5 and 10	Shake-flask study	59 , 51 and 46	Ramanan et al., (2010)
Spirulina platensis	1, 5 and 10	Shake-flask study	53, 41 and 39	Ramanan et al., (2010)
Mixed culture comprised of *Chlorella sp.*, *Scenedesmus sp.*, and *Ankistrodesmus sp.*	10	Photobioreactor	63.10	Rinanti et al., (2014)
Chlorella strains (FACHB-484, FACHB-729, FACHB-752 and ESP-6)	10	Photobioreactor	35.51, 32.26, 26.14 and 26.14	Hu et al., (2016)
B. cereus	13 (±1)	Shake-flask study	84.6 (± 5.76)	Present study
Mixed microbial population	15 (±1)	Shake-flask study	78.07 (± 0.014)	
E. cloacae	15 (±1)	Shake-flask study	56.44 (± 2.68)	
P. putida	15 (±1)	Shake-flask study	67.44 (± 2.44)	
P. aeruginosa	17 (±1)	Shake-flask study	92.37(± 2.47)	
H. stevensii	15 (±0.8)	Shake-flask study	98.59 (±0.59)	

Table 5.18: Comparison of biomass productivity on per day basis (P, g L^{-1} d^{-1}) and CO_2 fixation rate (R_{CO2}) obtained from STP and SSL cultures among reported studies

Species	CO_2 concentration (%v/v)	Biomass productivity per day (P, g L^{-1} d^{-1})	CO_2 fixaton rate (R_{CO2}, g L^{-1} d^{-1})	References
Chlorella kessleri	6	0.087	0.16	deMorais et al., (2007)
Scenedesmus obliquus	12	0.076	0.14	deMorais et al., (2007)
Chlorella sp.	2	0.171	0.857	Chiu et al., (2008)
Chlorella vulgaris	6	(Approx.) 0.025	0.04575	Chinnasamy et al., (2009)
Isochrysis galbana	5	0.51	0.933	Picardo et al., (2013)
B. cereus	13 (±1)	0.0512 (±0.002)	0.0638 (± 0.003)	Present study
Mixed microbial population	15 (±1)	0.078 (±0.004)	0.107 (± 0.018)	
E. cloacae	15 (±1)	0.036 (±0.0042)	0.0445 (± 0.005)	
P. putida	15 (±1)	0.056 (±0.0056)	0.07 (± 0.007)	
P. aeruginosa	17 (±1)	0.195 (±0.0025)	0.0302 (± 0.0031)	
H. stevensii	15 (±0.8)	0.174 (±0.016)	0.218	

Table 5.19: Comparison of bio-diesel productivity obtained from STP cultures among reported studies

Species	CO_2 concentration (% v/v)	Biodiesel production (mg g^{-1} biomass)	References
Tetraselmis elliptica	1.5	77.36	Abomohra et al., (2017)
Leptolyngbya sp.	$NaHCO_3$	16 - 21	Singh et al., (2014)
Scenedesmus sp. ISTGA1	15	179.86	Tripathi et al., (2015)
Botryococcus braunii	10	31.8 (±1.23)	Nascimento et al., (2015)
Botryococcus terribilis	20	29.7 (±1.38)	
B. cereus	13 (±1)	86.5 (±0.048)	Present study
Mixed microbial population	15 (±1)	91.55 (±0.198)	
E. cloacae	15 (±1)	77.49 (±0.1)	
P. putida	15 (±1)	38.69 (±1.66)	

Table 5.20: Comparison of fatty alcohols productivity of culture obtained from SSL among reported studies

Species	**Fatty alcohol production (mg of fatty alcohol per g biomass or g L^{-1})**	**Reference**
Engineered *Escherichia coli*	0.060 g L^{-1}	Steen et al., (2010)
Engineered *E. coli*	0.5986 g L^{-1}	Zheng et al., (2012)
Chelorella sorokinianna 21	540 mg of fatty alcohol per g of biomass	Yang et al., (2013)
Engineered *E. coli*	0.75 g L^{-1}	Liu et al., (2014)
Synechocystis sp. PCC	0.00287 mg of fatty alcohol per g of biomass	Yao et al., (2014)
P. aeruginosa	392 mg of fatty alcohol per g biomass	Present study
H. stevensii	310 mg of fatty alcohol per g biomass & 0.13 g L^{-1}	

5.11 CO_2 fixation mechanism

On the basis of theoretical and experimental evidences, the possible CO_2 fixation and its metabolic mechanism present in isolates of STP and SSL are described in following sections.

5.11.1 Microorganisms obtained from STP

In various studies, *Bacillus*, *Enterobacter* and *Pseudomonas* were found to be equipped with enzyme called as carbonic anhydrase (CA) which makes them capable of assimilating CO_2 into their cellular biomass (Santini et al., 2000; Sharma et al., 2008; Prabhu et al., 2011). Hence, CO_2 assimilation mechanism of the bacteria belonging to the group *Bacillus*, *Enterobacter* and *Pseudomonas* was very well established and reported in earlier studies (Lotlikar et al., 2013; Eminoglu et al., 2015; Aggarwal et al., 2015; Sundaram and Thakur, 2015).

The fatty acid production of bacteria was well established and rigorously studied by many researchers (Moazami et al., 2011; Bharti et al., 2014). The synthesis of fatty acids in bacteria involves: (1) initiation and (2) chain elongation. The initiation step involves the simultaneous condensation of primer acyl-CoA and malonyl-ACP with ATP as energy source and NADPH as source of reducing equivalent. The enzyme malonyl-COA:ACP transacylase catalyses the conversion of malonyl-CoA and bicarbonate to malonyl-ACP. The malonyl-ACP is the major building block of fatty acids. The branched acids synthesis is initiated by isovaleryl-CoA, isobutryl-CoA, or 2-methylbutryl-CoA (Wallace et al., 1995; Bharti et al., 2014). The branched keto acid dehydrogenase complex is responsible for the formation of these acyl-CoAs (Cropp et. al., 2000). The unsaturated fatty acid synthesis involves 3-hydroxydecanoyl-ACP dehydratase (FabA) catalyzing the dehydration of 3-hydroxydecanoyl- ACP to a mixture of trans-2-decenoyl-ACP and cis-3-decenoyl-ACP. The trans-intermediate is converted to saturated

fatty acids. The cis-intermediate is elongated, double bond is preserved and unsaturated fatty acids are formed (Leesong et al., 1996).

Thus, *B. cereus*, mixed microbial population, *E. cloacae* and *P. putida* are found capable of growth in a chemoautotrophic manner. These microorganisms may be following the above discussed mechanism for the production of saturated and unsaturated fatty acids using CO_2 as carbon source.

5.11.2 Microorganisms obtained from SSL

The overall metabolism of CO_2 fixation can be understood from the obtained experimental results. GC-MS analysis of cell lysate extract of *P. aeruginosa* and *H. stevensii* has shown the presence of fatty aldehyde cis-9-hexadecenal having match quality of 89% and 90%, respectively. The analysis further revealed that the cell lysate extract of *P. aeruginosa* and *H. stevensii* was comprised of fatty acids such as tetradecanoic acid (match quality of 92 % and 95%) and n-hexadecanoic acid (match quality of 96% and 95%) in trace amounts (Table 5.9 - 5.10).

Bacterial conversion of cellular fatty acids to fatty alcohols involves two step reaction mechanisms: (1) reduction of fatty acyl-CoA to the corresponding fatty aldehyde catalyzed by acyl-CoA reductase then, (2) the reduction of fatty aldehyde to the corresponding fatty alcohol catalyzed by fatty aldehyde reductase **(**Hofvander, et al., 2011**)**. Few studies have shown that an enzyme (Fatty acid reductase) which is analogous to fatty acyl reductase (in eukaryotes) and is isolated from bacterium *Marinobacter aquaeolei* VT8 has shown the possibility of single step fatty alcohol production (Willis et al., 2011). These studies have suggested that bacteria are capable of synthesizing long chain fatty alcohols. Thus in the present work, based on GC-MS

and FT-IR results, it may be concluded that *P. aeruginosa* and *H. stevensii* were following the above mentioned pathways for converting the assimilated fatty acids into fatty alcohol when cultivated under high concentration of CO_2 (Tables 5.9 - 5.10).

5.12. Semi-continuous studies using *H. stevensii*

5.12.1 CO_2 utilization studies

The culture of *H. stevensii* was cultivated for the total duration of 72 h in a laboratory scale bioreactor by continuous supply of CO_2 at concentration of 15 (±1)% (v/v). pH and dissolved oxygen (DO) of the culture medium were obtained in regular time interval of 12 h. The changes in pH and DO with time were plotted and are shown in Fig. 5.33. The pH of the medium was found to decrease from 10 to 6.05 in the 24 h of cultivation time. Further, it got increased up to 7.48 with increase in the cultivation period till the end. CO_2(g) supplied to the system (bioreactor) got dissolved into the culture medium and existed in the form of free CO_2 and carbonic acid (H_2CO_3).

The concentrations of HCO_3^-, CO_3^{2-} and free CO_2 were estimated using titration method in the regular time interval of 12 h and are shown in Fig. 5.34. The obtained results indicated that initially the concentration of HCO_3^- was approximately constant for the first 24 h of study. Later, the concentration of HCO_3^- decreased with time for the next 48 h of cultivation period. However, the continuous increase in concentration of CO_3^{2-} was observed with time. The concentration of free CO_2 was found to increase from 83 (±7) to 148 (±1.5) mg L^{-1} and then became approximately constant (Fig. 5.34). Initially pH of the culture medium was 10 and it started to decrease as CO_2 was induced into the medium. Due to this dissolved CO_2 concentration in the culture medium got increased. The microorganisms take time in adjusting to its changing

environment and hence, no change in HCO_3^- concentration was observed in the first 24 h of cultivation period. However, a decrease in HCO_3^- ion concentration, increase in CO_3^{2-} concentration and an increase in pH were observed as soon as the rate of biological utilization of CO_2 superseded the rate of dissolution of CO_2. The obtained results of HCO_3^-, CO_3^{2-} and free CO_2 concentration supported the obtained pH profile of the culture medium (Figs. 5.33 and 5.34). CO_2(g) concentration was monitored in regular interval of 24 h at the outlet of the bioreactor and no trace of CO_2(g) was observed in the outlet stream. This indicated that CO_2 supplied to the system was totally dissolved in the culture medium and its continuous supply into the system resulted in increase in the free CO_2 concentration. The evaluation of parameters such as P_{Max}, μ_{Max} and R_{CO2} are required for understanding the actual CO_2 utilization efficiency of *H. stevensii* in semi-continuous bioreactor.

The biomass growth of *H. stevensii* was determined in terms of dry weight (g L^{-1}) at regular interval of 12 h and the results are shown in Fig. 5.34. A continuous increase in biomass concentration was observed for the total period of cultivation. The maximum biomass concentration (X_{Max}) was obtained as 4.675 (±0.11) g L^{-1} at the end of cultivation period. CO_2 assimilated into the cellular biomass depends upon the availability of adequate amount of energy substrate (McCollom and Amend, 2005). Thiosulfate ion ($S_2O_3^{2-}$) was utilized as an energy source and CO_2 was continuously supplied to the system as carbon source in the present study. Hence, a continuous increase in the biomass was observed due to the presence of sufficient amount of energy substrate and carbon source. CO_2 utilization capability of *H. stevensii* was evaluated by estimating P (g L^{-1} d^{-1}), μ (d^{-1}) and R_{CO2}. The calculated values of P (g L^{-1} d^{-1}), μ (d^{-1}) and R_{CO2} were found as 1.55 (± 0.035), 0.19 (± 0.034) and 1.94 (± 0.044), respectively for semi-continuous studies. However, the obtained values of P (g L^{-1} d^{-1}), μ (d^{-1}) and R_{CO2} for *H.*

stevensii from batch studies at 100 mM $S_2O_3^{2-}$ were calculated as 0.175 g L^{-1} d^{-1}, 0.25 d^{-1} and 0.218 g L^{-1} d^{-1}, respectively (section 5.3.2). The higher values of P and R_{CO2} obtained in continuous study as comparison to batch study signifies the good response of *H. stevensii* in the changing environment of pH and high CO_2 concentration at laboratory semi-continuous bioreactor. The higher biomass productivity was the primary requirement of CCU for the profitable product recovery.

5.12.2 Downstream processing strategy

Biomass harvesting was carried out by following both centrifugation and filtration techniques (3.6.1). The maximum biomass concentrations of 6.5 (±0.34) g L^{-1} and 4.675 (±0.11) g L^{-1} were obtained by centrifugation and filtration methods, respectively. Hence, better harvesting efficiency and biomass yield were observed using centrifugation method. Energy required for centrifugation is significantly higher which makes this process expensive. Low biomass yield obtained from filtration process can be compensated by lower operating cost of the process (Grima et al., 2003; Kim et al., 2013). There was a scope in enhancing the efficiency of filtration process by combining it with flocculation method as described in previous literature (Grima et al., 2003; Kim et al., 2013). Hence, in the present study filtration method was used.

The fatty alcohols were extracted by following the two different strategies i.e. (1) directly from the wet biomass and (2) by cell disruption. The extraction methodologies of solvent-solvent extraction and reactive extraction were applied and the obtained organic phase was analyzed using GC-MS. The analysis results along with compound and their match quality are reported in Tables 5.21 - 5.22, respectively.

The extraction of the metabolites from the wet biomass and cell disruption followed by solvent extraction has shown the presence of fatty alcohols, hydrocarbons and fatty acids in the considerable amount (Table 5.21). The fatty alcohols and fatty acids contents were found as 8.96% and 17.43% from the wet biomass as compared to 5.27% of fatty alcohols and 0.44% fatty acids from cell lysate. The obtained results indicated that the strategy of direct extraction from the wet biomass was found to be superior to the strategy of cell disruption followed by extraction. The extraction of metabolites after de-watering the biomass along with the cell disruption is an energy intensive process that would add extra downstream processing cost. Few studies have demonstrated the direct extraction of valuable metabolites from the wet biomass. In general, the lower yield of metabolite is expected from wet biomass as compared to cell disruption (Kim et al., 2013). However, in the present study, the better recovery of metabolites from wet biomass was may be due to the thin cellular membrane of bacteria as compared to thick cellular membrane of microalgae (Kim et al., 2013; Nelson and Viamajala, 2016).

The GC-MS results obtained from reactive extraction of primary metabolite from cell disruption and wet biomass have shown the presence of fatty alcohols and hydrocarbons and are reported in Table 5.22. Fatty alcohols are comprised of 1.22 % of the total cell lyste extract and no traces of fatty acids were observed in the cell lysate extract (Table 5.22). The extraction of products using reactive extraction directly from wet biomass gave the fatty alcohol content as 1.31 % (Table 5.22). The contents of fatty alcohols and fatty acids obtained from cell disruption and wet biomass using reactive extraction were found to be approximately same. The recovered amounts of fatty alcohols and fatty acid were significantly less than the amounts obtained from solvent extraction. The lower yield by reactive extraction may be due to the extractant system considered for the recovery of metabolites. This system is mainly utilized to recover short chain

carboxylic acids and lower molecular weight alcohols from aqueous phase (Datta et al., 2015). The presence of long chain of hydrocarbons in the biomass was may be one of the reasons for the inefficacy of reactive extraction.

Based on the above discussion, biomass obtained from filtration and direct recovery of metabolites using solvent extraction from wet biomass can be an efficient and cost effective downstream processing strategy.

5.12.3 Product yield

The biomass and supernatant obtained from the solvent extraction of wet biomass were utilized for the quantifications of targeted compounds. Eqs. 5.7 - 5.9 are utilized to quantify the dodecanol, tetradecanol and pentadecanol, respectively.

The fatty alcohols obtained from biomass consist of 2.57 (±0.28) mg dodecanol, 2.72 (±0.14) mg tetradecanol and 2.97 (±0.007) mg pentadecanol. The quantities of dodecanol, tetradecanol and pentadecanol in supernatant extract were obtained as 190.9 (±0.14), 379.5 (±0.21), 28.06 (±0.035) mg, respectively. Hence, the leachate (biomass + supernatant) contained 193.47 (±0.19) mg of dodecanol, 382.22 (±0.6) mg of tetradecanol and 31.03 (±0.14) mg of pentadecanol. The total amount of fatty alcohols was obtained as 606.72 (± 0.35) mg with product recovery of 30.33 (±0.02)% per gram of biomass. This study concludes that the integration of CO_2 bio-mitigation with appropriate downstream processing of product recovery would be an economically viable solution for curbing down the CO_2 level from atmosphere.

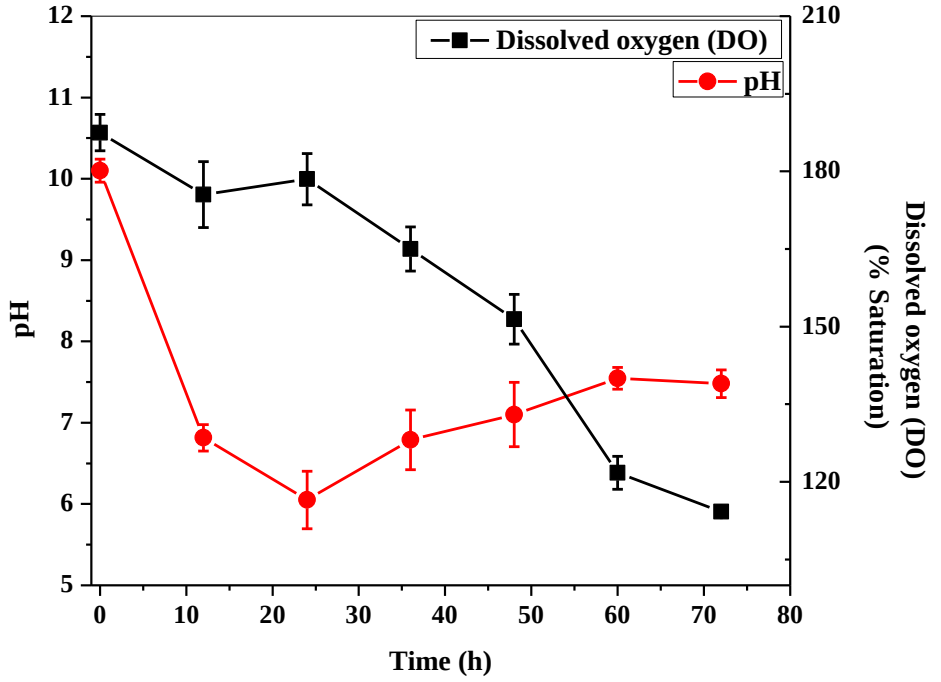

Fig. 5.33 pH and dissolved oxygen value obtained during semi-continuous studies using *H. stevensii*.

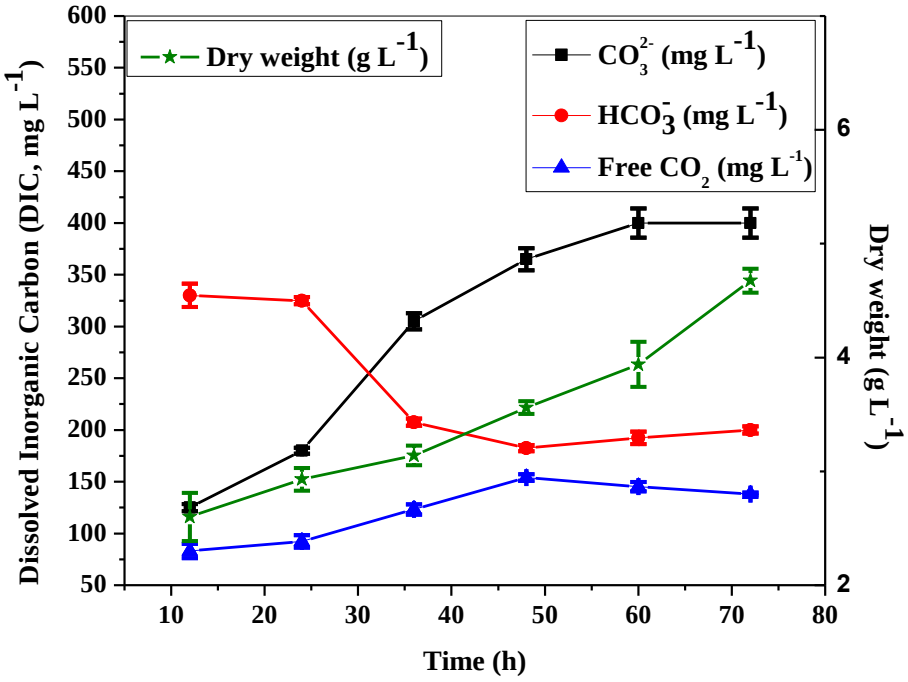

Fig. 5.34 Dissolved inorganic carbon (mg L^{-1}) and dry weight (g L^{-1}) of *H. stevensii*.

Table 5.21: GC-MS analysis results obtained for cell lysate extract product and wet biomass product extract using solvent-solvent extraction

	Run time (min)	**Formula**	**Compound**	**% Area**	**Relative molecular mass**	**Match quality (%)**
Cell lysate solvent-solvent extract products	6.916	$C_{12}H_{26}O$	1-dodecanol	3.09	186	95
	11.069	$C_{15}H_{32}O$	n-pentadecanol	0.28	228	95
	13.354	$C_{18}H_{38}O$	1-octadecanol	0.37	270	94
	15.204	$C_{16}H_{32}O_2$	hexadecanoic acid	0.44	256	84
	15.419	C21H44O	1-heneicosanol	0.57	312	91
	17.308	$C_{20}H_{42}O$	1-eicosanol	0.49	298	91
	19.538	$C_{27}H_{56}O$	1-heptacosanol	0.47	396	94
Total fatty alcohol				5.27%		
Wet biomass solvent-solvent extract products	11.156	$C_{17}H_{36}$	heptadecane	3.30	240	96
	13.169	$C_{14}H_{28}O_2$	tetradecanoic acid	10.44	228	93
	15.244	$C_{16}H_{32}O_2$	hexadecanoic acid	6.99	256	84
	15.421	$C_{19}H_{40}O$	n-nonadecanol-1	1.18	284	87
	17.155	$C_{18}H_{36}O_2$	octadecanoic acid	2.68	284	83
	17.309	$C_{20}H_{42}O$	1-eicosanol	2.05	298	91
	19.541	$C_{27}H_{56}O$	1-heptacosanol	2.51	396	90
	22.763	$C_{24}H_{50}O$	n-Tetracosanol-1	1.69	354	85
Total fatty alcohol				8.96%		

Table 5.22: GC-MS analysis results obtained for cell lysate extract product and wet biomass product extract using reactive extraction system

	Run time (min)	**Formula**	**Compound**	**% Area**	**Relative molecular mass**	**Match quality (%)**
Cell lysate products extract	5.512	$C_{11}H_{24}O$	1-undecanol	0.02	172	93
	5.864	$C_{12}H_{26}$	n-dodecane	0.01	170	95
	10.126	$C_{12}H_{26}O$	1-dodecanol	1.16	186	98
	12.169	$C_{14}H_{30}O$	1-tetradecanol	0.04	214	91
Total fatty alcohol				1.22%		
Wet biomass products extract	5.509	$C_{11}H_{24}O$	1-undecanol	0.02	172	94
	5.862	$C_{12}H_{26}$	n-dodecane	0.01	170	96
	10.126	$C_{12}H_{26}O$	1-dodecanol	1.26	186	96
	11.302	$C_{16}H_{34}$	hexadecane	0.02	226	96
	12.152	$C_{14}H_{30}O$	1-tetradecanol	0.03	214	92
Total fatty alcohol				1.31%		

5.12.4 Carbon balance and thermodynamic analysis

The actual CO_2 utilization efficiency of *H. stevensii* in laboratory scale reactor was demonstrated by applying approximate carbon balance on the bioreactor. The procedure adopted for approximate material balance and thermodynamic assessment was same as described in section 4.1 and 4.13, respectively.

The total amount of CO_2 supplied to the system ($M_{C,in}$) during cultivation period was calculated as 4.63 g. The CO_2 concentration at the outlet of bioreactor is monitored in regular interval of 12 h and no trace of CO_2 was observed. Therefore, the value of CO_2(g) in the outlet stream ($M_{C,go}$) was taken as 0. The amount of CO_2 assimilated as biomass in into the cellular biomass ($M_{C,\,bo}$) was found as 3.66 g (Ritmann and Mackarty, 2012). At the end of the study, the total carbon present in the liquid phase ($M_{C,CO2(l)}$) as CO_3^{2-}, HCO_3^-, free $CO_2$and fatty alcohols was estimated as 0.826 g using titration method and GC quantification, respectively. After substituting the above obtained values in Eq. 4.1, the RHS and LHS of the equation were found as 4.63 g and 4.48 g, respectively. Thus, material balance calculations revealed that out of total 4.63 g of carbon supplied to the bio-reactor, 3.66 g of carbon was assimilated into the cellular biomass of *H. stevensii*. Based on this the actual CO_2 utilization efficiency ($R.R_{CO2}$) of the process was obtained as 79.04 %.

Gibb's free energy of products and reactants was estimated as -6777.48 and -5917.68 kJ mol^{-1}, respectively. The change in Gibb's free energy for the Eq. 4.12 was obtained as -859.8 kJ mol^{-1}. As the fixation of 14 moles of CO_2 requires -859.8 kJ of energy then in present case 0.29 moles of CO_2 would require 17.81 kJ of energy for the fixation of CO_2 as tetradecanol.

The energy available in the system as $S_2O_3^{2-}$ was -440.58 kJ due to complete $S_2O_3^{2-}$ oxidation. This was much higher than the energy required (17.81 kJ) for the fixation of CO_2.

Therefore, the energy available in the system was sufficient to meet the requirement of CO_2 fixation and to further metabolize the same into cellular biomass as fatty alcohols. Hence, the approximate material balance and thermodynamic analysis confirmed the gaseous phase CO_2 fixation in the presence of $S_2O_3^{2-}$ as an energy source and its conversion into value added products.

5.12.5 Comparison with existing literature

Most of the studies in CCU have reported the production of valued chemicals by utilizing photoautotrophs (microalgae and cyanobacteria). Hence, the performance of present system in terms of *P* and R_{CO2} is compared with reported studies and given in Tables 5.23 and 5.24. *P* and R_{CO2} values for the reported microalgal strains were found in the range of 0.189 - 0.338 g L^{-1} d^{-1} and 0.12 - 1.21 g L^{-1}, respectively (Table 5.23). In present study, *P* and R_{CO2} values were obtained as 1.55 (±0.04) and 1.94 (±0.044), respectively. Thus, the results indicated that *P* and R_{CO2} values for *H. stevensii* were found to be higher as compared to the values obtained for other microbial strains (Table 5.23). Therefore, the higher CO_2 utilizing capability of *H. stevensii* makes it a promising candidate for the CO_2 mitigation from the industrial environment.

The amount of fatty alcohol content in per unit mass or volume of biomass or leachate should be higher for economically feasible process. Few studies are listed in Table 5.24 which have reported the production of fatty alcohols from different microorganisms such as bacteria, yeast, microalgae etc. The total fatty alcohol production yield of 540 mg of fatty alcohol per g biomass was observed for *Chelorella sorokinianna* 21 (Table 5.24). *Synechocystis sp.* PCC has shown the total fatty alcohol production of 0.00287 mg of fatty alcohol per g of biomass (Table 5.24). The *E. coli* was engineered for the production of fatty alcohols and the product yield was

obtained as 0.067, 0.5986 and 0.75 g L^{-1} in different studies (Table 5.24). In present study, the yield of fatty alcohol was observed as 606.72 (±0.35) mg per g of biomass of *H. stevensii* by CO_2 bio-mitigation in semi-continuous studies. The yield of fatty alcohols obtained in the present study was significantly higher as compared to reported studies except engineered *E. coli* (Table 5.24). Further, the studies related to the biological fatty alcohols production were mostly dependent on the engineered bacterial strain (Table 5.24). However, *H. stevensii* (pure isolate) was found capable to utilize CO_2(g) as a carbon source.

5.12.6 Process economics

The raw materials for the production of dodecanol and tetradecanol were lauric acid (C_{12}) (46% - 51%) and myristic acid (C_{14}) (17% - 19%,) obtained from coconut oil. Therefore, by material balance, approximately 2.5 kg and 5.5 kg virgin coconut oil was required, respectively for perkg production of dodecanol and tetradecanol. The virgin coconut oil is available at the market price of Rs 114.324 per kg (indexmundi.com). Thus, the cost of feedstock required for the production of 1 kg of dodecanol and tetradecanol was Rs 285.81 and Rs 628.78, respectively. The effect of factor "*f*" on the total cost for the production of dodecanol and tetradecanol using coconut oil as feedstock was calculated using Eq. 4.15 and is shown in Fig. 5.35. The market price of dodecanol and tetradecanol produced from coconut oil as raw material was estimated as 1143.24 Rs kg^{-1} and 2515.12 Rs kg^{-1}, respectively for the "*f*" factor value in between 0.7 and 0.8 (Fig. 5.35). These prices fall in accordance with the current market price of dodecanol (Rs. 1300.00) and tetradecanol (Rs. 2450.00), respectively (Fig. 5.36). The obtained "*f*" factor value for market price of coconut oil was in accordance with the reported values for bioprocesses in literature (Belrabi et al., 2000).

The maximum acceptable price of raw material i.e. bacterium biomass (*C*) was calculated using Eq. 4.18. The effect of factor "*f*" on *C* is shown in Fig. 5.36 and was estimated using Eq. 4.15. The maximum acceptable price of biomass was estimated by considering the "*f*" value in the range of 0.7 to 0.8. The obtained values of *C* were observed as 617.96 Rs kg^{-1} and 2687.91 Rs kg^{-1} for dodecanol and 2687.91 Rs kg^{-1} and 3263.89 Rs kg^{-1} for tetradecanol, respectively. The value of *C* for dodecanol production was well below the current market price of dodecanol and there is scope for the addition of extra separation, purification and energy cost. However, the obtained value of *C* for the production of tetradecanol was found to be higher than the current market price. The obtained value of *C* for tetradecanol production has to be further lowered in order to account for additional separation, purification and energy cost. The lower value of *C* for the dodecanol confirms that the *H. stevensii* can be utilized for the production of dodecanol.

In the above analysis, same fraction of dodecanol and tetradecanol was considered in the biomass of *H. stevensii* and coconut oil. However, the fraction of dodecanol and tetradecanol present in the biomass of *H. stevensii* was obtained as 9.1% and 19.5%, respectively which was quite low as compared to coconut oil. Therefore, it is necessary to evaluate the effect of the fraction of fatty alcohols on the value of *C*. This effect was calculated using Eq. 4.19 and was plotted in Figs. 5.37 and 5.38. The obtained results are shown in Fig. 5.37 and Fig. 5.38 at factor "*f*" value of 0.7 and 0.8 for dodecanol and tetradecanol, respectively. The result estimated the cost of biomass which was obtained from *H. stevensii* for perkg production of dodecanol and tetradecanol as Rs kg^{-1} 58.52, 121.60 and Rs kg^{-1} 271.81, 256.71 at factor "*f*" value of 0.7 and 0.8, respectively. These costs are acceptable or competitive with coconut oil at the obtained values. The acceptable price of the biomass depends on the factor "*f*" and was found to increase with increase in value of factor "*f*". This suggested that in order to maintain the factor between

0.7 and 0.8, the biomass price has to decrease. Study of process economics suggested the feasibility of downstream process for the production of dodecanol as compared to the tetradecanol.

Table 5.23: Comparison of *P* (g L^{-1} d^{-1}) and R_{CO2} of few reported studies with semi-continuos study using *H. stevensii*

Species	Mode	CO_2 concentration (% v/v)	Biomass productivity (*P*, g L^{-1} d^{-1})	CO_2 fixaton rate (R_{CO2}, g L^{-1} d^{-1})	References
Chlorella sorokiniana	Air-lift PBR	5	0.338	1.21	Kumar and Das, (2012)
Chaetoceros muelleri	Flask study	10	0.272	0.428	Wang et al., (2014)
Chlorella sp.	Bubble column PBR	10	0.271 (±0.07)	0.249 (±0.11)	Yadav et al., (2015)
Chlorella vulgaris	Bubble column PBR	15	0.282	Between 0.35 - 4.0	Mohsenpour and Willoughby, (2016)
Guzmania membranacea	Bubble column PBR	15	0.189	Between 0.12 - 0.15	Mohsenpour and Willoughby, (2016)
Chlorella PY-ZU1	Bubble column PBR	15	0.518	0.94	Cheng et al., (2016b)
H. stevensii	Laboratory scale bioreactor	15 (±1)	1.55 (±0.04)	1.94 (±0.044)	Present study

Table 5.24: Comparison of fatty alcohols productivity of few reported studies with *H. stevensii* during scale-up study

Species	Fatty alcohol production (mg of fatty alcohol per g biomass & g L^{-1})	Reference
Engineered *Escherichia coli*	0.060 g L^{-1}	Steen et al., (2010)
Engineered *E. coli*	0.5986 g L^{-1}	Zheng et al., (2012)
Chelorella sorokinianna 21	540 mg of fatty alcohol per g of biomass	Yang et al., (2013)
Engineered *E. coli*	0.75 g L^{-1}	Liu et al., (2014)
Synechocystis sp. PCC	0.00287 mg of fatty alcohol per g of biomass	Yao et al., (2014)
H. stevensii	606.72 (± 0.35) mg per g of biomass	Present study

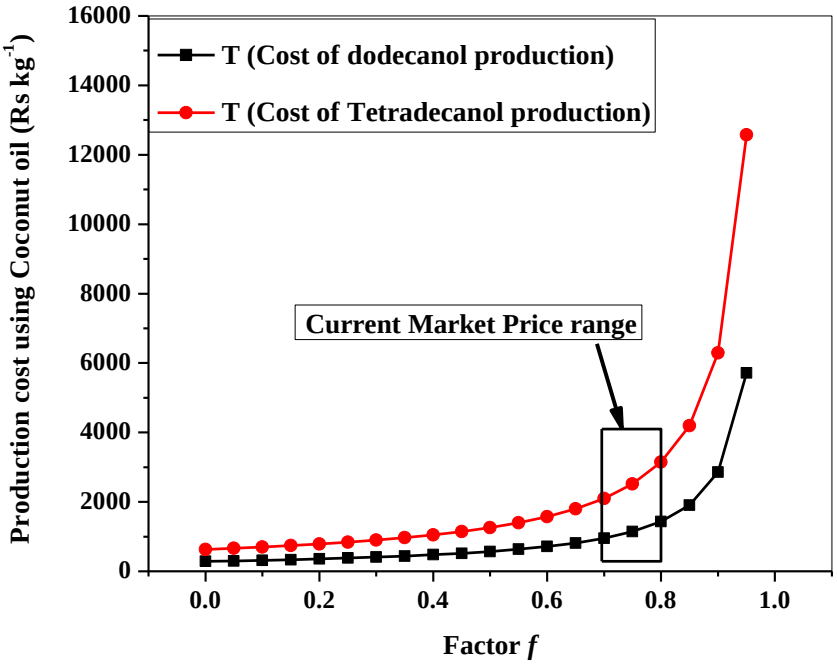

Fig. 5.35 Effect of factor "*f*" on the total cost of production of dodecanol and tetradecanol using coconut oil.

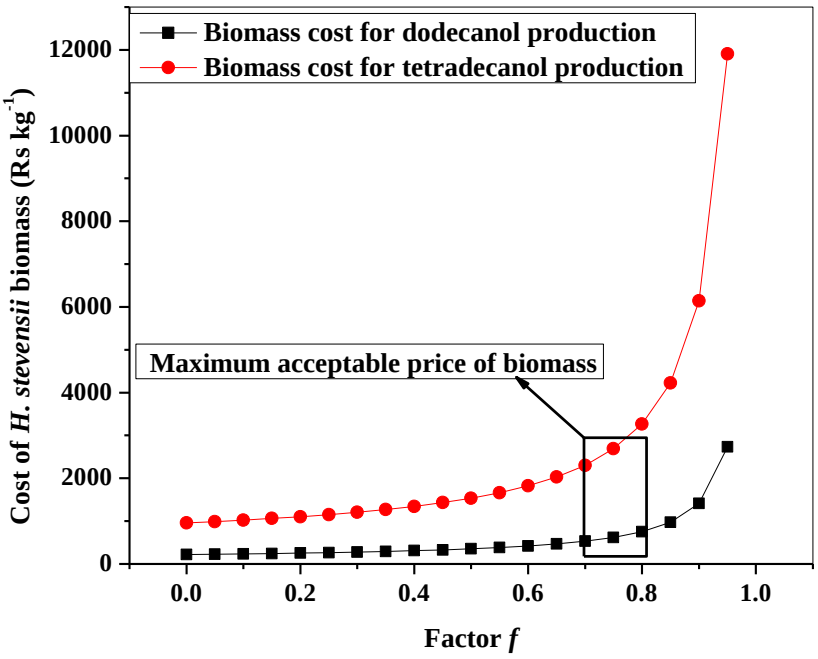

Fig. 5.36 Effect of factor "*f*" on the maximum acceptable cost of *H. stevensii* biomass.

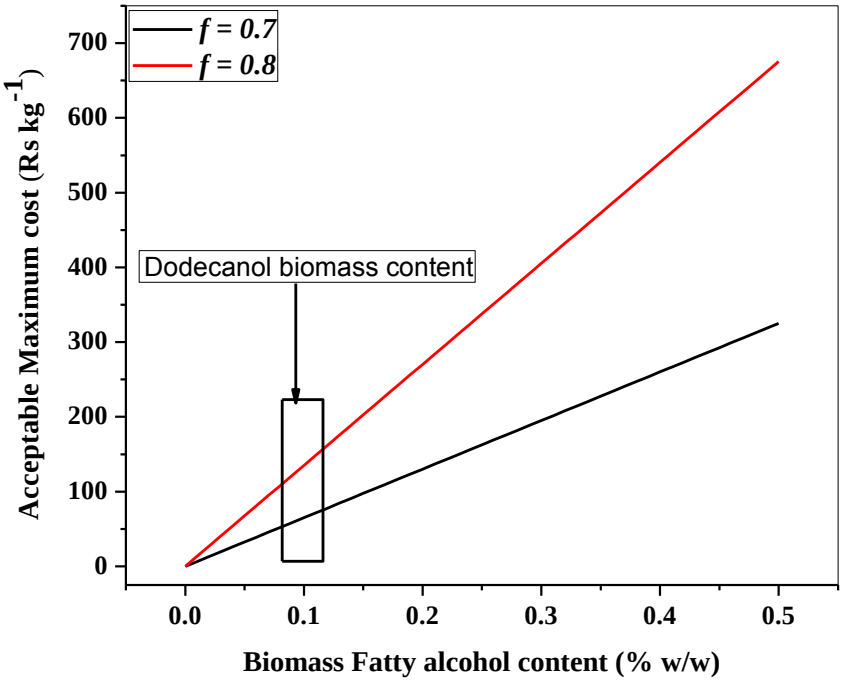

Fig. 5.37 Effect of dodecanol content on the maximum acceptable price of *H. stevensii*.

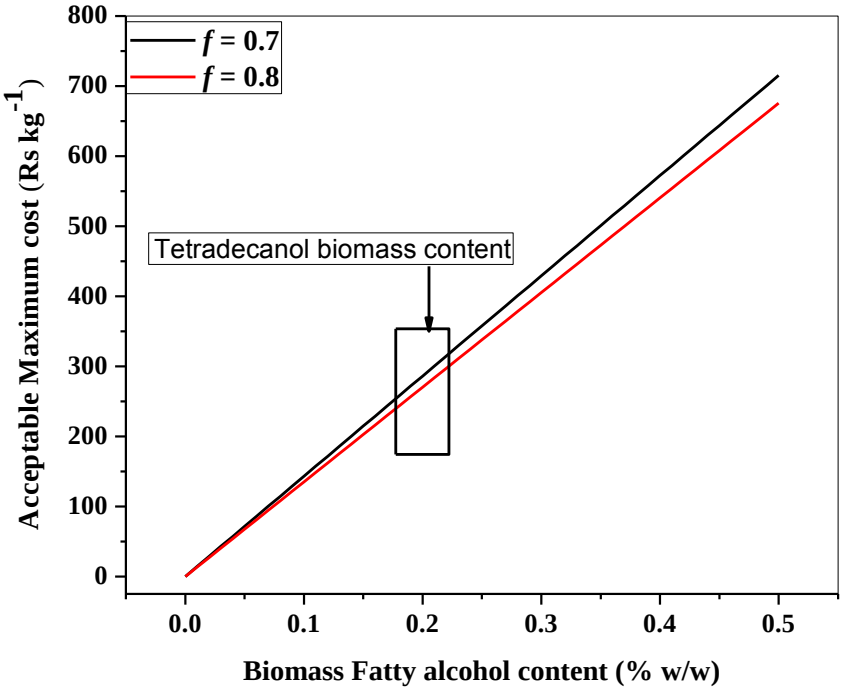

Fig. 5.38 Effect of dodecanol content on the maximum acceptable price of *H. stevensii*.

5.13 Performance of packed bed bioreactor for CO_2 mitigation

The removal of CO_2(g) from the mixture of CO_2(g) and air was investigated using continuous bioreactor packed with a mixture of coal and matured compost. The packed bed was inoculated with the mixed population of *B. cereus*, *E. cloacae*, *P. putida*, *P. aeruginosa* and *H. stevensii* for seven days. The effect of time on the performance of packed bed bioreactor was investigated at changing inlet concentration of CO_2(g). The performance of the column was measured in terms of CO_2(g) removal efficiency and biomass growth rate (CFU g^{-1} of packing material).

The effect of time on the inlet concentration, outlet concentration and removal efficiency of CO_2(g) at different inlet concentration was plotted and shown in Fig. 5.39. The packed bed bioreactor was operated for the duration of 77 days and the duration was divided into three phases according to packed bed bioreactor operating conditions. The biomass in terms of $CFUg^{-1}$ of packing material was also estimated at different heights of the packed bed (15, 30, 45, 60, 75 and 90 cm from the bottom of the packing) for different values of inlet CO_2(g) concentration and is reported in Table 5.25.

In phase I (acclimation period), CO_2(g) concentration was found to be more at the column outlet than the CO_2(g) supplied to the packed bed bioreactor for first 15 days of its operation. This may be due to the lower rate of microbial utilization of CO_2 as compared to the CO_2(g) supplied to the packed bed bioreactor during initial days of acclimation period. Thus, un-utilized CO_2(g) was accumulated in the upper part of the packed bed bioreactor as inlet flow rate of CO_2(g) to the packed bed bio-reactor was not equal to the outlet packed bed bioreactor flow rate. This resulted in the increased concentration of CO_2(g) on top of the reactor. However, the CO_2 removal efficiency was found to increase with increase in number of days and reached 100 % at the end of phase I (30 days) (Fig. 5.34). This may be due to the fact that microbial consortia

took some time to get acclimated in the changed environment of CO_2. The increase in CO_2(g) removal efficiency with increase in time may also be justified with the larger value of CFU (704 $\times 10^8$ CFU g^{-1} of packing material, 15 cm from bottom) at the end of acclimation period. The value of CFU was found to decrease from 704 $\times 10^8$ to 25 $\times 10^8$ CFU g^{-1} of packing material with increase in height from 15 cm to 90 cm, respectively.

Inlet CO_2(g) concentration to the column was sudden changed to 10 and 15% (v/v) at the start of phase II and phase III, respectively. The removal efficiency was found to decrease with change in inlet CO_2 concentration in the initial days of phase II and phase III. This may be due to the fact that microbial consortia took time to adjust in the changed environment. The increase in biomass growth with time may be one of the possible reasons for obtaining 100% CO_2(g) removal efficiency at higher inlet CO_2(g) concentration. The obtained results of sudden change in inlet CO_2(g) concentration indicate that biofilm developed in the packed bed bioreactor was quite stable. Hence, one set of continuous bio-mitigation studies using CO_2(g) has shown that the mixed microbial culture was responding well in the continuous mode as well.

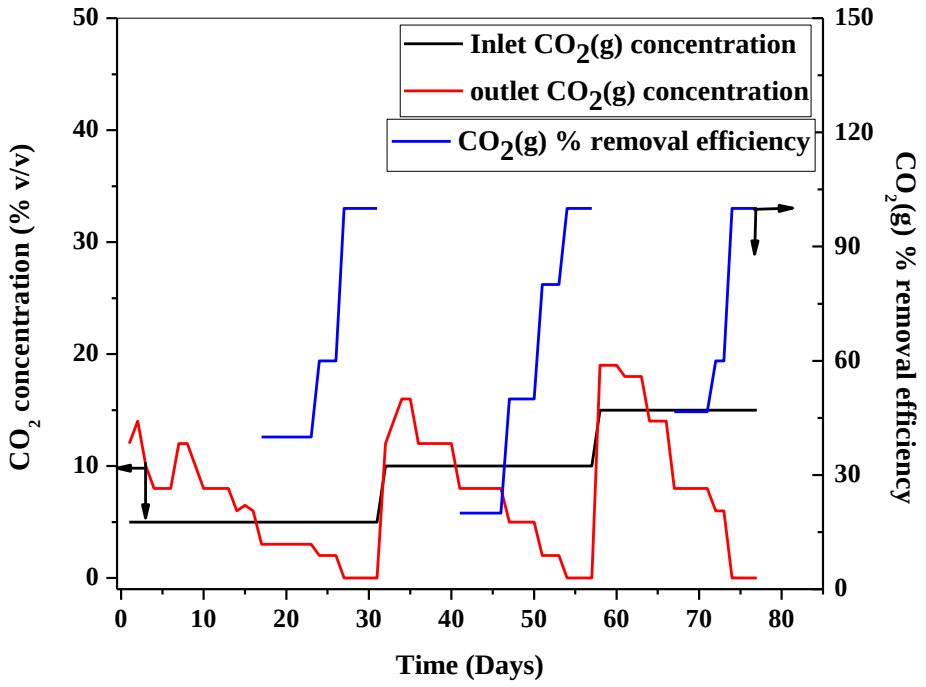

Fig. 5.39 Performance of packed bed bioreactor under shock loading condition for CO_2(g) removal.

Table 5.25: Biomass growth in terms of CFU g^{-1}

Sample port (from the bottom)	Phase I	Phase II	Phase III
	CFU g^{-1}		
1	704×10^8	1384×10^8	1402×10^8
2	656×10^8	976×10^8	987×10^8
3	136×10^8	328×10^8	411×10^8
4	103×10^8	177×10^8	208×10^8
5	38×10^8	131×10^8	156×10^8
6	25×10^8	144×10^8	148×10^8

Chapter 6

Concluding Remarks

In present chapter, conclusions, major contributions and future scope for research are discussed.

6.1 Conclusions

The following conclusions are drawn based on the results obtained in the present study:

1. Strains *B. cereus* SM1, *P. putida* SM2 and *E. cloacae* PP1 obtained from STP and strains *P. aeruginosa* SSL4 and *H. stevensii* SSL5 from SSL were successfully utilized for the bio-mitigation studies using CO_2.
2. *P. aeruginosa* SSL4 showed maximum η_{CO2}(g) value as 92.37 (±2.47)% among all iron utilizing bacterium at 100 ppm of Fe[II] concentration and among all microbial cultures used in the present study, *H. stevensii* showed maximum η_{CO2}(g) as 98.59 (±0.59)% at 100 mM $S_2O_3^{2-}$ concentration.
3. CO_2 fixation capability was found to increase with increase in Fe[II] concentration for *B. cereus* SM1, Mixed microbial population *P. putida* SM2, *E. cloacae* PP1 and *P. aeruginosa* SSL4 and also increased with $S_2O_3^{2-}$ for *H. stevensii*.
4. Optimum energy substrate concentration was obtained as 100 ppm Fe[II] for iron utilizing bacterium and 100 mM $S_2O_3^{2-}$ for sulfur oxidizing bacterium.
5. Maximum values for *P*, R_{CO2} and $R.R_{CO2}$ were obtained at 100 ppm for Fe[II] for iron utilizing bacterium and100 mM $S_2O_3^{2-}$ concentration for sulfur oxidizing bacterium.
6. As per the values obtained for η_{CO2}(g), *P*, R_{CO2} and $R.R_{CO2}$, *H. stevensii* was found to be a superior candidate for CO_2 fixation among all other species used in the present study.
7. FT-IR and GC-MS analysis of cell lysate and cell free supernatant extract of *B. cereus* SM1, mixed microbial population, *P. putida* SM2 and *E. cloacae* PP1, confirmed the presence of fatty acids and hydrocarbons comprised of carbon chain length in the range of C_5-C_{19} and C_{10}-C_{24}, respectively.
8. Fatty acids obtained from CO_2 fixation of STP cultures were successfully converted to biodiesel using transestrification reaction.

9. Biodiesel yield of 86.5 (±0.048), 91.55(±0.198), 77.49 (±0.1) and 38.69 (±1.66)% was observed for *B. cereus*, mixed microbial population, *E. cloacae* and *P. putida*, respectively.
10. Hydrocarbon obtained from CO_2 bio-fixation of STP cultures were comprised of saturated, unsaturated and branched hydrocarbons which could be utilized as a precursor for the production of compounds such as higher alcohols, alkanes, halides, polymer products, etc.
11. FT-IR and GC-MS analysis of cell lysate and cell free supernatant extract of *P. aeruginosa* SSL4 and *H. stevensii* SSL5 revealed the presence of fatty alcohols and hydrocarbons in considerable amount and fatty acids in trace amount.
12. Yield of fatty alcohols for the biomass obtained from CO_2 fixation using *P. aeruginosa* SSL4 and *H. stevensii* SSL5 was found as 0.392 (±0.14) and 0.32 (±0.016) g of fatty alcohols g^{-1} of biomass, respectively.
13. Values of salt concentration and temperature for maximum specific growth of *P. aeruginosa* SSL4 were found as 3% (w/v) and 37 ^{o}C, respectively.
14. Optimum growth parameters for the fixation of CO_2 using *H. stevensii* were obtained as 0.5 M salt concentration, pH of 8 and a temperature of 37 ^{o}C.
15. Product yield of fatty alcohols obtained from the leachate of *H. stevensii* was found to be significantly influenced by the physicochemical parameters such as inlet CO_2(g) concentration, salt concentration, pH and temperature.
16. Semi-quantification and quantification studies of carbon allocation established the fact that CO_2 was utilized to produce fatty alcohols at the expense of cellular carbohydrate and protein content.

17. Approximate material balance and thermodynamic assessment of the CO_2 bio-mitigation process of STP and SSL cultures supported CO_2(g) fixation in the presence of energy substrate [Fe[II] or $S_2O_3^{2-}$] into cellular biomass and its conversion into value added products.
18. Actual CO_2(g) utilization estimated from approximate material balance was found to decrease in order of *H. stevensii* > mixed microbial population > *B. cereus* > *P. putida* > *P. aeruginosa* > *E. cloacae*.
19. Higher values of P and R_{CO2} obtained from semi-continuous bioreactor in comparison to batch study proved a good response of *H. stevensii* in the changing environment of pH and higher CO_2 concentration.
20. Downstream processing results revealed that the biomass obtained from filtration and direct recovery of metabolites using solvent extraction from wet biomass may be an efficient and cost effective downstream processing strategy.
21. Product yields of fatty alcohols and $R.R_{CO2}$ were obtained as 79.81 (±0.014)% and 79.04%, respectively from semi-continuous studies of CO_2 fixation using *H. stevensii*.
22. Process economic study on semi-continuous study for fixation of CO_2 suggested the feasibility of downstream process for the production of dodecanol as compared to tetradecanol.
23. Packed bed bioreactor was developed and effectively utilized for the continuous mitigation of CO_2(g) from 15% (v/v) CO_2 and air mixture for 77 days of bioreactor operation.
24. Packed bed bioreactor was found stable at fluctuating inlet CO_2(g) concentration and confirmed its suitability for further scale-up.

6.2 Major contributions

1. Bacterial strains were identified as *B. cereus* SM1, *P. putida* SM2 and *E. cloacae* PP1 obtained from STP culture and strains *P. aeruginosa* SSL4 and *H. stevensii* SSL5 from SSL culture for bio-mitigation of CO_2(g) studies.
2. CO_2(g) fixation was carried out by microbial culture in absence of light by use of inorganic compounds [Fe[II] or $S_2O_3^{2-}$] as energy source.
3. Identification and utilization of extremophilic bacteria (*P. aeruginosa* SSL4 and *H. stevensii* SSL5) for the CO_2 fixation in extreme environmental conditions.
4. Successful demonstration of the conversion of CO_2(g) into valuable chemicals such as fatty acids, hydrocarbons, fatty alcohols, etc. by microbial culture.
5. Development of cost effective downstream process for the recovery of fatty alcohols from the culture obtained from semi-continuous fixation of CO_2 using *H. stevensii*.
6. Economic feasibility analysis of developed downstream process for the recovery of fatty alcohols with existing bio-based fatty alcohol processes.
7. Development of packed bed bioreactor for the continuous mitigation of CO_2 from CO_2 – air mixture.

6.3 Future scope

1. CO_2 bio-mitigation experiments can be performed with mixed microbial culture and isolated strains in the simulated environment having resemblance to flue gas.
2. Development of mixed microbial consortium from the species obtained in the present study and utilizing them for bio-mitigation studies of CO_2(g).

3. CO_2 bio-mitigation studies can be performed to evaluate the effect of utilization of industrial effluent containing inorganic chemicals [Fe[II], $S_2O_3^{2-}$, heavy metal ions in reduced form, NO_3^-, etc.] as growth media.
4. Cultivation strategy using CO_2(g) as carbon source needs to be investigated for increasing targeted metabolite contents in the leachate.
5. Exhaustive experimental studies on continuous bioreactor need to be performed for efficient scale-up of the process

REFERENCES

Abomohra, A-F., El-Sheekh, M., Hanelt D., (2017). Screening of marine microalgae isolated from the hypersaline Bardawil lagoon for biodiesel feedstock, Renewable Energy. 101, 1266-1272.

Aggarwal, M., Chua, K., T., Pinard, A., M., Szebenyi, M., D., McKenna, R., (2015). Carbon Dioxide "Trapped" in a β-Carbonic Anhydrase. Biochemistry, 54(43), 6631–6638.

Alonso-Sáez, L., Galand, P., E., Casamayor, E., O., Pedrós-Alió, C., Bertilsson, S., (2010). High bicarbonate assimilation in the dark by Arctic bacteria. The ISME Journal, 4(12), 1581–90.

Amend, P., J., and Shock, L., E., (2001). Energetics of overall metabolic reactions of thermophilic and hyperthermophilic Archaea and Bacteria, FEMS Microbiology Reviews 25(2), 175-243.

Amend, P., J., Rogers, L., K., Shock, L., E., Gurrieri, S., Inguaggiato, S., (2003). Energetics of chemolithoautotrophy in the hydrothermal system of Vulcano Island, southern Italy, Geobiology 1, 37-58.

Anderson, S., and Newell, R., (2004). Prospects for carbon capture and storage technologies. Annual Review of Environment and Resources, 29, 109 -142.

Andrews, S., C., Robinson, A., K., Rodríguez-Quiñones, F., (2003). Bacterial iron homeostasis. FEMS Microbiology Reviews, 27(2-3), 215-237.

Anjos, M., Fernandes, B., D., Vicente, A., A., Teixeira, J., A., Dragone, G., (2013). Optimization of CO_2 bio-mitigation by *Chlorella vulgaris*. Bioresource Technology, 139, 149–154.

American Public Health Association (APHA), Standard methods for the examination of water and wastewater, 17th ed. APHA AWWA WPCF, Washington, DC, 1989.

Aresta, M., Dibenedetto, A., Pastore, C., (2004). An Integrated Approach To the Synthesis of Organic Carbonates : Discovery of New Catalysts, 3(3), 356-357.

Aresta, M., and Dibenedetto, A., (2007). Utilisation of CO_2 as a chemical feedstock: opportunities and challenges. Dalton Transactions, 17(28), 2975-2992.

Basu, S., Roy, A. S., Mohanty, K., Ghoshal, A. K., (2013). Enhanced CO_2 sequestration by a novel microalga: *Scenedesmus obliquus* SA1 isolated from bio-diversity hotspot region of Assam, India. Bioresource Technology, 143, 369–77.

Battin, T., J., Luyssaert, S., Kaplan, L., Aufdenkampe, A., K., Richter, A., Tranvik, L., J., (2009). The boundless carbon cycle. Nature Geoscience, *2*(9), 598–600.

Baumann, H., Talmage, S., C., Gobler, C., J., (2011). Reduced early life growth and survival in a fish in direct response to increased carbon dioxide. Nature Climate Change, 2(1), 38-41.

Belarbi, E., Molina, E., Chisti, Y., (2000). A process for high yield and scaleable recovery of high purity eicosapentaenoic acid esters from microalgae and fish oil. Enzyme and Microbial Technology, 26(7), 516-529.

Berg, I., A., (2011). Ecological aspects of the distribution of different autotrophic CO_2 fixation pathways. Applied and Environmental Microbiology, 77(6), 1925-1936.

Cuellar-Bermudeza, P., S., Garcia-Pereza, S., J., Ritmann, E., B., Parra-Saldivara, R., (2015). Photosynthetic bioenergy utilizing CO_2: an approach on flue gases utilization for third generation biofuels. Journal of Cleaner Production, 98, 53-65.

Bharti, R., K., Srivastava, S., Thakur, I., S., (2014). Production and characterization of biodiesel from carbon dioxide concentrating chemolithotrophic bacteria, *Serratia* sp. ISTD04. Bioresource Technology, 153, 189-197.

Buckel, W., Thauer, R., K., (2013). Energy conservation via electron bifurcating ferredoxin reduction and proton/Na+ translocating ferredoxin oxidation. Biochimica et Biophysica Acta - Bioenergetics, 1827(2), 94-113.

Cannon, G., C., Heinhorst, S., Kerfeld, C., A., (2010). Carboxysomal carbonic anhydrases: Structure and role in microbial CO_2 fixation. Biochimica et Biophysica Acta, 1804(2), 382-392.

Cardoso, S., J., B., Enrich-Prast, A., C., Pace, M. L., Roland, F., (2014). Do models of organic carbon mineralization extrapolate to warmer tropical sediments?. Limnology and Oceanography, 59(1), 48–54.

Carroll, J., J., Slupsky, J., D., Mather, A., E., (1991). The solubility of carbon dioxide in water. Journal of Physical and Chemical Reference Data, 20(6), 1201-1209.

Chandra, S., T., Deepak, S., R., Kumar, M., M., Mukherji, S., Chauhan, S., V., Sarada, R., Mudliar, N., S., (2016). Evaluation of indigenous fresh water microalga *Scenedesmus obtusus* for feed and fuel applications: Effect of carbon dioxide, light and nutrient sources on growth and biochemical characteristics, Bioresource Technology, 207, 430-439.

Cheah, W., Y., Show, P., L., Chang, J.-S., Ling, T., C., Juan, J., C., (2014). Biosequestration of atmospheric CO_2 and flue gas-containing CO_2 by microalgae. Bioresource Technology, 184, 190-201.

Chen, C-Y., Kao, P-C., Tan, H., C., Show, L., P., Cheah, Y., W., Lee, W-L., Ling, C., T., Chang, J-S., (2016). Using an innovative pH-stat CO_2 feeding strategy to enhance cell growth and C-phycocyanin production from *Spirulina platensis*. Biochemical Engineering Journal, 112, 78-85.

Cheng, J., Huang, Y., Feng, J., Sun, J., Zhou, J., Cen, K., (2013a). Improving CO_2 fixation efficiency by optimizing *Chlorella* PY-ZU1 culture conditions in sequential bioreactors. Bioresource Technology, 144, 321-327.

Cheng, J., Huang, Y., Feng, J., Sun, J., Zhou, J., Cen, K., (2013b). Mutate *Chlorella* sp. by nuclear irradiation to fix high concentrations of CO_2. Bioresource Technology, 136, 496-501.

Cheng, Y., S., Labavitch, J., M., Vandergheynst, J., S., (2014). Elevated CO_2 concentration impacts cell wall polysaccharide composition of green microalgae of the genus *Chlorella*. Letters in Applied Microbiology, 60(1), 1-7.

Cheng, J., Li, K., Yang, Z., Lu, H., Zhou, J., Cen, K., (2016a). Gradient domestication of *Haematococcus pluvialis* mutant with 15% CO_2 to promote biomass growth and astaxanthin yield. Bioresource Technology, 216, 340-344.

Cheng, J., Ye, Q., Xu, J., Yang, Z., Zhou, J., Cen, K., (2016b). Improving pollutants removal by microalgae *Chlorella* PY-ZU1 with 15% CO_2 from undiluted anaerobic digestion effluent of food wastes with ozonation pretreatment. Bioresource Technology, 216, 273-279.

Chiang, C., L., Lee, C., M., Chen, P., C., (2011). Utilization of the cyanobacteria *Anabaena sp.* CH1 in biological carbon dioxide mitigation processes. Bioresource Technology, 102(9), 5400-5405.

Chiaramonti, D., Prussi, M., Casini, D., Tredici, M., R., Rodolfi, L., Bassi, N., Bondioli, P., (2013). Review of energy balance in raceway ponds for microalgae cultivation: Re-thinking a traditional system is possible. Applied Energy, 102, 101-111.

Chisti, Y., (2007). Biodiesel from microalgae. Biotechnology Advances, 25(3), 294-306.

Chiu, S., Y., Kao, C., Y., Chen, C., H., Kuan, T., C., Ong., S., C., Lin, C., S., (2008). Reduction of CO_2 by high density culture of *Chlorella sp.* in a semicontineous photobioreactor. Bioresource Technology, 99, 3389-3396.

Chinnasamy, S., Ramakrishnan, B., Bhatnagar, A., Das, C., K., (2009). Biomass production potential of a wastewater alga *Chlorella vulgaris* ARC 1 under elevated levels of CO_2 and temperature, International Journal Molecular Science, 10, 518-532.

Cropp, T., A., Smogowicz, A., A., Hafner, E., W., Denoya, C., D., McArthur, H., A., Reynolds, K., A., (2000). Fatty-acid biosynthesis in a branched-chain alpha-keto acid dehydrogenase mutant of *Streptomyces avermitilis* . Canadian journal of Microbiology, 46, 506-514.

Cuadros-Rodr´ıguez, L., Bagur-Gonz´alez, G., M., S´anchez-Vi˜nas, M., Gonz´alez-Casado, A., G´omez-S´aez, M., A., (2007). Principles of analytical calibration/quantification for the separation sciences. Jouurnal Chromatograph. A, 1158, 33-46.

Cuéllar-Franca, R., M., and Azapagic, A., (2015). Carbon capture, storage and utilisation technologies: A critical analysis and comparison of their life cycle environmental impacts. Journal of CO_2 Utilization, 9, 82–102.

Datta, D., Kumar, S., Uslu, H., (2015). Status of the Reactive Extraction as a Method of Separation, Journal of Chemistry, 1-16.

Daas, M., S., Rosana, A., R., R., Acedo, J., Z., Nateche, F., Kebbouche-Gana, S., Vederas, J., C., Case, R., J., (2017). Draft genome sequences of *Bacillus cereus* E41 and *Bacillus anthracis* F34 isolated from Algerian salt lakes. Genome Announc 5:e00383-17.

Dailey, C., R., Martin, G., R., Smiley, D., R., (2014). The effects of competition from non-pathogenic foodborne bacteria during the selective enrichment of Listeria monocytogenes using buffered Listeria enrichment broth. Food Microbiology 44, 173-179.

de Godos, I., Mendoza, J., L., Acièn, F., G., Molina, E., Banks, C., J., Heaven, S., Rogalla, F., (2014). Evaluation of carbon dioxide mass transfer in raceway reactors for microalgae culture using flue gases. Bioresource Technology, 153, 307–314.

de Morais, G., M., and Costa, V., A., J., (2007). Isoaltion and selection of microalgae from cola fired thermoelectric power plant for biofixation of carbon dioxide. Energy Conservation and Management, 48, 2169-2173.

de Visser, E., Hendriks, C., Barrio, M., Mølnvik, M., J., de Koeijer, G., Liljemark, S., Le Gallo, Y., (2008). Dynamis CO_2 quality recommendations. International Journal of Greenhouse Gas Control, *2*(4), 478-484.

Delhomenie, M-C., Heitz, M., (2005). Biofilteration of Air: A review, Critical Reviews in Biotechnology, 25, 53-72.

Duarte, J., H., Fanka, L., S., Costa, J., A., V., (2016). Utilization of simulated flue gas containing CO_2, SO_2, NO and ash for *Chlorella fusca* cultivation. Bioresource Technology, 214(10), 159-165.

Eminoğlu, A., Vullo, D., Aşık, A., Çolak, D., N., Supuran, C., T., Çanakçı, S., Osman Beldüz, A., (2016). Cloning, expression and biochemical characterization of a β -carbonic anhydrase from the soil bacterium *Enterobacter* sp. B13. Journal of Enzyme Inhibition and Medicinal Chemistry, 31(6), 1111-1118.

Fan, J., Xu, H., Luo, H., Wan, M., Huang, J., Wang, W., Li, Y., (2015). Impacts of CO_2 concentration on growth, lipid accumulation, and carbon-concentrating-mechanism-related gene expressionin oleaginous *Chlorella*. Applied Microbiology and Biotechnology, 99, 2451-2462.

Fdz-Polanco, F., M., Garcia, P., A, Villaverde, S., Uruen, M., A., (2001). Rapid communication new process for simultaneous removal of nitrogen and sulphur under anaerobic conditions. Water Research, 35(4), 1111-1114.

Fernandes, B., D., Mota, A., Teixeira, J., A., Vicente, A., A., (2015). Continuous cultivation of photosynthetic microorganisms: Approaches, applications and future trends. Biotechnology Advances, 33(6), 1228-1245.

Fernandes, T., Fernandes, I., Andrade, C., A., Cordeiro, N., (2016). Marine microalgae growth and carbon partitioning as a function of nutrient availability. Bioresource Technology, 214, 541-547.

Gaboyer, F., Vandenabeele-Trambouze, O., Cao, J., Ciobanu, M.-C., Jebbar, M., Le Romancer, M., Alain, K., (2014). Physiological features of *Halomonas lionensis* sp. nov., a novel bacterium isolated from a Mediterranean Sea sediment. Research in Microbiology, 165(7), 490–500.

Garcĭa, G., M., Mărquez, G., M. A., Moreno, H., C., X., (2016). Characterization of bacterial diversity associated with calcareous deposits and drip-waters, and isolation of calcifying bacteria from two Colombian mines. Microbiological Research, 182, 21-30.

Geider, R., Roche, J., La, Geider, R., J., (2002). Redfield revisited : variability of C : N : P in marine microalgae and its biochemical basis. European Journal of Phycology-British Phycological Society, 371(37), 1-17.

Giordano, M., Heraud, P., Beardall, J., Giordano, M., Al, E., T., (2001). Fourier transform infrared spectroscopy as a novel tool to investigate changes in intracellular macromolecular pools in the marine microalga *Chaetoceros muellerii* (*bacillariophyceae*). Journal of Phycology, 279, 271-279.

Grima, M., E., Belarbi, E., H., Acién Fernández, F., G., Robles Medina, A., Chisti, Y., (2003). Recovery of microalgal biomass and metabolites: process options and economics. Biotechnology Advances, 20, 491-515.

Goncalves, A., L., Rodrigues, C., M., Pires, J., C., M., Simoes, M., (2016). The effect of increasing CO_2 concentrations on its capture, biomass production and wastewater bioremediation by microalgae and cyanobacteria. Algal Research, 14, 127-136.

Gosh, W., Dam, B., (2009). Biogeochemistry and molecular biology of lithotrophic sulfur oxidation by taxonomically and ecologically diverse bacteria and archaea. FEMS Microbiology Review, 6(33), 999-1043.

Gupta, H., and Fan, L-S., (2002). Carbonation-Calcination Cycle using high reactivity calcium oxide for carbon dioxide separation from flue gas. Industrial and Engineering Chemistry Research, 41, 4035-4042.

Gupta, M., Aggarwal, S., Navani, N., K., Choudhury, B., (2014). Isolation and characterization of a protease-producing novel haloalkaliphilic bacterium *Halobiforma sp.* strain BNMIITR from Sambhar lake in Rajasthan, India. Annals of Microbiology, 65(2), 677-686.

https://www.co2.earth/. Date: 25 February 2017

Hedrich, S., Schlömann, M., and Johnson, D., B., (2011). The iron-oxidizing proteobacteria. Microbiology, 157(6), 1551-1564.

Ho, S-H., Chen, C-Y., Yeh, K-L., Chen, W-M., Lin, C-Y., Chang, J-S., (2010). Characterization of photosynthetic carbon dioxide fixation ability of indigenous *Scenedesmus obliquus* isolates. Biochemical Engineering Journal, 53(1), 57-62.

Ho, S-H., Chen, C-Y., Lee, D-J., Chang, J-S., (2011). Perspectives on microalgal CO_2-emission mitigation systems - a review. Biotechnology Advances, 29 (2), 189-198.

Hofvander, P., Doan, P., T., T., Hamberg, M., (2011). A prokaryotic acyl-CoA reductase performing reduction of fatty acyl-CoA to fatty alcohol, FEBS Letters, 585, 3538-3543.

Hu, Q., Sommerfeld, M., Jarvis, E., Ghirardi, M., Posewitz, M., Seibert, M., Darzins, A., (2008). Microalgal triacylglycerols as feedstocks for biofuel production: Perspectives and advances. The Plant Journal, 54(4), 621-639.

Hu, X., Zhou, J., Liu, G., Gui, B., (2016). Selection of microalgae for high CO_2 fixation efficiency and lipid accumulation from ten *Chlorella* strains using municipal wastewater. Journal of Environmental Science, 46, 83-91.

Inskeep, W., P., Ackerman, G., G., Taylor, W., P., Kozubal, M., Korf, S., Macur, R., E., (2005). On the energetics of chemolithotropy in nonequilibrium systems: case studies of geothermal springs in Yellowstone National Park. Geobiology, 3, 297-317.

http://www.indexmundi.com/commodities/. Date: 24 December 2016

IPCC, 2014: Climate Change 2014: Synthesis Report. Contribution of Working Groups I, II and III to the Fifth Assessment Report of the Intergovernmental Panel on Climate Change [Core Writing Team, Pachauri, K., R., Meyer, A., L.] IPCC, Geneva, Switzerland.

Jabeen, H., Iqbal, S., Anwar, S., Parales, R., E., (2015). Optimization of profenofos degradation by a novel bacterial consortium PBAC using response surface methodology. International Biodeterioration and Biodegradation, 100, 89-97.

Jiang, Y., Yoshida, T., Quigg, A., (2012). Photosynthetic performance, lipid production and biomass composition in response to nitrogen limitation in marine microalgae. Plant Physiology and Biochemistry, 54, 70-77.

Johannsdottir, L., and McInerney, C., (2016). Calls for carbon markets at COP21: A conference report. Journal of Cleaner Production, 124, 405-407.

Kais, S., and Sami, H., (2016). An econometric study of the impact of economic growth and energy use on carbon emissions: Panel data evidence from fifty eight countries. Renewable and Sustainable Energy Reviews, 59, 1101-1110.

Kaiwan-arporn, P., Hai, P., D., Thu, N., T., Annachhatre, A., P., (2012). Cultivation of cyanobacteria for extraction of lipids. Biomass and Bioenergy, 44, 142-149.

Kalsi, S., P., (2007). Spectroscopy of Organic Compounds, 6th edn. New age international, New Delhi, India.

Kao, C-Y., Chen, T-Y., Chang, Y-B., Chiu, T-W., Lin, H-Y., Chen, C-D., Lin, C-S., (2014). Utilization of carbon dioxide in industrial flue gases for the cultivation of microalga *Chlorella* sp. Bioresource Technology, 166, 485-493.

Kelly, D., P., (1999). Thermodynamic aspects of energy conservation by chemolithotrophic sulfur bacteria in relation to the sulfur oxidation pathways. Archives of Microbiology, 171(4), 219-229.

Ketheesan, B., and Nirmalakhandan, N., (2013). Modeling microalgal growth in an airlift-driven raceway reactor. Bioresource Technology, 136, 689-696.

Khan, N., E., Myers, J., A., Tuerk, A., L., Curtis, W., R., (2014). A process economic assessment

of hydrocarbon biofuels production using chemoautotrophic organisms. Bioresource Technology, 172, 201-211.

Kim, J., Yoo, G., Lee, H., Lim, J., Kim, K.,, W., C., Park, S., M., Yang J-W., (2013). Methods of downstream processing for the production of biodiesel from microalgae, Biotechnology Advncces, 31(6), 862-876.

Knothe, G., (2008). "Designer" biodiesel: optimizing fatty ester composition to improve fuel properties. Energy and Fuels, 22, 1358-1364.

Kumar, K., Dasgupta, N., C., Nayak, B., Lindblad, P., Das, D., (2011). Development of suitable photobioreactors for CO_2 sequestration addressing global warming using green algae and cyanobacteria. Bioresource Technology, 102(8), 4945-4953.

Kumar, K., and Das, D., (2012). Growth characteristics of *Chlorella sorokiniana* in airlift and bubble column photobioreactors. Bioresource Technology, 116, 307-313.

Kumar, A., Madden, G., D., Lusi, M., Chen, K-J., Daniels, A., E., Curtin, T., Perry, J., J., Zaworotko, J., M., (2015). Direct Air Capture of CO_2 by Physisorbent Materials. Angewandte Chemie International Edition, 54(48), 14372-14377.

Kwon, H-S., Lee, J-H., Kim, T., Kim, J-J., Jeon, P., Lee, C-H., Ahn, I-S., (2015). Biofixation of a high-concentration of carbon dioxide using a deep-sea bacterium: *Sulfurovum lithotrophicum* 42BKT T. RSC Advances, 5(10), 7151-7159.

Ladygina, N., Dedyukhina, E., G., Vainshtein, M., B., (2006). A review on microbial synthesis of hydrocarbons. Process Biochemistry, 41(5), 1001-1014.

Lal, R., (2008). Sequestration of atmospheric CO_2 in global carbon pools. Energy & Environmental Science, 1(1), 86-100.

Le Quéré, C., Raupach, M., R., Canadell, J., G., Marland, G., Woodward, F., I., (2009). Trends in the sources and sinks of carbon dioxide. Nature Geoscience, 2(12), 831-836.

Lee, J-Y., Yoo, C., Jun, S-Y., Ahn, C-Y., Oh, H-M., (2010). Comparison of several methods for effective lipid extraction from microalgae, Bioresource Technology, 101, 75-77.

Leesong, M., Henderson, B., S., Gillig, J., R., Schwab, J., M., Smith, J., L., (1996). Structure of a dehydratase-isomerase from the bacterial pathway for biosynthesis of unsaturated fatty acids: two catalytic activities in one active site. Structure, 4(3), 253-264.

Leu, J., Y., Lin, T., H., Selvamani, M., J., P., Chen, H., C., Liang, J., Z., Pan, K., M., (2013). Characterization of a novel thermophilic cyanobacterial strain from hot springs in Taiwan for

high CO_2 mitigation and C-phycocyanin extraction. Process Biochemistry, 48(1), 41-48.

Leung, D., Y., C., Caramanna, G., Maroto-Valer, M., M., (2014). An overview of current status of carbon dioxide capture and storage technologies. Renewable and Sustainable Energy Reviews, 39, 426-443.

Li, Y., Horsman, M., Wu, N., Lan, Q., C., (2008). Biofuels from microalgae. Biotechnology Progress, 24(4), 815-820.

Li, Y., Zhang, Q., Wang, Z., Wu, X., Cong, W., (2014). Evaluation of power consumption of paddle wheel in an open raceway pond. Bioprocess and Biosystems Engineering, 37(7), 1325-1336.

Liu, R., F., Zhu, L., Lu, A. Fu, J., Lu, Z., Deng, T., Liu., (2014). Metabolic engineering of fatty acyl-ACP reductase-dependent pathway to improve fatty alcohol production in *Escherichia coli*, Metabolic Engineering, 22, 10-21.

Lin, Q., and Lin, J., (2011). Effects of nitrogen source and concentration on biomass and oil production of a *Scenedesmus rubescens* like microalga. Bioresource Technology, 102(2), 1615-1621.

Lotlikar, S., R., Hnatusko, S., Dickenson, N., E., Choudhari, S., P., Picking, W., L., Patrauchan, M., A., (2013). Three functional α, β,γ-carbonic anhydrases in *Pseudomonas aeruginosa* PAO1: Role in survival in ambient air. Microbiology, 159(8), 1748-1759.

Lower, K., S., Carbonate equilibria in natural waters, Simon Fraser University (1999) 1-26. Available on the web at: http://www.chem1.com/acad/webtext/pdf/c3carb.pdf (October 2015).

Lynn, S., G., Kilham, S., S., Kreeger, D. A., Interlandi, S., J., (2000). Effect of Nutrient Availability on the biochemical and elemental stoichiometry in the freshwater diatom *Stephanodiscus Minutulus* (*Bacillariophyceae*). Journal of Phycology, 36, 510-522.

McCollom, M., T., and Amend, P., J., (2005). A thermodynamic assessment of energy requirements for biomass synthesis by chemolithoautotrophic micro-organisms in oxic and anoxic environments. Geobiology, 3(2), 135–144.

MacDowell, N., Florin, N., Buchard, A., Hallett, J., Galindo, A., Jackson, G., Fennell, P., (2010). An overview of CO_2 capture technologies. Energy and Environmental Science, 3(11), 1645-1669.

Majumder, S., Gupta, V., Raghuvanshi, S., Gupta, S., (2016). Simultaneous sequestration of

ternary metal ions (Cr^{6+}, Cu^{2+} and Zn^{2+}) from aqueous solution by an indigenous bacterial consortium. Process Safety and Environmental Protection, 102, 786-798.

Markewitz, P., Kuckshinrichs, W., Leitner, W., Linssen, J., Zapp, P., Bongartz, R., Müller, T., E., (2012). Worldwide innovations in the development of carbon capture technologies and the utilization of CO_2. Energy and Environmental Science, 5(6), 7281-7305.

Mata, T., M., Martins, A., A., Caetano, N., S., (2010). Microalgae for biodiesel production and other applications: A review. Renewable and Sustainable Energy Reviews, 14(1), 217-232.

McBeth, J., M., Little, B., J., Ray, R., I., Farrar, K. M., Emerson, D., (2011). Neutrophilic iron-oxidizing "*Zetaproteobacteria*" and mild steel corrosion in nearshore marine environments. Applied and Environmental Microbiology, 77(4), 1405-1412.

McGinn, P., J., Dickinson, K., E., Park, K., C., Whitney, C., G., MacQuarrie, S., P., Black, F., J., O'Leary, S., J., B., (2012). Assessment of the bioenergy and bioremediation potentials of the microalga *Scenedesmus sp*. AMDD cultivated in municipal wastewater effluent in batch and continuous mode. Algal Research, 1(2), 155-165.

Memmola, F., Mukherjee, B., Moroney, J., V., Giordano, M., (2014). Carbon allocation and element composition in four *Chlamydomonas* mutants defective in genes related to the CO_2 concentrating mechanism. Photosynthesis Research, 121(2-3), 201-211.

Mendoza, J., L., Granados, M., R., de Godos, I., Acién, F., G., Molina, E., Banks, C., Heaven, S., (2013). Fluid-dynamic characterization of real-scale raceway reactors for microalgae production. Biomass and Bioenergy, 54, 267-275.

Meng, Y., Yao, C., Xue, S., Yang, H., (2014). Application of fourier transform infrared (FT-IR) spectroscopy in determination of microalgal compositions. Bioresource Technology, 151, 347-354.

Mignone, C., F., and Donati, E., R., (2004). ATP requirements for growth and maintenance of iron-oxidizing bacteria. Biochemical Engineering Journal, 18(3), 211-216.

Mikkelsen, M., Jørgensen, M., Krebs, F., C., (2010). The Teraton Challenge. A review of fixation and transformation of carbon dioxide. Energy and Environmental Science, 3, 43-81.

Miethke, M., Monteferrante, G., C., Marahiel, A., M., Dij, V., M., J., (2013). The *Bacillus subtilis* EfeUOB transporter is essential for high affinity acquisition of ferrous and ferric iron. Biochmica et. Biophysica Acta, 1833, 2267-2278.

Mohsenpour, S., F., and Willoughby, N., (2016). Effect of CO_2 aeration on cultivation of

microalgae in luminescent photobioreactors. Biomass and Bioenergy, 85, 168-177.

Molina, L., Geoffroy, V., A., Segura, A., Udaondo, Z., Ramos, J-L., (2016). Iron Uptake Analysis in a Set of Clinical Isolates of Pseudomonas putida. Frontiers in Microbiology, 7:2100.

Moreira, D., and Pires, J., C., M., (2016). Atmospheric CO_2 capture by algae: Negative carbon dioxide emission path. Bioresource Technology, 215, 371-379.

Moazami, N., Ranjbar, R., Ashori, A., Tangestani, M., Nejad, S., A., (2011). Biomass and lipid productivities of marine microalgae isolated from the Persian Gulf and the Qeshm Island, Biomass and Bioenergy, 35, 1935-1939.

Muradov, N., (2014). Chapter 3: Anthropogenic CO_2 Emissions: Sources and Trends, 79-89, in Liberating Energy from Carbon: Introduction to Decarbonization; Springer: New York.

Mudge, M., S., (2005). Fatty Alcohols - A review of their natural synthesis and environmental distribution, The Soap and Detergent Association, 132, 1-141.

Nakanishi, A., Aikawa, S., Ho, S-H., Chen, C-Y., Chang, J-S., Hasunuma, T., Kondo, A., (2014). Development of lipid productivities under different CO_2 conditions of marine microalgae *Chlamydomonas* sp. JSC4. Bioresource Technology, 152, 247-252.

Nascimento, A., Cabanelas, I., T., D., dos Santos, J., N., Nascimento, M., A., Sousa, L., Sansone, G., (2015). Biodiesel yields and fuel quality as criteria for algal-feedstock selection: effects of CO_2-supplementation and nutrient levels in cultures, Algal Research, 8, 53-60.

Nelsona, R., D., and Viamajala, S., (2016). One-pot synthesis and recovery of fatty acid methyl esters (FAMEs) from microalgae biomass, Catalysis Today, 269, 29-39.

O'Fallon, J., V., Busboom, J., R., Nelson, M., L., Gaskins, C., T., (2007). A direct method for fatty acid methyl ester synthesis: Application to wet meat tissues, oils, and feedstuffs. Journal of Animal Science, 85(6), 1511-1521.

Ono, E., and Cuello, L., J., (2007). Carbon dioxide mitigation using thermophilic cyanobacteria. Biosystems Engineering, 96(1), 129-134.

Oren, A., (2002). Diversity of halophilic microorganisms: Environments, phylogeny, physiology, and applications, Journal of Industrial Microbiology and Biotechnology, 28, 56-63.

Ota, M., Kato, Y., Watanabe, H., Watanabe, M., Sato, Y., Smith, R., L., Inomata, H., (2009). Fatty acid production from a highly CO_2 tolerant alga, *Chlorocuccum littorale*, in the presence of inorganic carbon and nitrate. Bioresource Technology, 100(21), 5237-5242.

Ota, M., Kato, Y., Watanabe, M., Sato, Y., Smith, R., L., Rosello-Sastre, R., Inomata, H., (2011). Effects of nitrate and oxygen on photoautotrophic lipid production from *Chlorococcum littorale*. Bioresource Technology, 102(3), 3286-3292.

Palmucci, M., Ratti, S., Giordano, M., (2011). Ecological and evolutionary implications of carbon allocation in marine phytoplankton as a function of nitrogen availability: A fourier transform infrared spectroscopy approach. Journal of Phycology, 47(2), 313-323.

Pawlowski, A., Mendoza, J., L., Guzmán, J., L., Berenguel, M., Acién, F., G., Dormido, S., (2014). Effective utilization of flue gases in raceway reactor with event-based pH control for microalgae culture. Bioresource Technology, 170, 1-9.

Peters, G., Marland, G., Le Quéré, C., Boden, T., Canadell, J., G., Raupach, M., R., (2011). Rapid growth in CO_2 emissions after the 2008–2009 global financial crisis. Nature Climate Change, 2, 2–4.

Pirouzi, A., Nosrati, M., Shojaosadati, S., A., Shakhesi, S., (2014). Improvement of mixing time, mass transfer, and power consumption in an external loop airlift photobioreactor for microalgae cultures. Biochemical Engineering Journal, 87, 25-32.

Picardo, C., M., Medeiros, J., L., Araujo, F., Q., O., Chaloub, M., R., (2013). Effects of CO_2 enrichment and nutrients supply intermittency on batch cultures of *Isochrysis galbana*, Bioresource Technology, 143, 242-250.

Prabhu, C., Wanjari, S., Puri, A., Bhattacharya, A., Pujari, R., Yadav, R., Rayalu, S., (2011). Region-Specific Bacterial Carbonic Anhydrase for Biomimetic Sequestration of Carbon Dioxide, Energy and Fuels, 25(3), 1327-1332.

Pradhan, L., Bhattacharjee, V., Mitra, R., Bhattacharya, I., Chowdhury, R., (2015). Biosequestration of CO_2 using power plant algae (*Rhizoclonium hieroglyphicum* JUCHE2) in a flat plate photobio-bubble-reactor- experimental and modeling. Chemical Engineering Journal, 275, 381-390.

Putt, R., Singh, M., Chinnasamy, S., Das, K., C., (2011). An efficient system for carbonation of high-rate algae pond water to enhance CO_2 mass transfer. Bioresource Technology, 102(3), 3240-3245.

Raeesossadati, M., J., Ahmadzadeh, H., McHenry, M., P., Moheimani, N., R., (2014). CO_2 bioremediation by microalgae in photobioreactors: Impacts of biomass and CO_2 concentrations, light, and temperature. Algal Research, 6, 78-85.

Raghuvanshi, S., and Babu, B., V., (2009). Experimental studies and kinetic modeling for removal of methyl ethyl ketone using biofiltration. Bioresource Technology, 100(17), 3855-3861.

Ramanan, R., Kannan, K., Deshkar, A., Yadav, R., Chakrabarti, T., (2010). Enhanced algal CO_2 sequestration through calcite deposition by *Chlorella sp*. and *Spirulina platensis* in a mini-raceway pond. Bioresource Technology, 101 (8), 2616-2622.

Ramdin, M., De Loos, T., W., Vlugt, T., J., H., (2012). State-of-the-art of CO_2 capture with ionic liquids. Industrial and Engineering Chemistry Research, 51, 8149-8177.

Ritmann E., B., and McCarty, L., P., (2012). Environmental biotechnology: Principles and Applications, fourth ed., McGraw, Newyork, 2012.

Rinanti, A., Dewi, K., Kardena, E., Astuti, D., I., (2014). Biotechnology carbon capture and storage (CCS) by mix-culture green microalgae to enhancing carbon uptake rate and carbon dioxide removal efficiency with variation aeration rates in closed system photobioreactor. Jurnal Teknologi, 69 (6), 105-109.

Rosenzweig, C., Karoly, D., Vicarelli, M., Neofotis, P., Wu, Q., Casassa, G., Imeson, A., (2008). Attributing physical and biological impacts to anthropogenic climate change. Nature, 453(7193), 353-357.

Saini, R., Kapoor, R., Kumar, R., Siddiqi, T. O., Kumar, A., (2011). CO_2 utilizing microbes-A comprehensive review. Biotechnology Advances, 29(6), 949-960.

Sakakura, T., Choi, J., C., Yasuda, H., (2007). Transformation of carbon dioxide. Chemical Reviews, 107(6), 2365-2387.

Santini, M., J., Sly, I., L., Schnagl, D., R., Macy, M., J., (2000). A new chemolithoautotrophic arsenite-oxidizing bacterium isolated from a gold mine: phylogenetic, physiological, and preliminary biochemical studies. Applied and environmental microbiology, 66 (1), 92-97.

Segond, D., Ab- Khalil, E., Buisson, C., Daou, N., Kallassy, M., (2014). Iron Acquisition in *Bacillus cereus*: The Roles of IlsA and Bacillibactin in Exogenous Ferritin Iron Mobilization. PLOS Pathogens 10(2): e1003935.

Sharma, A., Bhattacharya, A., Pujari, R., Shrivastava, A., (2008). Characterization of carbonic anhydrase from diversified genus for biomimetic carbon-dioxide sequestration. Indian Journal of Microbiology, 48(3), 365-371.

Shene, C., Chisti, Y., Vergara, D., Burgos-D, C., Rubilar, M., Bustamante, M., (2016).

Production of eicosapentaenoic acid by *Nannochloropsis oculata*: Effects of carbon dioxide and glycerol. Journal of Biotechnology, 239, 47-56.

Shi, M., and Shen, Y., (2003). Recent progresses on the fixation of carbon dioxide. Current Organic Chemistry, 7, 737-745.

Shukla, R., Ranjith, P., Haque, A., Choi, X. (2010). A review of studies on CO_2 sequestration and caprock integrity. Fuel, 89(10), 2651-2664.

Sinetova, M., A., Červený, J., Zavřel, T., Nedbal, L., (2012). On the dynamics and constraints of batch culture growth of the cyanobacterium *Cyanothece sp*. ATCC 51142. Journal of Biotechnology, 162(1), 148–155.

Sinha, R., and Raymahashay, B., C., (2004). Evaporite mineralogy and geochemical evolution of the Sambhar Salt Lake, Rajasthan, India. Sedimentary Geology, 166(1-2), 59-71.

Singh, J., Tripathi, R., Thakur, S., I., (2014). Characterization of endolithic cyanobacterial strain, *Leptolyngbya* sp. ISTCY101, for prospective recycling of CO_2 and biodiesel production. Bioresource Technology, 166, 345-352.

Skjånes, K., Rebours, C., Lindblad, P., (2012). Potential for green microalgae to produce hydrogen, pharmaceuticals and other high value products in a combined process. Critical Reviews in Biotechnology, 33, 1-44.

Smith, K., S., Ferry, J., G., (2000). Prokaryotic carbonic anhydrases. FEMS Microbiology Reviews, 24(4), 335-366.

Solomon, S., Plattner, G-K., Knutti, R., Friedlingstein, P., (2009). Irreversible climate change due to carbon dioxide emissions. Proceedings of the National Academy of Sciences of the United States of America, 106(6), 1704-1709.

Solovchenko, A., Gorelova, O., Selyakh, I., Pogosyan, S., Baulina, O., Semenova, L., Lobakova, E. (2015). A novel CO_2-tolerant symbiotic *Desmodesmus* (*Chlorophyceae*, *Desmodesmaceae*): Acclimation to and performance at a high carbon dioxide level. Algal Research, 11, 399-410.

Sorokin, Y., D., (2003). Oxidation of Inorganic Sulfur Compounds by Obligately Organotrophic Bacteria. Microbiology, 72, 6, 641-653.

Sorokin, Y., D., Kuenen, G., J., (2005). Haloalkaliphilic sulfur-oxidizing bacteria in soda lakes. FEMS Microbiology Reviews, 29, 4, 685-702.

Sorokin, Y., D., Kuenen, G., J., Muyzer, G., (2011).The microbial sulfur cycle at extremely haloalkaline conditions of Sambhar lakes, FEMS Microbiology Review, 2(44), 1-16.

Steen, J., E., Kang, S., Y., Bokinsky, G., Hu, H., Z., Schirmer, A., McClure, A., del-Cardayre, B., S., Keasling, D., J., (2010). Microbial production of fatty-acid-derived fuels and chemicals from plant biomass. Nature, 463, 559-562.

Stover, C., K., Pham, X., Q., Erwin, L., Mizoguchi, S., D., Warrener, P., Hickey, M., J., Olson, M., V., (2000). Complete genome sequence of *Pseudomonas aeruginosa* PAO1, an opportunistic pathogen. Nature, 406(6799), 959-964.

Subashchandrabose, R., S., Ramakrishnan, B., Megharaj, M., Venkateswarlu, K., Naidu, R., (2011). Consortia of cyanobacteria/microalgae and bacteria: biotechnological potential Biotechnology Advances, 29, 896-907.

Sun, Y., Huang, Y., Liao, Q., Fu, Q., Zhu, X., (2016). Enhancement of microalgae production by embedding hollow light guides to a flat-plate photobioreactor. Bioresource Technology, 207, 31–38.

Sun, Y., Liao, Q., Huang, Y., Xia, A., Fu, Q., Zhu, X., Zheng, Y., (2016). Integrating planar waveguides doped with light scattering nanoparticles into a flat-plate photobioreactor to improve light distribution and microalgae growth. Bioresource Technology, 220, 215-224.

Sundaram, S., Thakur, I., S., (2015). Biosurfactant production by a CO_2 sequestering *Bacillus sp.* strain ISTS2. Bioresource Technology, 188, 247-250.

Supuran, C., T., (2016). Structure and function of carbonic anhydrases. Biochemical Journal, 473, 2023-2032.

Swarnalatha, G., V., Hegde, N., S., Chauhan, V., S., Sarada, R., (2015). The effect of carbon dioxide rich environment on carbonic anhydrase activity, growth and metabolite production in indigenous freshwater microalgae. Algal Research, 9, 151-159.

Sydney, E., B., Sturm, W., de Carvalho, J., C., Thomaz-Soccol, V., Larroche, C., Pandey, A., Soccol, C., R., (2010). Potential carbon dioxide fixation by industrially important microalgae. Bioresource Technology, 101(15), 5892-5896.

Tang, D., Han, W., Li, P., Miao, X., Zhong, J., (2011). CO_2 biofixation and fatty acid composition of *Scenedesmus obliquus* and *Chlorella pyrenoidosa* in response to different CO_2 levels. Bioresource Technology, 102, 3071-3076.

Tamura, K., Dudley, J., Nei, M., Kumar, S., (2007). MEGA4: Molecular Evolutionary Genetics Analysis (MEGA) software version 4.0. Molecular Biology Evolution, 24, 1596-1599.

Tekerlekopoulou, A., G., Vasiliadou, I., A., Vayenas, D., V., (2006). Physico-chemical and biological iron removal from potable water. Biochemical Engineering Journal, 31(1), 74-83.

Teske, A., Brinkhoff, T., Muyzer, G., Moser, P., D., Rethmeier, J., Jannasch, W., H., (2000). Diversity of thiosulfate-oxidizing bacteria from marine sediments and hydrothermal vents. Appl. Environ. Microbiol., 66 , 3125-3133

Tiel-Menkveld V., J., G., Mentjox-Vervuurt, M., J., Oudega, B., de Graaf, K., F., (1982). Siderophore production by Enterobacter cloacae and a common receptor protein for the uptake of aerobactin and cloacin DF13. Journal of Bacteriology, 150, 2, 490-497.

Tripathi, R., Singh, J., Thakur, I., S., (2015). Characterization of microalga *Scenedesmus sp.* ISTGA1 for potential CO_2 sequestration and biodiesel production. Reneweable Energy, 74, 774-781.

Toledo-Cervantes, A., Morales, M., Novelo, E., Revah, S., (2013). Carbon dioxide fixation and lipid storage by *Scenedesmus obtusiusculus*. Bioresource Technology, 130, 652-658.

Ugwu, C., U., Aoyagi, H., Uchiyama, H., (2008). Photobioreactors for mass cultivation of algae. Bioresource Technology, 99(10), 4021-4028.

Vasileva, A, Golub, P., Doroshenko, I., Pogorelov, V., Sablinskas, V., Balevicius, V., Ceponkus, J., (2014). Dataset Paper FT-IR Spectra of n-Octanol in Liquid and Solid States, 2014, 1-3.

VenkataMohan, S., AnnieModestra, J., Amulya, K., KishoreButti, S., Velvizhi, G., (2016). A Circular Bio-economy with Bio-based Products from CO_2 Sequestration. Trends in Biotechnology, 34(6), 506-519.

Wallace, K ., K., Zhao, B., McArthur, H., A., Reynolds, K., A., (1995). In vivo analysis of straight-chain and branched chain fatty acid biosynthesis in three actinomycetes. FEMS Microbiology Letters, 131, 227-234.

Wang, B., Li, Y., Wu, N., Lan, C., Q., (2008). CO_2 bio-mitigation using microalgae. Applied Microbiology and Biotechnology, 79(5), 707-718.

Wang, X., W., Liang, J., R., Luo, C., S., Chen, C., P., Gao, Y., H., (2014). Biomass, total lipid production, and fatty acid composition of the marine diatom *Chaetoceros muelleri* in response to different CO_2 levels. Bioresource Technology, 161, 124-130.

Willis, M., R., Wahlen, D., B., Seefeldt, C., L., Barney, M., B., (2011). Characterization of a fatty Acyl-CoA reductase from *Marinobacter aquaeolei* VT8: A bacterial enzyme catalyzing the reduction of fatty Acyl-CoA to fatty alcohol. Biochemistry, 50(48), 10550-10558.

Wu, L., F., Chen, P., C., Lee, C., M., (2013). The effects of nitrogen sources and temperature on cell growth and lipid accumulation of microalgae. International Biodeterioration and Biodegradation, 85, 506-510.

Wychen, V., S., Laurens, L., M., L., (2013) Determination of Total Lipids as Fatty Acid Methyl Esters (FAME) by in situ Transesterification - Laboratory Analytical Procedure (LAP), Contract 303: 275-3000.

Xue, S., Zhang, Q., Wu, X., Yan, C., Cong, W., (2013). A novel photobioreactor structure using optical fibers as inner light source to fulfill flashing light effects of microalgae. Bioresource Technology, 138, 141-147.

Yadav, G., Karemore, A., Dash, S., K., Sen, R., (2015). Performance evaluation of a green process for microalgal CO_2 sequestration in closed photobioreactor using flue gas generated in-situ. Bioresource Technology, 191, 399-406.

Yang, X., Zhang, R., Fu, J., Geng, S., Cheng, J., J., Sun, Y., (2013). Petrodiesel-like straight chain alkane and fatty alcohol production by the Microalga *Chlorella sorokiniana*, Bioresource Technology, 136, 126-130.

Yang, W., Zou, S., He, M., Fei, C., Luo, W., Zheng, S., Wang, C., (2016). Growth and lipid accumulation in three *Chlorella* strains from different regions in response to diurnal temperature fluctuations. Bioresource Technology, 202, 15-24.

Yao, L., Qi F., Tan, X., Lu, X., (2014). Improved production of fatty alcohols in cyanobacteria by metabolic engineering. Biotechnology and Biofuels. 7, 94.

Yen, H-W., Hu, I-C., Chen, C-Y., Ho, S-H., Lee, D.-J., Chang, J-S., (2013). Microalgae-based biorefinery - From biofuels to natural products. Bioresource Technology, 135, 166-174.

Yoo, C., Choib, G-G., Kima, S-C., Oh, H-M., (2013). *Ettlia* sp. YC001 showing high growth rate and lipid content under high CO_2. Bioresource Technology, 127, 482-488.

Yvon-Durocher, G., Dossena, M., Trimmer, M., Woodward, G., Allen, A., P., (2015). Temperature and the biogeography of algal stoichiometry. Global Ecology and Biogeography, 24(5), 562-570.

Zeng, X., Danquah, M., K., Zhang, S., Zhang, X., Wu, M., Chen, X., D., Lu, Y., (2012).

Autotrophic cultivation of *Spirulina platensis* for CO_2 fixation and phycocyanin production. Chemical Engineering Journal, 183, 192-197.

Zhang, Q., Xue, S., Yan, C., Wu, X., Wen, S., Cong, W., (2015). Installation of flow deflectors and wing baffles to reduce dead zone and enhance flashing light effect in an open raceway pond. Bioresource Technology, 198, 150-156.

Zhang, Q., Zhan, J., Hong, Y., (2015). The effects of temperature on the growth, lipid accumulation and nutrient removal characteristics of *Chlorella* sp. HQ. Desalination and Water Treatment, 57(22), 1-6.

Zheng, Y-N., Li, L-L., Liu, Q., Yang, J-M., Wang, X-W., Liu, W., Xu X., Liu H., Zhao G., Xian M., (2012). Optimization of fatty alcohol biosynthesis pathway for selectively enhanced production of C12/14 and C16/18 fatty alcohols in engineered *Escherichia coli*. Microbial Cell Factories, 11(1), 65.

List of Publications

International Journals

1. **Mishra, S.**, Singh, R., P., Raghuvanshi, S., Gupta, S., Jha, P., N., (2015). Deducing the bio-perspective capabilities of Fe[II] utilizing bacteria isolated from extreme environment, **Biochemistry and Analytical Biochemistry**, 4(2), 1-5.
2. **Mishra, S.**, Singh, P., R., Raghuvanshi, S., Jha, N., P., (2015). GC-MS analysis of change in fatty acid composition of halobacterium *Bacillus licheniformis* hsw-16 under varying salinity condition**, Journal of Microbiology, Biotechnology and Food Sciences**, 5 (3) 290-292.
3. **Mishra, S.**, Pal, P., Raghuvanshi, S., Gupta, S., (2016). Energetic assessment of fixation of CO_2 and subsequent biofuel production using *B. cereus* SM1 isolated from sewage treatment plant. **Bioprocess and Biosystems Engineering**, 39:1247–1258
4. **Mishra, S.**, Raj, K., Raghuvanshi, S., Gupta, S., (2017). Application of novel thermo-tolerant haloalkalophilic bacterium *Halomonas stevensii* for bio-mitigation of gaseous phase CO_2: Energy assessment and product evaluation studies. **Process Biochemistry**, 55:133-145
5. **Mishra, S.**, Chauhan P., Raghuvanshi, S., Gupta, S., Jha P. N., Singh, R. (2017). CO_2 sequestration potential of halo-tolerant bacterium *Pseudomonas aeruginosa* SSL4 and its application for recovery of fatty alcohols. **Process safety and Environmental Protection**, Available on-line, In Press.

Full Paper communicated

1. **Mishra, S.**, Raghuvanshi, S., Gupta, S., (2017). Utilization of mixed culture and isolated bacterial strains *Enterobacter cloacae* PP1 and *Pseudomonas putida* SM2 for CO_2 mitigation: Thermodynamic analysis and by-product characterization, **Bio-chemical Engineering journal**, Under review.
2. **Mishra, S.**, Pahari, S., Shiva, K, Sarit, A., Gupta, S., Raghuvanshi, S., (2017). Processes and economics for scalable product recovery from biomass obtained after CO_2 bio-mitigation: A commercialization approach. **Journal of CO_2 Utilization**, Under revision.

Manuscripts under Preparation

1. **Mishra, S.**, Raghuvanshi, S., Gupta, S., (2017). Biological perspective of CO_2 mitigation-A review
2. **Mishra, S.**, Raghuvanshi, S., Gupta, S., (2017). Design and performance of pilot scale packed bed bio-reactor for CO_2 mitigation utilizing mixed microbial population.
3. **Mishra, S.**, Raj K., Raghuvanshi, S., Gupta, S., (2017). A study on the effect of pH and Temperature on the growth of the CO_2 mitigating bacteria *Halomonas stevensii*, obtained from the Sambhar Salt Lake, Rajasthan, India.

International Conference Proceeedings

1. **Mishra, S.**, Raghuvanshi, S., Gupta, S., (2012). Feasibility of Mixed Culture to Mitigate CO_2, "Proceedings of National Conference (TACEE – 2012) on Technological

Advancements in Chemical and Environmental Engineering, March 23-24, 2012, Pilani, India.

2. **Mishra, S.**, Raghuvanshi, S., Gupta, S., (2012). Batch studies on biomitigation of Carbon dioxide (CO_2) using mixed culture , Proceedings of International Symposium & 65 th Annual Session of IIChE in association with International Partners (CHEMCON-2012), Department of Chemical Engineering, Dr. B.R. Ambedkar National Institute of Technology, Jalandhar, India, December 27-30, 2012.
3. Nagpurkar, I., **Mishra, S.**, Raghuvanshi, S., Gupta, S., (2012). Mitigation of CO_2 using microalgae *Chlorella minutissima*, Proceedings of International Symposium & 65 th Annual Session of IIChE in association with International Partners (CHEMCON-2012), Department of Chemical Engineering, Dr. B.R. Ambedkar National Institute of Technology, Jalandhar, India, December 27-30, 2012.
4. **Mishra, S.**, Raghuvanshi, S., Gupta, S., (2013). A green approach to mitigate CO_2 using mixed microbial culture. Proceedings of 2013 AIChE Annual Meeting, Hilton San Francisco Union Square, San Francisco, CA, November 3 – 8, 2013.
5. **Mishra, S.**, Pal, P., Raghuvanshi, S., Gupta, S., (2013). Experimental studies for CO_2 mitigation using acclimated mixed culture, Proceedings of International Symposium & 66th Annual Session of IIChE in association with International Partners (CHEMCON-2013), Department of Chemical Engineering, University Institute of Chemical Technology, Mumbai, India, December 27-30, 2013.
6. **Mishra, S.**, Pal, P., Raghuvanshi, S., Gupta, S., (2013). Utilizatilization of Mixed Culture and Isolated Species for Biomitigation of CO_2, 2014 AIChE Annual Meeting, Atlanta Marriott Marquis, Hilton Atlanta, November 16-21, 2014.

BIOGRAPHIES

Biography of the Candidate

Somesh Mishra did his B.Tech degree in Chemical Engineering from Kanpur University in 2009. He completed his M.E. degree in Chemical Engineering with specialization in Petroleum Engineering from BITS-Pilani, Pilani campus in 2011. He has 8 months of industrial experience in chemical process industry. He joined BITS-Pilani, Pilani campus in August, 2011 as a Research Scholar. He is currently a PhD Scholar in the Department of Chemical Engineering at Birla Institute of Technology and science (BITS), Pilani campus, Rajasthan, India. His current area of research includes experimental studies on biological route for CO_2 mitigation. His research interests include carbon capture and utilization, statistical methods, Green Technology, Renewable Energy Sources, Artificial photosynthesis and Smart Materials. He got UGC-BSR fellowship from year 2012-2013 and Senior Research Fellowship from CSIR (CSIR-SRF) from 2013-2017. He was also involved in the tutorials of courses such as Mass Transfer, Heat Transfer, Chemical Process Calculations, Basic Thermodynamics, Process Design and Decisions.

Biography of Supervisor

Dr. Smita Raghuvanshi is working as an Assistant professor in Department of Chemical Engineering, BITS-Pilani, Pilani campus, Rajasthan, India. She did her PhD from BITS-Pilani, Pilani campus. She is having a vast expertise in Environmental Engineering & Separation Process (bio-filtration for removal of VOCs and metals; CO_2 mitigation using bio-based techniques; design of bioreactor); kinetic modeling of bio-degradation & bio-filtration processes and Environmental Management systems (Environmental impact assessment of various processes and life cycle assessment of industrial processes). Dr Smita has completed the DST Fast Track Research Project entitled "Removal of volatile organic compounds, chlorinated VOCs, non-methane hydrocarbons, ethylene glycol) from waste streams using biofiltration"in year 2015. The project entitled "Removal of Heavy Metals from Industrial Wastewater using Biofiltration" was also completed as part of UGC major research project in June, 2015.

She has around 18 research publications in peer reviewed International Journals. She has also published 4 book chapters and invited articles in various books and technical notes. She has almost 52 conference publications so far. Dr Smita has also won 1st prize in the paper presentation on "Removal of Methyl Ethyl Ketone (MEK) using Bio-filtration" in National Conference on Environmental Conservation (NCEC-2006), held at BITS-Pilani in September 1-3, 2006. She is the reviewer of 4 internationals journals which include Journal of Physical Sciences, Biodegradation, Journal of Food Processing and Technology and Nano-sciences & Nanotechnology. She has shown exemplary acumen in application of life cycle concepts i.e. LCA of RO based filtration system in BITS-Pilani and has also carried out the LCA of STP, BITS-Pilani, She is a life member of Indian Institute of Chemical Engineers (IIChE) and Fellow member of International Congress of Chemistry and Environment (FICCE). She is also a member of American Institute of Chemical Engineers (AIChE), International Association of Engineers (IAENG) and Institute of Engineers, IEI, India.

She is currently convener of Department Research Committee (DRC) of Chemical Engineering Department. She has been nucleus member of Practice School Division, BITS-Pilani, Pilani campus, Rajasthan, India from 2003-2012. She has been actively involved in various departmental activities and involved in laboratory based up gradation work. She was the Convener of the Work shop on Analytical Instruments for Chemical and Environmental Engineers, (WAICEE-2015). Besides this, Dr Smita has been the organizing Committee member of life Cycle Engineering conference held at BITS-Pilani in 2015 and 2016. She has guided 5 dissertation students and 5 B.E. Thesis students so far. Currently, Dr Smita is guiding 1 PhD student, 1 M.E Dissertation student and 1 B.E Thesis student.

Biography of Co-Supervisor

Prof. Suresh Gupta is an Associate Professor in the Department of Chemical Engineering, BITS-Pilani, Pilani campus, Rajasthan, India. He completed his PhD from BITS-Pilani, Pilani campus, India. Dr Gupta`s research interests include Environmental Engineering and Separation Processes, Bioleaching of metal ion from industrial waste, Mathematical Modeling of Chemical Processes, Computational Transport Phenomena, Environmental management Systems (LCA, EIA) and Energy Integration. He has 15 years of Teaching and Research experience. Prof Gupta has around 35 research publications in peer reviewed journals. He has around 60 conference proceedings to his credit. Dr Gupta has also published 7 chapters and invited articles in various books, lecture notes, national and international journals. He has delivered around 7 lectures as distinguished speaker in universities across India. Prof. Gupta was invited as a member in the workshop to review the existing scheme of the Engineeing Services Examination conducted by the Commission organized by UPSC at the International Management Development Center (IMDC), Indian Institute of Management, Vastrapur, Ahemdabad. Prof Gupta is an External Academic Expert Member in Board of Students (BoS) Constitution for Chemical Engineering and Galgotia University, Noida. He has visited various industries such as Ultratech cement, Reddipalaym cement works, Indo Gulf Fertilizers, Birla Cellulosic Kharach, Bharat Aluminum Company Limited and Hindustan Zinc Limited for discussions on BITS Collaborative Programmes on Academic Development in Basic Process Engineering for their Employees. He also served as a resource faculty in Practice School Division, BITS-Pilani. He was also an External Examiner for B.Tech (Chemical Engg.) students at Banasthali University.

Prof Gupta is involved in various academic and administrative committees at BITS-Pilani. Prof Gupta has been the Head of Chemical Engineering Department from 2012 to 2016. He was the Coordinator for UGC Assistance to the Department of Chemical Engineering of DRS under special Assistance Programme. He is the member of Implementation Committee of DIST-FIST Support for Chemical Engineering Department as the chairperson. He was also the Nucleus Member of Instruction Division from Jan 2007 to August 2012. He has been in various committees such as Research Board and Standing committee of student Discipline in BITS-Pilani, Pilani campus. He has guided 9 M.E. Dissertation students. Currently, he is guiding 2 Ph.D. students. He currently has 4 research and sponsored projects from UGC, DST and BITS-Pilani. He successfully completed 3 research and consultancy projects of MHRD, UGC and Birla Cellulosic, Kharach. He is the PhD Examiner of 2 candidates.

He is currently the reviewer of 16 International reputed Journals. He is a Life Member of Indian Institute of Chemical Engineers (IIChE) and Fellow Member of International Congress of Chemistry and Environment (FICCE). He is also a member of American Institute of Chemical Engineers (AIChE), International Association of Engineers (IAENG) and Institute of Engineers, (IEI), India.